Phase Equilibria Modelling of Petroleum Reservoir Fluids Containing Water, Hydrate Inhibitors and Electrolyte Solutions

by

Hooman Haghighi

Submitted for the degree of Doctor of Philosophy in

Petroleum Engineering

Heriot-Watt University

Institute of Petroleum Engineering

October 2009

ABSTRACT

Formation of gas hydrates can lead to serious operational, economic and safety problems in the petroleum industry due to potential blockage of oil and gas equipment. Thermodynamic inhibitors are widely used to reduce the risks associated with gas hydrate formation. Thus, accurate knowledge of hydrate phase equilibrium in the presence of inhibitors is crucial to avoid gas hydrate formation problems and to design/optimize production, transportation and processing facilities. The work presented in this thesis is the result of a study on the phase equilibria of petroleum reservoir fluids containing aqueous salt(s) and/or hydrate inhibitor(s) solutions.

The incipient equilibrium methane and natural gas hydrate conditions in presence of salt(s) and/or thermodynamic inhibitor(s) have been experimentally obtained, in addition to experimental freezing point depression data for aqueous solution of methanol, ethanol, monoethylene glycol and single or mixed salt(s) aqueous solutions, are conducted.

A statistical thermodynamic approach, with the Cubic-Plus-Association equation of state, has been employed to model the phase equilibria. The hydrate-forming conditions are modelled by the solid solution theory of van der Waals and Platteeuw. Predictions of the developed model have been validated against independent experimental data from the open literature and the data generated in this work. The predictions were found to agree well with the experimental data.

Dedicated to my parents, Fereidoon and Manijeh

and my brother, Ali

ACKNOWLEDGMENTS

This thesis is submitted in partial fulfilment of the requirements for the Ph.D. degree at Heriot-Watt University. This work has been conducted at the Institute of Petroleum from February 2006 to February 2009 under the supervision of Professor Bahman Tohidi and Dr. Antonin Chapoy.

The project has been financed by grants by a Joint Industrial Project (JIP) conducted at the Institute of Petroleum Engineering, Heriot-Watt University. The JIP is supported by Petrobras, Clariant Oil Services, StatoilHydro, TOTAL and the UK Department of Business, Enterprise and Regulatory Reform (BERR), which is gratefully acknowledged.

I would like to thank my advisor, Professor Bahman Tohidi for providing me the opportunity to work with such a scientifically interesting and challenging project in the Centre for Gas Hydrate Research, and would like to express my sincere gratitude for his help and guidance throughout this project. Special and countless thanks go to Dr. Antonin Chapoy for all his continuous help and support, his inspiring discussions, and his huge enthusiasm during the time we worked together. Also in this regard, I would like to thank my colleague Mr. Rod Burgess for his close collaboration and fruitful discussions. Additionally, I greatly appreciate the help from Mr. Ross Anderson and all the colleagues as well as friends in the Centre for Gas Hydrate Research making my stay in Edinburgh very pleasant and provided me with any help needed. I wish to express my thanks to the Institute of Petroleum Engineering, Heriot-Watt University.

At the end but not at the least, I am grateful to my parents. Words can not express how much I thank them for their continuous support through my graduate research. It was not easy for them seeing their son leave Iran for another country far away.

Hooman Haghighi

ACADEMIC REGISTRY
Research Thesis Submission

Name*:*	Hooman Haghighi		
School/PGI:	Institute of Petroleum Engineering		
Version: *(i.e. First, Resubmission, Final)*	Final	Degree Sought (Award **and** Subject area)	PhD

Declaration

In accordance with the appropriate regulations I hereby submit my thesis and I declare that:

1) the thesis embodies the results of my own work and has been composed by myself
2) where appropriate, I have made acknowledgement of the work of others and have made reference to work carried out in collaboration with other persons
3) the thesis is the correct version of the thesis for submission and is the same version as any electronic versions submitted*.
4) my thesis for the award referred to, deposited in the Heriot-Watt University Library, should be made available for loan or photocopying and be available via the Institutional Repository, subject to such conditions as the Librarian may require
5) I understand that as a student of the University I am required to abide by the Regulations of the University and to conform to its discipline.

* *Please note that it is the responsibility of the candidate to ensure that the correct version of the thesis is submitted.*

Signature of Candidate*:*		Date:	

Submission

Submitted By *(name in capitals):*	Hooman Haghighi
Signature of Individual Submitting:	
Date Submitted:	

For Completion in Academic Registry

Received in the Academic Registry by *(name in capitals):*			
Method of Submission *(Handed in to Academic Registry; posted through internal/external mail):*			
*E-thesis Submitted (**mandatory for final theses from January 2009)***			
Signature:		Date:	

Please note this form should bound into the submitted thesis.

Updated February 2008, November 2008, February 2009

TABLE OF CONTENTS

LISTS OF TABLES

LISTS OF FIGURES

LISTS OF PUBLICATIONS BY THE CANDIDATE

Anderson R., Chapoy A., Haghighi H., Tohidi B., 2009, *Binary ethanol-methane clathrate hydrate formation in the system $CH_4-C_2H_5OH-H_2O$: phase equilibria and compositional analyses*, J. Phys. Chem. C, **113** (28), 12602–12607

Chapoy A., Haghighi H., Burgess R., Tohidi B., 2009, *Gas hydrates in low water content gases: experimental measurements and modelling using the CPA equation of state*, Submitted in the J. Fluid Phase Equilibr.

Haghighi H., Chapoy A., Tohidi B., 2009, *Modelling phase equilibria of complicated systems containing petroleum reservoir fluids*, published and presented in SPE Offshore Europe conference (Paper # 123170)

Haghighi H., Chapoy A., Burgess R., Mazloum S., Tohidi B., 2009, *Phase equilibria for petroleum reservoir fluids containing water and aqueous methanol solutions: Experimental measurements and modelling using the CPA equation of state*, J. Fluid Phase Equilibr., **278**, 109–116

Salehabadi M., Jin M., Yang J., Haghighi H., Tohidi B., 2009, *Finite element modelling of casing in gas hydrate bearing sediments*, J. SPE Drilling & Completion, (Paper # 113819)

Haghighi H., Chapoy A., Tohidi B., 2009, *Experimental and thermodynamic modelling of systems containing water and ethylene-glycol: application to flow assurance and gas processing*, J. Fluid Phase Equilibr., **276**, 24-30

Haghighi H., Chapoy A., Tohidi B., 2009, *Experimental data and modelling methane and water phase equilibria in the presence of single and mixed electrolyte solutions using the CPA equation of state*, J. Oil Gas Sci. Technol., **64**(2), 141-154

Najibi H., Chapoy A., Haghighi H., Tohidi B., 2008, *Experimental determination and thermodynamically prediction of methane hydrate stability in alcohols and electrolyte solutions*, J. Fluid Phase Equilibr., **275**, 127–131

Haghighi H., Chapoy A., Tohidi B., 2008, *Freezing point depression of common electrolyte solutions: experimental and prediction using the CPA equation of state*, J. Ind. Eng. Chem. Res., **47**, 3983-3989

Salehabadi M., Jin M., Yang J., Haghighi H., Tohidi B., 2008, *Finite element modelling of casing in gas hydrate bearing sediments*, published and presented in SPE Europec conference (Paper #: 113819)

Chapoy A., Anderson R., Haghighi H., Edwards T., Tohidi B., 2008, *Can n-propanol form hydrate?*, J. Ind. Eng. Chem. Res., **47**, 1689-1694

Anderson R., Chapoy A., Tanchawanich J., Haghighi H., Lachwa-Langa J., Tohidi B., 2008, *Binary ethanol−methane clathrate hydrate formation in the system $CH_4-C_2H_5OH-H_2O$: experimental data and thermodynamic modelling*, published and presented in the 6th International Conference on Gas Hydrates

Haghighi H., Burgess R., Chapoy A., Tohidi B., 2008, *Hydrate dissociation conditions at high pressure: experimental equilibrium data and thermodynamic modelling*, published and presented in the 6th International Conference on Gas Hydrates

Chapoy A., Haghighi H., Tohidi B., 2008, *Development of a Henry's constant correlation and solubility measurements of n-pentane, i-pentane, cyclopentane, n-hexane and toluene in water*, J. Chem. Thermodyn., **40**(6), 1030-1037

Haghighi H., Azarinezhad R., Chapoy A., Anderson R., Tohidi B., 2007, *HYDRAFLOW: Avoiding gas hydrate problem*, published and presented in SPE Europec conference (Paper # 107335)

LIST OF MAIN SYMBOLS

A	Constant in the binary interaction parameter of salt model/ Electrolyte model parameter/ Helmholtz function/ Constant
AAD	Average absolute deviation
AD	Absolute deviation
APACT	Associated Perturbed Anisotropic Chain Theory
B	Constant in the binary interaction parameter of salt model/ Electrolyte model parameter/ Types of bonding in real associating fluids/ Constant
BIP	Binary interaction parameter
PB	Bubble point
C	Constant in the binary interaction parameter of salt model/ Langmuir constant/ Types of bonding in real associating fluids/ Constant
C_1	Pure compound parameter in the energy part of the CPA EoS/ Methane
C_2	Ethane
C_2	Ethane
C_3	Propane
iC_4	Iso propane
nC_4	Normal propane
iC_5	Iso pentane
nC_5	Normal pentane
C_p	Average heat capacity of natural gas
CPA EoS	Cubic-Plus-Association equation of state
D	Constant in the binary interaction parameter of salt model (K^{-1})
DP	Dew point
DH	Debye-Hückel electrostatic term
E	Constant in the binary interaction parameter of salt model
EoS	Equation of state
EtOH	Ethanol
F	Parameter of the equation of state/ Molar fraction of phase / Correction factor/ Function/ Shape factor
FP	Freezing point
G	Gas/ Gibbs free energy
H	Hydrate

HC	Hydrocarbon
I	Ice/ Ionic strength based on molality of salt in pure water
i-POH	Iso propanol
K	Equilibrium ratio
L	Liquid
L_1	Aqueous phase
L2	Rich hydrocarbon phase
LLE	Liquid-liquid equilibrium
M	Molecular weight
MEG	Monoethylene glycol
MeOH	Methanol
Mol.	Mole
N	Number of experimental points/ Number of components
NDD	Non density dependent mixing rules
NG	Natural gas
n-POH	Normal propanol
P	Pressure
PC	Computer
PR	Peng – Robinson equation of state
PRT	Platinum resistance thermometer
PTx	Pressure, Temperature, and Mole fraction in the liquid phase
PTxy	Pressure, Temperature, Mole fraction in the liquid phase and Mole fraction in the vapour state
R	Universal gas constant
$\overline{R}$	Cavity radius
SAFT	Statistical associated fluid theory
SRK	Soave-Redlich-Kwang equation of state
T	Temperature
V	Vapour/ Volume
VLE	Vapour-liquid equilibrium
VLLE	Vapour – liquid – liquid equilibrium
VPT EoS	Valderrama modification of Patel-Teja equation of state
W	Salt concentration in weight percent in the salt model

Q	Quadruple point
X	Mole fraction of molecules that are not-bonded to the site
a	Attractive parameter of the equation of state/ Activity/ Constant
a_0	Constant part in the energy parameter of the EoS
b	Co volume parameter of the equation of state/ Constant in the binary interaction parameter of salt model
c	Parameter of the equation of state/ Constant in the binary interaction parameter of salt model/ a normalisation constant/ Constant
d	Constant in the binary interaction parameter of salt model/ Constant
e	Constant in the binary interaction parameter
f	Fugacity/ Function in salt model/ Constant
g	Gas / Radial distribution function in the CPA EoS/ Constant
h	Binary interaction parameter between the dissolved salt and a non-electrolyte component/ Constant
k	Binary interaction parameter for the classical mixing rules/ Correction factor/ Boltzmann's constant
n	Number of moles/ Number of ions that results from salt
ns	Number of slats
p	Pressure
$pts.$	Points
r	Distance/ Well width in the potential models/ Residual properties
sI	Structure-I
sII	Structure-II
sH	Structure-H
t	Temperature
v	Molar volume
$\bar{v}$	Number of cavities of type m per water molecule in the unite cell
w	Weight percent of salt
$w(r)$	Spherically symmetric cell potential function
x	Liquid mole fraction/ Mole fraction in the liquid phase/ Salt-free mixture mole fraction
y	Vapour mole fraction/ Mole fraction in the vapour state

z	Coordination number/ Specified molar composition of component *i* in the feed/ Mole fraction in natural gas/ Mole fraction in oil

Greek

Γ	Potential energy of interaction between two
Δ	Association strength in the CPA EoS
ΔC_{pw}	Heat capacity difference between the empty hydrate lattice and liquid water,
ΔC_{pw}°	Reference heat capacity difference between the empty hydrate lattice and liquid water at 273.15 K
ΔH_{fus}	Molar enthalpy of fusion
Δh_w	Enthalpy difference between the empty hydrate lattice and ice / liquid water
Δh_w^0	Enthalpy difference between the empty hydrate lattice and ice at ice point and zero pressure
ΔT	Hydrate suppression/ Freezing point depression temperature
Δv_w	Molar volume difference between the empty hydrate lattice and ice / liquid water
$\Delta \mu_w$	Chemical potential difference between the empty hydrate lattice and ice / liquid water
$\Delta \mu_w^{\circ}$	Chemical potential difference between the empty hydrate lattice and ice at ice point and zero pressure
$\Delta \mu_w^{\beta-H}$	Chemical potential difference of water between the empty hydrate lattice and the hydrate phase
$\Delta \mu_w^{\beta-I/L}$	Chemical potential difference of water between the empty hydrate lattice and the ice/liquid water phase
Ω	Parameter in the EoS
α	Kihara hard-core radius
β	Association volume in the CPA EoS
$\alpha(T_r)$	Temperature dependent function of EoS
k	Interaction volume in the potential energy

ε	Association energy in the CPA EoS (bar L mol-1)/ Well depth in the potential energy
ϕ	Fugacity coefficient/ reduced temperature in ice vapour pressure model/ Contact angle
γ	Activity coefficient/ Contribution of the electrostatic term in salt model
η	Salt-free mixture dielectric constant
μ	Chemical potential
π	Number of phases
ρ	Density
σ	Collision diameter/ Average deviation between experimental runs
σ^*	$\sigma^* = \sigma - 2\alpha$
ω	Acentric factor

Superscript

DH	Debye-Hückel electrostatic term
HC	Hydrocarbon
EL	Electrostatic term
H	Hydrate
I	Ice
L	Liquid
Sat	Property at saturation
T	Total
V	Vapour
β	Empty hydrate lattice
∞	Infinite dilution
0	Reference property
simp.	Simplified version of the radial distribution function in the CPA EoS

Subscripts

HC	Hydrocarbon compound
EL	*Debye-Hückel* electrostatic contribution
I	Ice
SRK	SRK EoS
association	association part of the CPA EoS

assoc.	association part of the CPA EoS
c	Capillary term
exp	Experimental property
hydrate	Hydrate
ice	Ice
Non-Electrolyte	Non-electrolyte term
pred	Predicted property
ref	reference
salt	Salt
g	Gas
i, j	Molecular species
m	Type *m* of cavities/ Salt-free mixture
r	Reduced properties
s	Salt/ Second
w	Water
0	Reference property/ Symbol of freezing point of pure water (273.15 K)

CHAPTER 1 – INTRODUCTION

The past decade has witnessed dramatic changes in the oil and gas industry with the advent of deepwater exploration and production. A major challenge in deepwater field development is to ensure unimpeded flow of hydrocarbons to the host platform or processing facilities. Managing solids such as hydrate, waxes, asphaltene and scale is the key to the viability of developing any deepwater prospect. Hydrate formation could be a serious threat to safe and economical operation of production facilities. One of the problems, other than blockage, is the movement of the hydrate plugs in the pipeline at high velocity, which can cause rupture in the pipeline.

Current methods for avoiding gas hydrate problems are generally based on one or a combination of the following three techniques: (1) injection of thermodynamic inhibitors (e.g. methanol, ethanol, monoethylene glycol) to prevent hydrate formation, (2) use of kinetic hydrate inhibitors (KHIs) to sufficiently delay hydrate nucleation/growth, and (3) maintaining pipeline operating conditions outside the hydrate stability zone by removing one of the elements required for hydrate formation. For example, thermal insulation and/or active heating are used to remove the low temperature element. Water can be removed by dehydration of the natural gas using a glycol system, and from a theoretical viewpoint lowering the operating pressure can reduce the tendency for hydrate to form in the production system (though its use is limited to hydrate blockage removal).

Currently the most common flow assurance strategy is to rely upon injection of organic inhibitors (e.g. methanol, monoethylene glycol) and in order to inhibit hydrate formation at deepwater exploration and production; the concentrations required are likely to be relatively high. Current industry practice for hydrate prevention is injecting hydrate inhibitors at the upstream end of pipelines based on the calculated/measured hydrate phase boundary, water cut, worst pressure and temperature conditions, and the amount of inhibitor lost to non-aqueous phases. Accurate knowledge of hydrate phase equilibrium in the presence of inhibitors is therefore crucial to avoid gas hydrate formation problems and to design/optimize production, transportation and processing facilities.

Based on the fact that there is limited information available on the hydrate stability zone and inhibitor loss in such systems, high safety margins and inhibitor injection rates are used by industry to ensure adequate protection against gas hydrate formation. Therefore, it is necessary to generate reliable experimental data on the effect of high concentrations of inhibitors on the hydrate stability zone as well as developing reliable predictive technique for such systems.

In this work, new experimental measurements of the locus of incipient hydrate-liquid water-vapour (H–L_W–V) curve for systems containing methane or natural gases in the presence of aqueous solution of methanol, ethanol, monoethylene glycol and salt(s) over a wide range of concentrations, pressures and temperatures are generated and presented. Furthermore, new experimental data on the freezing point depressions of water (S-L_W) in the presence of various concentrations of the noted components have been generated and presented in this thesis. The experimental procedure used in this work, and the generated experimental data have been outlined in Chapter 2, in addition to a list of the experimental data extracted form the literature.

There has always been industrial interest in improving the reliability of the models to predict phase behaviour of gas hydrate systems, especially for systems containing both organic inhibitors and electrolytes, the so-called mixed inhibitor systems. In practice, the aqueous phase in which inhibitors are added, in many cases, already contains electrolytes from either well completion fluids or from formation water. In such mixed inhibitor systems, both co-solvents and strong electrolytes are present in the aqueous phase, making the thermodynamics modelling of these highly non-ideal systems difficult. In this thesis, a comprehensive phase behaviour modelling of water – hydrocarbons systems in the presence of salt(s) and/or organic inhibitor(s) with or without gas hydrates along with practical industrial applications (in particular flow assurance) in petroleum production and transportation have been addressed. The study involves a combination of laboratory experiments and thermodynamic modelling of the above systems.

A rigorous thermodynamic model based on the equality of fugacities of each component throughout all phases is developed to model the phase equilibria. For systems containing a component(s), which can form hydrogen bond (e.g., water, methanol, etc), the Cubic-Plus-Association equation of state (CPA-EoS) (Kontogeorgis et al., 2006) has

been employed. The binary interaction parameters (BIPs) between components have been tuned using reliable experimental data, from both open literature and this work. The CPA-EoS has been extended to predict fluid phase equilibria in the presence of single or mixed electrolyte solutions over a wide range of operational conditions. The hydrate-forming conditions are modelled by the solid solution theory of van der Waals and Platteeuw (1959). Langmuir constants have been calculated using the Kihara potential model (Kihara, 1953). In Chapter 3, a detail description of the approach has been outlined.

Chapters 4 presents the validation of the model by comparing the predictions with the data generated in this laboratory as well as the most reliable data from the open literature for binary systems of water, hydrocarbons, hydrate inhibitor and salts (self association and cross association systems) with no hydrate presence. The hydrate inhibition effect of organic hydrate inhibitors and salts has been studied in Chapter 5. A large number of experimental methane and natural gas hydrate data covering a wide range of salt(s) and inhibitors (methanol and monoethylene glycol) concentrations, temperature and pressure conditions, have been used in the validation of developed model (as detailed in Chapter 5).

In Chapter 6, the thermodynamic model is applied to study *n*-propanol and ethanol to confirm whether *n*-propanol and ethanol, like *i*-propanol, form mixed hydrates with small help gases at elevated pressures. Freezing point data of *n*-propanol and ethanol solutions suggest existence of a peritectic point and formation of clathrate hydrate in the *n*-propanol/ethanol-water system. Hydrate dissociation conditions for aqueous solution of different concentration of *n*-propanol and ethanol in the presence of methane and natural gas up to high pressures were measured or gathered from open literature. The results show that *n*-propanol and ethanol do not display the same level of hydrate inhibition effect, which would be expected from them and may, in fact, take part in clathrate formation. *n*-propanol and ethanol have been modelled as hydrate-forming compounds using the extended thermodynamic model which has been outlined in Chapter 6.

Besides the flow assurance aspects in the petroleum industry, naturally occurring gas hydrates are also of great significance considering their potential as a strategic energy reserve and the possibilities for CO_2 disposal by sequestration. Methane gas hydrates

have been widely touted as a potential new source of energy as very large quantities of methane hydrates occur naturally in sediments. Although, the knowledge of the occurrence of in-situ gas hydrate is very incomplete, and is obtained from both indirect and direct evidence, methane hydrate deposits worldwide in permafrost regions and subsea sediments off continental margins is estimated to be two orders of magnitude greater than recoverable conventional gas resources (Sloan, 1998). In summary, important issues driving research include the potential for methane hydrates as a strategic energy resource, increasing awareness of the relationship between hydrates and seafloor slope stability, the potential hazard hydrates pose to deepwater drilling, installations, pipelines and subsea cables, and long-term considerations with respect to hydrate stability, methane (a potent greenhouse gas) release, and global climate change.

Methane hydrate has been found to form in various rocks or sediments given suitable pressures, temperatures, and supplies of water and methane, however, natural subsurface environments exhibit significant variations in formation water chemistry and pore diameter, and these changes create local shifts in the phase boundary. As one step towards a better understanding of the occurrence of gas hydrate in nature, the effects of salts and capillary pressure in porous media on phase equilibria as well as the boundary of hydrate formation must be known. The detail description of the hydrate phase equilibria modelling in porous media and the effect of capillary pressure and inhibition effect of salt in formation water has been addressed in Chapter 3. The ability of the model for predicting hydrate dissociation conditions in porous media in the presence of salt and alcohol has been investigated in Chapter 6.

It is worth noting that, the results of this study have been implemented in the latest version of the Heriot-Watt University Hydrate Programme, HWHYD 2.1 (released in June 2009 and commercialised by HYDRAFACT Ltd., a Heriot-Watt spin-out company). HWHYD is currently used by a large number of major oil, gas and service companies. The software thermodynamic core consists of a general user interface and a DELPHI processing code, which has been written in DELPHI 2006 as part of this work.

The conclusions of this thesis and recommendations for future work are presented in Chapter 7.

References

Kihara T., 1953, *Virial coefficient and models of molecules in gases*, Rev. Modern Phys., **25**(4), 831– 843

Kontogeorgis G.M., Michelsen M.L., Folas G.K., Derawi S., von Solms N., Stenby E.H., 2006, *Ten years with the CPA (Cubic-Plus-Association) equation of state. Part 2. cross-associating and multicomponent systems*, Ind. Eng. Chem. Res., **45**, 4855-4868

Sloan E.D., 1998, *Clathrate hydrates of natural gases*, Marcel Dekker Inc., New York

Van der Waals J.H., Platteeuw J.C., 1959, *Clathrate solutions*, Adv. Chem. Phys., **2**, 1-57

CHAPTER 2 – EXPERIMENTAL STUDY

2.1 Introduction

Clathrate hydrates belong to the class of clathrates formed through combination of water and suitably sized 'guest' molecules under low temperature and elevated pressure conditions. Within the clathrate lattice, water molecules form a network of hydrogen-bonded cage-like structures that enclose the 'guest' molecules - the latter comprising of single or mixed low-molecular diameter gases (e.g. methane, ethane and etc) and organic compounds (Sloan, 1998). The stability of the clathrate hydrates, which have an ice-like appearance, is so substantial that they can exist at temperatures appreciably higher than triple point of H_2O (T_0= 273.16 K). Gas hydrates could form in numerous hydrocarbon production and processing operations, causing serious operational and safety concerns, therefore making it essential to gain a better understanding of the behaviour of gas hydrates.

Although there is an obvious pressing requirement to study and understand gas hydrates, the existing experimental data are relatively limited especially for the real petroleum reservoir fluids. In addition to the scarcity of accurate and reliable hydrate dissociation point data, most of the existing experimental gas hydrate data are limited to low to medium pressure conditions. This is partly due to a lack of interest/application at high pressure conditions and also due to practical difficulties when conducting such measurements. However, production from deepwater reservoirs, and the need for long tiebacks, necessitates hydrate prevention at high pressure conditions. With the increasing number of deep offshore drilling operations, it is necessary to determine the hydrate phase boundary in drilling and/or hydraulic fluids at high pressure conditions. Extreme conditions encountered at these depths may require changes in the drilling and hydraulic fluids formulations, and oilfield chemicals to ensure hydrate formation is not an issue. Furthermore, the limited data that are available in the literature are scattered and show some discrepancies, highlighting the need for reliable measurements (Matthews et al., 2002).

In this work, hydrate dissociation point measurements were conducted using the isochoric step-heating method, which had been previously demonstrated as being considerably more reliable and repeatable than conventional continuous heating and/or visual techniques (Tohidi et al., 2000). A detailed description of the apparatus and test

procedure is detailed in the high pressure experimental section (Section 2.2.4). In this work, the hydrate dissociation point were determined for systems containing methane or natural gases in the presence of aqueous solution of methanol, ethanol, monoethylene glycol and salt(s) over a wide range of concentrations, from medium to high pressure. These data were used as independent data in the development and validation (using independent data) of the predictive techniques, presented in Chapter 3.

In addition to the hydrate formation data, freezing point depression of six single electrolyte aqueous solutions (H_2O-NaCl, H_2O-$CaCl_2$, H_2O-$MgCl_2$, H_2O-KOH, H_2O-$ZnCl_2$ and H_2O-$ZnBr_2$), four binary aqueous electrolyte solutions (H_2O-NaC1-KCl, H_2O-NaC1-$CaCl_2$, H_2O-KC1-$CaCl_2$, and H_2O-NaC1-$MgCl_2$) and aqueous solution of ethylene glycol or methanol and salts at atmospheric pressure were made using an apparatus and method developed at Heriot-Watt University (Anderson et al., 2003). A detailed description of the apparatus and test procedure is outlined in the atmospheric experimental section (Section 2.2.3) of this chapter. For each system, freezing points were measured at least 5 times to check the repeatability and consistency. The final freezing point of the aqueous solution is taken as the average of all the runs. These data have been used as independent data for the validation of the presented model.

In addition to the experimental data generated here, an extensive literature survey was conducted to gather experimental data on systems containing hydrocarbon(s), water, organic inhibitor(s) and salt(s). The available data from the literature used for tuning the binary interaction parameters were gathered and presented in this chapter. The purpose of the binary interaction parameters is to enhance the ability of an equation of state to predict the observed phase behaviour. More details on tuning of the binary interaction parameters are presented in Chapter 4.

2.2 Experimental Equipments and Procedures

2.2.1 *Materials*

Aqueous solutions of different salt(s) and organic inhibitor(s) used in this work were prepared gravimetrically in this laboratory. All the salts used were of analytical reagent grade and with reported purities of >99% for anhydrous NaCl and KCl (Aldrich) and >98% for anhydrous $ZnCl_2$ and $ZnBr_2$ (Aldrich). Dihydrate $CaCl_2$ (Aldrich), hexahydrate $MgCl_2$ (Aldrich) with reported purities of >98% and 45 mass% KOH solution in water (Sigma-Aldrich) were also used without further purification. Methanol and monoethylene glycols used in the experiments were 99.5%+ pure, supplied by Sigma-Aldrich. Ultra high purity grade methane gas (99.995% pure) supplied by BOC was used. The compositions of the natural gases, supplied by BOC, are given in Table 2.1. Solutions were prepared using deionized water throughout the experimental work.

Table 2.1 Composition of natural gases used in the tests reported in this work

Component	NG1 / Mole%	NG2 / Mole%	NG3 / Mole%	NG4 / Mole%	NG5 / Mole%
C_1	88.30	88.51	89.35	88.79	88.21
C_2	5.40	6.76	5.15	5.30	5.78
C_3	1.50	1.76	1.38	1.55	1.78
iC_4	0.20	0.21	0.17	0.17	0.19
nC_4	0.30	0.34	0.23	0.30	0.30
iC_5	0.10	0.08	0.07	0.07	0.06
nC_5	0.09	0.08	0.06	0.06	0.06
N_2	2.39	0.82	1.14	0.04	1.40
CO_2	1.72	1.44	2.45	2.04	2.15
Total	100.00	100.00	100.00	100.00	100.00

2.2.2 *Atmospheric Experimental Apparatus*

The apparatus is comprised of two cells each containing a platinum resistance temperature (PRT) probe (±0.1 K), surrounded by an aluminium sheath as shown in Figure 2.1, placed in a controlled temperature bath. One cell contains the aqueous electrolyte solution, while the second cell contains the bath fluid (as a reference fluid). The bath temperature can be ramped between different set points at a constant set rate.

The similarity of construction and the level of filling fluids ensure that the two probes have very similar thermal time constants, and will lag behind the bath temperature by nearly identical values, as long as there is no phase change. The temperature of each probe is measured during the ramp (either heating or cooling), by recording (with an appropriate interface board) the voltage generated across each PRT by a constant current generator. The resistance is sampled at pre-determined intervals and digitally stored. The temperature probe was calibrated against a platinum resistance probe that has a certificate of calibration issued in accordance with NAMAS Accreditation Standard and NAMAS Regulations.

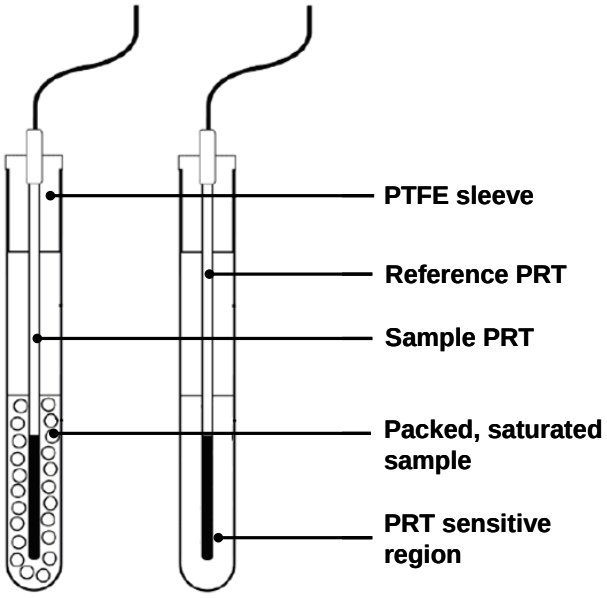

Figure 2.1 Schematic illustrations of the freezing point measurement apparatus

2.2.3. *Atmospheric Experimental Procedures*

The freezing point of a test solution is determined using an inflection point method. Initially the temperature of the test sample is reduced sufficiently to promote ice formation. This can be detected by a rise in sample temperature as the latent heat of formation is released. The temperature of the bath is then ramped up at a constant rate and the temperature of the bath, reference cell and the sample cells are recorded. The temperature of the sample will remain lower than the bath temperature as thermal energy is required to melt the ice. Once the last crystal of ice has melted the sample temperature will converge with the bath temperature. The point at which the bath and sample temperatures begin to converge can be easily identified and is taken as the freezing point of the sample or ice melting point (Figure 2.2). In fact in all experiments the melting point of ice in the presence of single or mixed aqueous electrolyte solutions is measured (i.e., correct thermodynamic equilibrium point) although this is commonly

reported as freezing point depression of the above aqueous solutions. For each system, the freezing points were measured 5 times to check the repeatability and consistency. The final freezing point of the aqueous solution is taken as the average of all the runs.

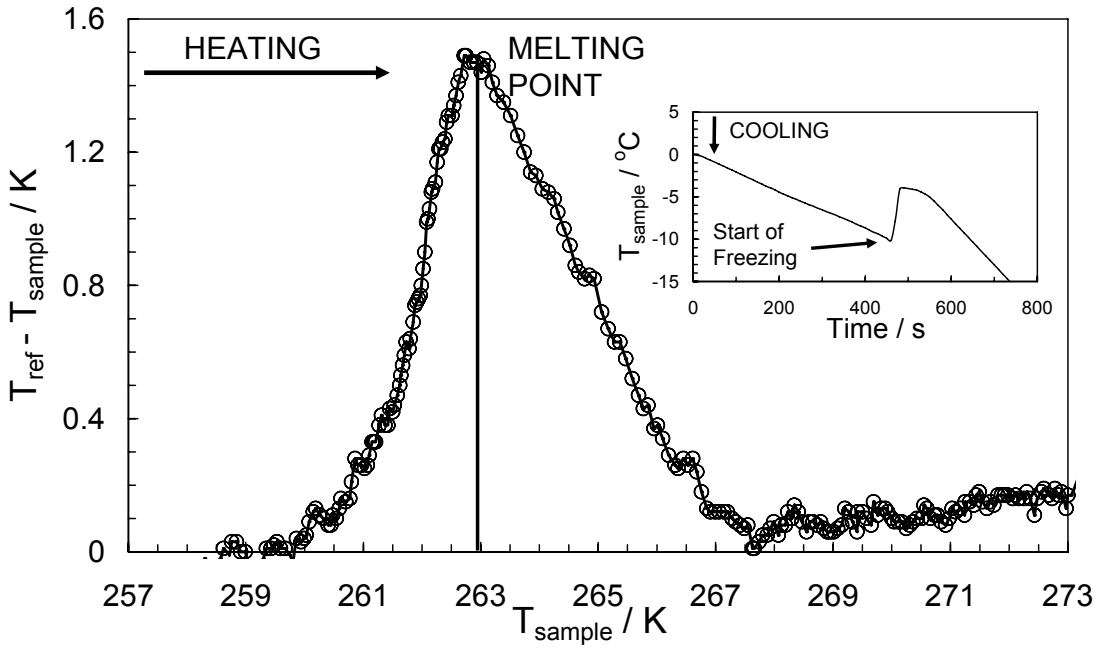

Figure 2.2 Illustration of a typical freezing point measurement.
Cooling: ice formation can be detected by a rise in sample temperature as the latent heat of formation is released. Heating: Once the last crystal of ice has melted the sample temperature converge with the bath temperature. The point at which the bath and sample temperatures begin to converge is taken as the freezing point of the sample or ice melting point

2.2.4 *High Pressure Experimental Apparatus*

Figure 2.3 shows the apparatus used to determine the phase equilibrium conditions. The phase equilibrium is achieved in a cylindrical cell made of stainless steel. The cell volume is about 500 ml and it can be operated up to 200 MPa between 233 K and 323 K. The equilibrium cell is held in a metallic jacket heated or cooled by a constant temperature liquid bath. The temperature of the cell is controlled by circulating coolant from a cryostat within the jacket surrounding the cell. The cryostat is capable of maintaining the cell temperature to within 0.1 K. To achieve good temperature stability, the jacket is insulated with polystyrene board and the pipes (which connect it to the cryostat) are covered with plastic foam. A platinum resistance probe monitors the temperature and is connected directly to a computer for direct acquisition. The pressure is measured by means of a strain gauge pressure transducer mounted directly on the cell and connected to the same data acquisition unit. This system allows real time readings and storage of temperatures and pressures throughout the different temperature cycles.

To achieve a fast thermodynamic equilibrium and to provide a good mixing of the fluids, a stirrer with a magnetic motor was used to agitate the test fluids.

The temperature probe was calibrated against a platinum resistance probe that has a certificate of calibration issued in accordance with NAMAS Accreditation Standard and NAMAS Regulations. The pressure transducer was checked for accuracy using a Budenberg dead weight tester up to a pressure of 80 MPa.

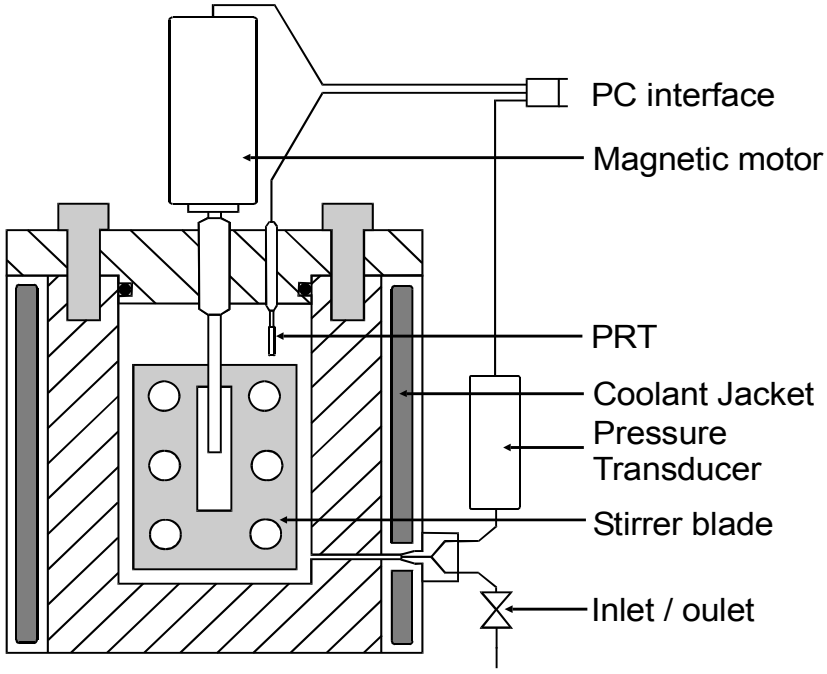

Figure 2.3 Schematic illustration of the experimental set-up

2.2.5 *High Pressure Experimental Procedures*

Prior to the tests the equilibrium cell was cleaned and evacuated. The aqueous solution of different salt(s) and/or organic inhibitor(s) was loaded into the cell and then gas was injected into the cell to achieve the desired starting pressure. Once the cell had been charged with the desired components the mixer was switched on and the temperature lowered to form hydrates, their presence being confirmed by pressure drop. The hydrate formation caused a rapid decline in the cell pressure as gas molecules were consumed during the process. The temperature was then increased stepwise, slowly enough to allow equilibrium to be achieved at each temperature step. At temperatures below the point of complete dissociation, gas is released from decomposing hydrates, giving a marked rise in the cell pressure with each temperature step (Figure 2.4). However, once the cell temperature has passed the final hydrate dissociation point, and all clathrates have disappeared from the system, a further rise in the temperature will

result only in a relatively small pressure rise due to thermal expansion. This process results in two traces with very different slopes on a pressure versus temperature (P/T) plot; one before and one after the dissociation point. The point where these two traces intersect (i.e., an abrupt change in the slope of the P/T plot) is taken as the dissociation point (see Figure 2.4). The procedure was repeated at different pressures in order to determine the hydrate phase boundaries over a wide temperature range. In this work, methane and natural gas hydrate dissociation points were measured in the presence of aqueous solutions containing different concentrations of organic inhibitor(s) and/or sat(s).

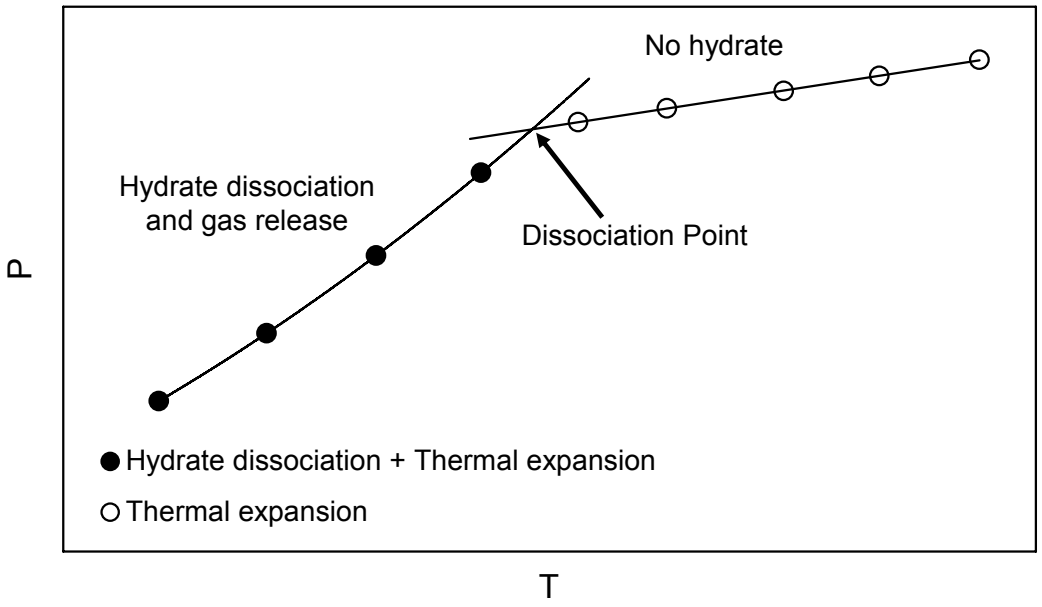

Figure 2.4 Dissociation point determination from equilibrium step-heating data. The equilibrium dissociation point is determined as being the intersection between the hydrate dissociation (pressure increase as a result of gas release due to temperature increase and hydrate dissociation, as well as thermal expansion) and the linear thermal expansion (no hydrate) curves

2.3 Experimental Results

2.3.1 *Freezing Point Measurements*

Freezing point measurements were carried out for aqueous solutions of NaCl, $CaCl_2$, $MgCl_2$, $ZnCl_2$ and $ZnBr_2$. The experimental data is presented in Table 2.2. Included in the Table is the average deviation between 5 runs for each aqueous solution.

Table 2.2 Freezing point depression (ΔT) of aqueous single electrolyte solutions (Haghighi et al., 2008)

	mass% of salt	ΔT_{exp} (±0.1 K)	σ_{exp}^{*} / K
NaCl	1.00	0.6	0.0
	5.00	3.0	0.2
	10.00	6.8	0.3
	15.00	11.0	0.0
	18.00	14.3	0.1
$CaCl_2$	4.70	2.5	0.1
	9.40	5.5	0.0
	14.10	10.2	0.1
	18.80	16.5	0.2
	23.50	25.9	0.1
$MgCl_2$	2.00	1.1	0.1
	5.00	3.1	0.1
	9.00	6.8	0.1
	12.00	10.7	0.1
	15.00	15.6	0.1

	mass% of salt	ΔT_{exp} (±0.1 K)	σ_{exp}^{*} / K
$ZnCl_2$	5.00	2.1	0.1
	10.00	4.6	0.0
	20.00	9.3	0.2
	30.00	17.6	0.0
$ZnBr_2$	5.00	1.2	0.1
	10.00	2.8	0.1
	20.00	7.3	0.2
	30.00	12.8	0.0
	45.00	25.1	0.2
KOH	1.00	0.7	0.0
	5.00	3.7	0.0
	10.00	8.5	0.2
	25.00	38.5	0.1

$^{*}\sigma_{exp}$: Average deviation between runs ($\sigma_{exp} = \frac{\sum \left| \Delta T_{exp} - \Delta T_{exp,i} \right|}{NP}$, where ΔT_{exp} is the mean value between the experimental data, $\Delta T_{exp,i}$ is the value of individual measured freezing point depression in each runs and NP is the number of measurements)

Experimental and calculated freeing point depression for four mixed electrolyte solutions (H_2O-NaC1-KCl, H_2O-NaC1-$CaCl_2$, H_2O-KC1-$CaCl_2$, and H_2O-NaC1-$MgCl_2$) measured by the above technique are presented in Table 2.3, including the average deviation between 5 runs for each aqueous solution. In addition to this, freezing points were obtained for solutions containing methanol, ethylene glycol, sodium chloride, calcium chloride and potassium chloride at different concentrations. The compositions of the solutions used in the experiments are shown in Table 2.4.

Table 2.3 Freezing point depression (ΔT) of aqueous solutions of mixed electrolyte solutions (Haghighi et al., 2008)

NaCl and 3 mass% $CaCl_2$			$CaCl_2$ and 3 mass% KCl		
mass% of NaCl in aqueous solution	ΔT_{exp} (±0.1 K)	σ_{exp}^{*} / K	mass% of $CaCl_2$ in aqueous solution	ΔT_{exp} (±0.1 K)	σ_{exp}^{*} / K
1.00	2.1	0.1	5.00	4.6	0.2
5.00	5.4	0.4	10.00	8.7	0.3
10.00	10.0	0.5	15.00	15.4	0.6
15.00	14.8	0.5	20.00	23.4	0.6
18.00	20.7	0.4	25.00	33.7	0.3

NaCl and 3 mass% KCl			$MgCl_2$ and 3 mass% NaCl		
mass% of NaCl in aqueous solution	ΔT_{exp} (±0.1 K)	σ_{exp}^{*} / K	mass% of $MgCl_2$ in aqueous solution	ΔT_{exp} (±0.1 K)	σ_{exp}^{*} / K
1.00	2.0	0.1	1.00	2.8	0.2
2.00	2.8	0.1	2.00	3.6	0.2
5.00	5.1	0.2	5.00	6.2	0.5
10.00	8.9	0.1	10.00	12.4	0.5
12.00	10.7	0.0	15.00	21.0	0.3

$^{*}\sigma_{exp}$: Average deviation between runs ($\sigma_{exp} = \frac{\sum |\Delta T_{exp} - \Delta T_{exp,i}|}{NP}$, where ΔT_{exp} is the mean value between the experimental data, $\Delta T_{exp,i}$ is the value of individual measured freezing point depression in each runs and NP is the number of measurements)

Table 2.4 Compositions of aqueous solutions (Najibi et al., 2008 and this work)

Solutions	Methanol (mass%)*	Monoethylene glycol (mass%)	NaCl (mass%)	KCl (mass%)	$CaCl_2$ (mass%)
Na8Me9	9.20		8.31		
Na3Me30	30.00		3.00		
Na3EG30		30.01	3.02		
Na5EG30		30.00	5.01		
K7Me9	9.01			7.01	
Ca8EG12		12.00			8.00
Ca10Me14	14.00		8.30		10.02

**All mass% on water basis.*

The freezing points of the aqueous solutions, defined in Table 2.4, have been reported in Table 2.5 along with the average deviation between 3 runs for each aqueous solution.

Table 2.5 Experimental ice melting point temperatures in aqueous solutions defined in Table 2.4 (Najibi et al., 2008)

Solutions	ΔT_{exp} (±0.1 K)	σ_{exp}^{*} / K
Na8Me9	14.7	0.1
Na3Me30	30.6	0.2
Na3EG30	18.6	0.1
K7Me9	10.7	0.2
Ca8EG12	10.1	0.2
Ca10Me14	20.55	0.2

$^{*}\sigma_{exp}$: Average deviation between runs ($\sigma_{exp} = \frac{\sum \left| \Delta T_{exp} - \Delta T_{exp,i} \right|}{NP}$, where ΔT_{exp} is the mean value between the experimental data, $\Delta T_{exp,i}$ is the value of individual measured freezing point depression in each runs and NP is the number of measurements)

2.3.2 *Methane Hydrate Dissociation Point Measurements*

In this thesis, an extensive number of experimental dissociation points have been measured for hydrates formed from methane in the presence of aqueous solutions of methanol, ethylene glycol and/or salt(s) in a wide range of concentrations. The data points were measured at pressures of up to 66 MPa thereby covering the range of interest for these systems. The new experimental data measured in this work have been presented in Table 2.6 through 2.9 below. Table 2.6 summarizes the experimental results for methane hydrate formation conditions in the presence of aqueous single electrolyte solutions. The results for methane hydrates in the presence of methanol (between 10 to 60 mass%) and monoethylene glycol (between 10 to 50 mass%) are presented in Table 2.7 and 2.8, respectively.

Additionally, hydrate equilibrium measurements were conducted for methane in equilibrium with solutions containing methanol, ethylene glycol, sodium chloride, calcium chloride and potassium chloride at different concentrations for a pressure range of 6.89 MPa to 29 MPa. The compositions of the solutions used in the experiments have been outlined in Table 2.4. The measured equilibrium hydrate dissociation conditions are presented in Table 2.9.

Table 2.6 Methane hydrate dissociation points in the presence of aqueous single electrolyte solutions (Haghighi et al., 2009c)

15.00 mass% NaCl	
T / K (±0.1)	P / MPa (±0.008)
269.4	3.93
282.2	17.81
285.1	26.50

20.00 mass% NaCl	
T / K (±0.1)	P / MPa (±0.008)
268.5	5.02
274.9	10.31
277.2	15.38

15.00 mass% KCl	
T / K (±0.1)	P / MPa (±0.008)
276.4	6.24
281.1	10.89
284.9	17.28

10.00 mass% $MgCl_2$	
T / K (±0.1)	P / MPa (±0.008)
274.3	4.32
280.9	10.27
284.0	15.00
287.4	24.78

Table 2.7 Experimental methane hydrate dissociation conditions in the presence of methanol aqueous solutions (Haghighi et al., 2009a)

Methanol		T / K	P / MPa
Mass %	Mol. %	(±0.1)	(±0.008)
10.00	5.88	274.2	4.378
		278.7	7.019
		282.7	10.963
		284.2	13.079
		287.0	19.305
20.00	12.32	266.3	3.516
		273.6	6.915
		278.4	13.190
		281.7	19.650
30.00	19.41	261.1	3.985
		267.3	7.584
		273.0	14.479
		274.7	18.705
40.00	27.26	249.4	2.654
		263.8	11.411
		267.8	19.712
		271.1	33.819
50.00	35.98	251.4	6.819
		241.8	2.592
		257.0	13.555
		259.7	21.070
60.00	45.74	239.4	4.716
		244.3	8.577
		248.4	15.734
		253.1	33.922

Table 2.8 Experimental methane hydrate dissociation conditions in the presence of monoethylene glycol aqueous solutions (Haghighi et al., 2009b and this work)

Monoethylene Glycol		T / K	P / MPa
Mass %	Mol. %	(±0.1)	(±0.008)
10.00	3.12	279.4	6.379
		288.2	17.600
		293.9	37.448
20.00	6.76	277.7	7.159
		284.9	17.779
		289.2	29.917
30.00	11.06	273.3	6.862
		281.1	18.586
		284.8	31.690
		290.1	57.707
40.00	16.21	264.9	5.055
		274.1	15.255
		277.0	23.166
		279.0	31.386
		285.0	65.843
50.00	22.49	265.3	12.621
		269.6	21.724
		270.8	28.073
		271.5	30.910
		276.7	64.723

Table 2.9 Experimental methane hydrate dissociation conditions in the presence of the aqueous solutions defined in Table 2.4 (Najibi et al., 2008)

Na3Me30	
T / K (±0.1)	P / MPa (±0.008)
269.3	13.990
272.8	21.015
274.35	25.642

Na3EG30	
T / K (±0.1)	P / MPa (±0.008)
271.8	7.667
277.1	15.237
279.4	20.298

Ca8EG12	
T / K (±0.1)	P / MPa (±0.008)
271.5	4.268
276.4	6.998
283.5	18.657

K7Me9	
T / K (±0.1)	P / MPa (±0.008)
275.9	7.446
282.4	17.258
286.3	28.889

Ca10Me14	
T / K (±0.1)	P / MPa (±0.008)
274.0	11.859
277.5	17.581
280.3	26.076

Na8Me9	
T / K (±0.1)	P / MPa (±0.008)
273.8	7.826
278.7	13.555
283.4	26.338

It is worth noting; the available experimental data have been collected from the literature to compare with the data generated in this work. None of the experimental data generated in this laboratory have been used in the optimization process, thus providing independent data for validation of the model in Chapters 4 and 5.

2.3.3 *Natural Gas Hydrate Dissociation Point Measurements*

In this work in addition to the data generated for methane hydrate, new experimental measurements of the locus of incipient hydrate-liquid water-vapour (H–L_W–V) curve for systems containing natural gases with aqueous solution of methanol, ethanol, monoethylene glycol and/or salt(s) over a wide range of concentrations, pressures and temperatures were measured and are presented in Tables 2.10 through 2.14. The compositions of the natural gases, used in this work, have been given in Table 2.1 previously. Table 2.10 summarizes the experimental results for natural gas hydrate formation condition in the presence of aqueous single electrolyte solutions and the results in the presence of methanol, ethanol and monoethylene glycol (between 10 to 70 mass%) are presented in Tables 2.11 and 2.13, respectively.

For further investigation, hydrate equilibrium conditions were obtained for natural gas in solutions containing methanol, ethylene glycol, and salt(s) at different concentrations for a pressure range of 3.5 MPa to 20.5 MPa. The compositions of the solutions used in the experiments have been outlined in Table 2.4. The measured equilibrium hydrate dissociation conditions are presented in Table 2.14.

Table 2.10 Natural gas hydrate dissociation points in the presence of aqueous single electrolyte solutions (this work)

10.00 mass% KCl		10.00 mass% $MgCl_2$	
T / K (±0.1)	P / MPa (±0.008)	T / K (±0.1)	P / MPa (±0.008)
278.9	3.282	277.8	3.307
284.0	6.440	282.6	6.832
286.4	10.392	285.8	10.320
290.2	20.247	288.9	20.912

Table 2.11 Experimental natural gas hydrate dissociation conditions in the presence of methanol aqueous solutions (Haghighi et al., 2009a and this work)

Methanol		T / K	P / MPa	NG type
Mass %	Mol. %	(±0.1)	(±0.008)	
10.00	5.88	280.7	3.806	NG1
		285.9	7.032	
		287.6	10.342	
		290.2	16.651	
20.00	12.32	276.2	3.633	NG1
		280.4	6.164	
		287.2	23.379	
30.00	19.41	266.6	2.392	NG1
		273.4	5.757	
		279.0	18.657	
		282.7	37.473	
40.00	27.26	260.0	2.516	NG1
		264.7	3.868	
		269.4	8.363	
		272.9	20.229	
		275.5	36.066	
50.00	35.98	256.1	3.068	NG2
		259.4	4.723	
		263.2	9.928	
		263.9	13.396	
		265.3	20.201	
		268.2	35.315	
		267.8	34.129	NG4
		272.8	61.467	NG4
60.00	45.74	242.5	2.010	NG3
		249.1	4.140	
		253.4	8.050	
		254.7	14.600	
		256.5	21.031	
		257.5	28.052	
		258.9	36.341	
70.00	56.74	240.4	6.131	NG3
		242.6	16.232	
		244.9	24.622	
		245.7	33.023	

Table 2.12 Experimental natural gas hydrate dissociation conditions in the presence of ethanol aqueous solutions (this work)

Ethanol		T / K	P / MPa	NG type
Mass %	Mol. %	(±0.1)	(±0.008)	
38.00	19.40	271.1	3.890	NG1
		278.6	9.442	
		282.8	20.623	
		286.5	36.831	
49.00	27.30	267.0	3.332	NG1
		277.1	11.182	
		280.7	22.331	
		283.0	33.983	

Table 2.13 Experimental natural gas hydrate dissociation conditions in the presence of monoethylene glycol aqueous solutions (Haghighi et al., 2009b and this work)

Monoethylene glycol		T / K	P / MPa	NG type
Mass %	Mol. %	(±0.1)	(±0.008)	
10.00	3.12	280.2	2.780	NG1
		289.7	10.631	
		292.7	20.261	
20.00	6.76	278.7	3.192	NG1
		286.3	10.433	
		289.4	19.991	
30.00	11.06	276.5	4.002	NG1
		282.6	10.451	
		285.3	19.591	
		287.4	29.823	
		293.0	69.522	NG4
40.00	16.21	283.4	36.562	NG1
		277.5	12.001	
		270.6	3.521	
		281.1	24.554	
		288.3	72.122	NG4
50.00	22.49	258.8	1.851	NG1
		267.8	5.522	
		272.4	14.963	
		273.9	27.792	
		275.1	35.761	
		280.6	68.731	NG4
60.00	30.33	254.9	2.942	NG1
		260.9	7.952	
		262.4	17.534	
		266.3	36.542	
		270.0	55.631	NG3
70.00	40.37	246.5	5.071	NG3
		247.9	7.973	
		248.2	13.602	
		249.4	23.791	
		251.7	37.3620	
		252.6	45.364	
		254.4	63.872	

Table 2.14 Experimental natural gas hydrate dissociation conditions in the presence of the aqueous solutions defined in Table 2.4 (this work)

Na5EG30	
T / K (±0.1)	P / MPa (±0.008)
272.6	3.520
276.3	6.866
279.8	11.952
282.0	20.510

It should be noted that these data could be regarded as independent as hydrate dissociation data were not used in the development and optimisation of the thermodynamic model in Chapters 4 and 5.

2.4 Review of Available Experimental Data

Knowledge of phase diagram and fluid properties is fundamental in petroleum and chemical engineering. It is necessary to have the most accurate tool to predict these properties. Use of a cubic equation of state in thermodynamic models requires appropriate values of empirical parameters, called Binary Interaction Parameters (BIP), in the equation of state. Correct values of binary interaction parameters between components are essential for an equation of state to predict the correct phase behaviour of the fluid. The VLE (vapour-liquid equilibrium), LLE (liquid-liquid equilibrium) and SLE (solid-liquid equilibrium) data are necessary for tuning of the binary interaction parameters between components.

An extensive literature survey has been performed and the available experimental data (vapour-liquid, liquid-liquid and solid-liquid data for the binary systems) have been collected from the literature and the original sources of experimental data are presented in this section. The reliability of these data has been evaluated by comparing the experimental data to check the consistency between them. The most reliable literature data were used in tuning the binary interaction parameters between various components.

2.4.1 *Binary Systems Containing Water*

The solubility of hydrocarbons (e.g. methane, ethane etc) in pure water and aqueous electrolyte solutions have been measured over a wide pressure and temperature range by many researchers. As methane is the main component in natural gas (normally more

than 87 mole%), there are many measurements on CH_4 solubility in water and water content in the gas phase. The ethane-water system has not been as widely examined as the methane-water system. Studies reporting intermediate and high-pressure solubility data are far more limited. Only a few researchers have conducted solubility experiments on this system (see Table 2.16). The same is observed for propane, n-butane, *i*-butane, *n*-pentane and *i*-pentane (see Tables 2.17 to 2.19). At atmospheric conditions, a large quantity of solubility data are available for nitrogen, hydrogen sulphide and carbon dioxide and limited data for intermediate and high pressure have been recently published (see Tables 2.20 to 2.22). The sources of the experimental data for binary mixture of each of the components and water used in this work are given in Tables 2.15 through 2.22. These data has been extracted and employed for tuning the binary interaction parameters used in equations of state.

Table 2.15 Vapour liquid data for methane – water binary systems

Reference	Type of Data	T / K	P / MPa	*N.pts*
Frolich et al. (1931)	*PTx*	298.15	3 – 12	6
Michels et al. (1936)	*PTx*	298.15 – 423.15	4.06 – 46.91	9
Culberson et al. (1950a)	*PTx*	298.15	3.62 – 66.74	8
Culberson and Mc Ketta (1951)	*PTxy*	298.15 – 444.26	2.23 – 68.91	73
Morrison and Billet (1952)	*PTx*	285.05-348.35	0.1 (atm)	11
Davis and McKetta (1960)	*PTx*	310.93 – 394.26	0.35 – 3.84	9
Duffy et al. (1961)	*PTx*	298.15 – 303.15	0.32 – 5.17	17
McAuliffe (1963)	*PTx*	298.15	0.1 (atm)	1
Pierotti (1965)	*PTx*	298.15	0.1 (atm)	1
O'Sullivan and Smith (1970)	*PTx*	324.65 – 398.15	10.13 – 61.61	17
Sultanov et al. (1971)	*PTxy*	423.15 – 633.15	4.90 – 107.87	127
Amirijafari and Campbell (1972)	*PTx*	310.93 – 344.26	4.13 – 34.46	8
Maharajh and Walkley (1973)	*PTx*	298.15	0.1 (atm)	1
Tokunaga and Kawai (1975)	*PTx*	293.15	0.1 (atm)	1
Sanchez and De Meer (1978)	*PTx*	423.15 – 573.15	10 – 250	10
Price (1979)	*PTx*	427.15 – 627.15	3.54 – 197.20	5
Stoessel and Byrne (1982)	*PTx*	298.15	2.41 – 5.17	8
Crovetto et al. (1982)	*PTx*	297.5 - 518.3	1.9 -6.4	7
Cramer (1984)	*PTx*	277.15 – 573.15	3 – 13.2	6
Yarym-Agaev et al. (1985)	*PTxy*	313.15 – 338.15	2.5 – 12.5	5
Yokoyama et al. (1988)	*PTxy*	298.15 – 323.15	3 – 8	6
Abdulgatov et al. (1993)	*PTx*	523.15 – 653.15	2 – 64	15
Wang et al. (1995)	*PTx*	283.15 – 298.15	1.15 – 5.18	21
Reichl (1996)	*PTx*	283.1 6 – 343.16	0.18 – 0.26	6
Lekvam and Bishnoi (1997)	*PTx*	274.19 – 285.68	0.57 – 9.08	18
Song et al. (1997)	*PTx*	273.15 – 288.15	3.45	1
Yang et al. (2001)	*PTx*	298.1 – 298.2	2.33 – 12.68	19
Servio and Englezos (2002)	*PTx*	278.65 – 284.35	3.5 – 6.5	5
Kim et al. (2003)	*PTx*	298.15	2.3 – 16.6	5
Wang et al. (2003)	*PTx*	283.2 – 303.2	2 – 40.03	17
Chapoy et al. (2004a)	*PTxy*	275.11 – 313.11	0.97 – 18.0	36

Table 2.16 Vapour liquid data for ethane – water binary systems

Reference	Type of Data	T / K	P / MPa	*N.pts*
Winkler (1901)	*PTx*	275.5-353.12	0.1 (atm)	5
Culberson and Mc Ketta (1950)	*PTx*	310.93 – 444.26	0.407 – 68.499	30
Culberson et al. (1950b)	*PTx*	310.93 – 444.26	0.407 – 8.377	71
Eucken and Hertzberg (1950)	*PTx*	273.15 -293.15	0.1 (atm)	2
Claussen and Polglase (1952)	*PTx*	274.7 -312.5	0.1 (atm)	6
Morrison and Billet (1952)	*PTx*	285.5 -345.6	0.1 (atm)	14
Czerski and Czaplinski (1962)	*PTx*	273.15	0.1 (atm)	1
McAuliffe (1963)	*PTx*	298.15	0.1 (atm)	1
Wetlaufer et al. (1964)	*PTx*	278.15-318.15	0.1 (atm)	3
Anthony and McKetta (1967)	*PTx*	344.3 – 377.65	3.48 – 28.170	5
Danneil et al. (1967)	*PTx*	473.15 – 673.15	20 – 370	6
Wen and Hung (1970)	*PTx*	278.15-308.15	0.1 (atm)	4
Ben-Naim et al. (1973)	*PTx*	278.15 -293.15	0.1 (atm)	5
Yaacobi and Ben-Naim (1973)	*PTx*	283.15 -303.15	0.1 (atm)	5
Yaacobi and Ben-Naim (1974)	*PTx*	283.15 -303.15	0.1 (atm)	5
Rudakov and Lutsyk (1979)	*PTx*	329.15-363.15	0.1 (atm)	2
Rettich et al. (1981)	*PTx*	275.4 -318.7	0.07- 0.1	23
Sparks and Sloan (1983)	*PTx*	283.17 – 343.16	3.477	6
Reichl (1996)	*PTx*	298.15	0.063 – 0.267	8
Kim et al. (2003)	*PTx*	283.2 – 303.2	1.4 – 3.9	9
Wang et al. (2003)	*PTx*	283.2 – 303.2	0.5 – 4	17
Mohammadi et al (2004)	*PTxy*	274.3 - 343.1	0.4-4.9	49

Table 2.17 Vapour liquid data for propane – water binary systems

Reference	Type of Data	T / K	P / MPa	*N.pts*
Morrison and Billet (1952)	*PTx*	285.45-347.25	0.1 (atm)	12
Claussen and Polglase (1952)	*PTx*	292.95-302.95	0.1 (atm)	2
Kobayashi and Katz (1953)	*PTx*	278.87-422.04	0.496-19.210	59
Umano and Nakano (1958)	*PTx*	273.15	0.01-0.1	25
Azarnoossh and McKetta (1958)	*PTx*	288.71-410.93	0.101-3.528	71
Namiot (1961)	*PTx*	273.15-283.15	0.1 (atm)	2
Wehe and McKetta (1961)	*PTx*	344.26	0.514-1.247	8
Wishnia (1963)	*PTx*	288.15-308.15	0.1 (atm)	5
Wetlaufer et al. (1964)	*PTx*	278.15-318.15	0.1 (atm)	3
Kresheck et al. (1965)	*PTx*	274.15-328.15	0.1 (atm)	26
Barone et al. (1966)	*PTx*	298.15	0.1 (atm)	1
McAuliffe (1966)	*PTx*	298.15	0.1 (atm)	1
Wen and Hung (1970)	*PTx*	278.15-308.15	0.1 (atm).	4
Yano et al. (1974)	*PTx*	298.15	0.1 (atm)	1
Sanchez and Coll (1978)	*PTx*	473.15-663.15	20-330	30
Rudakov and Lutsyk (1979)	*PTx*	298.15	0.1 (atm)	1
Sparks and Sloan (1983)	*PTx*	246.66-276.43	0.77	9
Cargill and MacPhee (1989)	*PTx*	277-327.8	0.1 (atm)	9
Jou et al. (2002)	*PTx*	313.15-343.15	1.7-5.5	5
Chapoy et al. (2004c)	*PTxy*	277.62-368.16	0.4-3.9	59

Table 2.18 Vapour liquid data for n-butane – water and i-butane – water binary systems

Reference	Type of Data	T / K	P / MPa	*N.pts*
n-Butane - Water				
Brooks et al. (1951)	*PTx*	310.93-377.59	7.3-69.4	15
Morrison and Billet (1952)	*PTx*	284.05-349.25	0.1 (atm)	14
Claussen and Polglase (1952)	*PTx*	292.95-302.95	0.1 (atm)	2
Reamer et al. (1952)	*PTx*	310.93-510.95	0.14-68.9	75
Umano and Nakano (1958)	*PTx*	273-293	0.1 (atm)	5
Namiot (1961)	*PTx*	283.15	0.1 (atm)	1
Wishnia (1963)	*PTx*	283.15-308.15	0.1 (atm)	6
Wetlaufer et al. (1964)	*PTx*	278.15-318.15	0.1 (atm)	3
Le Breton and McKetta (1964)	*PTx*	310.93-410.93	0.36-3.38	60
Kresheck et al. (1965)	*PTx*	274.15-349.25	0.1 (atm)	22
Barone et al. (1966)	*PTx*	298.15	0.1 (atm)	1
McAuliffe (1966)	*PTx*	298.15	0.1 (atm)	1
Danniel et al. (1967)	*PTx*	628.15	25.5-112.5	8
Wen and Hung (1970)	*PTx*	278.15-308.15	0.1 (atm)	4
Ben-Naim et al. (1973)	*PTx*	278.15-298.15	0.1 (atm)	5
Denton et al. (1973)	*PTx*	298.15	0.1 (atm)	1
Moudgil et al. (1974)	*PTx*	298.15	0.1 (atm)	1
Rice et al. (1976)	*PTx*	276.15-292.15	0.1 (atm)	5
Rudakov and Lutsyk (1979)	*PTx*	293.15-363.15	0.1 (atm)	2
Cargill and MacPhee (1989)	*PTx*	277.1-331.1	0.1 (atm)	10
i-Butane - Water				
Wetlaufer et al. (1964)	*PTx*	278.15-318.15	0.1 (atm)	3
McAuliffe (1966)	*PTx*	298.15	0.1 (atm)	1
Rudakov and Lutsyk (1979)	*PTx*	298.15	0.1 (atm)	1

Table 2.19 Vapour liquid data for n-pentane – water and i-pentane – water binary systems

Reference	Type of Data	T / K	P / MPa	*N.pts*
n-Pentane - Water				
Führer (1924)	*PTx*	298.15	0.1 (atm)	1
Namiot (1960)	*PTx*	293.15-344.55	3.2	3
Barone et al. (1966)	*PTx*	298.15	0.1 (atm)	1
McAuliffe (1966)	*PTx*	298.15	0.1 (atm)	1
Connolly (1966)	*PTx*	573.15-625	15.2-42.5	45
Nelson and de Ligny (1968)	*PTx*	277.15-303.15	0.1 (atm)	5
Pierotti and Liabastre (1972)	*PTx*	278.26-303.36	0.1 (atm)	4
Polak and Lu (1973)	*PTx*	273.15-298.15	0.1 (atm)	2
Korenman and Arefeva (1977)	*PTx*	293.15	0.1 (atm)	1
Krzyzanowska (1978)	*PTx*	298.15	0.1 (atm)	1
Rudakov and Lutsyk (1979)	*PTx*	298.15	0.1 (atm)	1
Price (1979)	*PTx*	298.15-422.65	0.1 (atm)	7
Jonsson (1982)	*PTx*	288.15-308.15	0.1 (atm)	5
Gillespie and Wilson (1982)	*PTx*	310.93-588.71	0.8-20.7	26
Jou and Mather (2000)	*PTx*	273.2-453.2	0.02-3.6	12
i- Pentane - Water				
McAuliffe (1966)	*PTx*	298.15	0.1 (atm)	1
Polak and Lu (1973)	*PTx*	273.15-298.15	0.1 (atm)	7
Price (1976)	*PTx*	298.15	0.1 (atm)	1
Krzyzanowska (1978)	*PTx*	298.15	0.1 (atm)	1

Table 2.20 Vapour liquid data for nitrogen – water binary system

Reference	Type of Data	T / K	P / MPa	*N.pts*
Winkler (1901)	*PTx*	273.23-353.15	0.1 (atm)	9
Fox (1909)	*PTx*	273.68-323.15	0.1 (atm)	24
Bohr (1910)	*PTx*	294.35	0.1 (atm)	1
Muller (1913)	*PTx*	289.35-290.35	0.1 (atm)	2
Adeney and Becker (1919)	*PTx*	276.7-308.3	0.1 (atm)	7
Goodman and Krase (1931)	*PTx*	273.15 - 442.15	10.13 - 30.39	12
Frolich et al. (1931)	*PTx*	298.15	2.027-19.252	8
Wiebe et al. (1932)	*PTx*	298.15	2.53 - 101.32	25
Saddington and Krase (1934)	*PTx*	323.15 - 513.15	10.13 - 30.398	11
Morrison and Billet (1952)	*PTx*	285.65-345.65	0.1 (atm)	12
Pray et al. (1952)	*PTx*	533.15 - 588.71	1.034 - 2.757	55
Clever et al. (1957)	*PTx*	298.15	0.1 (atm)	1
Smith et al. (1962)	*PTx*	303.15	1.103 - 5.895	5
Fahri et al. (1963)	*PTx*	276.25-310.2	0.1 (atm)	6
Klots and Benson (1963)	*PTx*	275.01-300.16	0.1 (atm)	5
Douglas (1964)	*PTx*	276.25-302.65	0.1 (atm)	33
O'Sullivan et al. (1966)	*PTx*	324.65	10.13 - 60.79	6
Murray et al. (1969)	*PTx*	273.73-303.86	0.1 (atm)	10
Maslennikova et al. (1971)	*PTy*	298.15 – 623.15	5.07 – 50.7	134
Maharajh and Walkey (1973)	*PTx*	298.15	0.1 (atm)	1
Wilcock and Battino (1974)	*PTx*	298.15	0.1 (atm)	2
Tokunaga (1975)	*PTx*	293.15 -313.15	0.1 (atm)	11
Cosgrove and Walkey (1981)	*PTx*	278.15-313.15	0.1 (atm)	8
Gillespie and Wilson (1982)	*PTx*	310.93 - 588.7	0.3-13.8	48
Japas and Frank (1985)	*PTxy*	480 - 658	15.5 - 270.5	54
Althaus (1999)	*PTy*	248.15 - 293.15	0.5 - 10	43
Purwanto et al. (2001)	*PTx*	277.15-281.15	0.1 (atm)	12
Chapoy et al. (2004d)	*PTxy*	274.2 - 363.0	0.1 (atm)	52

Table 2.21 Vapour liquid data for carbon dioxide – water binary system

Reference	Type of Data	T / K	P / MPa	*N.pts*
Verdet (1855)	*PTx*	273.15-293.15	0.1 (atm)	21
Bunsen (1855)	*PTx*	277.55-295.55	0.1 (atm)	6
de Khanikof and Loughinine (1867)	*PTx*	288.15	0.1-0.4	10
Bohr and Book (1891)	*PTx*	310.44-373.15	0.1-0.18	17
Prytz and Holtt (1895)	*PTx*	273.15	0.1 (atm)	2
Bohr (1899)	*PTx*	273.25-334.55	0.1 (atm)	5
Findlay and Creighton (1910)	*PTx*	298.15	0.1-0.18	10
Findlay and Shen (1912)	*PTx*	298.15	0.1-0.18	11
Kunerth (1922)	*PTx*	293.15-307.15	0.1 (atm)	8
Buch (1926)	*PTx*	292.15-293.15	0.1 (atm)	14
Morgan and Pyne (1930)	*PTx*	298.15	0.1 (atm)	
Morgan and Mass (1931)	*PTx*	273.15-298.15	0.008-0.11	21
Kritschewsky et al. (1935)	*PTx*	293.15 – 303.15	0.486 – 2.986	9
Kobe and Williams (1935)	*PTx*	298.15	0.1 (atm)	1
Shedlovsky and MacInnes (1935)	*PTx*	298.15	0.1 (atm)	1
Zel'vinskii (1937)	*PTx*	273.15-373.15	1.082 -9.12	21
Curry and Hazelton (1938)	*PTx*	298.15	0.1 (atm)	1
Wiebe and Gaddy (1939)	*PTx*	298.15-373.15	4.955	5
van Slyke (1939)	*PTx*	295.95-298.65	0.1 (atm)	6
Wiebe and Gaddy (1940)	*PTx*	291.15 – 373.15	2.53 – 70.9	25
Markam and Kobe (1941)	*PTx*	273.35-313.15	0.1 (atm)	3
Harned and Davis (1943)	*PTx*	273.15-323.15	0.1 (atm)	18
Morrison and Billet (1952)	*PTx*	286.45-347.85	0.1 (atm)	19
Bartholomé and Friz (1956)	*PTx*	283.15 – 303.15	0.101 – 2.027	25
Malinin (1959)	*PTx*	473.15-603.15	9.8-29.4	79
Ellis and Golding (1963)	*PTx*	450.15-607.15	2.5-19.5	15
Yeh and Peterson (1964)	*PTx*	298.15-318.15	0.1 (atm)	4
Matous et al. (1969)	*PTx*	303.15-353.15	0.99 – 3.891	13
Stewart and Munjal (1970)	*PTx*	273.15-298.15	1-4.6	12
Li and Tsui (1971)	*PTx*	273.19-303.15	0.1 (atm)	5
Murray and Riley (1971)	*PTx*	274.19-308.15	0.1 (atm)	8
Malinin and Savelyeva (1972)	*PTx*	298.15	1.11 – 5.689	79
Malinin and Kurovskaya (1975)	*PTx*	298.15 -348.15	4.955	6
Shagiakhmetov and Tarzimanov (1981)	*PTx*	323.15 – 373.15	10 – 60	14
Zawisza and Malesinska (1981)	*PTx*	323.15 – 373.15	0.488 – 4.56	24
Gillespie and Wilson (1982)	*PTxy*	298.15 – 366.45	5.07 –20.7	35
Cramer (1982)	*PTx*	306.15-486.25	0.8-5.8	7
Dohrn et al. (1983)	*PTx*	323.15	10-30	3
Oleinik (1986)	*PTx*	283.15 – 343.15	1 – 16	14
Postigo and Katz (1987)	*PTx*	288.15-308.15	0.1 (atm)	5
Muller et al. (1988)	*PTx*	373.15	0.3 – 1.8	8
Versteeg and VanSwaij (1988)	*PTx*	291-360.1	0.1 (atm)	18
Li and Lai (1995)	*PTx*	303.15-323.15	0.1 (atm)	3
Althaus (1999)	*PTy*	248.15 – 293.15	0.5 - 10	43
Yang et al. (2000)	*PTx*	298.31 – 298.57	2.7 – 5.33	9
Bamberger et al. (2000)	*PTx*	323.15 – 353.15	4 – 13.1	14
Anderson (2002)	*PTx*	274.15-288.15	0.07 – 2.18	13
Addicks et al. (2002)	*PTx*	293.15	1-2.5	4
Chapoy et al. (2004b)	*PTxy*	274.14-343.51	0.19-9.3	28
Valtz et al. (2004)	*PTx*	278.2-318.2	0.4-7.9	36

Table 2.22 Vapour liquid data for hydrogen sulphide – water binary system

Reference	Type of Data	T / K	P / MPa	*N.pts*
Winkler (1906)	*PTx*	273.15 – 363.15	0.1 (atm)	7
Kendal and Andrews (1921)	*PTx*	298.15	0.1 (atm)	1
Wright and Maas (1932)	*PTxy*	278.15 - 333.15	0.04 - 0.5	52
Kiss et al. (1937)	*PTx*	273.2 –298.1	0.1 (atm)	2
Selleck et al. (1952)	*PTxy*	310.93 – 444.26	0.7 –20.7	63
Pohl (1961)	*PTxy*	303.15 – 316.15	1.7	15
Hinners (1963)	*PTx*	353.15	0.1 (atm)	1
Kozintseva (1964)	*PTxy*	502.15 - 603.15	2.8 - 12.6	12
Burgess and Germann (1969)	*PTxy*	323.15 – 443.15	1.7 -2.3	35
Clarke and Glew (1971)	*PTx*	273.15 –323.15	0.05 –0.1	35
Gerrard (1972)	*PTx*	273.15 – 293.15	0.1 (atm)	5
Lee and Mather (1977)	*PTx*	283.15 –453.15	5.6 – 3.0»	29
Douabul and Riley (1979)	*PTxy*	275.25 – 303.07	0.1 (atm)	7
Gillespie and Wilson (1982)	*PTxy*	310.93 – 588.7	0.3 - 13.8	18
Byeseda et al. (1985)	*PTx*	297.1	0.1 (atm)	1
Barrett et al. (1988)	*PTx*	297.15 – 367.15	0.1 (atm)	39
Carroll and Mather (1989)	*PTxy*	313.15 –378.15	2.8 – 9.24	10
Suleimenov and Krupp (1994)	*PTx*	293.95 – 594.15	0.2 – 13.9	49
Kuranov et al. (1996)	*PTx*	313.15	0.5 – 2.5	9
Chapoy et al. (2005)	*PTx*	298.15 - 338.34	0.5 - 3.9	46

2.4.2 *Binary Systems Containing Methanol*

For the time being methanol is probably one of the most versatile chemicals in the natural gas processing industry. Methanol is and has been used for dehydration, gas sweetening and liquid recovery as well as hydrate inhibition. Accurate knowledge of thermodynamic properties of water-methanol equilibrium over a wide range of temperature and pressure conditions is therefore crucial for petroleum industry. These properties are essential throughout natural gas production and transportation to avoid hydrate formation and blockage, to optimise the process and the use of inhibitors. It is also necessary to have the most accurate data to provide a means for developing or improving the accuracy of predictive equilibria models by tuning binary interaction parameters. Data (i.e., solubilities, methanol distribution and mutual solubilities) of main components in natural gas (methane, ethane, propane, *i*-butane, *n*-butane, *n*-pentane, nitrogen, carbon dioxide and hydrogen sulphide) have been gathered and are reported here.

The sources of the experimental data for binary mixture of each of the components and water are given in Tables 2.23 through 2.30. These data has been extracted for tuning the binary interaction parameters used in equations of state in the following chapters.

Table 2.23 Vapour liquid data for methane – methanol binary systems

Reference	Type of Data	T / K	P / MPa	*N.pts*
Krichevsky and Koroleva (1941)	*PTy*	273.15 – 348.15	2.5 – 70	38
Shenderei et al. (1961)	*PTx*	213.15 – 248.15	0.1 (atm)	4
Hemmaplardh and King (1972)	*PTy*	288.15 – 333.15	3.61 – 6.46	27
Yaacobi and Ben-Naim (1974)	*PTx*	283.15-303.15	0.1 (atm)	5
Schneider (1978)	*PTx*	273.15 – 323.15	0.0004 – 10.3	17
Lazalde-Crabtree et al. (1980)	*PTy*	227.55 – 273.15	4.14 – 5.681	5
Francesconi et al. (1981)	*PTy & PTx*	282.45 – 566.65	24 – 208	115
Yarym-Agaev et al. (1985)	*PTxy*	298.15 – 338.15	2.5 – 12.5	15
Brunner et al. (1987)	*PTx & PTy*	298.15 – 373.15	3 – 105.1	78
Hong et al. (1987)	*PTxy*	220 – 330	1.38 – 41.37	83
Schlichting et al. (1993)	*PTy*	242.15-283.15	2.0 – 10.0	17
Ukai et al. (2002)	*PTx*	280.15	2.112-6.027	9
Wang et al. (2003)	*PTx*	283.15 – 303.15	5 – 40	24

Table 2.24 Vapour liquid data for ethane – methanol binary systems

Reference	Type of Data	T / K	P / MPa	*N.pts*
McDaniel (1911)	*PTx*	295.65-318.35	0.1 (atm)	4
Ma and Kohn (1964)	*PTxy*	248.15 – 373.15	1.013 – 6.08	30
Hemmaplardh and King (1972)	*PTy*	288.15 – 333.15	1.196 – 3.506	22
Yaacobi and Ben-Naim (1974)	*PTx*	283.15-303.15	0.1 (atm)	5
Ohgaki et al. (1976b)	*PTxy*	298.15	1.094 – 4.125	5
Lazalde-Crabtree et al. (1980)	*PTy*	267.15 – 278.15	1.911 – 2.204	4
Brunner (1985)	*Critical Curves*	250.85-512.64	3.7-17.9	25
Zeck and Knapp (1985)	*PTx*	240 – 298.15	0.41– 4.195	38
Lam and Luks (1991)	*PTx*	263.15 – 303.15	1.825 – 4.488	18
Ishihara et al. (1998)	*PTxy*	298.15	0.97-6.77	11
Wang et al. (2003)	*PTx*	283.2 - 303.2	0.5-3	20
Ruffine et al. (2005)	*PTx*	273.15	0.174-2.323	10

Table 2.25 Vapour liquid data for propane – methanol binary systems

Reference	Type of Data	T / K	P / MPa	*N.pts*
Nagahama et al. (1971)	*PTx*	293.15	0.27 – 0.80	11
Brunner (1985)	*Critical Curves*	370-512.6	4.2-8.7	25
Galivel-Solastiouk et al. (1986)	*PTxy*	313.1 – 373.1	0.35 – 4.28	32
Leu et al. (1992b)	*PTxy*	310.07– 352.2	0.032 – 3.173	24
Ma and Xu (1993)	*PTx*	273.15-298.15	0.1 (atm)	6
Yonker et al. (1998)	*PTxy*	394.15	1.2- 6	20

Table 2.26 Vapour liquid data for n-butane – methanol, i-butane – methanol and n-pentane – methanol binary systems

Reference	Type of Data	T / K	P / MPa	*N.pts*
n-Butane – Methanol				
Kretschmer and Wiebe (1952)	*PTx*	298.15 -323.15	0.05 – 0.102	12
Petty and Smith (1955)	*PTy*	322.04 – 410.93	0.103 – 3.544	29
Miyano and Hayduk (1986)	*PTx*	283.15-313.15	0.1 (atm)	4
Leu et al. (1992)	*PTxy*	469.9	3.787 – 6.917	7
Ma and Xu (1993)	*PTx*	298.15 -323.15	0.1 (atm)	8
i-Butane – Methanol				
Kretschmer and Wiebe (1952)	*PTx*	298.15 -323.15	0.04 – 0.102	12
Leu and Robinson (1992c)	*PTx*	273.15-373.15	0.004-2.0	49
Ma and Xu (1993)	*PTx*	298.15 -323.15	0.1 (atm)	8

Table 2.27 Vapour liquid data for nitrogen – methanol binary systems

Reference	Type of Data	T / K	P / MPa	*N.pts*
Krichevskii and Ilinskaya (1945)	*PTy*	273.15 – 348.15	0.004 – 70.928	41
Krichevskii and Koroleva (1945)	*PTx*	273.15 – 348.15	2.5 – 30	38
Kretschmer et al. (1946)	*PTx*	248.15-323.15	0.007-0.05	4
Krichevskii and Lebedewa(1947)	*PTx*	273.15 – 348.15	4.904 – 29.485	21
Hemmaplardh and King (1972)	*PTy*	288.15 – 333.15	2.938 – 6.363	28
Lazalde-Cabtree et al. (1980)	*PTy*	227.55 – 283.15	3.84 – 6.12	7
Weber et al. (1984)	*PTxy*	223.15 – 300	2.1 – 17.93	29
Brunner et al. (1987)	*PTy & PTx*	298.15 – 373.15	2.635 – 100	55
Schlichting et al. (1993)	*PTy*	241.15-282.15	1.0 – 11.5	34
Laursen and Andersen (2002)	*PTy & PTx*	298.15-318.15	4.6-10.1	24

Table 2.28 Vapour liquid data for carbon dioxide – methanol binary systems

Reference	Type of Data	T / K	P / MPa	*N.pts*
Kunerth (1922)	*PTx*	291.15 –309.15	0.1 (atm)	10
Krichevsky and Koroleva (1941)	*PTy*	298.15 – 348.15	0.004 – 70.928	19
Krichevskii and Lebedeva (1947)	*PTx*	273.15-348.15	6.9-697	27
Bezdel and Teodorovich (1958)	*PTx*	223.15-348.15	0.1-3.04	50
Shenderei et al. (1958)	*PTx*	194.45-273.15	0.01-0.1	28
Shenderei et al. (1959)	*PTx*	213.15-247.15	0.1-1.62	31
Usyukin and Shleinikov (1963)	*PTx*	203.15-273.15	0.1 (atm)	10
Yorizane et al. (1969)	*PTx*	243.15-273.15	0.4 -3.3	21
Katayama et al. (1975)	*PTxy*	298.15	0.219 – 6.128	13
Ohgaki and Katayama (1976a)	*PTx*	298.15-313.15	0.6-8.06	17
Semenova et al. (1979)	*PTxy*	323.15-398.15	0.5-18.5	70
Weber et al. (1984)	*PTx*	233.15-298.15	0.3-5.1	59
Brunner et al. (1987)	*PTxy*	241.8 – 282.9	0.4– 3.5	16
Hong and Kobayashi (1988)	*PTxy*	230 – 330	0.69– 10.65	64
Schroedter et al. (1991)	*PTx*	260 - 298.2	0.2 - 5.5	38
Leu et al. (1991)	*PTxy*	323.2-477.6	0.0558-12.75	40
Yoon et al. (1993)	*PTxy*	313.2	0.7-8.21	13
Schlichting et al. (1993)	*PTy*	241.15-283.15	0.4-3.6	16
Page et al. (1991)	*PTxy*	333.15-393.15	9.3-15.3	67
Reighard et al. (1996)	*PTx*	298.25 – 373.05	1.54 – 15.55	70
Chang et al. (1997)	*PTxy*	291.15 – 313.14	0.56 – 8.03	75
Chiehming et al. (1998)	*PTxy*	291.15-313.15	5.6-7.22	77
Elbaccouch et al. (2000)	*PTxy*	312.95-313.05	1.139-7.534	11
Joung et al. (2001)	*PTxy*	313.15-342.8	0.67-7.37	60
Bezanehtak et al. (2002)	*PTxy*	278.15-308.15	1.5-7.43	34
Zhu et al. (2002)	*PTxy*	323.15 - 473.15	6 - 16.2	25
Laursen et al. (2002)	*PTxy*	298.15-313.15	1.24-6.34	16
Xia et al (2004)	*PTx*	313.75 - 395	0.3-9.7	29

Table 2.29 Vapour liquid data for hydrogen sulphide – methanol binary systems

Reference	Type of Data	T / K	P / MPa	*N.pts*
Bezdel and Teodorovich (1958)	*PTx*	223.2-303.2	0.002-0.005	15
Yorizane et al. (1969)	*PTx*	248.15 -273.15	0.2-0.1	22
Short et al. (1983)	*PTx*	263-298.15	0.1 (atm)	5
Leu et al. (1992c)	*PTxy*	298.15– 448.15	0.017 – 11.20	55
Fischer et al. (2002)	*PTx*	298.15	0.02-0.414	22

Table 2.30 Vapour-Liquid or Solid – Liquid equilibrium data for water – methanol binary systems (BP: bubble point, DP: dew point and FP: freezing point)

Reference	Type of Data	T / K	P / MPa	*N.pts*
Washburn (1930)	*FP*	217-266	0.1 (atm)	7
Feldman and Dahlstrom (1936)	*FP*	233-266	0.1 (atm)	6
Frank et al. (1940)	*FP*	217-263	0.1 (atm)	7
Gristvold and Buford (1949)	*BP*	340.95-364.25	0.1 (atm)	8
Ross (1954)	*FP*	188-266	0.1 (atm)	8
Dalager (1969)	*BP & DP*	337.85-373.15	0.1 (atm)	26
Kato et al. (1970)	*BP & DP*	337.15-373.15	0.1 (atm)	24
Maripuri and Ratcliff (1972)	*BP & DP*	338.8-370.0	0.1 (atm)	16
McGlashan and Williamson(1976)	*BP*	308.15-338.15	0.006-0.1	39
Ott et al. (1979)	*FP*	157-273	0.1 (atm)	30
Ochi and Kojima (1987)	*BP*	371.15-373.15	0.1 (atm)	20
Pushin and Glagoleva (1992)	*FP*	177-260	0.1 (atm)	15
Kurihara et al. (1995)	*BP & DP*	323.15-333.15	0.03-0.07	50
Green and Venek (1995)	*BP*	291.15	0.1 (atm)	11
Khlfaoui et al. (1997)	*BP & DP*	337.15-373.15	0.1 (atm)	12
Christensen (1998)	*BP & DP*	333.15-373.15	0.02-0.1	5
Yao et al. (1999)	*BP & DP*	318.15	0.01-0.04	11
Lide (2004)	*FP*	176-272	0.1 (atm)	57

2.4.3 *Binary Systems Containing Ethanol*

Ethanol (EtOH) is used as a hydrate inhibitor in oil and gas production operations, particularly in areas of high industrial production (e.g. South America). Depending on operating conditions, solubility loss of ethanol into the sales gas can be very high and loss to the liquid hydrocarbon phase can also be important. The high vapour pressure of ethanol appears to be a significant drawback because of high chemicals losses. Therefore, it is of practical significance to study the mutual solubility of the major constituents of natural gas with ethanol.

In order to tune the interaction parameters between ethanol and other components, the available solubility data of the main components in the natural gas (methane, ethane, propane, *i*-butane, *n*-butane, *n*-pentane, nitrogen, and hydrogen sulphide, see Tables 2.31 through 2.33) have been gathered and presented here. Ethanol-gas binary systems have not been as widely examined as the methanol-gas systems. Studies reporting intermediate and high-pressure solubility data are far more limited. Only a few researchers have conducted solubility experiments on these systems (see Tables 2.31 through 2.33).

Table 2.31 Vapour liquid data for binary systems containing ethanol

Reference	Type of Data	T / K	P / MPa	*N.pts*
Methane – Ethanol				
Brunner et al. (1990)	*PTx*	298.15-498.15	4.2-36.5	75
Suzuki et al. (1990)	*PTxy*	313.15-333.15	1.8 – 10.5	10
Ukai et al. (2002)	*PTy*	280.15	1.5-11.5	10
Ethane – Ethanol				
Ellis et al. (1968)	*PTxy*	348.15	1.46-11	7
Suzuki et al. (1990)	*PTxy*	313.15-333.15	1.5-8	14
Brunner et al. (1990)	*PTxy*	298.15	0.25-11.8	77
Kato et al. (1999)	*PTxy*	311.15	4-7.9	7
Propane – Ethanol				
Kretschmer and Wiebe (1951)	*PTx*	273.15-373.15	0.001 – 0.1	13
Nagahama et al. (1971)	*PTx*	293.05	0.2 – 0.8	10
Gomez-Nieto and Thodos (1978)	*PTxy*	325-500	0.03 – 6.2	80
Horizoe et al. (1993)	*PTxy*	325-375	0.3-4.3	19
Zabaloy et al. (1994)	*PTxy*	325.15-375.15	1-4.5	17
n-Butane - Ethanol				
Kretschmer and Wiebe (1951)	*PTx*	298.15 -323.15	0.007 – 0.1	17
Holderbaum et al. (1991)	*PTx*	298.45-345.65	0.008 – 0.9	72
Deak et al. (1995)	*BP*	323.15-513.15	0.2-6.2	222
Dahlhoff et al. (2000)	*PTxy*	293.15	0.005-0.2	15
i-Butane - Ethanol				
Kretschmer and Wiebe (1951)	*PTx*	283.15-323.15	0.003 – 0.1	18
Zabaloy (1994)	*PTxy*	308.5-363.5	0.3-1.6	32
n-Pentane - Ethanol				
Campbell et al. (1987)	*PTxy*	372.6-422.6	0.2-1.6	34
Reimers et al. (1992)	*PTx*	303.15	0.01-.09	26
Seo et al. (2000)	*PTxy*	422.6-500	1.3-4.2	32
Hydrogen sulphide - Ethanol				
Gerrard (1972)	*PTx*	265.15-293.15	*P. atm*	5
Nitrogen - Ethanol				
Just (1901)	*PTx*	293.15 – 298.15	0.1 (atm)	2
Metschl (1924)	*PTy*	298.15	0.1 (atm)	1
Kretschmer and Nowakowska(1946)	*PTx*	248.15-323.15	0.1 (atm)	4
Boyer and Bircher (1960)	*PTx*	298.15	0.1 (atm)	1
Katayama and Nitta (1976)	*PTx*	213.15-298.15	0.1 (atm)	5

Table 2.32 Vapour liquid data for carbon dioxide – ethanol binary systems

Reference	Type of Data	T / K	P / MPa	*N.pts*
Takishima et al. (1986)	*PTxy*	304.2-308.2	3.75-7.7	19
Suzuki et al. (1990)	*PTxy*	313.14-333.4	0.514-9.949	23
Cho et al. (1991)	*PTxy*	313.2-333.2	6.3-10.5	21
Jennings et al. (1991)	*PTxy*	314.7-337.1	5.55-10.654	23
Hirohama et al. (1993)	*PTxy*	283.1-308.2	0.9-7.2	17
Yoon et al. (1993)	*PTxy*	313.2	0.6-8.2	11
Tanaka and Kato (1995)	*PTxy*	308.15	1.5-7.8	20
Chang et al. (1997a)	*PTxy*	291.15-313.15	0.514-7.92.	60
Chen et al. (2000)	*PTxy*	323.15	5-8.2	4
Elbaccouch et al. (2000)	*PTxy*	323.55-333.45	4.3-10	22
Galicia-Luna eta l. (2000)	*PTxy*	312.8-373	0.476-14.345	48
Yeo et al. (2000)	*BP*	298.15-413.15	6.2-15.2	35
Joung et al. (2001)	*PTxy*	313.15-342.8	0.6-12.4	61
Tian et al. (2001)	*PTxy*	333.15-453.15	6-12.6	24
Zhu et al. (2001)	*PTxy*	333.2-453.2	6-12.6	19
Gonzalez et al. (2002)	*PTx*	314.45-324.17	7.5-8.3	17
Zhu et al. (2002)	*PTxy*	200-453.15	4-16.2	48

Table 2.33 Vapour-Liquid equilibrium data for water – ethanol binary systems

Reference	Type of Data	T / K	P / MPa	*N.pts*
Rieder and Thompson (1949)	*BP*	351.45-372.45	0.1 (atm)	34
Barr-David and Dodge (1959)	*BP*	423.15-623.15	0.56-19	84
Dalager (1969)	*BP*	351.35-373.15	0.1 (atm)	27
D'Avila and Sila (1970)	*BP*	283.15-303.15	0.002-0.01	25
Kolbe and Gmehling (1985)	*BP*	363.25-423.65	0.1-1	114
Ochi and Kojima (1987)	*BP*	370.3-373.13	0.1 (atm)	22
Kurihara et al. (1995)	*BP*	323.15-363.15	0.004-0.16	202
Lide (2004)	*FP*	228-273	0.1 (atm)	32
Anderson et al. (2008)	*FP*	230-273	0.1 (atm)	85

2.4.5 *Binary Systems Containing n-Propanol*

There is a limited number of experimental data available in the literature for binaries of *n*-propanol. The methane/water and *n*-propanol equilibrium data have been gathered and used for tuning the binary interaction parameters. The sources of experimental data are outlined in Table 2.34.

Table 2.34 Vapour-Liquid equilibrium data for methane – n-propanol binary and Solid – Liquid equilibrium data for the water – n-propanol binary system (BP: bubble point, DP: dew point and FP: freezing point)

Reference	Type of Data	T / K	P / MPa	*N.pts*
Methane – *n*-Propanol				
Boyer and Bircher (1960)	*PTx*	298.15	0.101325	1
Yaacobi and Ben-Nain (1974)	*PTx*	283.15 – 303.15	0.101325	5
Suzuki et al. (1990)	*PTx*	313.40 – 333.40	1.4 –10.2	10
Bo et al. (1993)	*PTx*	298.15	0.101325	1
Water – *n*-Propanol				
Dawe et al. (1973)	*FP*	360.7 – 371.3	Around 0.1	16
Ziekiewicz and Konitz (1991)	*FP*	313.40	0.008 - 0.011	25
Gabaldon et al. (1996)	*FP*	331.8 – 372.8	0.03 – 0.1	82
Chapoy et al. (2008)	*FP*	264.55 – 271.55	0.101325	12
Orchille´s (2008)	*BP & DP*	360.49 – 372.81	0.1	56

2.4.4 *Binary Systems Containing Monoethylene Glycol (MEG)*

Monoethylene glycol's high boiling point and affinity for water makes it an ideal dehydrator in natural gas production. In the field, excess water vapour is usually removed by glycol dehydration. Glycols do not have the significant drawback of methanol that is its high solvent loss. However depending on operating conditions, the solubility of hydrocarbons in glycols is not negligible. Therefore, accurate knowledge of the thermodynamic properties of the hydrocarbons and monoethylene glycol equilibrium over a wide range of temperature and pressure conditions is crucial for gas processing industry and for developing or improving the accuracy of predictive equilibria models. Equilibrium data (i.e., solubilities and glycol vaporisation losses) on MEG and main components of natural gases have been gathered. The sources of the experimental data for binary mixture of each of the components and monoethylene glycol are given in Table 2.35 and Table 2.36. These data have been extracted and used for tuning the binary interaction parameters used in equations of state in the following chapters.

Table 2.35 Vapour liquid data for binary systems containing monoethylene glycol

Reference	Type of Data	T / K	P / MPa	*N.pts*
Methane - Monoethylene glycol				
Jou et al. (1994)	*PTx*	298.15 – 398.15	0.105 – 20.35	34
Zheng et al. (1999)	*PTx*	323.15 – 398.15	0.2 – 39.62	31
Wang et al. (2003)	*PTx*	283.2 – 303.2	5 – 40.06	24
Folas et al. (2007)	*PTxy*	278.15-323.15	5-20	9
Ethane - Monoethylene glycol				
Gjaldbaek and Nieman (1958)	*PTx*	298.16-308.15	0.1 (atm)	7
Wang et al. (2003)	*PTx*	283.2 – 303.2	0.5 – 4	14
Propane - Monoethylene glycol				
Lenoir et al. (1971)	*PTx*	298.15	0.1 (atm)	1
Byseda et al. (1985)	*PTx*	297.04	0.1 (atm)	1
Jou et al. (1993)	*PTx*	298.15 – 398.15	0.082 – 20.29	35
Nitrogen - Monoethylene glycol				
Gjaldbaek and Nieman (1958)	*PTx*	298.16	0.1 (atm)	2
Yamamoto and Tokunaga (1994)	*PTxy*	298.15	0.1 (atm)	1
Zheng et al. (1999)	*PTx*	323.15 – 398.15	1.47 – 39.6	34
Carbon dioxide - Monoethylene glycol				
Wallace (1985)	*PTx*	296 – 319	8.3	3
Byseda et al. (1985)	*PTx*	297.03	0.1 (atm)	1
Adachi et al. (1986)	*PTy*	308.15 – 333.15	2.76 – 22.06	32
Jou et al. (1988)	*PTx*	298.15-348.15	0.00324-6.75	40
Kaminishi et al. (1989)	*PTy*	313.15 – 333.15	2.36 – 15.04	13
Jou et al. (1990)	*PTx*	298.15-348.15	0.00324-6.75	40
Zheng et al. (1999)	*PTx*	323.15 – 398.15	0.895 – 38.4	34
Hydrogen sulphide - Monoethylene glycol				
Lenoir et al. (1971)	*PTx*	298.15	0.1 (atm)	1
Gerrard (1972)	*PTx*	265.15-293.15	0.1 (atm)	5
Short et al. (1983)	*PTx*	263.15-333.15	0.1 (atm)	12
Byseda et al. (1985)	*PTx*	297.03	0.1 (atm)	1
Jou et al. (1988)	*PTx*	298.15-348.15	0.00324-6.75	40
Jou et al. (1990)	*PTx*	298.15-348.15	0.00324-6.75	40

Table 2.36 Vapour-Liquid or Solid – Liquid equilibrium data for the water – monoethylene glycol binary system (BP: bubble point, DP: dew point and FP: freezing point)

Reference	Type of Data	T / K	P / MPa	*N.pts*
Olsen et al. (1930)	*FP*	227-270	0.1 (atm)	9
Washburn (1930)	*FP*	236-273	0.1 (atm)	6
Trimble and Potts (1935)	*BP*	342.15-469.15	0.033-0.1	79
Conrad et al. (1940)	*FP*	223-270	0.1 (atm)	7
Spangler and Davies (1943)	*FP*	237-270	0.1 (atm)	6
Ross (1954)	*FP*	252-270	0.1 (atm)	10
Mellan (1977)	*BP*	373.15-470.5	0.1 (atm)	41
Nath and Bendert (1983)	*BP & DP*	338.25-363.45	0.018-0.7	42
Villamanan et al. (1984)	*BP*	333.15	0.0002-.019	24
Lee et al. (1992)	*BP*	383.15-457.15	0.1 (atm)	18
Chiavone-Filho (1993)	*BP*	343.15-363.15	0.0061-0.07	40
Cordray et al. (1996)	*FP*	217-273	0.1 (atm)	16
Lancia et al. (1996)	*BP*	371.15-395.15	0.004-0.15	42
Lide (2004)	*FP*	222-273	0.1 (atm)	26

References

Abdulgatov I.M., Bazaev A.R., Ramazanova A.E., 1993, *Volumetric properties and virial coefficients of (water+methane)*, J. Chem. Therm., **25**, 249-259

Adachi Y., Malone P.V., Yonemoto T., Kobayashi R., 1986, *Glycol vaporization losses in supercritical CO2*, Gas Process. Assoc., Res. Rep. 98

Addicks J., Owren G.A., Fredheim A.O., Tangvik K., 2002, *Solubility of Carbon Dioxide and Methane in Aqueous Methyldiethanolamine Solutions*, J. Chem. Eng. Data, **47**, 855-860

Adeney W.E., Becker H.G., 1919, Royal Dublin Soc. Scientific Pro., **15**, 609-628. (Quoted in: IUPAC Solubility Data Series, Volume 10: Nitrogen and Air, Pergamon Press, 1982)

Althaus K., 1999, *Relationship Between Water Content and Water Dew Point Keeping in Consideration the Gas Composition in the Field of Natural Gas*, Fortschritt - Berichte VDI. Reihe., **3**, 350

Amirijafari R., Campbell J., 1972, *Solubility of gaseous hydrocarbon mixtures in water*, Soc. Pet. Eng. J., 21-27

Anderson G.K., 2002, *Solubility of carbon dioxide in water under incipient clathrate formation conditions*, J. Chem. Eng. Data, 47, 219–222

Anderson R., Chapoy A., Tanchawanich J., Haghighi H., Lachwa-Langa J., Tohidi B., 2008, *Binary ethanol−methane clathrate hydrate formation in the system $CH_4−C_2H_5OH−H_2O$: experimental data and thermodynamic modelling*, the 6th International Conference on Gas Hydrates (ICGH)

Anderson R., Llamedo M., Tohidi B., Burgass R.W., 2003, *Experimental Measurement of Methane and Carbon Dioxide Clathrate Hydrate Equilibria in Mesoporous Silica*, J. Phys. Chem. B, **107**, 3507- 3514

Anthony R.G., McKetta J.J., 1967, *Phase Equilibrium in the Ethylene-Water System*, J. Chem. Eng. Data., **12**(1), 17-20

Azarnoosh A., McKetta J.J., 1958, *The solubility of propane in water*, Petrol. Refiner, **37**, 275-278

Bamberger A., Sieder G., Maurer G., 2000, *High-pressure (vapour+liquid) equilibrium in binary mixtures of (carbon dioxide and water or acetic acid) at temperatures from 313 to 353 K*, J. Supercrit. Fluid., **17**, 97–110

Barone G., Crescenzi V., Pispisa B., Quadrifoglio F.J., 1966, *Hydrophobic Interactions in Polyelectrolyte Solutions. II. Solubility of some C3-C6 Alkanes in Poly(methacrylic acid) Solutions*, J. Macromol. Chem., **1**, 761-771

Barr-David F., Dodge B.F., 1959, *Vapor-Liquid Equilibrium at High Pressures. The Systems Ethanol-Water and 2-Propanol-Water*, J. Chem. Eng. Data, **4**, 107-121

Barrett T.J., Anderson G.M., Lugowski J., 1988, *The solubility of hydrogen sulphide in 0-5m NaCL solutions at 25-95oC and one atmosphere*, Geochim. Cosmochim. Ac., **52**, 807-811

Bartholomé E., Friz H., 1956, *Solubility of CO2 in water*, Chem. Ing. Tech. **28**, 706–708

Ben-Naim A., Wilf J., Yaacobi M., 1973, *Hydrophobic interaction in light and heavy water*, J. Phys. Chem., **77**, 95-102

Bezanehtak K., Combes G.B., Dehghani F., Foster N.R., Tomasko D.L., 2002, *Vapor-liquid equilibrium for binary systems of carbon dioxide + methanol, hydrogen + methanol, and hydrogen + carbon dioxide at high pressures*, J. Chem. Eng. Data, **47**, 161-168

Bezdel L.S., Teodorovich V.P., 1958, *Solubility of CO2, H2S, CH4, and C2H6 in methanol at low temperatures*, Gazov. Prom-st, **3**(8), 38-43

Bo S., Battino R., Wilhelm E., 1993, *Solubility of gases in liquids. 19. Solubility of He, Ne, Ar, Kr, Xe, N2, O2, CH4, CF4, and SF6 in normal 1-alkanols n-ClH2l+1OH (1 <= l < =11) at 298.15 K*, J. Chem. Eng. Data, **38**, 611-616

Bohr C.Z., 1910, Physik. Chem., **71**, 47-50

Bohr C., Book J., 1891, Ann. Phys. Chem., **44**, 318-343

Bohr C, 1899, Ann. Phys. Chem., **68**, 500-525

Boyer F.L., Bircher L.J., 1960, *The solubility of nitrogen, argon, methane, ethylene and ethane in normal primary alcohols*, J. Phys. Chem., **64**, 1330-1331

Brooks W.B., Gibbs G.B., McKetta J.J., 1951, *Mutual solubilities of light hydrocarbon-water systems*, Petrol. Refiner, **30**, 118-120

Brunner E., 1985, *Fluid mixtures at high pressures II. Phase separation and critical phenomena of (ethane + an n-alkanol) and of (ethene + methanol) and (propane + methanol)*, J. Chem. Thermodyn., **17**, 871 –885

Brunner E., Hueltenschmidt W., 1990, *Fluid mixture at high pressures VIII. Isothermal phase equilibria in the binary mixtures: (ethanol + hydrogen or methane or ethane)*, J. Chem. Thermodyn., **22**, 73-84

Brunner E., 1985, *Fluid mixtures at high pressures I. Phase separation and critical phenomena of 10 binary mixtures of (a gas + methanol)*, J. Chem. Thermodyn., **17**, 671 –679

Brunner E., Hueltenschmidt W., Schlichthaerle G., 1987, *Fluid mixtures at high pressures IV. Isothermal phase equilibria in binary mixtures consisting of (methanol + hydrogen or nitrogen or methane or carbon monoxide or carbon dioxide)*, J. Chem. Thermodyn., **19**, 273-291

Buch K., 1926, Nord. Kemistmotet, 184-192

Bunsen R.W.E., 1855, Memoire *sur la loi de l'absorption des gaz par les liquids*, Phil. Mag., **9**, 116-130, 181-201

Burgess M.P., Germann R.P., 1969, *Physical properties of hydrogen sulfide water mixtures*, AIChE J., **15**, 272-275

Byeseda J.J., Deetz J.A., Manning W.P., 1985, *The Optisol TM Gas Sweetening Solvent*, Laurance Reid gas conditioning conference

Byseda J.J., Deetz J.A., Manning W.P., 1985, *New gas-sweetening solvewnt proves successful in four fiel trials*, Oil Gas J., **83**(23), 144-146

Campbell S.W., Wilsak R.A., Thodos G., 1987, *(Vapor + liquid) equilibrium behavior of (n-pentane + ethanol) at 372.7, 397.7, and 422.6 K*, J. Chem.Thermodyn., **19**, 449-460

Cargill R.W., MacPhee D.E., 1989, *A Phase separation caused by the solubility of butane in 2-methylpropan-2-ol-water mixtures*, J. Chem. Soc., Faraday Trans. 1., **85**, 2665-2668

Carroll J.J., Mather A.E., 1989, *Phase equilibrium in the system water – hydrogen sulphide: Experimental determination of the LLV locus*, Can. J. Chem. Eng., **67**, 468-470

Chang C.J., Day C.Y., Ko C.M., Chiu K.L., 1997, *Densities and P-x-y diagrams for carbon dioxide dissolution in methanol, ethanol, and acetone mixtures*, Fluid Phase Equilibr., **131**, 243-258

Chang T., Rousseau R.W., 1985, *Solubilities of carbon dioxide in methanol and methanol - water at high pressures*, Fluid Phase Equilibr., **23**, 243-258

Chapoy A., Mohammadi A.H., Tohidi B., Valtz A., Richon D., 2005, *Experimental measurement and phase behavior modeling of hydrogen sulfide-water binary system*, Ind. Eng. Chem. Res., **44**, 7567-7574

Chapoy A., Anderson R., Haghighi H., Edwards T., Tohidi B., 2008, *Can n-propanol form hydrate?*, Ind. Eng. Chem. Res., **47**, 1689-1694

Chapoy A., Mohammadi A.H., Richon D., Tohidi B., 2004a, *Gas Solubility Measurement and Modeling for Methane – Water and Methane – Ethane – n-Butane - Water Systems near Hydrate Forming Conditions*, Fluid Phase Equilibr., **220**, 113-121

Chapoy A., Mohammadi A.H., Chareton A., Richon D., Tohidi B., 2004b, *Measurement and Modeling of Gas Solubility and Literature Review of the Properties for the Carbon Dioxide - Water System*, Ind. Eng. Chem., **43**, 1794-1802

Chapoy A., Mokraoui S., Valtz A., Richon D., Mohammadi A.H., Tohidi B., 2004c, *Vapor-liquid equilibria for propane-water system from 277.62 to 368.16 K*, Fluid Phase Equilibr., **226**, 213-220

Chapoy A., Richon D., Mohammadi A.H., Tohidi B., 2004d, *Gas Solubility Measurement and Modeling for Nitrogen + Water System from 274.18 K to 363.02 K*, J. Chem. Eng. Data, **49**, 1110 -1115

Chen H.I., Chang H.Y., Huang E.T.S., Huang T.C., 2000, *A new phase behavior apparatus for supercritical fluid extraction study*, Ind. Eng. Chem. Res., **39**, 4849-4852

Chiehming C.J., Kou-Lung C., Chang-Yih D., 1998, *A new apparatus for the determination of P-x-y diagrams and Henry's constants in high pressure alcohols with critical carbon dioxide*, J. Supercrit. Fluids, **12**, 223-237

Cho J.S., Park S.K., Lim J.S., Kim J.D., Lee Y.Y., Chun H.S., 1991, *A Study on concentration of ethanol by supercritical fluis and Salts(I)*, Hwahak Konghak, **29**, 111-117

Christensen S.P., 1998, Measurement of dilute mixture vapor–liquid equilibrium data for aqueous solutions of methanol and ethanol with a recirculating still, Fluid Phase Equilibr., **150-151**, 763–773

Clarke E.C.W., Glew D.N., 1971, *Aqueous non electrolyte solutions. Part VIII. Deuterium and hydrogen sulfide solubilities in deuterium oxide and water*, Can. J. Chem. Eng., **49**, 691-698

Claussen W.F., Polglase M.F., 1952, *Solubilities and Structures in Aqueous Aliphatic Hydrocarbon Solutions*, J. Am. Chem. Soc., **74**, 4817-4819

Clever H.L., Battino R., Saylor J.H., Gross D.M., 1957, *The Solubility of Helium, Neon, Argon and Krypton in Some Hydrocarbon Solvents*, J. Phys. Chem., **61**, 1078-1082

Conrad F.H., Hill E.F., Ballman E.A., 1940, *Freezing points of the system ethylene glycol-methanol-water*, Ind. Eng. Chem., **32**, 542-543

Connolly J.F., 1966, *Solubility of hydrocarbons in water near the critical solution temperatures*, J. Chem. Eng. Data, **11**, 13-16

Cordray D.R., Kaplan L.R., Woyciesjes P.M., Kozak T.F., 1996, *Solid - liquid phase diagram for ethylene glycol + water*, Fluid Phase Equilibr., **117**, 146 - 152

Cosgrove B.A., Walkley J., 1981, *Solubilities of gases in H_2O and $2H_2O$*, J. Chromatogr., **216**, 161-167

Cramer, S. D., 1984, *Solubility of methane in brines from 0 to 300^oC*, Ind. Eng. Chem. Pr. Des. Dev., **23**, 533-538

Cramer S.D., 1982, *The solubility of methane, carbon dioxide, and oxygen in brines from 0 to 300 ◦C*, US Bureau of Mines Report of Investigations, vol. 8706

Crovetto R., Fernandez-Prini R., Japas M.L., 1982, *Solubilities of inert gases and methane in H2O and in D2O in the temperature range of 300 to 600 K*, J. Chem. Phys., **76**(2), 1077-1086

Culberson O.L., McKetta J.J., 1950, *Phase Equilibria in Hydrocarbon-Water Systems II-, The Solubility of Ethane in Water at Pressures to 10000 psi*, Petr. Trans. AIME, **189**, 319-322

Culberson O.L., Horn A.B., Mc Ketta Jr J. J., 1950, *Phase Equilibria in Hydrocarbon-Water Systems: the solubility of Ethane in Water at Pressures up to 1200 Pounds per Square Inch*, AIME, **189**, 1-6

Culberson O.L., Mc Ketta Jr, J.J., 1951, *Phase Equilibria in Hydrocarbon-Water Systems III-, The solubility of methane in water at 10000 psia*, AIME, **192**, 223-226

Curry J., Hazelton C.L., 1938, *The Solubility of Carbon Dioxide in Deuterium Oxide at 25oC*, J. Am. Chem. Soc., **60**, 2771-2773

Czerski L., Czaplinski A., 1962, Ann. Soc. Chim. Polonorum (Poland), **36**, 1827-1834

D'Avilia S.G., Silva R.S.F., 1970, *Isothermal vapor-liquid equilibrium data by total pressure method. Systems acetaldehyde-ethanol, acetaldehyde-water, and ethanol-water*, J. Chem. Eng. Data, **15**, 421-424

Dahlhoff G., Pfennig A., Hammer H., Van Oorschot M., 2000, *Vapor-liquid equilibria in quaternary mixtures of dimethyl ether + n-butane + ethanol + water*, J. Chem. Eng. Data, ***45***, 887-892

Dalager P., 1969, *Vapor-liquid equilibriums of binary systems of water with methanol and ethanol at extreme dilution of the alcohols*, J. Chem. Eng. Data, **14**, 298-301

Danneil A., Tödheide K., Franck E.U., 1967, *Verdampfungsleichgewichte und kritische Kurven in den Systemen Äthan/Wasser und n-Butan/Wasser bei hohen Drücken*, Chem. Ing. Tech., **13**, 816-821

Davis J.E., Mc Ketta Jr J.J., 1960, *Solubility of methane in water*, Petrol. Refiner., **39**, 205-206

Dawe R.A., Newsham D.M.T., Ng S.B., 1973, *Vapor-liquid equilibria in mixtures of water, n-propanol, and n-butanol, journal of chemical engineering data*, **18**, 44-616

de Khanikof N., Loughinine V., 1867, Ann. Chim. Phys. Ser. 4, **11**, 412-433

Deak A., Victorov A.I., de Loos T.W, 1995, *High pressure VLE in alkanol + alkane mixtures. Experimental results for n-butane + ethanol, + 1-propanol, + 1-butanol systems and calculations with three EOS methods*, Fluid Phase Equilibr., **107**, 277-301

Denton W.H., Smith M.J.S., Klaschka J.T., Forgan R., 1973, Proceedings of the Fourth International Symposium on Fresh Water from the Sea, **3**, 291-311

Dohrn R., Bünz A.P., Devlieghere F., Thelen D., 1983, *Experimental measurements of phase equilibria for ternary and quaternary systems of glucose, water, CO2 and ethanol with a novel apparatus*, Fluid Phase Equilibr., **83**, 149-158

Douabul A.A., Riley J.P., 1979, *The solubility of gases in distilled water and seawater - V. Hydrogen sulphide*, Deep-Sea Res., **26**A, 259-272

Douglas E., 1964, *Solubilities of oxygen, argon, and nitrogen in distilled water*, J. Phys. Chem., **68**, 169-174

Duffy, J. R. Smith, N. O. and Nagy, B., 1961, *Solubility of natural gases in aqueous salt solutions—I: liquidus surfaces in the system CH4-H2O-NaCl2-CaCl2 at room temperatures and at pressures below 1000 psia*, Geochim. Cosmochim. Acta, **24**, 23-31

Elbaccouch M.M., Raymond M.B., Elliott J.R., 2000, *High-pressure vapor-liquid equilibrium for R-22 + ethanol and R-22 + ethanol + water,* J. Chem. Eng. Data, **45**, 280-287

Ellis A.J., Golding R.M., 1963, *The solubility of carbon dioxide above 100^{o}C in water and in sodium chloride solutions*, Am. J. Sci., **261**, 47-60

Ellis S.R.M., Valteris R.L., Harris G., 1968, J. Chem. Eng. Prog. Symp. Ser., **64**, 16-21

Eucken A., Hertzberg G., 1950, *Aussalzeffekt and ionenhydration*, Z. Physik Chem., **195**, 1-23

Fahri L.E., Edwards A.W.T., Homa T.J., 1963, Appl. Physiol., 18, 97-106

Feldman H.B., Dahlstrom W.G., 1936, *Freezing points of the ternary system glycerol-methanol-water*, Ind. Eng. Chem., 28, 1316

Findlay A., Creighton H.J.M., 1910, *The influence of colloids and fine suspensions on the solubility of gases in water. Part I. Solubility of carbon dioxide and nitrous oxide*, J. Chem. Soc., **97**, 536-561

Findlay A and Shen, B., 1912, *The influence of colloids and fine suspensions on the solubility of gases in water. Part II. Solubility of carbon dioxide and of hydrogen*, J. Chem. Soc., **101**, 1459-1468

Fischer K., Chen J., Petri M., Gmehling J., 2002, *Solubility of H2S and CO2 in N-octyl-2-pyrrolidone and of H2S in methanol and benzene,* AIChE J., **48**, 887-893

Folas G.K., Berg O.J., Solbraa E., Fredheim A.O., Kontogeorgis G.M., Michelsen M.L., Stenby E.H., 2007, *High-pressure vapor–liquid equilibria of systems containing ethylene glycol, water and methane: Experimental measurements and modelling*, Fluid Phase Equilibr., **251**, 52–58

Fox C.J.J., 1909, *On the coefficients of absorption of nitrogen and oxygen in distilled water and sea-water, and of atmospheric carbonic acid in sea-water,* Trans. Faraday Soc., **5**, 68-87

Frank, H., Conard, E. F. Hill, E. A. Ballmak, 1940, *Freezing points of the system ethylene glycol-methanol- water,* Ind. Eng. Chem., **32**, 542-543

Francesconi A.Z., Lentz H., Franck E.U., 1981, *Phase equilibria and PVT data for the methane-methanol system to 300 MPa and 240 ^{o}C*, J. Phys. Chem., **85**, 3303-3307

Frolich K., Tauch E.J., Hogan J.J., Peer A.A., 1931, *Solubility of gases in liquids at high pressures*, Ind. Eng. Chem., **23**(5), 548-550

Fühner H., 1924, Ber. Dtsch. Chem. Ges., **57**, 510-515

Gabaldon C., Marzal P., Monton J., Rodrigo M.A., 1996, *Isobaric vapor-liquid equilibria of the water + 1-propanol system at 30, 60, and 100 kPa*, J. Chem. Eng. Data, **41**, 1176-1180

Galicia-Luna L.A., Ortega-Rodriguez A., Richon D., 2000, *New apparatus for the fast determination of high-pressure vapor-liquid equilibria of mixtures and of accurate critical pressures*, J. Chem. Eng. Data, **45**, 265-271

Galivel-Solastiouk F., Laugier S., Richon D., 1986, *Vapor-liquid equilibrium data for the propane - methanol and propane - methanol - carbon dioxide system*, Fluid Phase Equilibr., **28**, 73-85

Gerrard, W., 1972, *Solubility of hydrogen sulphide, dimethyl ether, methyl chloride and sulphur dioxide in liquids. The prediction of solubility of all gases*, J. Appl. Chem.. Biothechnol., **22**, 623-650

Chiavone-Filho O., Proust P., Rasmussen P., 1993, Vapor-liquid equilibria for glycol ether + water systems, J. Chem. Eng. Data, **38**, 128-131

Gillespie P.C., Wilson G.M., 1982, *Vapor liquid and liquid liquid equilibria: methane-water; water – carbon - dioxide; water – hydrogen sulphide;water – npentane; water – methane - npentane*, Gas Processors Association, Tulsa, Research Report RR 48

Gjaldbaek J.C., Niemann H., 1958, *The solubility of nitrogen, argon and ethane in alcohols and water*, Acta Chem. Scand., **12**, 1015-1023

Gomez-Nieto M., Thodos G., 1978, *Vapor-liquid equilibrium measurements for the propane-ethanol system at elevated pressures*, AlChE J., **24**, 672-678

Gonzalez A.V., Tufeu R., Subra P., 2002, *High-pressure vapor-liquid equilibrium for the binary systems carbon dioxide + dimethyl sulfoxide and carbon dioxide + dichloromethane*, J. Chem. Eng. Data, **47**, 492-495

Goodman J.B., Krase N.W., 1931, *Solubility of nitrogen in water at high pressures and temperature*s, Ind. Eng. Chem., **23**(4), 401-404

Green S.J., Venek I.E., 1995, *Vapor-liquid equilibria of formaldehyde-methanol-water*, Ind. Eng. Chem., 47, 103-109

Gristwold J., Buford C.B., 1949, Separation of synthesis mixtures vapor-liquid equilibria of acetone-methanol-water, Ind. Eng. Chem., **41**, 2347-2351

Haghighi H., Chapoy A., Tohidi B., 2008, *Freezing point depression of electrolyte solutions: experimental measurements and modeling using the CPA equation of state*, Ind. Eng. Chem. Res., **47**, 3983–3989

Haghighi H., Chapoy A., Burgess R., Mazloum S., Tohidi B., 2009a, *Phase equilibria for petroleum reservoir fluids containing water and aqueous methanol solutions: experimental measurements and modelling using the CPA equation of state*, Fluid Phase Equilibr., **278**, 109–116

Haghighi H., Chapoy A., Burgess R., Tohidi B., 2009b, *Experimental and thermodynamic modelling of systems containing water and ethylene-glycol: application to flow assurance and gas processing*, Fluid Phase Equilibr., **276**, 24-30

Haghighi H., Chapoy A., Tohidi B., 2009c, *Methane and water phase equilibria in the presence of single and mixed electrolyte solutions using the Cubic-Plus-Association equation of state*, J. Oil Gas Sci. Technol., **64**(2), 141-154

Harned H.S., Davis Jr R., 1943, *The ionization constant of carbonic acid in water and the solubility of carbon dioxide in water and aqueous salt solutions from 0 to 50°C*, J. Am. Chem. Soc., **65**, 2030-2037

Hemmaplardh B., King Jr. A.D., 1972, *Solubility of methanol in compressed nitrogen, argon, methane, ethylene, ethane, carbon dioxide and nitrous oxide. Evidence for association of carbon dioxide with methanol in the gas phase*, J. Phys. Chem., **76**, 2170-2175

Hinners N.W., 1963, *The solubility of sphalerite in aqueous solutions at 80°C*, Ph.D. thesis, Princeton University

Hirohama S., Takatsuka T., 1993, Miyamoto S., Muto T., *Measurement and correlation of phase equilibria for the carbon dioxide-ethanol-water system*, J. Chem. Eng. Jpn., **26**, 408-415

Holderbaum T., Utzig A., Gmehling J., 1991, *Vapour-liquid equilibria for the system butane/ethanol at 25.3, 50.6 and 72.5 C*, Fluid Phase Equilibr., **63**, 219-226

Hong J.H., Kobayashi R., 1988, *Vapor-liquid equilibrium studies for the carbon dioxide - methanol system*, Fluid Phase Equilibr., **41**, 269-276

Hong J.H., Malone P.V., Jett M.D., Kobayashi R., 1987, *The measurement and interpretation of the fluid phase equilibria of a normal fluid in a hydrogen bonding solvent: the methane-methanol system*, Fluid Phase Equilibr., **38**, 83-96

Hong S.P., Patton C.L., Luks K.D, 1994, *Multiphase equilibrium behavior of the mixture carbon dioxide + ethane + methanol*, J. Chem. Eng. Data, **39**, 90-94

Horizoe H., Tanimoto T., Yamamoto I., Kano Y., 1993, *Phase equilibrium model for the separation of ethanol-water solution using super- and subcritical propane solvent extraction*, J. Chem. Eng. Jpn., **26**, 482-489

Ishihara K., Tanaka H., Kato M., 1998, *Phase equilibrium properties of ethane + methanol system at 298.15 K*, Fluid Phase Equilibr., **144**,131-144

Japas M.L., Franck E.U., 1985, *High Pressure Phase Equilibria and PVT-Data of the Water-Nitrogen System to 673 K and 250 MPa.*, Ber. Bensunges. Phys. Chem., **89**, 793-800

Jennings D.W., Lee R., Teja A., 1991, *Vapor-liquid equilibria in the carbon dioxide + ethanol and carbon dioxide + 1-butanol systems*, J. Chem. Eng. Data, **36**, 303-307

Jonsson J.A., Vejrosta J., Novak J., 1982, *Air/water partition coefficients for normal alkanes (n-pentane to n-nonane),* Fluid Phase Equilibr., **9**, 279-286

Jou F.Y., Mather A.E., 2000, *Vapor-liquid-liquid locus of the system pentane + water*, J. Chem. Eng. Data, **45**, 728-729

Jou F.Y., Ng H.J., Critchfield J.E., Mather A.E., 2002, *Solubility of propane in aqueous alkanolamine solutions*, Fluid Phase Equilibr., **194–197**, 825–830

Jou F.Y., Deshmukh R.D., Otto F.D., Mather A.E., 1990, *Vapor-liquid equilibria of H2S and CO2 and ethylene glycol at elevated pressures*, Chem. Eng. Commun., **87**, 223-231

Jou F.Y., Otto F.D., Mather A.E., 1994, *Solubility of methane in glycols at elevated pressures*, Can. J. Chem. Eng., **72**, 130-133

Jou F.Y., Otto F.D., Mather A.E., 1993, *The solubility of propane in 1,2-ethanediol at elevated pressures*, J. Chem. Thermodyn., **25**, 37-40

Jou F.Y., Otto F.D., Mather A.E., 1988, *Solubility of H2S and CO2 in Ethylene Glycol at Elevated Pressures*, Energy Progress, **8**, 218-219

Joung S.N., Yoo C.W., Shin H.Y., Kim S.Y., Yoo K.P., Lee C.S., Huh W.S., 2001, *Measurement and correlation of high-pressure VLE of binary CO_2-alcohol systems (methanol, ethanol, 2-methoxyethanol and 2-ethoxyethanol),* Fluid Phase Equilibr., **185**, 219-230

Just G., 1901, *Solubility of Uses in Organic Solvents*, Z.Phys.Chem.(Leipzig), **37**, 342-367

Kaminishi G.I., Takano S., Yokoyama C., Takahashi S., Takeuchi K., 1989, *Concentration of triethylene glycol, diethylene glycol and ethylene glycol in supercritical carbon dioxide up to 16 MPa at 313.15 and 333.15 K*, Fluid Phase Equilibr., **52**, 365-372

Katayama T., Nitta T., 1976, *Solubilities of hydrogen and nitrogen in alcohols and n-hexane*, J. Chem. Eng. Data, **21**, 194-196

Katayama T., Ohgaki K., Maekawa G., Goto M., Nagano T., 1975, *Isothermal vapor-liquid equilibria of acetone - carbon dioxide and methanol - carbon dioxide systems at high pressures,* J. Chem. Eng. Jpn., **8**, 89-92

Kato M., Konishi H., Hirata M., *New apparatus for isobaric dew and bubble point method. Methanol-water, ethyl acetate-ethanol, water-1-butanol, and ethyl acetate-water systems*, J. Chem. Eng. Data, 1970, **15**(3), 435–439

Kato M., Tanaka H., Yoshikawa H., 1999, *High-pressure phase equilibrium for ethane + ethanol at 311.15 K,* J. Chem. Eng. Data, **44**, 116-117

Kendal J., Andrews J.C., 1921, *The solubilities of acids in aqueous solutions of other acids*, J. Am. Chem. Soc., **43**, 1545-1560

Khlfaoui B., Meniai A.H., Borja R., 1997, *Thermodynamic properties of water + normal alcohols and vapor-liquid equilibria for binary systems of methanol or 2-propanol with* water, Fluid Phase Equilibr., **127**, 181-80

Kim Y.S., Ryu S.K., Yang S.O., Lee C.S., 2003, *Liquid water-hydrate equilibrium measurements and unified predictions of hydrate-containing phase equilibria for methane, ethane, propane, and their mixtures*, Ind. Eng. Chem. Res., **42**, 2409-2414

Kiss A.V., Lajtai I., Thury G., 1937, *Über die löslichkeit von gasen in wasser - nichtelektrolytgemischen,* Z. Anorg. Allg. Chem., **233**, 346-352

Klots C.E., Benson B.B., 1963, *Solubilities of nitrogen, oxygen, and argon in distilled water*, J. Marine Res., **21**, 48-57

Kobayashi R., Katz D.L., 1953, *Vapor-liquid equilibria for binary hydrocarbon-water systems*, Ind .Eng.Chem., **45**(2), 440-447

Kobe K.A., Williams J.S., 1935, *Confining liquids for gas analysis: solubility of carbon dioxide in salt solutions*, Ind. Eng. Chem. Anal. Ed., **7**, 37-38

Kolbe B., Gmehling J., 1985, *Thermodynamic properties of ethanol + water. I. Vapour-liquid equilibria measurements from 90 to 150°C by the static method*, Fluid Phase Equilibr., **23**, 213-226

Korenman I.M., Aref'eva R.P., 1977, Patent USSR, 553 524, C.A. 87:87654

Kozintseva T.N., 1964, *Solubility of hydrogen sulphide in water at elevated temperature*, Geochem. Intl., **1**, 750-756

Kresheck G.C., Schneider H., Scheraga H.A., 1965, *The effect of D_2O on the thermal stability of proteins. thermodynamic parameters for the transfer of model compounds from H2O to D2O*, J. Phys. Chem., **69**, 3132-3144

Kretschmer C.B., Nowakowska J., Wiebe R., 1946, *Solubility of oxygen and nitrogen in organic solvents from -25 to 50^oC,* Ind. Eng. Chem., **38**, 506-509

Kretschmer C.B., Wiebe R., 1951, *The solubility of propane and the butanes in ethanol*, J. Am. Chem. Soc., **73** ,3778-3781

Kretschmer C.B., Wiebe R., 1952, *Solubility of gaseous paraffins in methanol and isopropyl alcohol*, J. Am. Chem. Soc., **74**(5), 1276-1277

Krichevskii I.R., Ilinskaya A.A., 1945, Zh. Fiz. Khim., 19, 621

Krichevskii I.R., Lebedeva E.S., 1947, Zh. Fiz. Khim., 21, 715

Krichevsky I., Koroleva M., 1945, *Partial molar volumes of gases dissolved in liquids. (A contribution to the thermodynamics of dilute solutions of non-electrolytes),* Acta Physicochim. (URSS), **15**, 327-348

Krichevsky I., Koroleva M., 1941, *The solubility of methanol in compressed gases,* Acta Physicochim. URSS, **15**, 327-342

Kritschewsky I.R., Schaworonkoff N.M., Aepelbaum V.A., 1935, *Combined solubility of gases in liquids under pressure: I. Solubility of carbon dioxide in water from its mixtures with hydrogen of 20 and 30 °C and total pressure of 30 kg/cm2*, Z. Phys. Chem., A **175**, 232-238

Krzyzanowska, T. and Szeliga, J., 1978, *A method for determining the solubility of individual hydrocarbons*, Nafta (Katowice), **28**, 414-417

Kunerth W., 1922, *Solubility of CO_2 and N_2O in certain solvents*, Phys. Rev., **19**, 512-524

Kunerth W., 1922, *Solubility of carbon dioxide and nitrous oxide in certain solvents*, Phys. Rev., **2**, 512-524

Kuranov G., Rumpf B., Smirnova N.A., Maurer G., 1996, *Solubility of single carbon dioxide and hydrogen sulphide in aqueous solutions of N methyldiethanolamine in the temperature range 313 -413 K at pressure up to 5 MPa*, Ind. Eng Chem. Res., **35**, 1959-1966

Kurihara K., Minoura T., Takeda K., Kojima K., 1995, *Isothermal Vapor-Liquid Equilibria for Methanol + Ethanol + Water, Methanol + Water, and Ethanol + Water*, J. Chem. Eng. Data, **40**, 679-684

Lam D.H., Luks K.D., 1991, *Multiphase equilibrium behavior of the mixture ethane + methanol +1-decanol*, J. Chem. Eng. Data, **36**(3), 307-311

Lancia A., Musmarra D., Pepe F., 1996, *Vapor-liquid equilibria for mixtures of ethylene glycol, propylene glycol, and water between 98° and 122°C*, J. Chem. Eng. Jpn., **29**, 449-455

Laursen, T. and Andersen, S. I., 2002, *High-pressure vapor-liquid equilibrium for nitrogen + methanol*, J. Chem. Eng. Data, **47**, 1173-1174

Laursen T., Rasmussen P., Andersen S.I., 2002, *VLE and VLLE measurements of dimethyl ether containing systems*, J. Chem. Eng. Data, **47**, 198-202

Lazalde-Crabtree H., Breedveld G.J.F., Prausnitz J.M., 1980, *Solvent losses in gas absorption. solubility of methanol in compressed natural and synthetic gases*, AIChE J., **26**(3), 462-470

Lazalde-Crabtree H., Breedveld G.J.F., Prausnitz J.M., 1980, *Solvent losses in gas absorption. Solubility of methanol in compressed natural and synthetic gases*, AIChE J., **26**, 462-470

Le Breton J.G., McKetta J.J., 1964, Low-*pressure solubility of n-butane in water*, Hydrocarb.Proc.& Petr.Ref., **43**(6), 136-138

Lee J.I., Mather A.E., 1977, *Solubility of hydrogen sulphide in water*, Ber. Besunges. Phys., **81**, 1021-1023

Lee H.S., Yoon J.H., Lee H., 1992, *VLE for the systems water-ethylene glycol, methanol-ethylene glycol and pentanol-ethylene glycol*, HWAHAK KONGHAK, **30**, 553-558

Lekvam K., Bishnoi P.R., 1997, *Dissolution of methane in water at low temperatures and intermediate pressures,* Fluid Phase Equilibr., **131**, 297-309

Lenoir J.Y., Renault P., Renon H., 1971, *Gas chromatographic determination of Henry's constants of 12 gases in 19 solvents*, J. Chem. Eng. Data, **16**, 340-342

Leu A.D., Robinson D.B., 1992a, *Equilibrium phase properties of the methanol-isobutane binary system,* J. Chem. Eng. Data, **37**,10-13

Leu A.D., Robinson D.B. Chung, S.Y., Chen, C.J., 1992b, *The Equilibrium Phase Properties of the Propane-Methanol and n-Butane-Methanol Binary Systems*, Can. J. Chem. Eng., **70** 330-334

Leu A.D., Carroll J.J., Robinson D.B., 1992c, *The equilibrium phase properties of the methanol-hydrogen sulfide binary system*, Fluid Phase Equilibr., **72**, 163-172

Leu A.D., Chen C.J., Robinson D.B., 1989, *Vapor-liquid equilibrium in selected binary systems,* AIChE Symp. Ser., **85**(271), 11-16

Leu A.D., Chung S.Y.K., Robinson D.B., 1991, *The equilibrium phase properties of (carbon dioxide + methanol),* J. Chem. Thermodyn., **23**, 979-985

Lide D.R., Hand Book of Chemistry and Physics, 85th ed., CRC Press, Boca Raton, FL, 2004

Li M.H., Lai M.D., 1995, *Solubility and Diffusivity of N2O and CO2 in (Monoethanolamine + N-Methyldiethanolamine + Water) and in (Monoethanolamine + 2-Amino-2-methyl-1-propanol + Water)*, J. Chem. Eng. Data, **40**, 486-492

Li Y.H., Tsui T.F., 1971, *The solubility of CO_2 in water and sea water*, J. Geophys. Res., **76**, 4203-4207

Ma P., Xu M., 1993, *Solubility data of various gases in methanol*, Tianranqi Huagong, **18**(2), 54-56

Ma Y.H., Kohn J.P., 1964, *Multiphase and Volumetric Equilibria of the Ethane-Methanol System at Temperatures between -40oC. and 100 oC*, J. Chem. Eng. Data, **9**, 3-5

Maharajh D.M., Walkley J., 1973, *Thermodynamic solubility: properties of gas mixtures. Part 1.—Two component gas mixtures in water at 25°C*, J. Chem. Soc., Faraday Trans., **1**, 842-848

Malinin S.D., Kurovskaya N.A., 1975, *Investigation of CO_2 solubility in a solution of chlorides at elevated temperatures and pressures of CO_2*, Geochem. Int., **12**, 199-201

Malinin S.D., Savelyeva N.I., 1972, *The solubility of CO2 in NaCl and CaCL2 solutions at 25, 50 and 75°C under elevated CO2 pressures*, Geochem. Int., **9**, 410-418

Malinin S.D., 1959, The *system water-carbon dioxide at high temperatures and pressures*, Geokhimiya, **3**, 235-245

Maslennikova V.Y., Vdovina N.A., Tsiklis D.S., 1971, *Solubility of water in compressed nitrogen*, Zh. Fiz. Khim., **45**, 354

Maripuri V.O., Ratcliff G.A., 1972, *Measurement of isothermal vapor-liquid equilibriums for acetone-n-heptane mixtures using modified Gillespie still*, J. Chem. Eng. Data, **17**, 366-369

Markam A.E., Kobe K.A., 1941, *The Solubility of Carbon Dioxide and Nitrous Oxide in Aqueous Salt Solutions*, J. Am. Chem. Soc., **63**, 449-454

Matous J., Sobr J., Novak J.P., Pick J., 1969, *Solubilities of carbon dioxide in water at pressure up to 40 atm*, Collect. Czech. Chem. Commun., **34**, 3982-3985

Matthews P.N., Subramanian S., Creek J., 2002, *High impact, poorly understood issues with hydrates in flow assurance*, Proceeding of the 4th international conference on gas hydrates, Yokohama, Japan

McAuliffe C., 1963, *Solubility in Water of C_1-C_9 Hydrocarbons*, Nature, **200**, 1092-1093

McAuliffe C., 1966, *Solubility in Water of paraffin, cycloparaffin, olefin, acetylene, cycloolefin, and aromatic hydrocarbons*, J. Phys. Chem., **70**, 1267-1275

McDaniel A.S., 1911, *The absorption of hydrocarbon gases by non-aqueous liquids*, J. Phys. Chem., **15**, 587-610

McGlashan M.L., Williamson A.G., 1976, *Isothermal liquid-vapor equilibriums for system methanol-water*, J. Chem. Eng. Data, **21**, 196-199

Mellan I., 1977, Industrial Solvents Handbook, Noyes Publishing: New Jersey, USA

Metschl J., 1924, *The Supersaturation of Gases in Water and Certain Organic Liquids*, J. Phys. Chem., **28**(5), 417-437

Michels A., Gerver J., Bijl A., 1936, *The influence of pressure on the solubility of gases*, Physica III, 3819-3822

Miyano Y., Hayduk W., 1986, *Solubility of butane in several polar and nonpolar solvents and in an acetone-butanol solvent solution*, J. Chem. Eng. Data, **31**, 77-80.

Mohammadi A.H., Chapoy A., Richon D., Tohidi B., 2004, *Measurements and thermodynamic modeling of vapor-liquid equilibria in ethane –water systems from 274.26 to 343.08 K*, Ind. Eng. Chem., **43**, 5418-5424

Morgan J.L.R., Pyne H.R., 1930, *Solubility relations in gas-liquid systems. I*, J. Phys. Chem., **34**, 1578-1582

Morgan O.M., Mass O., 1931, *An investigation of the equilibrium existing in gas water systems forming electrolytes*, Can. J. Res., **5**, 162-199

Morrison T.J., Billet F., 1952, *The salting-out of non-electrolytes. Part II. The effect of variation in non-electrolyte*, J. Chem. Soc., 3819-3822

Moudgil B.M., Somasundaran P., Lin L.J., 1974, *Automated constant pressure reactor for measuring solubilities of gases in aqueous solutions*, Rev Sci Instrum., **45**, 406-409

Muller C.Z., 1913, *Absorption of Oxygen, Nitrogen, and Hydro-gen by Aqueous Solutions of Non-electrolytes*, Z. physik. Chem., **81**, 483-503

Muller G., Bender E., Maurer G., 1988, *Das Dampf-Flüssigkeitsgleichgewicht des ternären systems ammonik-kolhendioxid wasser bei hohen wassergehalten im bereich zwischen 373 und 473 K*, Ber. Bunsenges. Phys. Chem., **92**, 148-160

Murray C.N., Riley J.P., 1971, *Solubility of gases in distilled water and sea water .4. carbon dioxide*, Deep. Sea. Res., **18**, 533-541

Murray C.N., Riley J.P., Wilson T.R.S., 1969, *The solubility of gases in distilled water and sea water—I. Nitrogen*, Deep Sea Res., **16**, 297-310

Nagahama K., Suda S., Hakuta T., Hirata M., 1971, *Determination of vapor-liquid equilibrium from total pressure measuremen*t, Sekiyu Gakkaishi, **14**, 252-258

Nagahama K., Suda S., Hakuta T., Hirata M., 1971, *Determination of vapor-liquid equilibrium from total pressure measurement. C_3 hydrocarbon/solvent*, Sekiyu Gakkaishi, **14**, 252-256

Najibi H., Chapoy A., Haghighi H., Tohidi B., 2008, *Experimental determination and prediction of methane hydrate stability in alcohols and electrolyte solutions*, Fluid Phase Equilibr., **275**, 127–131

Namiot A.Y., 1961, *Solubility of nonpolar gases in water*, J. Struct. Chem., **2**, 381-389

Namiot, A.Y., Bender S.Y., 1960, Khim. Tekhnol. Topl. Nasel, **7**, 52-55

Nath A., Bendert E., 1983, *Isothermal vapor-liquid equilibriums of binary and ternary mixtures containing alcohol, alkanolamine, and water with a new static device*, J. Chem. Eng. Data, **28**, 370-375

Nelson H.D., de Ligny C.L., 1968, *The determination of the solubilities of some n-alkanes in water at different temperatures, by means of gas chromatography*, Rec. Trav. Chim. Pays-Bas, **87**, 528-544

Ochi K., Kojima K., 1987, J. Chem. Eng. Japan, **20**, 6-10

Ohgaki K., Katayama T., 1976a, *Isothermal vapor-liquid equilibrium data for binary systems containing carbon dioxide at high pressuers: methanol - carbon dioxide, n-hexane - carbon dioxide, and benzene - carbon dioxide*, J. Chem. Eng. Data, **21**, 53-55

Ohgaki K., Sano F., Katayama T., 1976b, *Isothermal vapor-liquid equilibrium data for binary systems containing ethane at high pressure*, J. Chem. Eng. Data, **21**(1), 55-58

Oleinik P.M., 1986, *Method of evaluating gases in liquids and volumetric properties of solutions under pressure*, Neft. Prom-st., Ser. "Neftepromysl. Delo"(in Russian)

Olsen J.C., Brunjes A.S., Qlsen J.W., 1930, *Freezing and flow points for glycerol, prestone, denatured alcohol, and methanol*, Ind. Eng. Chem., **22**, 1315-1317

Orchille´s A.V., Miguel P.J., Vercher E., Martı´nez-Andreu A., 2008, *Isobaric vapor-liquid equilibria for 1-propanol + water + 1-ethyl-3-methylimidazolium trifluoromethanesulfonate at 100 kPa*, J. Chem. Eng. Data, **53**, 2426–2431

O'Sullivan T.D., Smith N.O., 1970, *The solubility and partial molar volume of nitrogen and methane in water and aqueous sodium chloride*, J. Phys. Chem., **74**, 1460-1466

O'Sullivan T.D., Smith N.O., Nagy B., 1966, *Solubility of natural gases in aqueous salt solutions—III Nitrogen in aqueous NaCl at high pressures*, Geochim. Cosmochim. Acta., **30**, 617-619

Ott J.B., Goates J.R., *Waite B.A., (Solid + liquid) phase equilibria and solid-hydrate formation in water + methyl, + ethyl, + isopropyl, and + tertiary butyl alcohols*, J. Chem. Thermodyn., **11**, 1979, 739-746

Page S.H., Goates S.R., Lee M.L., 1993, *Methanol/CO2 phase behavior in supercritical fluid chromatography and extraction*, J. Supercrit. Fluids, **4**, 109-117

Petty L.B. Smith J.M., 1955, *Volumetric behavior of the methanol - n-butane system*, Ind. Eng. Chem., **47**, 1258-1265

Pierotti R.A., 1965, *Aqueous Solutions of Nonpolar Gases*, J. Phys. Chem., **69**, 281-288

Pierotti R.A., Liabastre A.A., 1972, *Structure and properties of water solutions*, U.S. Nat. Tech. Inform. Serv., PB Rep., No. 21163, 113

Pohl H.A., 1961, *Thermodynamics of the hydrogen sulfide -water system relevant to the dual temperature process for the production of heavy water*, J. Chem. Eng. Data, **6**(4), 515- 521

Polak J., Lu B.C.Y., 1973, *Mutual solubilities of hydrocarbons and water at 0 and 25^{o}C*, Can. J. Chem., **51**, 4018-4023

Postigo M.A., Katz M., 1987, *Solubility and thermodynamics of carbon-dioxide in aqueous ethanol solutions*, J. Solution Chem., **16**, 1015-1024

Pray H.A., Schweickert C.E., Minnich B.H., 1952, *Solubility of hydrogen, oxygen, nitrogen, and helium in water*, Ind. Eng. Chem., **44**(5), 1146-1151

Price L.C., 1979, *Aqueous Solubility of Methane at elevated Pressures and Temperatures*, Am. Assoc. Pet. Geo. Bull., **63**, 1527-1533

Prytz K., Holtt H., 1895, Ann. Phys. Chem., **54**, 130-138

Purwanto Y.A., Oshita S., Seo Y., Kawagoe Y., 2001, *Concentration of liquid foods by the use of gas hydrate*, J. Food Eng., **47**, 133-138

Pushin N.A., Glagoleva A.A., 1922, J. Chem. Soc. Trans., **121**, 2813-2834

Reamer H.H., Sage B.H., Lacey W.N., 1952, *Phase equilibria in hydrocarbon systems. n-butane-water system in the two-phase region*, Ind. Eng. Chem., **44**, 609-615

Reichl, 1996, PhD Dissertation, Technical University, Berlin

Reighard T.S., Lee S.T., Olesik S.V., 1996, *Determination of methanol/CO_2 and acetonitrile/CO_2 vapor-liquid phase equilibria using a variable-volume view cell*, Fluid Phase Equilibr., **123**, 215-230

Reimers J.L., Bhethanabotla V.R., Campbell S.W., 1992, *Total pressure measurements for pentane + methanol + ethanol at 303.15 K*, J. Chem. Eng. Data, **37**, 127-130

Rettich T.R., Handa Y.P., Battino R., Wilhelm E., 1981, *Solubility of gases in liquids. 13. High-precision determination of Henry's constants for methane and ethane in liquid water at 275 to 328 K*, J. Phys. Chem., **85**, 3230-3237

Rice P.A., Gale R.P., Barduhn A.J., 1976, *Solubility of butane in water and salt solutions at low temperatures*, J. Chem. Eng. Data, **21**, 204-206

Rieder R.M., Thompson A.R., 1949, *Vapor–liquid equilibria measured. by a Gillespie still. ethyl alcohol–water system*, Ind. Eng. Chem., **41**, 2905-2908

Ross, H.K., 1954, *Cryoscopic studies - concentrated solutions of hydroxy compounds*, Ind. Eng. Chem., **46**(3), 601-610

Rudakov E.S., Lutsyk A.I., 1979, *The solubility of sturated hydrocarbons in aqueous sulphuric acid*, Russ. J. Phys. Chem., **53**, 731 –733

Ruffine L., Barreau A., Brunella I., Mougin P., Jose J., 2005, *New apparatus for low-temperature investigations: measurements of the multiphase equilibrium of mixtures containing methane, ethane, propane, butane, methanol, and carbon dioxide*, Ind. Eng. Chem. Res., **44**, 8387-8392

Saddington A.W., Krase N.W., 1934, *Vapor-liquid equilibria in the system nitrogen-water*, J. Am. Chem. Soc., **56**(2), 353-361

Sanchez M., Coll R., 1978, *Water-propane system at high-pressures and temperatures .1. 2-phase region*, An. Quim., *74, 1329-1335* and Sanchez, M. and Coll, R., 1978,

Water-propane system at high-pressures and temperatures .2. homogeneous region, An. Quim., **74**, 1336-1339

Sanchez M., de Meer F., 1978, *Equilibrio liquido-vapor del sistema metano-agua para altas presiones y temperaturas comprendidas entre 150 y 300°C*, An. Quim., **74**, 1325-1328

Schlichting H., Langhorst R., Knapp H., 1993, *Saturation of high pressure gases with low volatile solvents: Experiments and correlation*, Fluid Phase Equilibr., **84**, 143-163

Schneider R., 1978, PhD Thesis, TUB, Berlin

Schroedter F., Melzer W.M., Knapp H., 1991, *Investigation of phase equilibria in multicomponent mixtures consisting of propane, carbon dioxide, water and various organic solvents : Part I: Experimental methods, equipment and procedures; results with test systems consisting of CO_2, C_3H_8 and CH_3OH*, Gas Sep. Purif., **5**, 161-172

Selleck F.T., Carmichael L.T., Sage B.H., 1952, *Phase behavior in the hydrogen sulfide – water system*, Ind. Eng. Chem., **44**(9), 2219-2226

Semenova A.I., Emelyanova E.A.,Tsimmerman S.S., Tsiklis D.S., 1979, *Phase equilibria in the methanol - carbon dioxide system*, Russ. J. Phys. Chem. (Engl. Transl.), **53**, 1428-1430

Semenova, A. I.; Emelyanova, E.A., Tsimmerman S.S., Tsiklis D.S., 1979, *Phase equilibria in the methanol - carbon dioxide system*, Zh. Fiz. Khim., **53**, 2502

Seo J., Lee J., Kim H., 2000, *Isothermal vapor-liquid equilibria for ethanol and n-pentane system at the near critical region*, Fluid Phase Equilibr., **172**, 211-219

Servio P., Englezos P., 2002, *Measurement of dissolved methane in water in equilibrium with its hydrate*, J. Chem. Eng. Data, **47**, 87–90

Shagiakhmetov R.A., Tarzimanov A.A., 1981, *Measurements of CO_2 solubility in water up to 60 MPa*, Deposited Document SPSTL 200khp-D81-1982

Shedlovsky T., Mac Innes D.A., 1935, *The first ionization constant of carbonic acid, 0 to 38, from conductance measurements*, J. Am. Chem. Soc., **57**, 1705-1710

Shenderei E.R., Zelvenskii Y.D., Ivanovskii F.P., 1961, Gazov. Prom-st, **6**(3), 42-45

Shenderei E.R., Zelvenskii Y.D., Ivanovskii F.P., 1961, Khim. Prom-st (Moscow), **5**, 309

Shenderei E.R., Zelvenskii Y.D., Ivanovskii F.P., 1959, *Solubility of carbon dioxide in methanol at low temperatures and high pressures*, Khim. Prom-st (Moscow), **4**, 328

Shenderei E.R., Zelvenskii Y.D., Ivanovskii F.P., 1958, *The solubility of carbon dioxide in alcohols at low temperatures*, Gazov. Prom-st, **3**(12), 36-42

Short I., Sahgal A., Hayduk W., 1983, *Solubility of ammonia and hydrogen sulfide in several polar solvents*, J. Chem. Eng. Data, **28**, 63-66

Sloan E.D., 1998, Clathrate Hydrates of Natural Gases. Marcel Dekker Inc., New York

Smith N.O., Kelemen S., Nagy B., 1962, *Solubility of natural gases in aqueous salt solutions—II : Nitrogen in aqueous NaCl, $CaCl_2$, Na_2SO_4 and $MgSO_4$ at room temperatures and at pressures below 1000 psia*, Geochim. Cosmochim. Acta., **26**, 921-926

Song K.Y., Fneyrou G., Martin R., Lievois J., Kobayashi R., 1997, *Solubility measurements of methane and ethane in water and near hydrate conditions*, Fluid Phase Equilibr., **128**, 249-260

Spangler J., Davies E., 1943, *Freezing points, densities, and refractive indexes of system glycerol-ethylene glycol-water*, Ind. Eng. Chem. Anal. Ed., 15, 96-99

Sparks K.A., Sloan E.D., 1983, *Water content of NGL in presence of hydrates*, Research Report 71, GPA, Tulsa, OK

Stewart P.B., Munjal P., 1970, *Solubility of carbon dioxide in pure water, synthetic sea water, and synthetic sea water concentrates at -5.deg. to 25.deg. and 10- to 45-atm. pressure*, J. Chem. Eng. Data., **15**, 67-71

Stoessel R.K., Byrne P.A., 1982, *Salting-out of methane in single-salt solutions at 25°C and below 800 psia,* Geochim. Cosmochim. Acta, **46**, 1327-1332

Suleimenov O.M., Krupp R.E., 1994, *Solubility of hydrogen sulphide in pure water and in NaCl solutions from 20 to 32^oC and at saturation pressures*, Geochimica et Cosmochimica Acta, **58**(11), 2433-2444

Sultanov R.G., Skripka V.G., Namiot A.Y., 1971, *Rastvormost metana v vode pri novysjennykh temperaturakh I davlenijakh*, Gaz. Prom., **16**, 6-7

Suzuki K., Sue H., Itou M., Smith R.L., Inomata H., 1990, *Isothermal vapor-liquid equilibrium data for binary systems at high pressures: carbon dioxide-methanol, carbon dioxide-ethanol, carbon dioxide-1-propanol, methane-ethanol, methane-1-propanol, ethane-ethanol, and ethane-1-propanol systems*, J. Chem. Eng. Data, **35**, 63-66

Takishima S., Saiki K., Arai K., Saito S., 1986, *Phase equilibria for CO_2-C_2H_5OH-H_2O system*, J. Chem. Eng. Jpn., **19**, 48–56

Tanaka H., Kato M., 1995, *Vapor-liquid equilibrium properties of carbon dioxide + ethanol mixtures at high pressures*, J. Chem. Eng. Jpn., **28**, 263-266

Tian Y.L., Han M., Chen L., Feng J.J., Qin Y., 2001, *Study on vapor-liquid phase equilibria for CO2-C2H5OH system*, Chin. J. Inorg. Chem., **17**, 155-160

Tokunaga J., 1975, *Solubilites of oxygen, nitrogen, and carbon dioxide in aqueous alcohol solutions,* J. Chem. Eng. Data, **20**, 41-46

Tokunaga J., Kawai M., 1975, *Solubilities of methane in methanol water and ethanol water solutions*, J. Chem. Eng. Jpn., **8**, 326-327

Tokunaga J., 1975, *Solubilities of oxygen, nitrogen, and carbon dioxide in aqueous alcohol solutions*, J. Chem. Eng. Data, **20**, 41-46

Tokunaga J., Nitta T., Katayama T., 1969, *Solubility of carbon dioxide in aqueous alcohol solutions*, **33**, 775-779

Trimble H.M., Potts W., 1935, Glycol-water mixtures vapor pressure-boiling point-composition relations, Ind. Eng. Chem., **27**, 66-68

Ukai T., Kodama D., Miyazaki J., Kato M., 2002, *Solubility of methane in alcohols and saturated density at 280.15 K*, J. Chem. Eng. Data, **47**, 1320-1323

Umano S., Nakano Y., 1958, Kogyo Kagaku Zasshi, 61, 536

Usyukin I.P., Shleinikov V.M., 1963, Nauchn. Tekhn.., **1**, 39

Valtz A., Chapoy A., Coquelet C., Paricaud P., Richon D., 2004, *Vapour - Liquid Equilibria in the Carbon Dioxide – Water System, Measurement and Modelling from 278.2 to 318.2 K*, Fluid Phase Equilibr., **226**, 333-344

van Slyke D.D., 1939, *Determination of solubilities of gases in liquids with use of the van slyke-neill manometric apparatus for both saturation and analysis*, J. Biol. Chem., **130**, 545-554

Verdet M., 1855, Ann. Chim. Phys., **43**, 496-507

Versteeg G.F., VanSwaij W.V., 1988, *Solubility and diffusivity of acid gases (carbon dioxide, nitrous oxide) in aqueous alkanolamine solutions*, J. Chem. Eng. Data, **33**, 29-48

Villamanan M.A., Gonzalez C., van Ness H.C., 1984, *Excess thermodynamic properties for water/ethylene glycol*, J. Chem. Eng. Data, **29**, 427-429

Wallace C.B., 1985, *Drying supercritical CO2 demands care*, Oil Gas J., **83**(25), 98–104

Wang L.K., Chen G.J., Han G.H., Guo X.Q., Guo T.M., 2003, *Experimental study on the solubility of natural gas components in water with or without hydrate inhibitor*, Fluid Phase Equilibr., **207**(1-2), 143-154

Wang Y., Han B., Yan H., and Liu, R., 1995, *Solubility of CH_4 in the mixed solvent t-butyl alcohol and water*, Thermochim. Acta., **253**, 327-334

Washburn E.W., 1926–1930, International Critical Tables (ICT) of Numerical Data, Physics, Chemistry and Technology. National Research Council

Weber W., Zeck S., Knapp H., 1984, *Gas solubilities in liquid solvents at high pressures: apparatus and results for binary and ternary systems of N2, CO2 and CH3OH*, Fluid Phase Equilibr., **18**, 253-278

Wehe A.H., McKetta J.J., 1961, *Method for determining total hydrocarbons dissolved in water*, Anal. Chem., **33**(2), 291-293

Wen W.Y., Hung J.H., 1970, *Thermodynamics of hydrocarbon gases in aqueous tetraalkylammonium salt solutions*, J. Phys. Chem., **74**, 170-180

Wetlaufer D.B., Malik S.D., Stoller L., Coffin R.L., 1964, *Nonpolar group participation in the denaturation of proteins by urea and guanidinium salts. Model compound studies*, J. Am Chem Soc., **86**, 508-515

Wiebe R., Gaddy V.L., 1939, *The solubility in water of carbon dioxide at 50, 75 and 100°C, at pressures to 700 atmospheres*, J. Am. Chem. Soc., **61**, 315–318

Wiebe R., Gaddy V.L., 1940, *The solubility in water of carbon dioxide from 12 to 40°C and at pressures to 500 atmospheres: Critical Phenomena*, J. Am. Chem. Soc., **62**, 815–817

Wiebe R., Gaddy V.L., Heins C., 1932, *Solubility of nitrogen in water at 25°C from 25 to 1000 atmospheres*, Ind. Eng. Chem., **24**, 927-933

Wilcock R.J., Battino R., 1974, *Solubility of oxygen-nitrogen mixture in water*, Nature, **252**, 614-615

Winkler L.W., 1901, *Die Loslichkeit der gas in wasser*, Chem. Ber., **34**, 1408-1422

Winkler L.W., 1906, *Gesetzmäßigkeitbei der Absorption der gase in Flüssigkeiten*, Z. Phys. Chem., **55**, 344-354

Wishnia A., 1963, *The hydrophobic contribution to micelle formation: the solubility of ethane, propane, butane, and pentane in sodium dodecyl sulfate solution*, J. Phys. Chem., **67**, 2079 –2082

Wright R.H., Maas O., 1932, *The solubility of hydrogen sulphide in water from the vapor pressures of the solutions*, Can. J. Res., **6**, 94–101

Xia J., Jodecke M., Perez-Salado Kamps A., Maurer G., 2004, *Solubility of CO_2 in (CH3OH + H2O)*, J. Chem. Eng. Data, **49**(6), 1756-1759

Yaacobi M., Ben-Naim A., 1973, *Hydrophobic interaction in water-ethanol mixtures*, J. Soln. Chem., **2**, 425-443

Yaacobi M., Ben-Naim A., 1974, *Solvophobic interaction*, J. Phys. Chem., **78**, 175-178

Yamamoto H., Tokunaga J., 1994, *Solubilities of nitrogen and oxygen in 1,2-ethanediol + water at 298.15 K and 101.33 kPa*, J. Chem. Eng. Data, **39**, 544-547

Yang S.O., Cho S.H., Lee H., Lee C.S., 2001, *Measurement and prediction of phase equilibria for methane + water in hydrate forming conditions*, Fluid Phase Equilibr., **185**, 53-63

Yang S.O., Yang I.M., Kim Y.S., Lee C.S., 2000, *Measurement and prediction of phase equilibria for water + CO2 in hydrate forming conditions*, Fluid Phase Equilibr., **175**, 75–89

Yano T., Suetaka T., Umehara T., Horiuchi A., 1974, *Solubilities of methane, ethylene, and propane in aqueous electrolyte solutions*, Kagaku Kogaku, **38**(4), 320-323

Yao J., Li H., Han S., 1999, *Vapor–liquid equilibrium data for methanol-water-NaCl at 45°C*, Fluid Phase Equilibr., **162**, 253–260

Yarym-Agaev N.L., Sinyavskaya R.P., Koliushko I.I., Levinton L.Y., 1985, Zh. Prikl. Khim., **58**, 165-168

Yeh S.Y., Peterson R.E., 1964, *Solubility of carbon dioxide, krypton and. xenon in aqueous solutions*, J. Pharm. Sci., **53**, 822-824

Yeo S.D., Park S.J., Kim J.W., Kim J.C., 2000, *Critical properties of carbon dioxide + methanol, + ethanol, + 1-propanol, and + 1-butanol*, J. Chem. Eng. Data, **45**, 932-935

Yokoyama C., Wakana S., Kaminishi G.I., Takahashi S., 1988, *Vapor-Liquid Equilibria in the Methane-Diethylene Glycol-Water System at 298.15 and 323.15 K*, J. Chem. Eng. Data, **33**, 274 -276

Yonker C.R., Linehan J.C., Fulton J.L., 1998, *The use of high pressure NMR for the determination of phase behavior for select binary solvent systems*, J. Supercrit. Fluids, **14**, 9-16

Yoon J.H., Lee H.S., Lee H., 1993, *High-pressure vapor-liquid equilibria for carbon dioxide + methanol, carbon dioxide + ethanol, and carbon dioxide + methanol + ethanol*, J. Chem. Eng. Data, **38**, 53-55

Yorizane M., Sadamoto S., Masuoka H., Eto Y., 1969, *Gas solubilities in methanol at high pressures*, Kogyo Kagaku Zasshi, **72**, 2174

Zabaloy M.S., Gros H.P., Bottini S.B., Brignole E.A., 1994, *Isothermal Vapor-Liquid Equilibrium Data for the Binaries Isobutane-Ethanol, Isobutane-1-Propanol, and Propane-Ethanol,* J. Chem. Eng. Data, **39**, 214

Zawisza A., Malesinska B., 1981, *Solubility of carbon dioxide in liquid water and of water in gaseous carbon dioxide in the range 0.2 – 5 MPa and at temperatures up to 473 K*, J. Chem. Eng. Data, **26**, 388–391

Zeck S., Knapp H., 1985, *Solubilities of ethylene, ethane and carbon dioxide in mixed solvents consisting of methanol, acetone and water*, Int. J. Thermophys., **6**, 643-656

Zeck, 1984, PhD Thesis, University of Amsterdam, Spain

Zel'vinskii Y.D., 1937, *On the solubility of carbon dioxide in water under pressure*, Zhurn. Khim. Prom., **14**, 1250–1257

Zheng D.Q., Ma W.D., Wei R., Guo T.M., 1999, *Solubility study of methane, carbon dioxide and nitrogen in ethylene glycol at elevated temperatures and pressures*, Fluid Phase Equilibr., **155**, 277-286

Zhu H.G., Tian Y.L., Chen L., Feng J.J., Fu H.F., 2002, *Studies on vapor-liquid phase equilibria for CO_2 + CH_3OH and CO_2 + C_2H_5OH supercritical systems*, Gaodeng Xuexiao Huaxue Xuebao, **23**, 1588-1591

Zhu H., Tian Y.L., Chen L., Qin Y., Feng J.J., 2001, *High-pressure phase equilibria for binary ethanol system containing supercritical CO2*, Chin. J. Chem. Eng., **9**, 322-325

Zielkiewicz J., Konitz A., 1991, *(Vapor + liquid) equilibria of (N, N-dimethylformamide + water + propan-1-ol) at the temperature 313.15 K.*, J. Chem. Thermodyn., **23**, 59-65

CHAPTER 3 – THERMODYNAMIC MODELLING

3.1 Introduction

An equation of state (EoS) is an analytical expression relating pressure (P) to temperature (T) and volume (V). A proper description of this PVT relationship for real hydrocarbon fluids plays an important role in chemical and petroleum engineering design and they have assumed an expanding role in the study of phase equilibria of fluids and fluid mixtures. Many equations of state have been proposed in the literature with either an empirical, semi-empirical or theoretical basis. Finding the proper EoS for a given system is a real challenge (Orbey and Sandler, 1998, and Reid et al., 1987). These equations have two or more adjustable parameters which can be fitted to experimental data. These EoS often give good results for mixtures of nonpolar (Soave, 1972, and Peng and Robinson, 1976) and slightly polar components (Huron et al., 1978, Asselineau et al., 1978, and Graboski and Daubert, 1978). However, for substances that have the ability to form strong associating bonding interactions between molecules, like hydrogen bonding, predictions are poor. In the last fifteen to twenty years, as a result of advances in statistical mechanics and computer power, significant progress has been made in the statistical theory of associating fluids. The idea behind the statistical theory is that the Helmholtz free energy of a fluid can be split into several contributions. Each contribution covers a specific kind of interaction within the molecules or between the molecules. Examples of EoS resulting from this are SAFT (Statistical Associating Fluid Theory) using Wertheim's theory, (Chapman et al., 1990, and Huang and Radosz, 1990) and APACT (Associated Perturbed Anisotropic Chain Theory) (Ikonomou and Donohou, 1988).

These EoS give much more insight into how the physics on a molecular level determines the macroscopic behaviour of a fluid. Once the parameters of these EoS have been fitted to experimental data, they are able to predict the phase behaviour of highly non-ideal systems. Moreover, for systems for which no experimental data are available, parameters can often be extrapolated from similar systems. The disadvantage of these EoS is their complexity, even for non-associating fluid mixtures. It has therefore been proposed to combine the association term from the statistical associating fluid theory with a cubic equation of state. In short, these models are called CPA, which stands for cubic plus association. In a number of papers by Kontogeorgis et al.

the Soave-Redlich-Kwong (SRK) EoS in combination with the association term of SAFT has proven to give good descriptions of the phase behaviour of mixtures of alkanes, alcohols and water (Kontogeorgis et al., 2006a). The equation combines the simplicity of a cubic equation of state, SRK (the Soave-Redlich-Kwong, 1972), and the theoretical background of the perturbation theory employed for the association part. The predictions are comparable to the predictions from the original SAFT model by Huang and Radosz (Yakoumis et al., 1998, and Voutsas et al., 2000). The price of this gain in simplicity is of course the loss of physical insight. However, if the main goal is to have an accurate description of the phase behaviour of a system, and experimental data to which parameters can be fitted are available, then CPA is to be preferred to equations like SAFT.

Further to the above, a rigorous thermodynamic model based on the equality of chemical potential of each component throughout all phases is developed to model the phase equilibria. In this thesis, for systems containing a compound(s), which can form hydrogen bond (e.g., water, methanol, monoethylene glycol and etc), the Cubic-Plus-Association equation of state (CPA-EoS) has been employed. The CPA-EoS has been extended to predict fluid phase equilibria in the presence of single or mixed electrolyte solutions over a wide range of operational conditions. The hydrate-forming condition has been modelled by the solid solution theory of van der Waals and Platteeuw (1959). Langmuir constants have been calculated using the Kihara potential model (Kihara, 1953). A detail description of the approach is outlined in this chapter. Model predictions were validated against independent experimental data and a good agreement between predictions and experimental data has been observed, supporting the reliability of the developed model.

3.2 Thermodynamic Modelling

For a system at equilibrium, from a thermodynamic view point, the chemical potential of each component throughout the system must be uniform. For an isothermal system this will reduce to the equality of fugacity of each component in different phases. The fugacity of components in each phase has been calculated by the Cubic-Plus-Association (CPA) EoS. The CPA EoS combines the well known Soave-Redlich-Kwong (SRK) EoS for describing the physical interactions with the Wertheim's first-order perturbation theory (1987), which can be applied to different types of hydrogen-bonding compounds. The parameters for pure water, alcohols and glycols (associating

compounds) in the CPA EoS have been determined by Kontogeorgis et al. (1999). When salt is present, the fugacity of non-electrolyte compound in the aqueous phase is calculated by combining the EoS with the Debye-Hückel electrostatic contribution term (Aasberg-Petersen et al., 1991 and Tohidi-Kalorazi, 1995). The CPA EoS has been selected for the modelling as it adequately describes the effect of alcohols and water on phase equilibria (Folas et al., 2005). In the present work, the CPA EoS has been extended to take into account the effect of eight different salts on the fluid phase equilibria of mixtures when aqueous electrolytes solution presents. As mentioned above, the hydrate-forming conditions are modelled by the solid solution theory of van der Waals and Platteeuw (1959). Langmuir constants have been calculated by using Kihara potential parameters tuned to methane hydrate dissociation data (Kihara, 1953).

3.3 Introduction to CPA

Species forming hydrogen bonds often exhibit unusual thermodynamic behaviour due to the strong attractive interactions between molecules of the same species (self-association) or between molecules of different species (cross-association) (Atkins and de Paula, 2006). These interactions may strongly affect the thermodynamic properties of the fluids. Thus, chemical equilibria between clusters should be taken into account in order to develop a reliable thermodynamic model.

The Cubic-Plus-Association (CPA) model is an equation of state that combines the cubic SRK equation of state and an association (chemical) term described below and can be expressed in terms of compressibility factors Z as:

$$\begin{aligned} Z^{CPA} &= Z^{SRK} + Z^{Assoc.} \\ Z^{SRK} &= \frac{v}{v-b} - \frac{a}{RT(v+b)} \\ Z^{Assoc.} &= -\frac{1}{2}\left(1+\rho\frac{\partial \ln g}{\partial \rho}\right)\sum_i \sum_{A_i} x_i\left(1-X^{A_i}\right) \end{aligned} \qquad (3.1)$$

The compressibility factor contribution from the SRK equation of state is Z^{SRK} and the contribution from the association term is Z^{CPA}.

Where v is the molar volume, X_{A_i} is the mole fraction of the molecule i not bonded to the site A, i.e., the monomer fraction, and x_i is the superficial (apparent) mole fraction of component i. The small letter i is used to index the molecules and capital letter A is used to index the bonding sites on a given molecule.

While the SRK model accounts for the physical interaction contribution between the species, the association term in CPA takes into account the specific site-site interaction due to hydrogen bonding. The association term employed in CPA is identical to the one used in SAFT.

Before describing the model, it is essential to give the definitions of "sites" and "site-related" parameters used in CPA and SAFT models.

3.4 Association Energy and Volume

The key features of the hydrogen-bonds are their strength, short range and highly orientation dependent site to site attraction. In Figure 3.1 a simple example of prototype spheres, or spherical segments, with one associating site, A is shown. The associating sites are modelled in CPA as square-well sites as seen in Figure 3.1 (Kontogeorgis et al., 1996). Such spheres can only form an AA-bonded dimer when both distance and orientation are favourable.

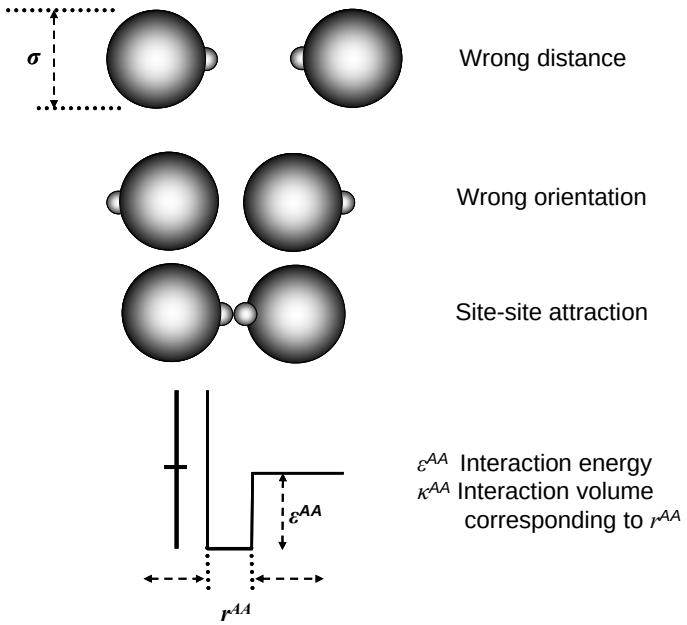

Figure 3.1 Square-well potential and an illustration of site-to-site distance and orientation (Chapman et al., 1990)

The associating bond strength is quantified by a square-well potential, which, in turn, is characterised by three parameters. The flexibility arises from the square-well potential's three parameters: The parameter ε^{AA} characterises the association energy

(well depth), and the parameter κ^{AA} characterises the association volume (corresponds to the well width r^{AA}).

3.5 Fraction of Non-bonded Associating Molecules, X_A

Since the mixture contains not only monomer species but also associated clusters, it is necessary to define the mole fraction (X) for all the components. The mole fraction of all the molecules of component i is x_i. The mole fraction of (chain) molecules i that are not-bonded to the site A is X^{Ai}, and hence $1\text{-}X^{Ai}$ is the mole fraction of molecules i that are bonded to the site A. This definition applies to both pure self-associated compounds and to mixtures.

The CPA EoS can be expressed for mixtures in terms of pressure P (Kontogeorgis et al., 1999):

$$P = \frac{RT}{V_m - b} - \frac{a_0.\alpha(T)}{V_m(V_m + b)} - \frac{1}{2}\frac{RT}{V_m}\left(1 + \rho\frac{\partial \ln(g)}{\partial \rho}\right)\sum_i x_i \sum_{A_i}\left(1 - X^{A_i}\right) \qquad (3.2)$$

where the physical term is that of the SRK EoS and the association term is taken from the SAFT EoS (Huang and Radosz, 1990), x_i is the mole fraction of the component i and X^{A_i} is the mole fraction of molecule i not bonded to the site A which is rigorously related to the association strength. Both depend on the structure of the molecule and the number and type of sites.

The site fraction, X^{A_i} is related to the association strength between the site A on a molecule i, the site B on another molecule j, $\Delta^{A_iB_j}$ and the fractions X_B of all other kind of association sites B by:

$$X^{A_i} = \frac{1}{1 + \rho\sum_j n_j \sum_{B_i} X^{B_i}\Delta^{A_iB_i}} \qquad (3.3)$$

where ρ is the molar density of the fluid, x_j is the mole fraction of substance j, X^{A_i} is related to the association strength between site A and site B on the molecule, and $\Delta^{A_iB_j}$, the association strength, is the key quantity in the CPA EoS. Both X^{A_i} and $\Delta^{A_iB_j}$ depend on the structure of the molecule and the number and type of sites. The association strength between site A on molecule i and site B on molecule j is given by:

$$\Delta^{A_iB_j} = g(d)^{simp.}\left[\exp\left(\frac{\varepsilon^{AB}}{RT}\right)-1\right]\beta^{A_iB_j}b \tag{3.4}$$

where $g(d)^{simp.}$ is the simplified expression of the radial distribution function as suggested by Kontogeorgis et al. (1999), b is the co–volume parameter from the cubic part of the model, β and ε are the association volume and energy parameters of CPA, respectively. The latter two parameters are in most cases estimated, together with the three physical term parameters, using vapour pressure and density of pure compounds. The simplified expression of the radial distribution function is:

$$g(d)^{simp.} = \frac{1}{1-1.9\eta} \tag{3.7}$$

where η is the reduced fluid density given as:

$$\eta = \frac{1}{4}b\rho = \frac{b}{4V_m} \tag{3.6}$$

where ρ is the fluid density and the co–volume parameter, b, is assumed to be temperature independent, in agreement with most popular equations of state.

The energy parameter of Equation 3.2, $\alpha(T)$, is defined using a Soave type temperature dependency for the association compound used for the fugacity calculations in this work.

$$\alpha(T) = \left[1 + C_1\left(1-\sqrt{T_r}\right)\right]^2 \tag{3.8}$$

where C_1 is the pure component parameter of CPA and reduced temperature (T_r) is defined in the conventional way T/T_C. The CPA model has five pure compound parameters; three for non-associating compounds (a_0, b and C_1) and two for additional parameters for associating compounds ($\varepsilon^{A_iB_j}$ and $\beta^{A_iB_j}$). The CPA EoS parameters for the association compound used in this work are listed in Table 3.1.

For inert compounds, the CPA parameters a and b are calculated from critical point conditions, similar to the van der Waals EoS. Mathias & Copeman alpha function (Mathias and Copeman, 1983) is used for temperature dependency of the attractive term to ensure an accurate representation of vapour pressures of pure compounds, as detailed below:

$$a = \frac{\Omega_a R^2 T_c^2}{P_c}$$

$$b = \frac{\Omega_b R T_c}{P_c} \tag{3.9}$$

$$\Omega_a = 0.66121 - 0.76105 Z_c$$

$$\Omega_b = 0.02207 + 0.20868 Z_c$$

where Z_c is the critical compressibility factor, and ω is the acentric factor. The Mathias & Copeman alpha function parameters for the inert compounds used in this work is presented below:

$$a(T) = \left[1 + C_1\left(1 - \sqrt{T_r}\right) + C_2\left(1 - \sqrt{T_r}\right)^2 + C_3\left(1 - \sqrt{T_r}\right)^3\right]^2$$

$$\text{if } T > T_C \text{ then} \tag{3.10}$$

$$a(T) = \left[1 + C_1\left(1 - \sqrt{T_r}\right)\right]^2$$

Table 3.1 CPA Parameters for the associating compounds considered in this work

	a_0 (bar L^2 mol^{-2})	b (L/mol)	C_1	ε (bar L mol^{-1})	β ($\times 10^3$)	Reference
Water	1.228	0.01452	0.6736	166.55	69.2	Kontogeorgis et al. (1999)
Methanol	4.053	0.03098	0.4310	245.91	16.1	Kontogeorgis et al. (1999)
Ethanol	8.672	0.04908	0.7369	215.32	8.0	Folas et al. (2005)
MEG	10.819	0.05140	0.6744	197.52	14.1	Derawi et al. (2003a)

In order to predict the two phase VLE equilibrium condition at a given temperature and pressure, the algorithm with a flow diagram presented in Figure 3.2 for the CPA EoS has been applied. The procedure is the same for liquid-liquid equilibria.

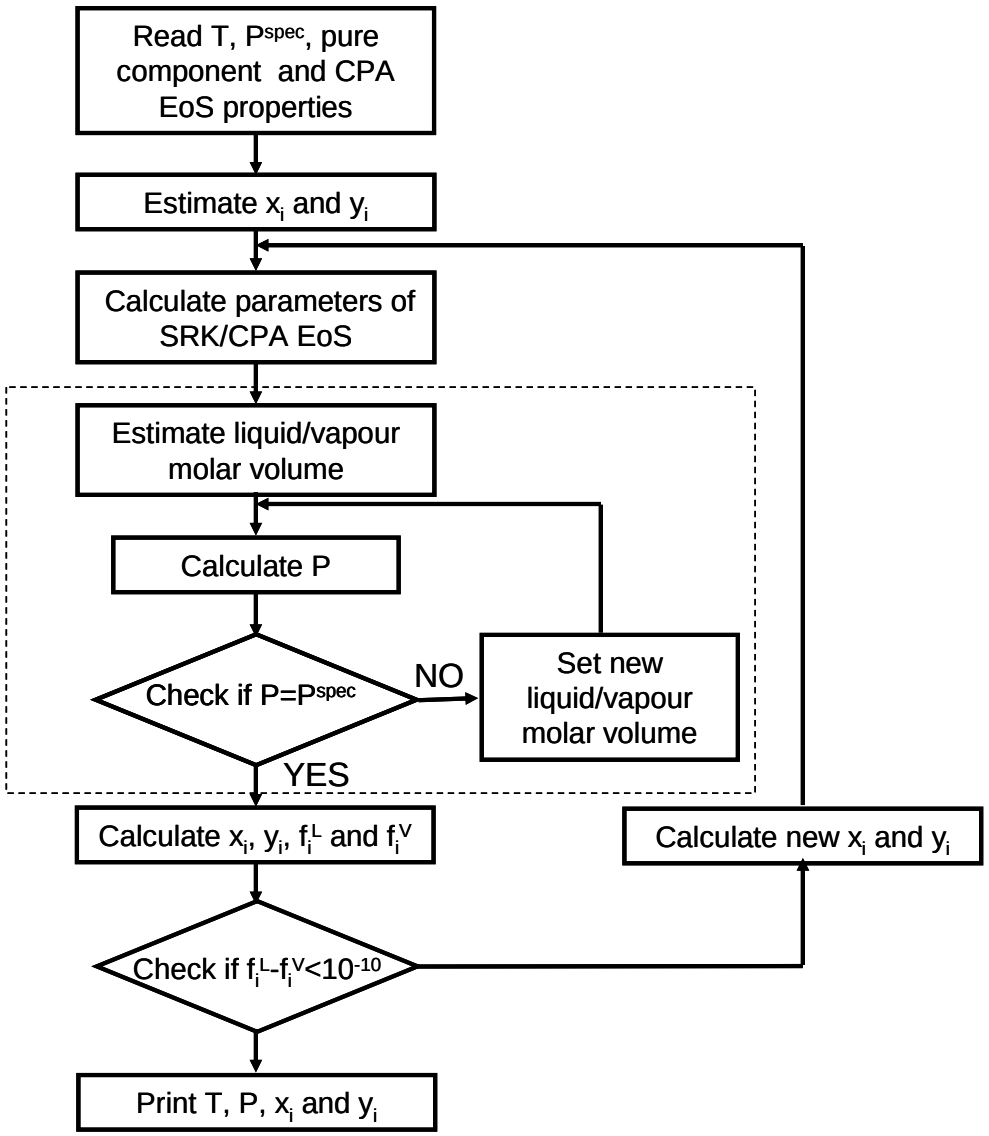

Figure 3.2 Block diagram for the VLE calculation for the CPA EoS

As it is shown in the algorithm, an extra loop from the traditional VLE calculation method is necessary in order to calculate the molar volume in each phase. In this work the Newton-Raphson iteration method has been applied for calculation of volume.

3.6 Association Schemes

The selection of the association scheme and the maximum number of association sites can be found for a compound by looking at the location of its constituting hydrogen atoms and lone pairs on acceptor atom (oxygen for water molecules). Furthermore, information about whether the molecule form dimers, trimers, oligomers (chains), or even three-dimensional structures like water give an indication of how many of the sites actually are used. Steric hindrance is also a factor and larger molecules could exhibit the possibility of an atom associating with another atom within the same molecule.

Huang and Radosz (1990) have classified eight different association schemes, which can be applied to different molecules depending on the number and type of associating sites. Based on the fact that the association term depends on the number and type of association sites for the associating compound, for a highly hydrogen-bonded substances like water and glycols a four-site (4C) association scheme was adopted since it is considered that hydrogen bonding occurs between the two hydrogen atoms and the two lone pairs of electrons in the oxygen atom of water molecules. For alcohols, the two-site (2B) or the three-site (3B) association schemes may be applied. The results from Huang and Radosz (1990) and from Kontogeorgis et al. (2006b) suggest the use of the two-site association (2B) scheme for methanol, which proposes that hydrogen bonding occurs between the hydroxyl hydrogen and one of the lone pairs of electrons from the oxygen atom in another alcohol molecule (Table 3.2). The CPA EoS pure compound parameters for associating compounds, used for fugacity calculations in this thesis were listed in Table 3.1.

Table 3.2 Types of bonding in real associating fluids (Huang and Radosz, 1990)

Species	Formula	Assigned type
Alcohols	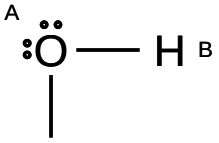	2B
Water	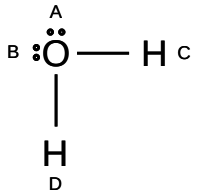	4C
Glycols	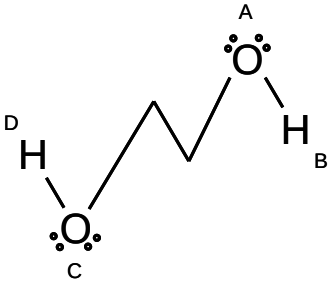	4C

3.7 Mixing Rules

The extension of the CPA-EoS to mixtures containing multi-associating compounds requires mixing rules only for parameters of the SRK part. When the CPA-EoS is used for mixtures, the SRK part requires the conventional van der Waals mixing rules for b and $a(T)$, while the association part requires only combining rules for $\varepsilon^{A_iB_j}$ and $\beta^{A_iB_j}$. The mixing and combining rules for $a(T)$ and b are the classical van der Waals equations:

$$b = \frac{\sum_i n_i \sum_{A_i} n_j b_{ij}}{n^2}$$
$$a(T) = \frac{\sum_i n_i \sum_{A_i} n_j a_{ij}(T)}{n^2} \tag{3.19}$$

where the classical combining rules are used:

$$a_{ij} = (1 - k_{ij})\sqrt{a_i a_j}$$
$$b_{ij} = \frac{b_i + b_j}{2} \tag{3.20}$$

Combining rules for the association energy and volume parameters are needed for different associating molecules, i.e., $i \neq j$ (e.g., water-glycol systems), in order to calculate the value of the association strength. As recently shown by Derawi et al. (2003b), the arithmetic mean for the cross-association energy is proportional to the enthalpy of hydrogen bonding and the geometric mean for the cross association volume is also related to the cross entropy of the hydrogen bonding. These combining rules have been applied to calculate the association energy and volume parameters between different associating molecules.

$$\varepsilon^{A_iB_j} = \frac{\varepsilon^{A_iB_i} + \varepsilon^{A_jB_j}}{2}$$
$$\beta^{A_iB_j} = \sqrt{\beta^{A_iB_i}\beta^{A_jB_j}} \tag{3.21}$$

3.8 Fugacity Coefficients from the CPA EoS

The thermodynamic properities are calculated as partial derivatives of the Helmholtz function, $A(T,V,n)$, however, it is in many cases more convenient to use the partial derivatives of the reduced residual Helmholtz function. The fugacity coefficient of a component in a mixture (Φ_i) is given by (Michelsen and Mollerup, 2004):

$$RT\ln\Phi_i = \left(\frac{\partial A^r}{\partial n_i}\right)_{T,V,n_j} - RT\ln Z \tag{3.11}$$

where Z is the compressibility factor. As the CPA EoS combines the SRK EoS with the association term, the Helmholtz function is the summation of the two parts:

$$A^r = A^r{}_{SRK} + A^r{}_{association} \tag{3.14}$$

According to Michelsen and Mollerup (2004) the fugacity coefficient for the *SRK* term can be calculated as follow:

$$\frac{\partial}{\partial n_i}\left(\frac{A^r{}_{SRK}}{RT}\right)_{T,V,n_j} = F_n + F_B B_i + F_D A_i \tag{3.14}$$

where:

$$F_n = -\ln\left(1-\frac{B}{V}\right)$$

$$F_B = -g_B - \frac{A}{T} f_B \tag{3.14}$$

$$F_D = -\frac{f}{T}$$

with:

$$f = \frac{\ln\left(1+\frac{B}{V}\right)}{RB}$$

$$g_B = -\frac{1}{V-B} \tag{3.14}$$

$$f_B = -\frac{f + V f_V}{B}$$

$$f_V = -\frac{1}{RV(V+B)}$$

where A_i and B_i are the composition derivatives of the co-volume term and the energy term, given by the following equation:

$$B_i = \frac{\partial}{\partial n_i}\left(n^2 b\right)_{n_j} = \frac{2\sum_j n_j b_{ij} - B}{n}$$
$$A_i = \frac{\partial}{\partial n_i}\left(n^2 a\right)_{n_j} = 2\sum_i n_j a_{ij} \qquad (3.14)$$

Similarly, the association contribution to the chemical potentials is calculated by the simplified equations introduced by Michelsen and Hendricks (2001):

$$\frac{\partial}{\partial n_i}\left(\frac{A^r{}_{association}}{RT}\right) = -\sum_{A_i} \ln X_{A_i} + \frac{h}{2}\frac{\partial \ln g}{\partial ni}$$
$$h = \sum_i n_i \sum_{A_i}\left(1 - X_{A_i}\right) \qquad (3.14)$$
$$\frac{\partial \ln g^{simp.}}{\partial n_i} = \frac{0.475B}{V - 0.475B}$$

3.9 Modelling of Electrolyte Solutions

When electrolytes are present the fugacity of non-electrolyte compound is calculated by combining the equation of state with the Debye-Hückel electrostatic contribution for taking into the account the effect of salt (Aasberg-Petersen et al., 1991):

$$\ln \phi_i = \ln \phi_i^{EoS} + \ln \gamma_i^{EL} \qquad i = 1, 2, ..., N \qquad (3.22)$$

where N is the number of non-electrolyte components, ϕ_i is the fugacity coefficient of component i, ϕ_i^{EoS} is the fugacity coefficient of component i calculated by an EoS, neglecting the electrostatic effect, and γ_i^{EL} is the contribution of the electrostatic term. Using the Debye-Hückel activity coefficient, the final form of the second term on the right hand side in Equation 3.22 becomes:

$$\ln \gamma_i^{DH} = \frac{2AM_m h_{is}}{B^3} f\left(BI^{1/2}\right) \qquad (3.23)$$

where M_m is the salt-free mixture molecular weight determined as a molar average, and h_{is} is the interaction coefficient between the dissolved salt and a non-electrolytic compound. The function $f\left(BI^{1/2}\right)$ is obtained from:

$$f\left(BI^{1/2}\right)=1+BI^{1/2}-\frac{1}{\left(1+BI^{1/2}\right)}-2\ln\left(1+BI^{1/2}\right) \tag{3.24}$$

where I is the ionic strength. The parameters A and B are given by:

$$A=\frac{1.327757\cdot 10^{5} d_m^{1/2}}{\left(\eta_m T\right)^{3/2}}$$
$$B=\frac{6.359696 d_{\mathrm{m}}^{1/2}}{\left(\eta_m T\right)^{1/2}} \tag{3.25}$$

where d_m is the density of the salt-free mixture and η_m is the salt-free mixture dielectric constant which can be calculated from:

$$\eta_m = x_w \eta_w \tag{3.26}$$

x_w and η_w are the salt-free mole fraction and dielectric constant of water, respectively. The dielectric constants of dissolved non-electrolyte compounds have been neglected, relative to that of water.

The binary interaction parameter, h_{ws}, between water and dissolved salt for nine electrolytes has been re-optimized by expressing h_{ws} as a function of salt concentration and temperature by using experimental freezing point depression data of aqueous solutions in the presence of salt, by optimizing constants A-E in the binary interaction parameter relation (shown below). The re-optimisation was required due to the change from VPT to CPA EoS. The new numerical expression developed in this work to achieve the best match between the experimental data and predictions is given below in Equation 3.27.

$$h_{ws}=\frac{A}{W}+B\times W^{2}+\frac{C}{W^{2}}+D+E\times T, \quad if\ W\neq 0 \tag{3.27}$$

where T is temperature in degrees Celsius and W is salt concentration in weight percent. A, B, C, D and E are fitting constants. The optimized interaction parameters are presented in Table 3.3.

Table 3.3 Optimized water-salt interaction coefficients for different salts ($\times 10^6$)

	A	B	C	D / K	E
NaCl	-3879.89	-6.09	-45.95	-8137.28	10.43
KCl	-6427.25	-2.68	-308.79	-7445.30	6.16
KOH	-1465.19	-13.31	-2129.45	-9338.45	23.58
CaCl2	-3566.60	-9.67	385.81	-3960.14	16.19
MgCl2	-813.23	-14.41	-76.81	-4469.65	20.12
CaBr2	-3727.05	-5.02	-76.83	-4392.45	17.12
ZnCl2	-1183.00	-1.37	-39.08	-4481.42	24.21
ZnBr2	81.12	-1.27	-4451.44	-4741.98	6.08

The change in gas solubility due to the presence of salts has been taken into account using the method introduced by Tohidi-Kalorazi (1995) in which the gas-salt interaction parameters expressed as functions of temperature and salt concentration.

The Patwardhan and Kumar's approach (1986) was employed (as detailed by Tohidi-Kalorazi, 1995) to extend the model to mixed electrolyte solutions instead of finding a mixing rule to relate the interaction coefficients of mixed electrolyte solutions to those of single electrolyte solutions. Activity coefficient of mixed electrolyte solutions from activity coefficient of single electrolyte solutions has been calculated in this work based on the relationship comes as follow (Patwardhan and Kumar, 1986):

$$\log a_w = \sum_i^{ns} y_i \log a_{w,i}^{\ o} \qquad (3.27)$$

a_w is the activity of water in a solution of mixed electrolytes, $a_{w,i}^{\ o}$ represents the activity of water in a single electrolyte solution of the same ionic strength as that of mixed electrolyte solution. i and y_i represent electrolyte, and ionic strength fraction of electrolyte I, respectively.

3.10 Modelling of Ice Phase

The fugacity of a pure solid can (as for a supersaturated pure liquid) be calculated using the Poynting correction, i.e., assuming that the volume of the supersaturated phase is constant at the volume for the saturated phase (Smith and Van Ness, 1987 and Anderson and Prausnitz, 1986). For ice the expression becomes:

$$f_w^I = \phi_w^{sat} P_I^{sat} \exp\left(\frac{v_I\left(P - P_I^{sat}\right)}{RT}\right) \tag{3.28}$$

where f_w^I is the fugacity of water in the ice phase, ϕ_w^{sat} is the water fugacity coefficient in the vapour phase at pressure equal to the ice vapour pressure, P_I^{sat} is the ice vapour pressure (Pa), v_I is the ice molar volume (m^3/mol), R is the universal gas constant, and P and T is the system pressure (Pa) and temperature (K), respectively.

The ice molar volume, v_I, (m^3/mol) is calculated using the following expression (Tohidi et al., 1995):

$$v_I = 19.629 \cdot 10^{-6} + 2.2364 \cdot 10^{-9}\left(T - 273.15\right) \tag{3.29}$$

and the ice vapour pressure, P_I^{Sat}, is calculated using (Wagner et al., 1994):

$$\begin{aligned} &\ln\left(\frac{P_I^{sat}}{P_n}\right) = a_1(1-\theta^{-1.5}) + a_2(1-\theta^{-1.25}) \\ &a_1 = -13.9281690 \\ &a_2 = 34.7078238 \\ &P_n / Pa = 611.657 \\ &T_n / K = 273.16 \end{aligned} \tag{3.30}$$

where θ is reduced temperature (T/T_n) and P_I^{sat} is the ice vapour pressure in Pa.

3.11 Modelling of Hydrate Phase

The statistical thermodynamic model of van der Waals and Platteeuw (1959) provides a bridge between the microscopic properties of the clathrate hydrate structure and macroscopic thermodynamic properties, i.e., the phase behaviour. The hydrate phase is modelled by using the solid solution theory of van der Waals and Platteeuw (1959), as implemented by Parrish and Prausnitz (1972). The Kihara model for spherical molecules is applied to calculate the potential functions for compounds forming the hydrate phase (Kihara, 1953). In order to predict the three phase L_w-H-V hydrate formation pressure at a given temperature the algorithm with a flow diagram presented in Figure 3.3 for the CPA EoS has been applied.

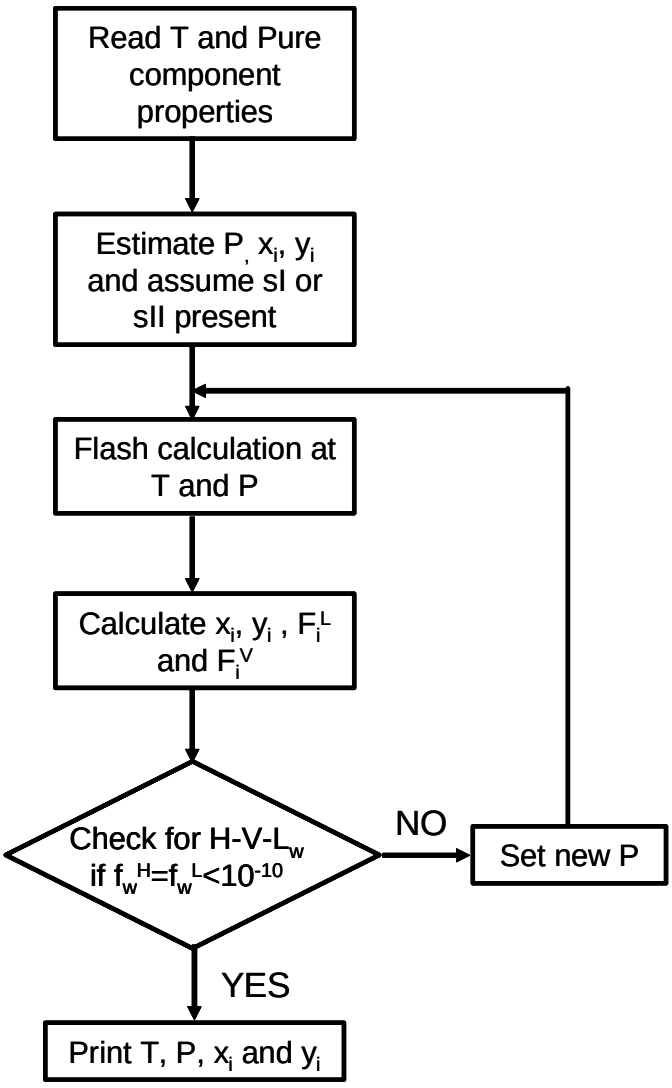

Figure 3.3 Block diagram for the L_w-H-V hydrate formation calculation

The fugacity of water in the hydrate phase is given by the following equation (Anderson and Prausnitz, 1986):

$$f_w^H = f_w^\beta \exp\left(-\frac{\Delta\mu_w^{\beta-H}}{RT}\right) \tag{3.31}$$

where superscripts H and β refer to hydrate and empty hydrate lattice, respectively and μ stands for chemical potential. f_w^β is the fugacity of water in the empty hydrate lattice. $\Delta\mu_w^{\beta-H}$ is the chemical potential difference of water between the empty hydrate lattice, μ_w^β, and the hydrate phase, μ_w^H, which is obtained by the van der Waals and Platteeuw expression:

$$\Delta\mu_w^{\beta-H} = \mu_w^\beta - \mu_w^H = RT\sum_m \bar{v}_m \ln\left(1+\sum_j C_{mj} f_j\right) \tag{3.32}$$

where $\bar{v}_m$ is the number of cavities of type m per water molecule in the unit cell, f_j is the fugacity of the gas component j. C_{mj} is the Langmuir constant, which accounts for the gas-water interaction in the cavity. The Langmuir constants are temperature dependent functions that describe the potential interaction between the encaged guest molecule and the water molecules surrounding it. Numerical values for the Langmuir constant can be calculated by choosing a model for the guest-host interaction (van der Waals, and Platteeuw, 1959):

$$C_{mj}(T) = \frac{4\pi}{kT}\int_0^\infty \exp\left(-\frac{w(r)}{k^{'}T}\right) r^2 dr \tag{3.33}$$

where k is Boltzmann's constant. The function $w(r)$ is the spherically symmetric cell potential in the cavity, with r measured from the centre, and depends on the intermolecular potential function chosen for describing the encaged gas-water interaction. In the present work, the Kihara potential function (Kihara, 1953) is used as described in McKoy and Sinanoglu (Mckoy and Sinanoglu, 1963).

$$\begin{aligned} \Gamma(r) &= \infty && r \le 2\alpha \\ \Gamma(r) &= 4\varepsilon\left[\left(\frac{\sigma^*}{r-2\alpha}\right)^{12} - \left(\frac{\sigma^*}{r-2\alpha}\right)^{6}\right] && r > 2\alpha \end{aligned} \tag{3.34}$$

where $\Gamma(r)$ is the potential energy of interaction between two molecules when the distance between their centres is equal to r. ε is the characteristic energy, α is the radius of the spherical molecular core and $\sigma^* = \sigma - 2\alpha$ where σ is the collision diameter, i.e., the distance where $\Gamma = 0$. The Kihara potential parameters, α, σ, and ε, for hydrate formers are taken from Tohidi-Kalorazi (1995).

Based on the chosen potential energy function the spherically symmetric cell potential in the cavities (Equation 3.33) needs to be derived. The fugacity of water in the empty hydrate lattice, f_w^β in Equation 3.31, is given by:

$$f_w^\beta = f_w^{I/L} \exp\left(\frac{\Delta\mu_w^{\beta-I/L}}{RT}\right) \tag{3.35}$$

where $f_w^{I/L}$ is the fugacity of pure ice or liquid water and $\Delta\mu_w^{\beta-I/L}$ is the difference in the chemical potential between the empty hydrate lattice and pure liquid water. $\Delta\mu_w^{\beta-I/L}$ is given by the following equation:

$$\frac{\Delta\mu_w^{\beta-I/L}}{RT} = \frac{\mu_w^{\beta}(T,P)}{RT} - \frac{\mu_w^{I/L}(T,P)}{RT} = \frac{\Delta\mu_w^{0}}{RT_0} - \int_{T_0}^{T} \frac{\Delta h_w^{\beta-I/L}}{RT^2} dT + \int_{P_0}^{P} \frac{\Delta v_w^{\beta-I/L}}{RT} dP \qquad (3.36)$$

where superscript *0* stands for the triple point of water and *h* refers to molar enthalpy. μ_w^{β} and $\mu_w^{I/L}$ are the chemical potential of the empty hydrate lattice and of pure water in the ice (*I*) or the liquid (*L*) state, respectively. $\Delta\mu_w^{0}$ is the reference chemical potential difference between water in the empty hydrate lattice and pure water at 273.15 K. $\Delta h_w^{\beta-I/L}$ and $\Delta v_w^{\beta-I/L}$ are the molar enthalpy and molar volume differences between an empty hydrate lattice and ice or liquid water. $\Delta h_w^{\beta-I/L}$ is given by the following equation (Anderson and Prausnitz, 1986 and Holder et al., 1980):

$$\Delta h_w^{\beta-I/L} = \Delta h_w^{0} + \int_{T_0}^{T} \Delta C'_{Pw} dT \qquad (3.37)$$

where *C'* and subscript *P* refer to molar heat capacity and pressure, respectively. Δh_w^{0} is the enthalpy difference between the empty hydrate lattice and pure water, at the triple point. The heat capacity difference between the empty hydrate lattice and the pure liquid water phase, $\Delta C'_{Pw}$ is also temperature dependent and the equation recommended by Holder et al. (1980) is used:

$$\Delta C'_{Pw} = -37.32 + 0.179(T - T_0) \qquad T > T_0 \qquad (3.38)$$

where $\Delta C'_{Pw}$ is in J.mol^{-1}.K^{-1}. Furthermore, the heat capacity difference between hydrate structures and ice is set to zero. The reference properties used are summarized in Table 3.4.

Table 3.4 Thermodynamic reference properties for structures I and II hydrates

Reference property	Structure I	Structure II	Reference
$\Delta\mu_w^\circ$ /J.mol^{-1}	1297	937	Dharmawardhana et al., 1980
Δh_w° / J.mol^{-1} †	1389	1025	Dharmawardhana et al., 1980
Δv_w/cm^3.mol^{-1} ‡	3.0	3.4	Parrish and Prausnitz, 1972

† In the liquid water region subtract 6009.5 J mol^{-1} from Δh_w°.

‡ In the liquid water region add 1.601 cm^3 mol^{-1} to Δv_w.

3.12 The Capillary Effect on Hydrate Stability Condition

To model the hydrate dissociation conditions in porous media, the approach introduced by Llamedo et al. (2004) has been used to take into account the effect of capillary pressure. To account for capillary pressure effects on phase fugacities, a correction similar to the Poynting correction for saturated liquids has been applied (Smith and Van Ness, 1987).

$$f_i^{pore} = f_i^{bulk} \times \exp\left(\frac{v_i P_c}{RT}\right)$$
$$P_c = P_h - P_l \tag{3.39}$$

where, f_i^{pore} is the fugacity in the pores, f_i^{bulk} is the fugacity in the bulk. v_i is the molar volume, P_c is the capillary pressure. P_h and P_l are the pressure in the hydrate and liquid phases, respectively. The model assumes water to be the wetting phase on silica surface as observed by Tohidi et al. (2001) and that the porous media is saturated with the liquid phase. Within the pore space, clathrates are subjected to a higher pressure due to the capillary pressure effects, resulting in inhibition.

For cylindrical pores, the pressure of the solid hydrate phase, P_h, in contact with an aqueous liquid phase (of varying dissolved gas concentration) within a capillary of radius *r* at any given temperature is defined as (Clennell et al., 1999):

$$P_h = P_l + \left(\frac{F\gamma_{hl}\cos\theta_{hl}}{r}\right) \tag{3.40}$$

where γ_{hl} is the specific surface energy of the hydrate-liquid interface, and θ_{hl} is the contact angle between hydrate and liquid phases, and is considered to be 0^o in this work.

r is the nominal pore radius and F, is the shape factor which is dependent on the solid-liquid interfacial curvatures. This model assumes cylindrical pores, and the shape factor equal to one has been considered for modelling the dissociation condition, in accordance with accepted capillary theory (Anderson et al., 2006). For modelling purposes, the value for the specific surface energy of the hydrate-liquid interface, the only parameter required for the modelling, was considered to be 0.032 J/m^2. More details about the modelling of gas hydrate growth and dissociation in narrow pores and capillary inhibition effect can be found elsewhere (Anderson et al., 2006 and Llamedo et al., 2004).

3.13 Conclusions

Popular engineering equations of state such as SRK and PR become inaccurate when applied to mixtures containing polar materials such as water or alcohols. Their performance can be improved by using non-density dependent mixing rules. Many attempts have been made to find a suitable equation of state for predicting the phase behaviour and volumetric properties of hydrocarbon fluids (Danesh et al., 1991). Finding/developing the proper EoS for a system containing water, organic inhibitor(s) and salt(s) in addition to the petroleum reservoir fluids is a real challenge and the thermodynamics of these highly non-ideal systems is difficult to model. In this work, a more complicated approach applied to model alcohols/glycols, salts and water in hydrocarbon mixtures by using a robust general-purpose implementation of the CPA (Cubic plus Association) model, has been introduced.

The thermodynamic approach for modelling fluid phases and hydrates, as well as the effect of porous media on phase behaviour has been detailed in this chapter.

References

Aasberg-Petersen K., Stenby E., Fredenslund A., 1991, *Prediction of high-pressure gas solubilities in aqueous mixtures of electrolytes*, Ind. Eng. Chem. Res., **30**, 2180-2185

Anderson F.E., Prausnitz J.M., 1986, *Inhibition of gas hydrates by methanol*, AIChE J., **32**, 1321-1333

Asselineau L., Bogdanic G., Vidal J., 1978, *Calculation of thermodynamic properties and vapour-liquid equilibria of refrigerants, Chem. Eng. Sci.,* **33**, 1269-1276

Atkins P., de Paula J., 2006, *Physical chemistry*, Oxford University Press

Chapman W.G., Gubbins K.E., Jackson G., Radosz M., 1990, *New reference equation of state for associating liquids*, Ind. Eng. Chem. Res., **29**, 1709–1721

Clennell M.B., Hovland M., Booth J.S., Henry P., Winters W. J., 1999, *Formation of natural gas hydrates in marine sediments; 1, Conceptual model of gas hydrate growth conditioned by host sediment properties,* J. Geophys. Res. B., **104**, 22985-23003.

Danesh A., Xu D.H., Todd A.C., 1991, *Comparative study of cubic equatins of state for predicting phase behaviour and volumetric properties of injection gas-reservoir oil systems*, Fluid Phase Equilibr., **63**, 259-278

Derawi S.O., Michelsen M.L., Kontogeorgis G.M., Stenby E.H., 2003a, *Application of the CPA equation of state to glycol/hydrocarbons liquid-liquid equilibria*, Fluid Phase Equilibr., **209**, 163-184

Derawi S.O., Kontogeorgis G.M., Michelsen M.L., Stenby E.H., 2003b, *Extension of the Cubic– Plus–Association equation of state to glycol–water cross–associating systems*, Ind. Eng. Chem. Res., **42**, 1470–1477

Dharmawardhana P.B., Parrish W.R., Sloan E.D., 1980, *Experimental thermodynamic parameters for the prediction of natural gas hydrate dissociation conditions*, Ind. Eng. Chem. Fundam., **19**, 410-414

Folas G.K., Derawi S.O., Michelsen M.L., Stenby E.H., Kontogeorgis G.M., 2005, *Recent applications of the Cubic-Plus-Association (CPA) equation of state to industrially important systems*, Fluid Phase Equilibr., **228**, 121-126

Graboski M.S., Daubert T.E., 1978, *A modified soave equation of state for phase equilibrium calculations*, Ind. Eng. Chem. Process. Des. Dev., **17**, 443-454

Holder G.D., Corbin G., Papadopoulos K.D., 1980, *Thermodynamic and molecular properties of gas hydrate from mixtures containing methane, argon and krypton*, Ind. Eng. Chem. Fundam., **19**, 282-286

Huang S.H., Radosz M., 1990, *Equation of State for Small, Large, Polydisperse and associating molecules*, Ind. Eng. Chem. Res., **29**, 2284–2294

Huron M.J., Dufour G.N., Vidal J., 1978, *Vapour - liquid equilibrium and critical locus curve calculations with the soave equation for hydrocarbon systems with carbon dioxide and hydrogen sulfide*, Fluid Phase Equilibr., **1**, 247-265

Ikonomou G.D., Donohue M.D., 1988, *Extension of the associated perturbed anisotropic chain theory to mixtures with more than one associating component*, Fluid Phase Equilibr., **39**, 129-159

Kihara T., 1953, *Virial coefficient and models of molecules in gases*, Rev. Modern Phys., **25**(4), 831– 843

Kontogeorgis G.M., Yakoumis I.V., Meijer H., Hendriks E.M., Moorwood T., 1999, *Multicomponent phase equilibrium calculations for water–methanol–alkane mixtures*, Fluid Phase Equilibr., **158**, 201-209

Kontogeorgis G.M., Michelsen M.L., Folas G.K., Derawi S., von Solms N., Stenby E.H., 2006a, *Ten years with the CPA (Cubic-Plus-Association) equation of state. part 1. pure compounds and self-associating systems*, Ind. Eng. Chem. Res., **45**, 4855-4868

Kontogeorgis G.M., Michelsen M.L., Folas G.K., Derawi S., von Solms N., Stenby E.H., 2006b, *Ten years with the CPA (Cubic-Plus-Association) equation of state. part 2. cross-associating and multicomponent systems*, Ind. Eng. Chem. Res., **45**, 4869- 4878

Kontogeorgis G.M., Voutsas E.C., Yakoumis I.V., Tassios D.P., 1996, *An equation of state for associating fluids*, J. Ind. Eng. Chem. Res., **35**, 4310–4318

Mathias P.M., Copeman T.W., 1983, *Extension of the Peng-Robinson equation of state to polar fluids and fluid mixtures*, Fluid Phase Equilibr., **13**, 91–108

McKoy V., Sinanoglu O., 1963, *Theory of dissociation pressures of some gas hydrates*, J. Chem. Physics, **38**(12), 2946-2956

Michelsen M.L., Hendriks E.M., 2001, *Physical properties from association models*, Fluid Phase Equilibr., **180**, 165–174

Michelsen M.L., Mollerup J., 2004, *Thermodynamic models, fundamentals and computational aspects*, Tie-Line Publications, Denmark

Orbey H., Sandler S.I., 1998, *Modeling vapor-liquid equilibria; cubic equations of state and their mixing rules*, Cambridge University Press, Cambridge

Parrish W.R., Prausnitz J.M., 1972, *Dissociation pressures of gas hydrates formed by gas mixtures*, Ind. Eng. Chem. Process Des. Dev., **11**(1), 26–35

Patwardhan V.S., Kumar A., 1986, *A unified approach for the prediction of thermodynamic properties of aqueous mixed electrolyte solutions, part I: vapour pressure and heat of vaporisation*, AIChE J., **32**, 1419-1428

Peng D.Y., Robinson D.B., 1976, *A new two-constant equation of state*, Ind. Eng. Chem. Fundam., **15**, 58-64

Redlich O., Kwong J.N.S., 1949, *On the thermodynamics of solutions. v: an equation of state. fugacities of gaseous solutions*, Chem. Rev., **44**, 233-244

Reid R.C., Prausnitz J.M., Poling B.E., 1987, *The properties of gases and liquids*, McGraw Hill Book Company, New York

Smith J.M., Van Ness H.C., 1987, *Introduction to chemical engineering thermodynamics*; McGraw-Hill Inc., New York

Soave G., 1972, *Equilibrium constants from a modified Redlich-Kwong equation of state*, J. Chem. Eng. Sci., **27**, 1197-1203

Tohidi B., Danesh A., Todd A.C., 1995, *Modelling single and mixed electrolyte solutions and its applications to gas hydrates*, Trans. IChemE, **73**, 464-472

Tohidi-Kalorazi B., 1995, *Gas hydrate equilibria in the presence of electrolyte solutions*, Ph.D. thesis, Heriot-Watt University

Van der Waals J.H., Platteeuw J.C., 1959, *Clathrate solutions*, Adv. Chem. Phys., **2**, 1–57

Voutsas E.C., Boulougouris G.C., Economou I.G., Tassios D.P., 2000, *Water/hydrocarbon phase equilibria using the thermodynamic perturbation theory*, Ind. Eng. Chem. Res. **39**, 797

Wagner W., Saul A., Pruss A., 1994, *International equations for the pressure along the melting and along the sublimation curve of ordinary water substance*, J. Phys. Chem. Ref. Data, **23**, 515-527

Wertheim M.S., 1987, *Thermodynamic perturbation theory of polymerization*, J. Chem. Phys., **87**, 7323-7331

Yakoumis I.V., Kontogeorgis G.M., Voutsas E.C., Hendriks E.M., Tassios D.P., 1998, *Prediction of phase equilibria in binary aqueous systems containing alkanes, cycloalkanes and alkenes with the cubic-plus-association equation of state*, Ind. Eng. Chem. Res., **37**, 4175-4182

CHAPTER 4 – DEVELOPMENT AND VALIDATION OF THERMODYNAMIC MODEL (No hydrate present)

4.1 Introduction

As detailed in Chapter 3, a thermodynamic formulation using the Cubic-Plus-Association (CPA) Equation of State to model all fluid phases was presented. The model was extended to predict fluid phase equilibria in the presence of single or mixed electrolyte solutions over a wide range of operating conditions. In order to enable an equation of state to predict the correct phase behaviour of the fluid, correct binary interaction parameters between molecules are essential. In this chapter, the available experimental data (see Chapter 2) from the literature was used for tuning the binary interaction parameters between molecules to enhance the capability of the equation of state used in the thermodynamic model to predict the desired phase behaviour. This optimisation has been performed by adjusting the binary interaction parameter to achieve the best match between predictions and experimental data

After tuning the binary interaction parameters, the extent of the validity and reliability of the model is investigated in this chapter by presenting some examples for each case. The experimental data used for tuning and validation can be divided into the following groups:

- Gas solubility in water/methanol/ethanol/*n*-propanol/MEG.
- Water content and inhibitor distribution in vapour phase.
- Vapour pressure depression of single and mixed electrolyte solutions.
- Freezing point depression of single and mixed electrolyte solutions.

The predictions of the model have been compared with independent experimental data (this work and literature data), that has not been used in developing the model, demonstrating the reliability of the model. This validation is an essential step towards developing/evaluating the model under more complex conditions such as, presence of hydrates, hydrate inhibition effect of electrolyte solutions and/or organic inhibitors, as described in Chapter 5.

This chapter can be divided into three parts. The first part being the application of the model on the self-association systems, covering binary systems of water, methanol, ethanol, monoethylene glycol (MEG) and *n*-propanol with natural gas components. The second part covers application of the CPA EoS to cross-associating systems and binaries of associating compounds. The third part describes an investigation into the reliability of the model in predicting vapour pressure and freezing point depression of single and mixed electrolyte solutions.

4.2 Application of the CPA EoS to Self-Associating Systems

The presence of water and/or alcohols in a hydrocarbon mixture can affect the product quality and damage the operating equipment due to corrosion and formation of gas hydrates. Tracing the concentration of hydrocarbons in aqueous phase is also important for technical purposes like preventing oil spills, inhibitor loss and for ecological concerns such as predicting the fate of these organic pollutants in the environment. In spite of its obvious importance there is no reliable predictive model for providing qualitative description of such systems over a wide range of thermodynamic conditions.

This section details the modelling results of binary mixtures containing non-associating compounds, such as light to heavy hydrocarbons, and associating components such as water, methanol, ethanol, *n*-propanol and monoethylene glycol by using the CPA EoS over a broad range of pressure and temperature conditions.

For binary systems containing a self-associating compound (water, methanol, monoethylene glycol etc) in addition to non-associating compounds (methane, ethane, propane, etc), the binary interaction parameters k_{ij} are the only adjustable parameters and thus no combining rules are required for the associating energy and volume. Experimental data on water content and inhibitor distribution in the vapour phase, at low temperatures, for hydrocarbons and non-hydrocarbon gases are scarce and often rather dispersed. This is partly due to the fact that the amount of components such as water and monoethylene glycol in the vapour phase is very low at low temperature and high pressure conditions and hence generally very difficult to measure, however, measuring gas solubility is easier than measuring for example the water content of gases. Due to this fact, the binary interaction parameters between non-associating and self-associating compounds have been adjusted directly to experimental data through a

modified Simplex algorithm (Åberg and Gustavsson, 1982) using the following objective function based on the minimization of the difference between the calculated and experimental data:

$$OF = \frac{1}{NP} \times \sum_{i}^{NP} \left(\frac{x_i^{calc.} - x_i^{\exp.}}{x_i^{\exp.}} \right)^2 \tag{4.1}$$

where x_i is the gas solubility in the liquid phase. By minimizing above function, a temperature dependent k_{ij} has been established, for each binary system. The literature used for tuning the binary interaction parameters between each of non-associating compounds and water are presented in Chapter 2.

4.2.1 *Binary Systems Containing Water*

Natural gases are not very soluble in water even at high pressures. As mentioned before, the solubility of light hydrocarbons (C_1-C_5), carbon dioxide, nitrogen and hydrogen sulphide in pure water and aqueous solutions of electrolytes have been measured over a wide pressure and temperature range by many researchers and therefore measurements of gas solubility in water are extensive. The sources of the experimental data for binary mixture of each component and water are presented in Chapter 2 (Tables 2.15 to 2.22).

By minimizing the objective function as presented in Equation 4.1, using solubility of each compound in water in the range of 273.15 K up to 393.15 K, a temperature dependent k_{ij} has been established. The following form was found to be the best representation of temperature dependency:

$$k_{ij} = A + B/T \tag{4.2}$$

The optimized parameters for interaction parameters between water and each of the non-associating compounds are presented in Table 4.1.

Table 4.1 Optimized values for interaction parameters between each of the non-associating compounds and water

Component	***A***	***B***
methane	0.8613	-251.0540
ethane	0.5409	-160.4000
propane	0.5519	-152.0200
butane	0.2828	-73.7300
pentane	0.3705	-108.0710
hexane	0.3764	-116.8110
heptane	0.3926	-121.8260
octane	0.2224	-77.6656
nonane	0.0297	-54.4144
decane	-0.0309	0
undecane	-0.1780	0
dodecane	-0.0846	0
tridecane	-0.2676	0
tetradecane	-0.2588	0
pentadecane	-0.3403	0
hexadecane	-0.2066	0
heptadecane	-0.3840	0
octadecane	-0.3792	0
nonadecane	-0.4126	0
eicosane	-0.4460	0
carbon dioxide	0.1099	-53.7586
nitrogen	0.9909	-379.9691

After gathering the available data from the literature and tuning the binary interaction parameters for each component and water, experimental solubility data were used to evaluate the predictions of the model based on sCPA EoS.. Figures 4.1a, b, c, and d presents the predicted and experimental gas solubility for methane, ethane, propane, and nitrogen in water, respectively. Figure 4.2 shows experimental and predicted water content in the gas phase (methane).

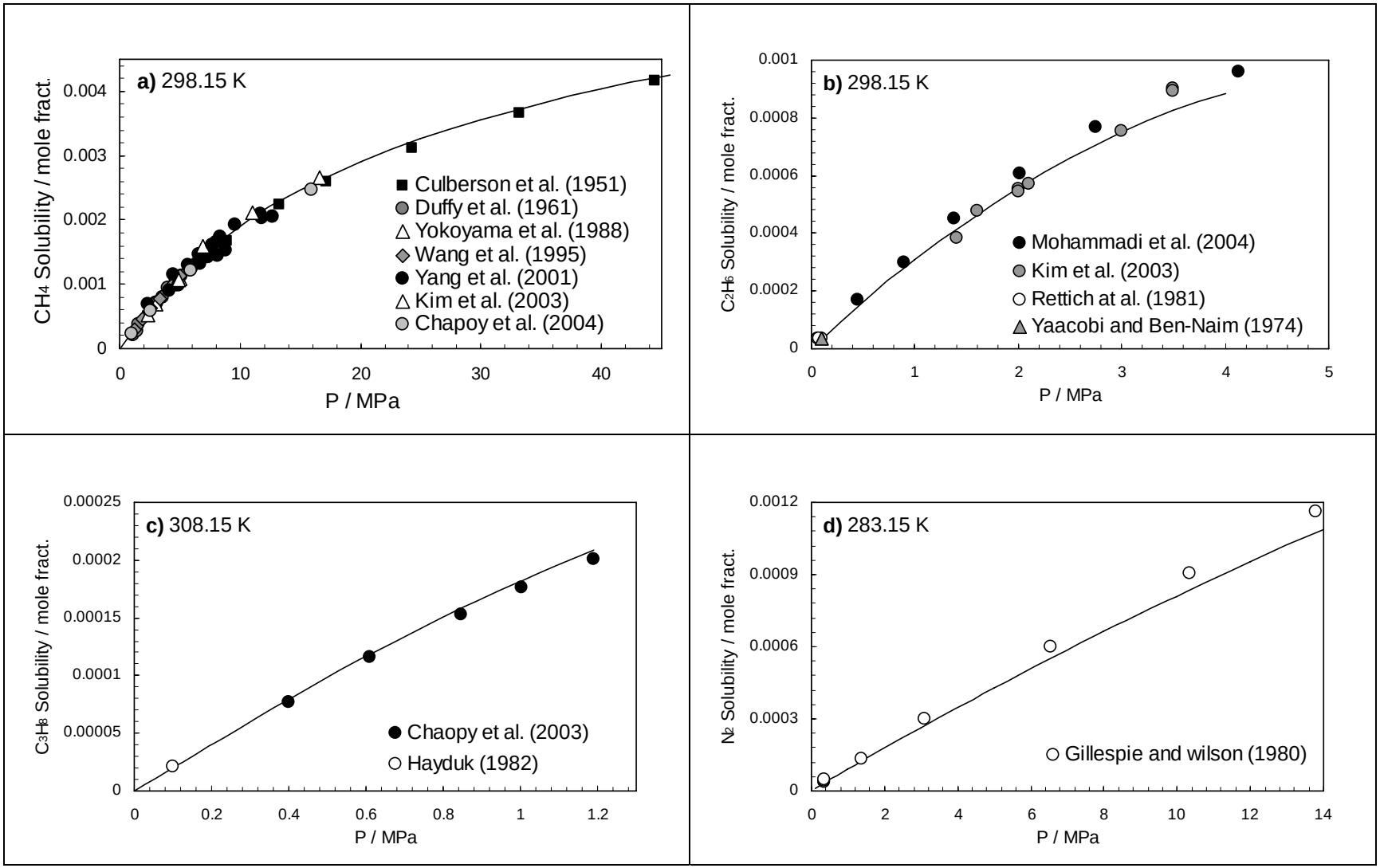

Figure 4.1 Experimental and calculated solubility of methane (a), ethane (b), propane (c) and nitrogen (d) in water. Black lines are the calculated solubilities in water by using the optimised BIPs.

It can be seen from Figures 4.1a-d that the gas solubility predicted by the CPA EoS for each compound in water phase is in a good agreement with the experimental data.

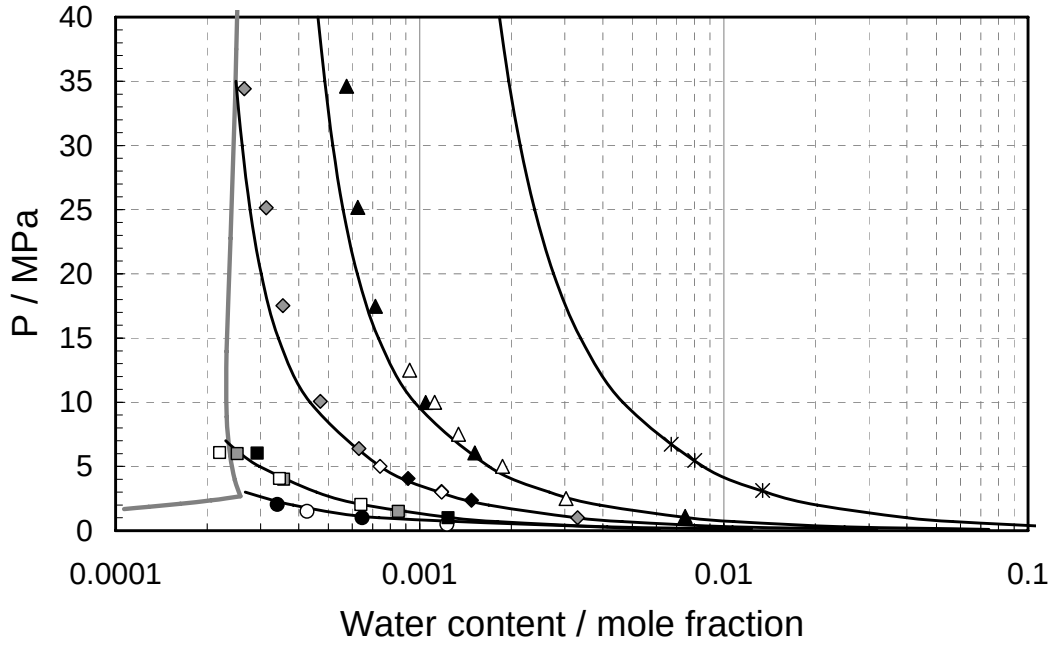

Figure 4.2 Experimental and predicted water content of methane in equilibrium with liquid water.
Experimental data at 273.11 K from Kosyakov et al., 1982 (●) and Althaus, 1999 (○).Experimental data at 283.1 K from Kosyakov et al., 1982 (□), Althaus, 1999 (■) and Chapoy et al. , 2003(■). Experimental data at 298.1 K from Rigby and Prausnitz, 1968 (◆), Yokoyama et al., 1988 (◇) and Chapoy et al., 2003 (◆). Experimental data at 313.13 K from Yarym-Agaev et al., 1985 (△) and Chapoy et al., 2003 (▲). Experimental data at 348.15 K from Rigby and Prausnitz, 1968 (✱). Black lines are model predictions for the water content of methane using CPA EoS. Gray line shows the methane hydrate phase boundary.

Figure 4.2 shows that predictions of the water content of methane in equilibrium with liquid water using the CPA EoS appear to be in an excellent agreement with experimental results, demonstrating the reliability of the developed model.

4.2.2 *Binary Systems Containing Methanol*

Methanol is probably one of the most versatile chemical in the natural gas processing and transportation. In addition to its conventional application as a hydrate inhibitor, methanol usage is reported in gas dehydration, sweetening and liquids recovery (Esteban et al., 2000). Methanol's most significant drawback is its high vapour loss (obviously this could be an advantage if methanol transfer in the gas phase is desirable, for example, in hydrate blockage removal). Depending on operating conditions, solubility loss of methanol into the sales gas can be very high and loss to the liquid

hydrocarbon phase can also be important. Therefore, it is of practical significance to study the mutual solubility of the major constituents of natural gas with methanol.

Binary interaction parameters between hydrocarbons and methanol have been obtained, by forcing the model to match experimental vapour-liquid equilibrium data on binary systems. Original sources of experimental data for binary mixtures of methane and methanol were presented in Chapter 2 (Tables 2.23 to 2.29). By minimizing the deviations between experimental solubility data and model predictions using the objective function presented in Equation 4.1, the following simple expression has been developed for binary interaction parameters between methanol and hydrocarbons:

$$k_{ij} = A + B \times T \tag{4.3}$$

where A and B are two constants and T is the temperature in Kelvin. The optimized values for interaction parameters are presented in Table 4.2. BIPs between methanol and hydrocarbons heavier than butane have been set to zero, due to observed scatter in the reported experimental data, therefore the developed model is not recommended for calculating the solubility of these compounds in methanol. However, it is believed that this assumption will not have any significant effect on the calculated solubility of gas in methanol due to low concentration of these compounds in the gas phase.

Table 4.2 Optimized values for interaction parameters between each of the non-associating compounds and methanol

Component	***A***	***B***
methane	0.04869	0
ethane	-0.02398	0.00018
propane	-0.04571	0.00031
iso-butane	-0.22227	0.00073
n-butane	0.29791	-0.00092
carbon dioxide	0.08676	-0.00028
nitrogen	0.17438	-0.00073

After gathering the available data from the literature and tuning the binary interaction parameters between methanol and each of the components, experimental solubility data were used to evaluate the CPA. Figures 4.3a, b, c, and d presents the experimental data and the CPA predicted gas solubility in methanol for methane, propane, nitrogen,

carbon dioxide, respectively. Figure 4.4 presents methanol content in the gas phase in methane-methanol systems. As methane is the main component of natural gases (about 87 mole%), a methane-methanol system could be regarded as the key system for predicting the concentrations of methanol in the vapour phase in natural gas-methanol systems (where the loss of methanol could be an issue of economical importance). The model predictions (Figure 4.4) are in an excellent agreement with the experimental data, demonstrating the reliability of the developed model.

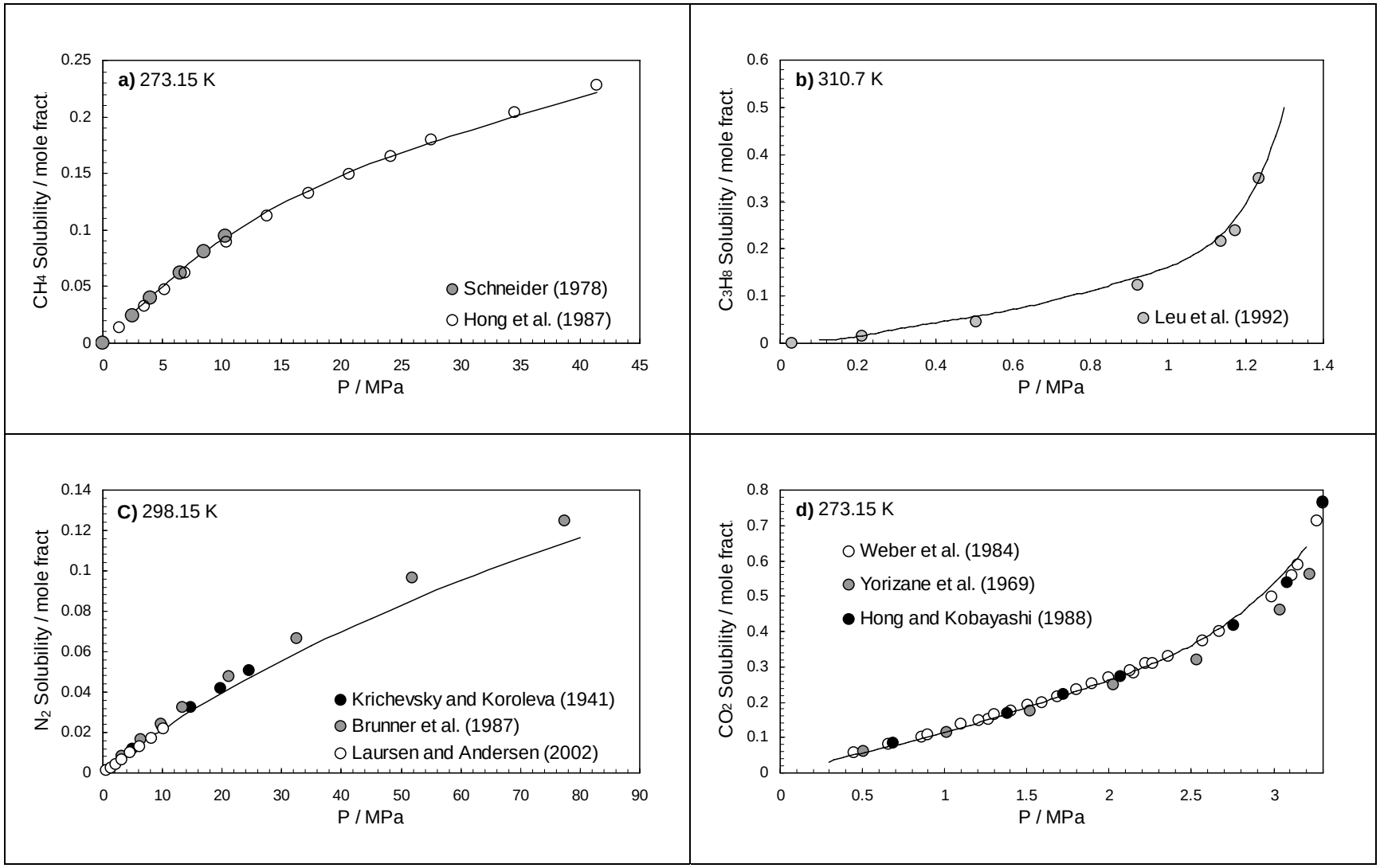

Figure 4.3 Experimental and calculated solubility of methane (a), propane (b), nitrogen (c) and carbon dioxide (d) in methanol. Black lines are the calculated solubilities in methanol by using the optimised BIPs.

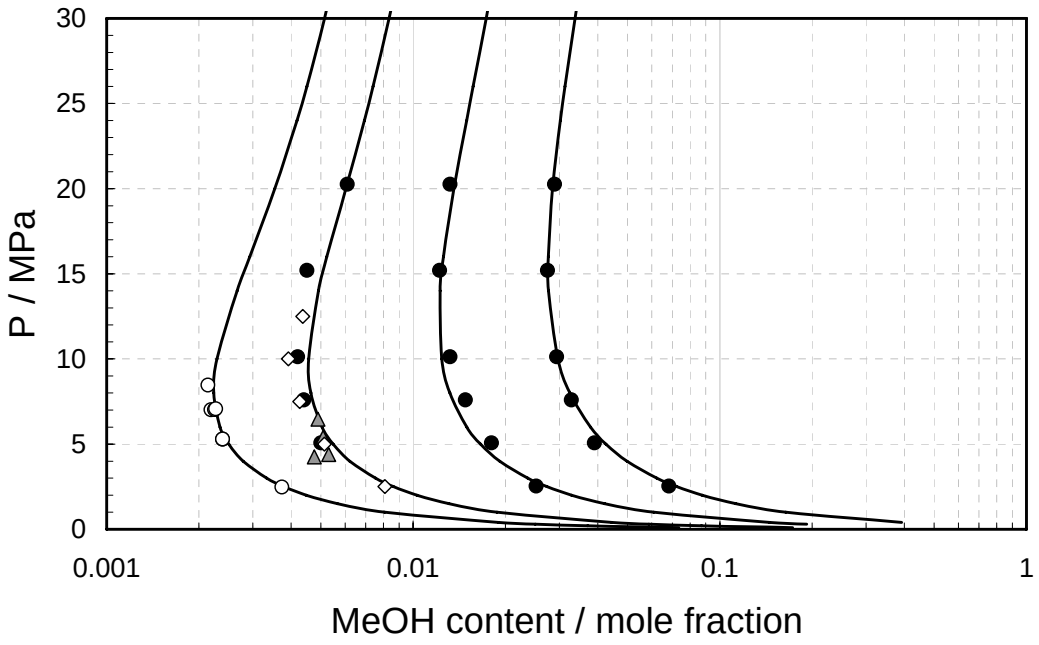

Figure 4.4 Experimental and predicted (black lines) methanol content in the gas phase of the methane-methanol systems.
Experimental data at 348.15 K and 323.15 K from Krichevsky and Koroleva, 1945 (●). Experimental data at 298.15 K from Krichevsky and Koroleva, 1945 (●), Hemmaplardh and King, 1972 (▲) and Yarym-Agaev et al., 1985 (◇). Experimental data at 283.15 K from Schlichting et al., 1993 (○).

4.2.3 *Binary Systems Containing Ethanol*

Ethanol is being used widely in some parts of the world for various reasons, including, advance ethanol industry (e.g. Brazil), less processing limitation (e.g., titanium heat exchangers), and less toxicity compare to methanol. Due to better environmental acceptability and relatively low cost of ethanol, many operators can save CAPEX on ethanol regeneration units. However, it is often injected at a higher rate than is actually necessary owing to uncertainties in its inhibition characteristics and partition in other phases.

The available data (i.e.: solubilities and ethanol vaporisation losses) on ethanol-gas equilibria have been gathered and presented in Chapter 2 (Tables 2.31 and 2.32) for main components of natural gases. By minimizing the deviations between experimental and predicted gas solubility in ethanol (Equation 4.1), a temperature dependent binary interaction parameter, k_{ij}, has been established, between ethanol and various components of natural gases. The following simple expressions are used:

$$k_{ij} = A + B \times T \tag{4.4}$$

where A and B are two constants and T is the temperature in Kelvin. The optimized parameters for interaction parameters are presented in Table 4.3 (BIPs between hydrocarbons heavier than propane and ethanol have been set to zero, due to the lack of experimental data. Therefore the developed model is not recommended for calculating the solubility of these compounds in ethanol. However, it is believed that this assumption will not have any significant effect on the calculated solubility of gas in ethanol due to low concentration of these compounds in the gas phase.).

Table 4.3 Optimized values for interaction parameters between each of the non-associating compounds and ethanol

Component	***A***	***B***
methane	0.05656	-0.00012
ethane	0.01534	-0.00006
propane	-0.03398	0.00019
carbon dioxide	0.00537	0
nitrogen	-0.00076	0.10414

Figure 4.5a, b, c, and d present the experimental and the predictions of the CPA model for the solubility of methane in ethanol at different temperatures. Figure 4.6 shows the CPA model predicted ethanol content in the gas phase (methane) against experimental data from literature.

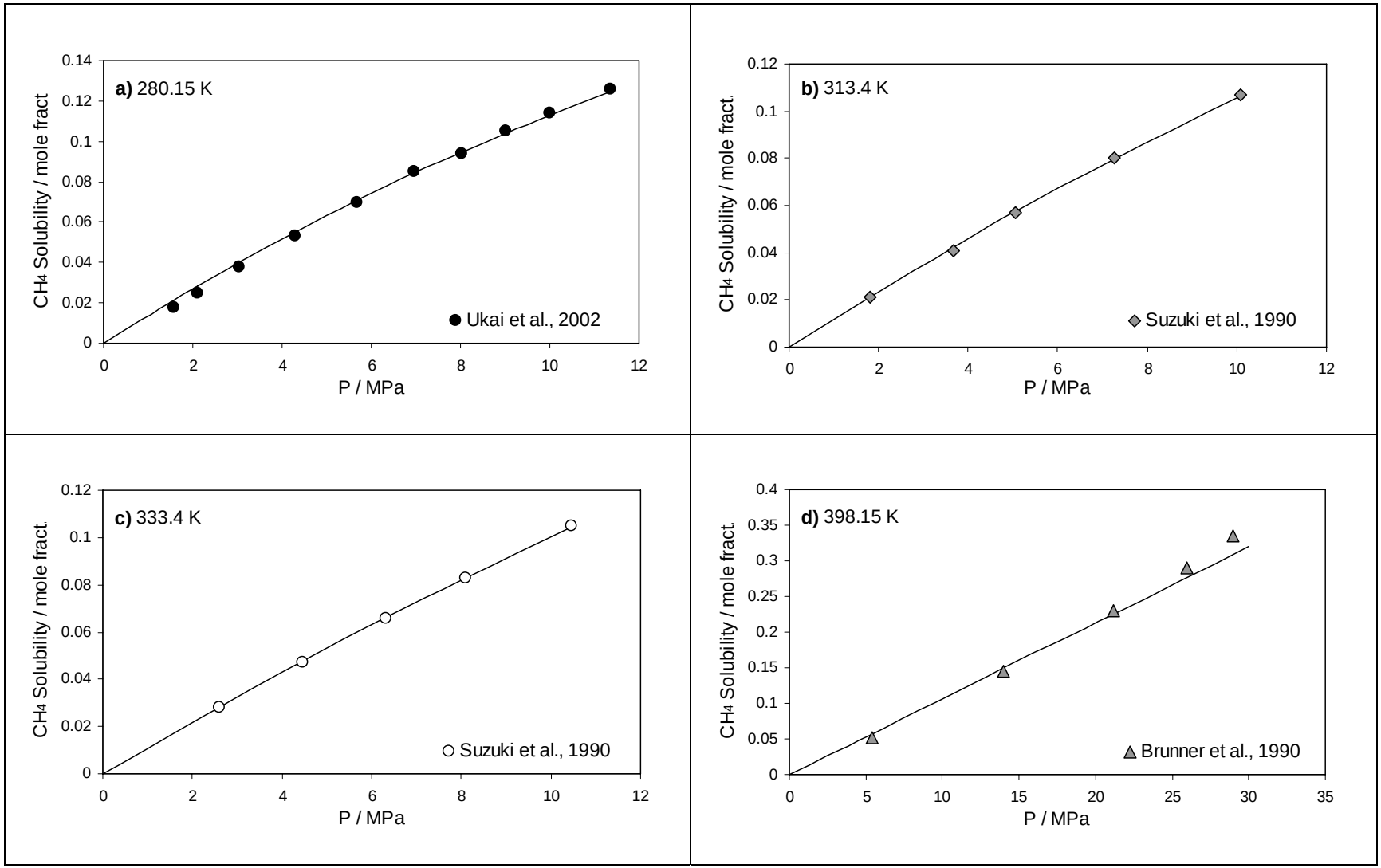

Figure 4.5 Experimental and calculated methane solubility in ethanol at 280.15, 313.4, 33.4 and 398.15 K. Black lines are the calculated solubilities in ethanol by using the optimised BIPs.

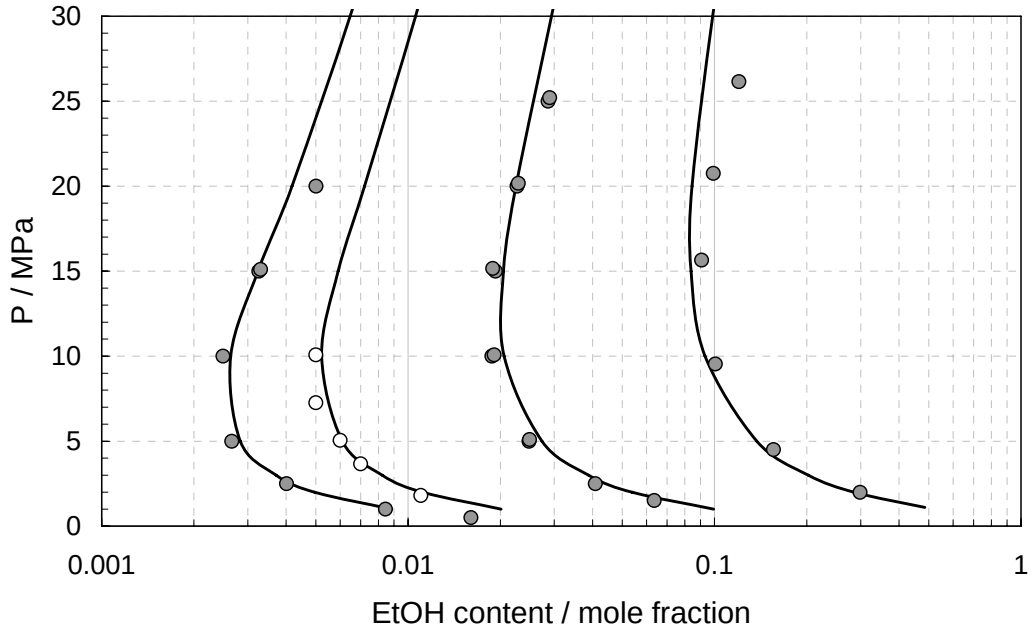

Figure 4.6 Experimental and predicted (black lines) ethanol content in the gas phase of methane-ethanol systems.
Experimental data at 398.15 K and 348.15 K and 298.15 from Brunner and Hueltenschmidt, 1990 (●). Experimental data at 313.15 K from Suzuki et al., 1990 (○).

4.2.4 *Binary Systems Containing n-Propanol*

In petroleum exploration and production, *n*-propanol is often used during stimulation and workover to aid in the rapid recovery of injected fluids (Keeney and Frost, 1978 and Grass, 1976). In recent years, *n*-propanol has also found use in prevention and remediation of hydrate-related problems in offshore operations, e.g., formulation of some chemicals. Therefore more investigation on its phase behaviour is required.

In this section, the available experimental data on the solubility of methane as the main component of natural gas (gathered and presented in Chapter 2, Table 2.34) in *n*-propanol has been used to tune the binary interaction parameter. Due to lack of experimental data to cover the whole temperature range of interest, a non-temperature dependent binary interaction parameter has been considered and has been set to the value of 0.007757 in this model. Figure 4.7 presents the results of the CPA model for predicting the solubility of methane in *n*-propanol against experimental data from literature, and a good match has been observed.

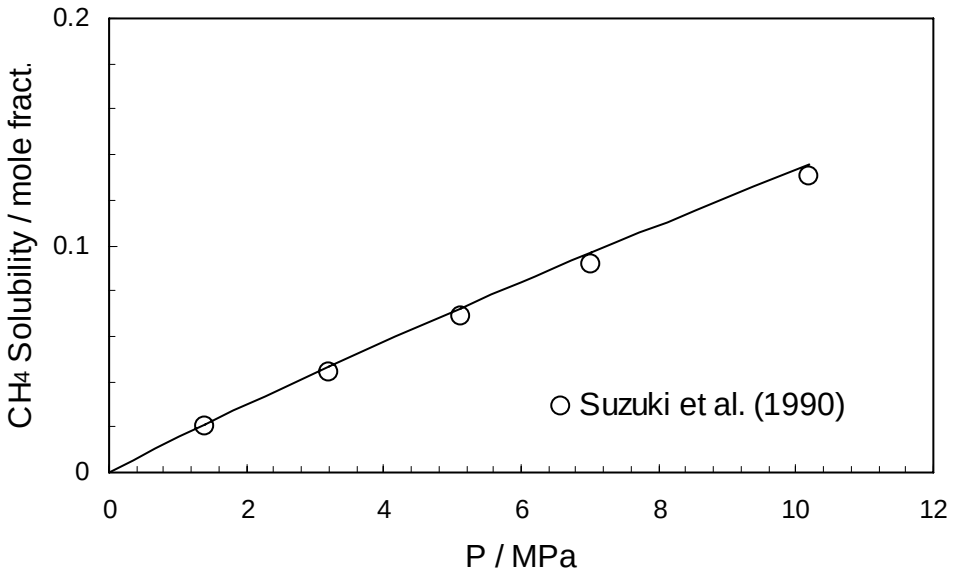

Figure 4.7 Experimental and calculated solubility of methane in n-propanol at 333.4 K. Black line is the calculated solubilities in n-propanol by using the optimised BIPs.

4.2.5 *Binary Systems Containing Monoethylene Glycol*

Glycols such as monoethylene glycol (MEG), diethylene glycol (DEG), triethylene glycol (TEG) are commonly used in gas dehydration processes. MEG is preferred over DEG for applications where the temperature is expected to be −10 °C or lower due to its high viscosity at low temperatures. TEG has too low vapour pressure to be suitable for use as an inhibitor injected into a gas stream. Ethylene glycol's high boiling point and affinity for water makes it an ideal dehydration agent for natural gas production. In the field, excess water vapour is usually removed by glycol dehydration. Glycols do not have the drawback of methanol, i.e., its high solvent loss. However depending on operating conditions, solubility of hydrocarbons and in particular aromatics and organic hydrocarbons in glycol aqueous solutions are not negligible. Accurate knowledge of the thermodynamic properties of the glycol/hydrocarbon equilibrium in a wide range of temperatures and pressures is also crucial for the gas processing industry and for developing or improving the accuracy of predictive models. Data (i.e.: solubilities and glycol vaporisation losses) on glycol-gas system for main components of natural gases have been gathered and presented in Chapter 2 (Table 2.35). The above experimental data have been used in tuning the developed model.

By minimizing the deviations between predicted and experimental gas solubility in glycol (Equation 4.1), a temperature dependent binary interaction parameter, k_{ij}, has

been established between glycol and natural gas components. The following simple expressions are used:

$$k_{ij} = A + B \times T \tag{4.5}$$

where A and B are two constants and T is the temperature in Kelvin. The optimized parameters for interaction parameters are presented in Table 4.4 (BIPs between hydrocarbons heavier than propane and MEG have been set to zero, due to the lack of experimental data. As a result the developed model is not recommended for calculating the solubility of these compounds in MEG. However, it is believed that this assumption will not have any significant effect on the calculated solubility of gas in MEG due to low concentration of these compounds in the gas phase.). After gathering the available data from the literature and tuning the binary interaction parameters for each component and MEG, experimental solubility data were used to examine the accuracy of the tuning for the CPA EoS (Figure 4.8).

Table 4.4 Optimized values for interaction parameters between each of the non-associating compounds and MEG

Component	***A***	***B***
Methane	0.0004	0.0498
Ethane	0.1155	0
Propane	0.0002	0.0348
carbon dioxide	-0.0002	0.1141
Nitrogen	0.1731	0
Hydrogen sulphide	-0.0126	0

Figure 4.8a, b, c, and d present the experimental and predicted (using the developed the CPA model) solubility of methane, ethane, nitrogen, and carbon dioxide in monoethylene glycol, respectively.

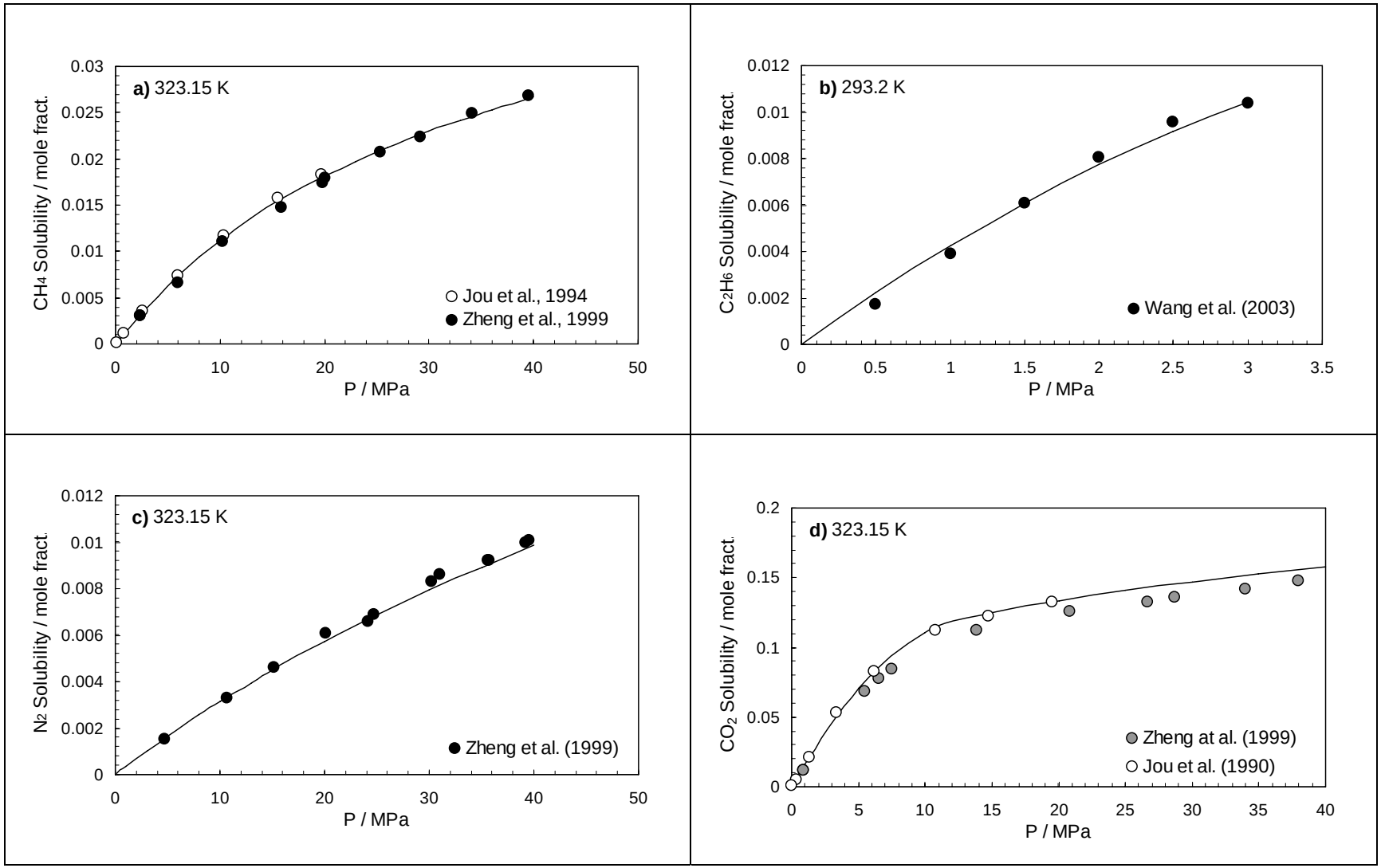

Figure 4.8 Experimental and calculated solubility of methane (a), ethane (b), nitrogen (c) and carbon dioxide (d) in MEG. Black lines are the calculated solubilities in MEG by using the optimised BIPs.

To estimate the amount of monoethylene glycol loss into the gas, the composition of monoethylene glycol in the gas phase has been calculated using the CPA model developed in this work (Figure 4.9). The model predictions appear to be in reasonable agreement with the experimental data, considering the fact that the amount monoethylene glycol loss into the gas phase is in order of ppm.

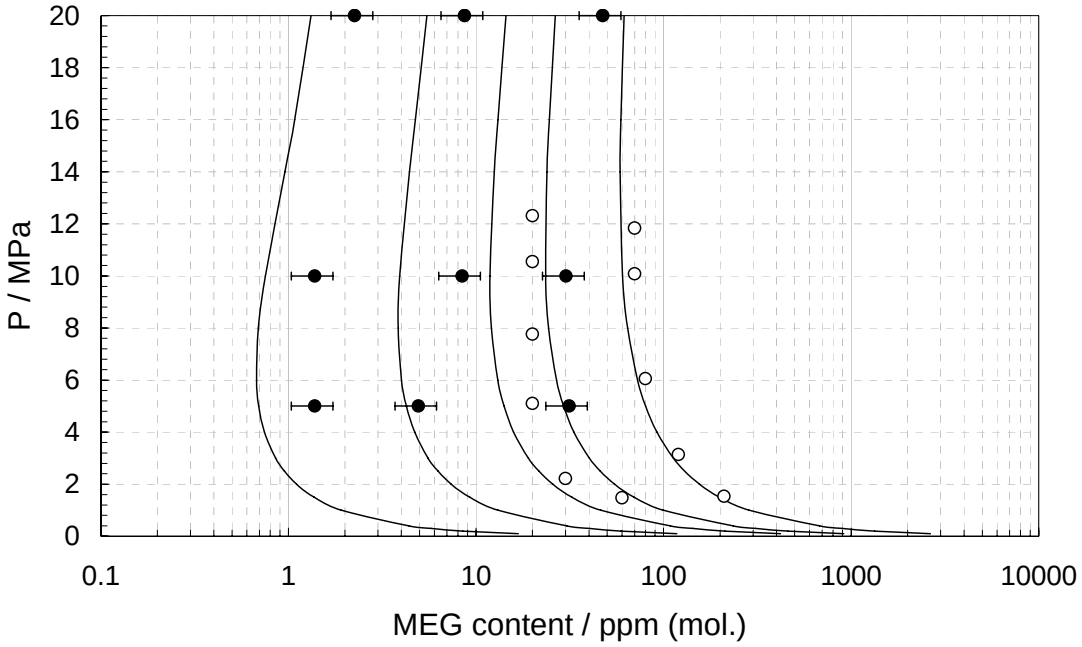

Figure 4.9 Experimental and predicted MEG (black lines) content in the gas phase of methane-MEG system.
Experimental data at 323.15 K, 298.15 K, 278.15 K from Folas et al., 2007 (●).
Experimental data at 338.15 K, 313.15 K from Schlichting, 1991 (○).

4.3 Application of the CPA EoS to Cross-Associating Systems

Mixtures of associating components, and in particular mixtures of water and alcohols or glycols with hydrocarbons, are of great interest to the oil and gas industry. In this section the capability of the CPA EoS to describe VLE and SLE of alcohol/glycol – water mixtures over an extended temperature and pressure range using a temperature dependent interaction parameter is studied. Binary interaction parameters for methanol/ethanol/*n*-propanol/MEG and water have been obtained, by forcing appropriate models to fit experimental binary data for vapour-liquid (bubble and dew point data) or solid-liquid (freezing point depression data) equilibrium conditions over the temperature range of interest. Original sources of experimental data for binary mixtures have been given in Chapter 2. Here we are presenting the modelling results

for the binary of methanol/ethanol/*n*-propanol/MEG and water system as an application of the CPA EoS to cross associating systems.

The binary interaction parameters between cross-associating compounds have been adjusted directly to experimental data through a modified Simplex algorithm (Åberg and Gustavsson, 1982) using the following objective function based on the minimization of the difference between the calculated and experimental data:

$$OF = \begin{cases} \frac{1}{NP} \times \sum_{i}^{NP} \left(\frac{P_i^{calc.} - P_i^{\exp.}}{P_i^{\exp.}} \right)^2, \textit{for VLE data} \\ \frac{1}{NP} \times \sum_{i}^{NP} \left(\frac{T_i^{calc.} - T_i^{\exp.}}{T_i^{\exp.}} \right)^2, \textit{for SLE data} \end{cases} \tag{4.6}$$

By minimizing the average absolute deviations, a temperature dependent k_{ij} has been established, for each binary system. The available data from the literature used for the tuning of the binary interaction parameters between the cross-associating compounds were gathered and presented in Chapter 2.

4.3.1 *Binary Systems of Water/Methanol*

The experimental VLE binary data for water and methanol, (with the exception of the data of Kuihara et al., 1995), which were kept as independent data for validation of the model), and the ice-liquid equilibrium conditions (using the melting point data reported in the CRC Handbook, 2004) which have been reported in Chapter 2 (Table 2.30), were used for tuning the binary interaction parameters between water and methanol. The following expression is proposed for binary interaction parameter between methanol and water:

$$k_{ij} = 3.4463 \times 10^{-6} T^2 - 9.5986 \times 10^{-4} T - 0.1197 \tag{4.7}$$

Both VLE and SLE phase equilibria calculations have been performed for the binary cross-associating mixture of methanol and water. As shown in Figure 4.10 the model accurately calculates freezing points of aqueous methanol solutions. Also as demonstrated in Figures 4.11 and 4.12, it can predict accurately methanol - water vapour-liquid equilibrium.

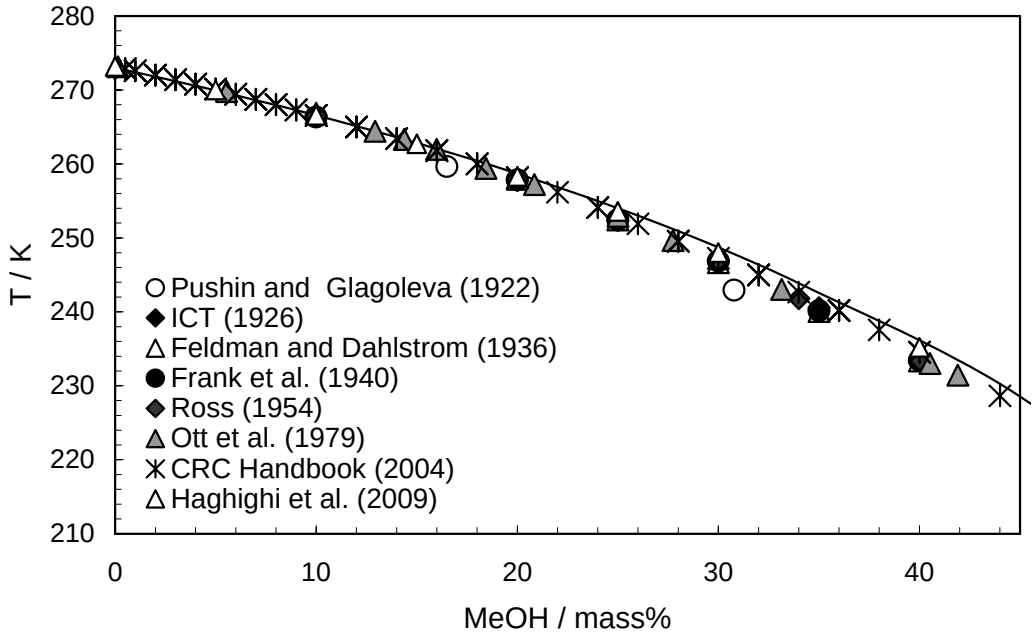

Figure 4.10 Experimental and calculated (black line) water freezing point temperatures in the presence of various concentrations of methanol

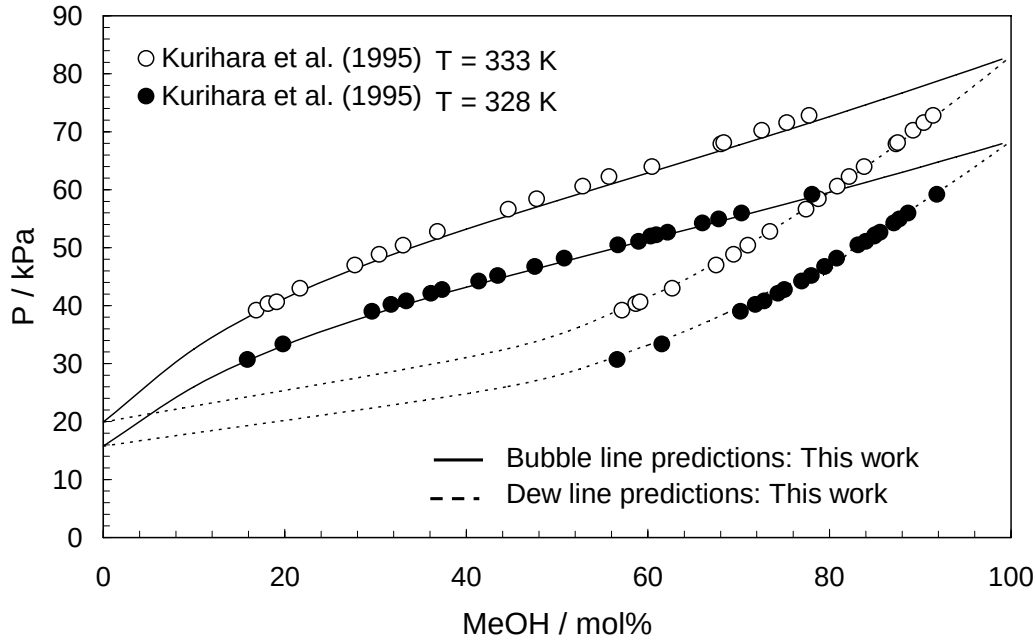

Figure 4.11 Experimental and predicted methanol concentrations in vapour and liquid phases for methanol - water systems at 333 K and 328 K

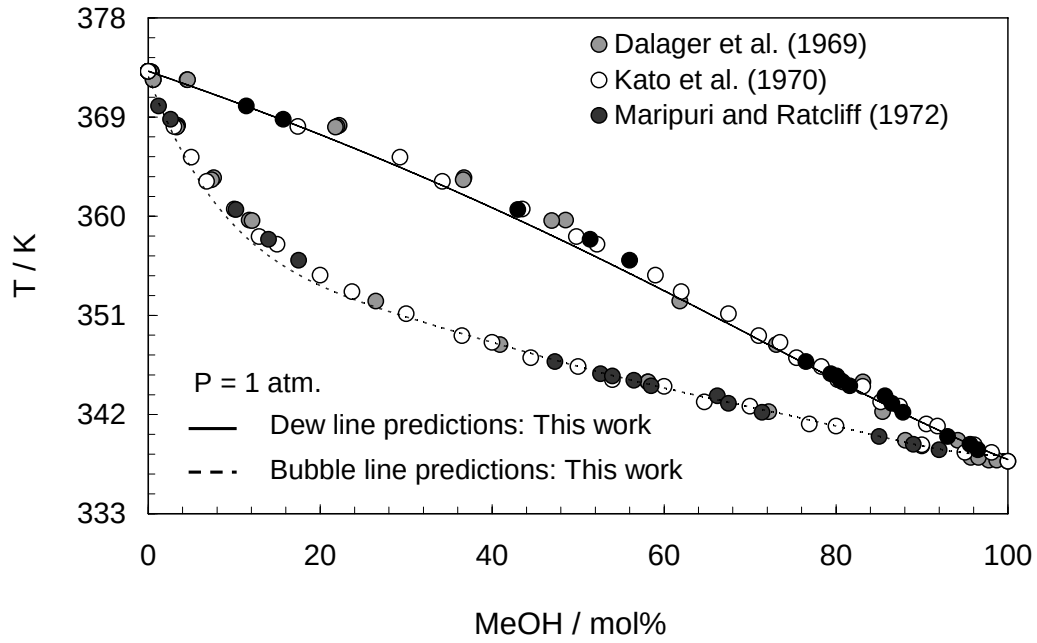

Figure 4.12 Experimental and predicted methanol concentrations in vapour and liquid phases for methanol - water systems at 1 atm

4.3.2 *Binary Systems of Water/Ethanol*

The experimental VLE binary data of water and ethanol, and freezing point of aqueous ethanol solutions (with the exception of the data of Reider and Thompson, 1949 and Anderson et al., 2008) which have been reported in Chapter 2 (Table 2.33), were used for tuning the binary interaction parameters between water and ethanol. The following expression is proposed for ethanol and water:

$$k_{ij} = -5.6946\times10^{-7}T^3 + 4.9661\times10^{-4}T^2 - 0.1412\times T - 13.0024 \qquad (4.8)$$

Both VLE and SLE phase equilibria calculations have been performed for the binary cross-associating mixture of ethanol and water. As Figure 4.13 shows the model calculates freezing points of water-ethanol system for different concentrations of ethanol with satisfactory accuracy. Also as demonstrated in Figure 4.14, it can predict accurately ethanol - water vapour-liquid equilibrium.

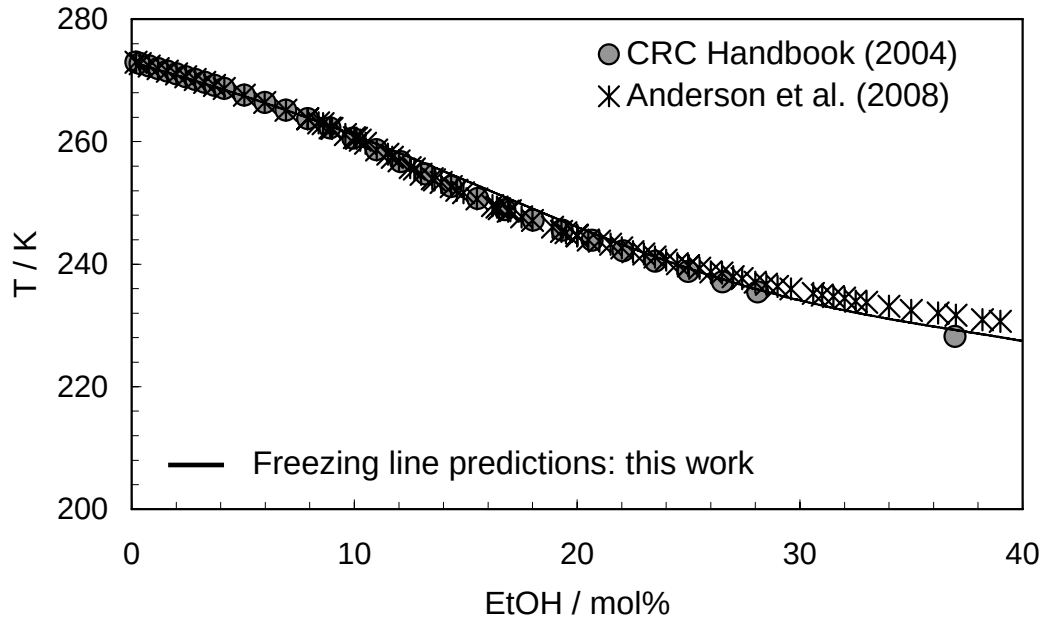

Figure 4.13 Experimental and calculated water freezing point temperatures in the presence of various concentrations of ethanol

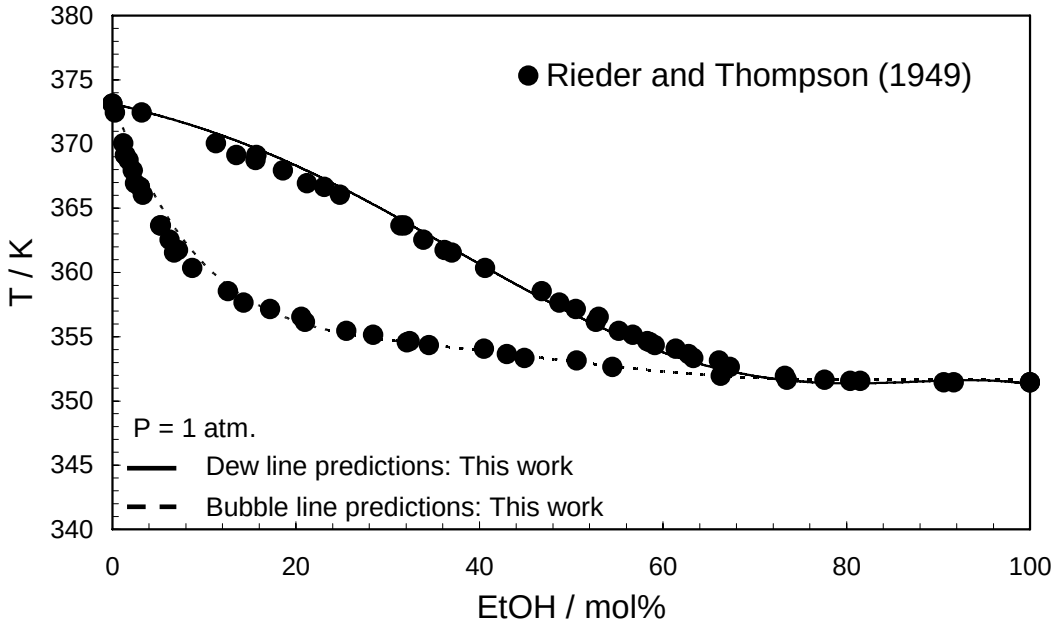

Figure 4.14 Experimental and predicted ethanol concentrations in vapour and liquid phases for ethanol - water systems at 1 atm

4.3.3 *Binary Systems of Water/n-Propanol*

The binary interaction parameters between water and *n*-propanol have been optimized using VLE data and melting point data reported in Chapter 2 (Table 2.34). A similar Simplex algorithm and the objective function, FOB, displayed in Equation 4.6 were used to optimize the binary interaction parameters. The following expression is proposed for *n*-propanol and water:

$$k_{ij} = -4.7125\times10^{-5}T^2 + 3.0303\times10^{-2}T - 4.8741 \qquad (4.9)$$

4.3.4 *Binary Systems of Water/Monoethylene Glycol*

The binary interaction parameters between water and monoethylene glycol have been optimised, by minimising the deviation between predictions and the experimental VLE binary data reported in Chapter 2, Table 2.36 (with the exception of the data of Chiavone-Filho et al. (1993), which were kept as independent data for validation of the model), and the ice-liquid equilibrium conditions (using the melting point data reported in the CRC Handbook, 2004). The following simple expression is proposed for monoethylene glycol and water:

$$k_{ij} = 5.6294\times10^{-4}T - 0.2313 \qquad (4.10)$$

Both VLE and SLE phase equilibria calculations have been performed for the binary cross-associating mixture of monoethylene glycol and water. As shown in Figure 4.15, the model accurately calculates freezing points of water-MEG system for different concentrations of MEG. Also as demonstrated in Figures 4.16 and 4.17, it can predict accurately the vapour-liquid equilibrium in monoethylene glycol – water systems.

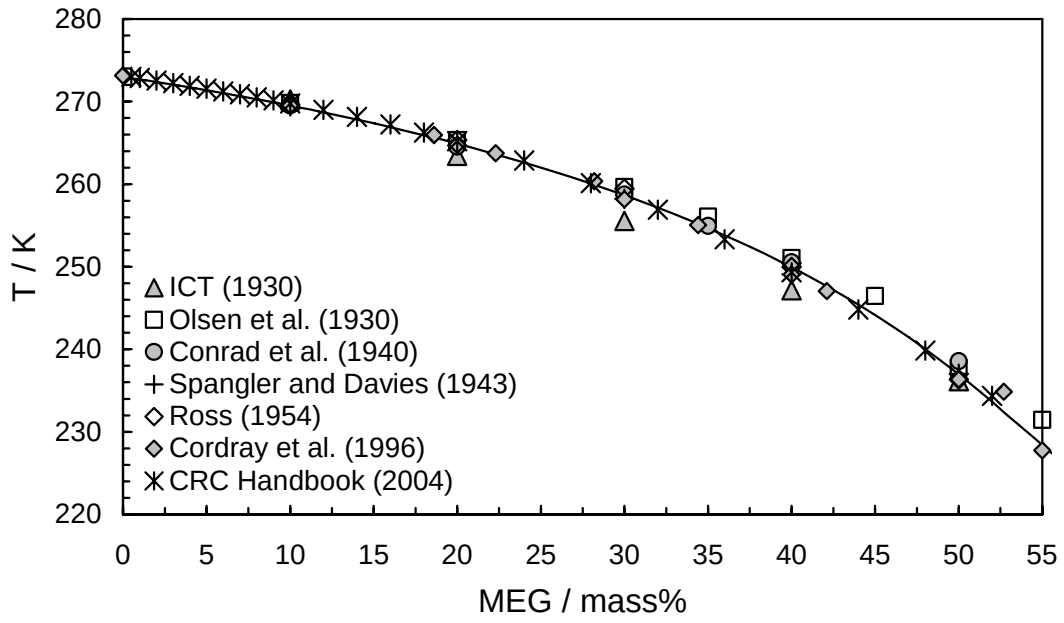

Figure 4.15 Experimental and calculated (black line) water freezing point temperatures in the presence of various concentrations of MEG

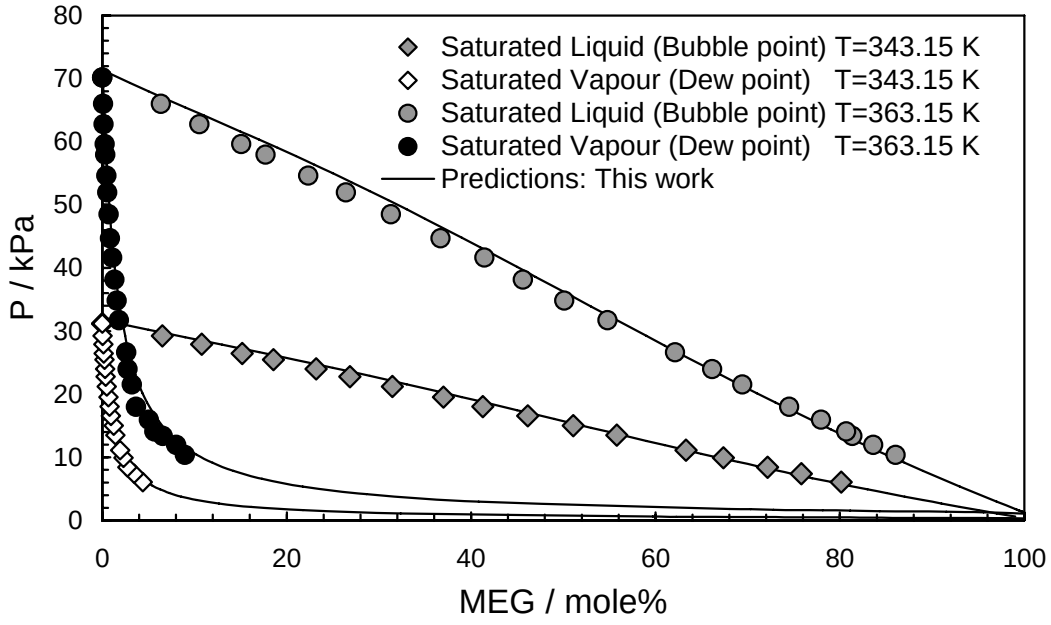

Figure 4.16 Experimental and predicted MEG concentrations in vapour and liquid phases for MEG - water systems at 343.15 K and 363.15 K (Experimental data from Chiavone-Filho et al., 1993)

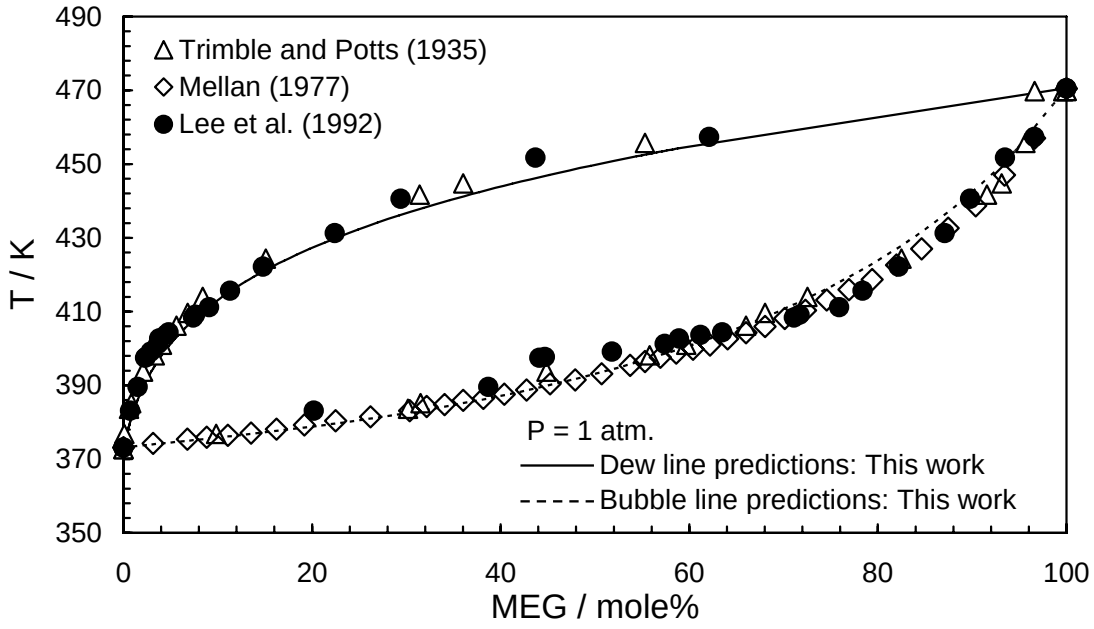

Figure 4.17 Experimental and predicted MEG concentrations in vapour and liquid phases for MEG - water systems at 1 atm

4.4 Vapour Pressure and Freezing Point of Electrolyte Solutions

There has been a strong interest in developing either predictive thermodynamic models or correlations capable of predicting hydrate phase boundaries in systems containing single and mixed electrolytes solutions. Accurate models describing phase behaviour of these systems are necessary for analysing, designing and optimising processes and equipment in the chemical and petroleum industries. Studying the effect of electrolyte

solutions on thermodynamic phase behaviour of electrolyte solutions is the first step to gain a better understanding of the effect of salts on gas hydrate stability conditions.

The available experimental data (vapour pressure and freezing point depression of single and mixed electrolyte solutions) have been collected from the literature and were used for tuning of interaction coefficients. The binary interaction parameter between water and dissolved salts for nine electrolytes has been previously presented in Chapter 3 (Table 3.3). The new experimental freezing point depressions of different concentrations of single salt measured in this work have been described in Chapter 2 (Table 2.2). None of the experimental data generated in this laboratory have been used in the optimisation process, hence can be used as independent data for validation of the model.

Figures 4.18 through 4.22 present the experimental and predicted freezing point depression of various salts, as well as some new experimental data generated in this work. The thermodynamic model based on CPA EoS developed in this work has been used in all predictions. As shown in the figures, the predictions are in good agreement with the experimental data, demonstrating the reliability of the model developed in this work. Figures 4.23 through 4.25 present the predicted vapour pressure of water for different concentrations of single salts against literature data and Figures 4.26 through 4.29 show the experimental and predicted freezing point depression in the presence of mixed electrolyte solutions as well as the new experimental data generated in this work.

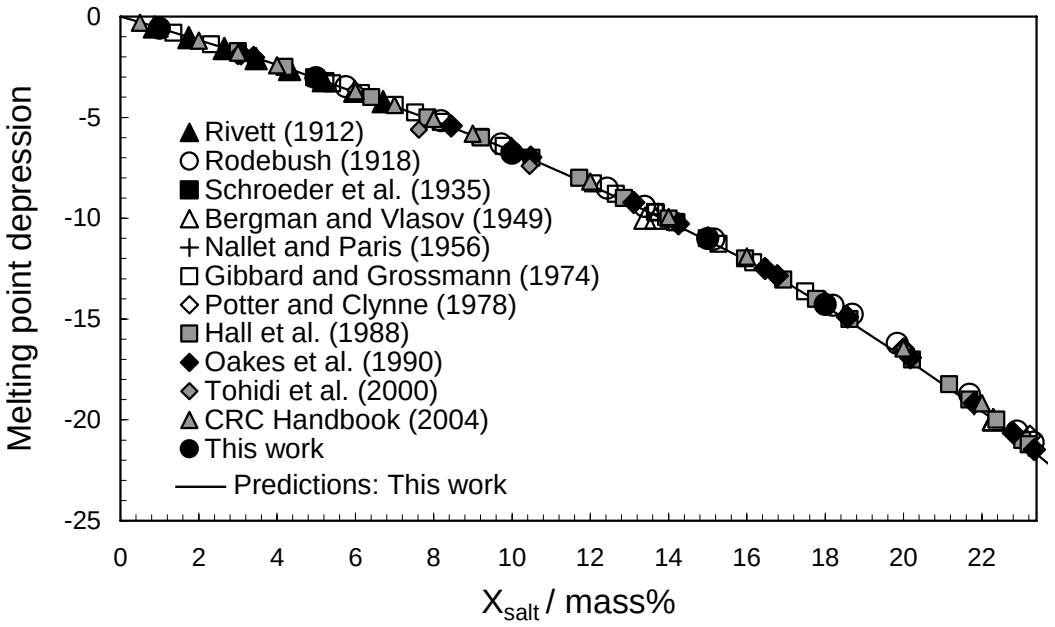

Figure 4.18 Freezing point depression in the presence of different concentrations of NaCl.
Black line: the CPA model predictions. Experimental data from Rivett, 1912 (▲), Rodebush, 1918 (○), Schroeder et al., 1935 (■), Bergman and Vlasov, 1949 (△), Nallet and Paris, 1956 (+), Gibbard and Grossmann, 1975 (□), Potter et al., 1978 (◊), Hall et al., 1988 (■), Oakes et al., 1990 (▲), Tohidi et al., 2001 (◆), CRC Handbook (▲) and this work (●).

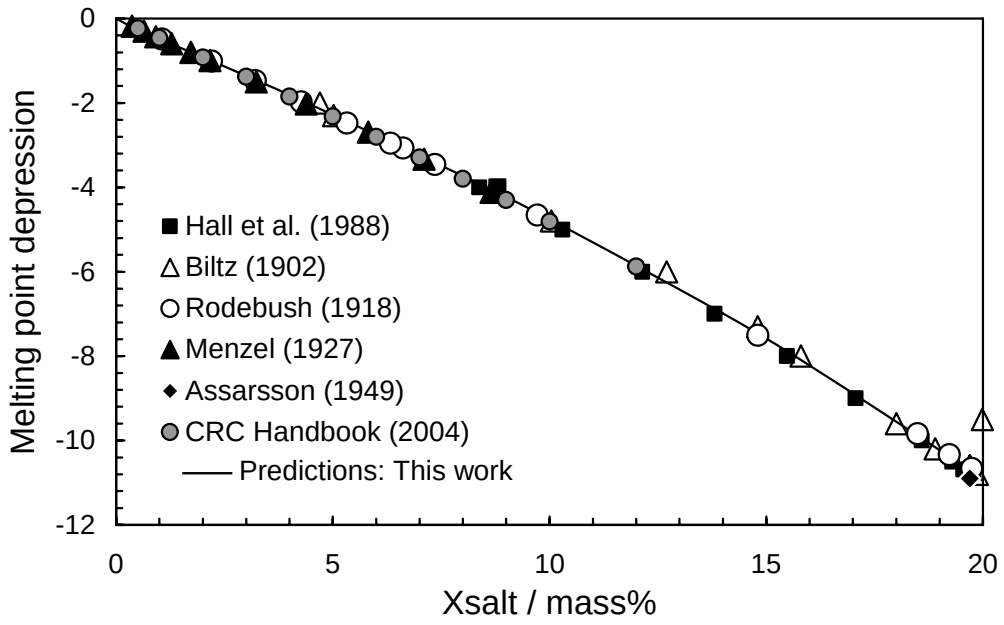

Figure 4.19 Freezing point depression in the presence of different concentrations of KCl.
Black lines: the CPA model predictions. Experimental data from Hall et al., 1988 (■), Biltz, 1902 (△), Rodebush, 1918 (○), Menzel, 1927 (▲), Assarsson, 1949 (◆) and CRC Handbook (●).

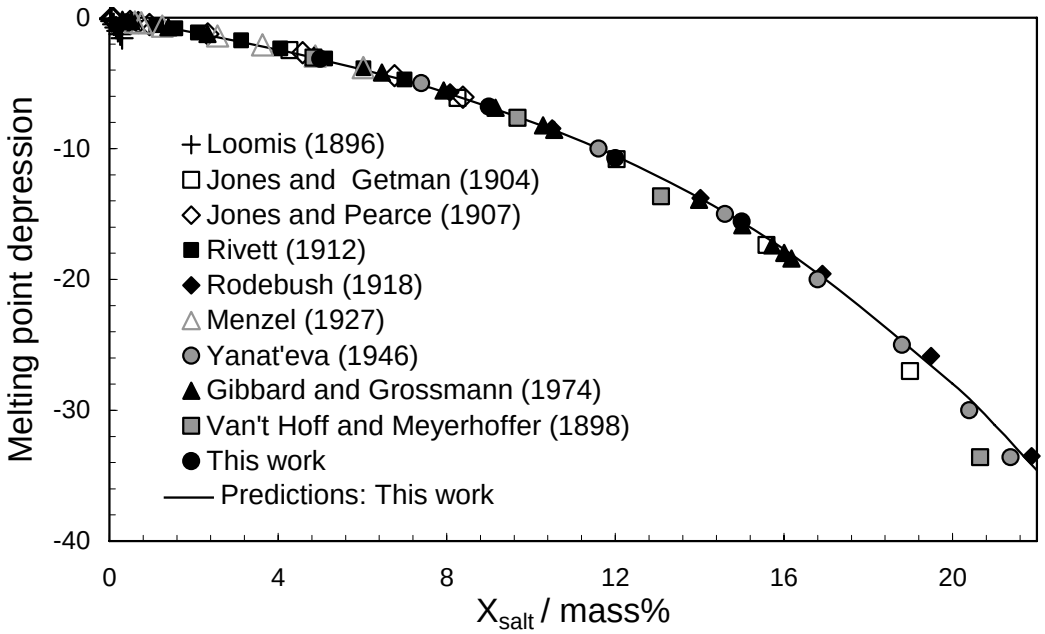

Figure 4.20 Freezing point depression in the presence of different concentration of $MgCl_2$.
Black lines: the CPA model predictions. Experimental data from Loomis, 1896 (+), Jones and Getman, 1904 (□), Jones and Pearce, 1907 (◇), Rivett, 1912 (■), Rodebush, 1918 (◆), Menzel, 1927 (△), Yanateva, 1946 (●), Gibbard and Grossmann, 1975 (▲), Van't Hoff and Meyerhoffer, 1898 (■) and this work (●).

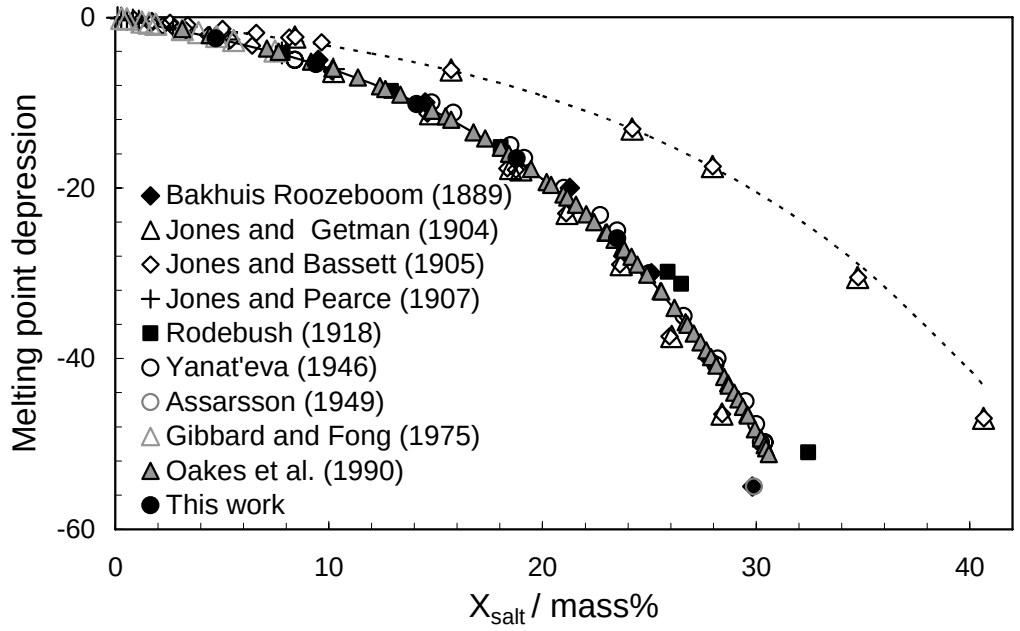

Figure 4.21 Freezing point depression in the presence of different concentration of $CaCl_2$ and $CaBr_2$.
Black lines: the CPA model predictions for the $CaCl_2$-water system. Experimental data from Bakhuis Roozeboom, 1889 (◆), Jones and Getman, 1904 (△), Jones and Bassett, 1905 (◇), Jones and Pearce, 1907 (+), Rodebush, 1918 (■), Yanateva, 1946 (○), Gibbard and Fong, 1975 (△), Oakes et al., 1990 (▲) and this work (●). Dotted black lines: model predictions for the $CaBr_2$-water system, experimental data from Jones and Getman, 1904 (△) and Jones and Bassett, 1905 (◇).

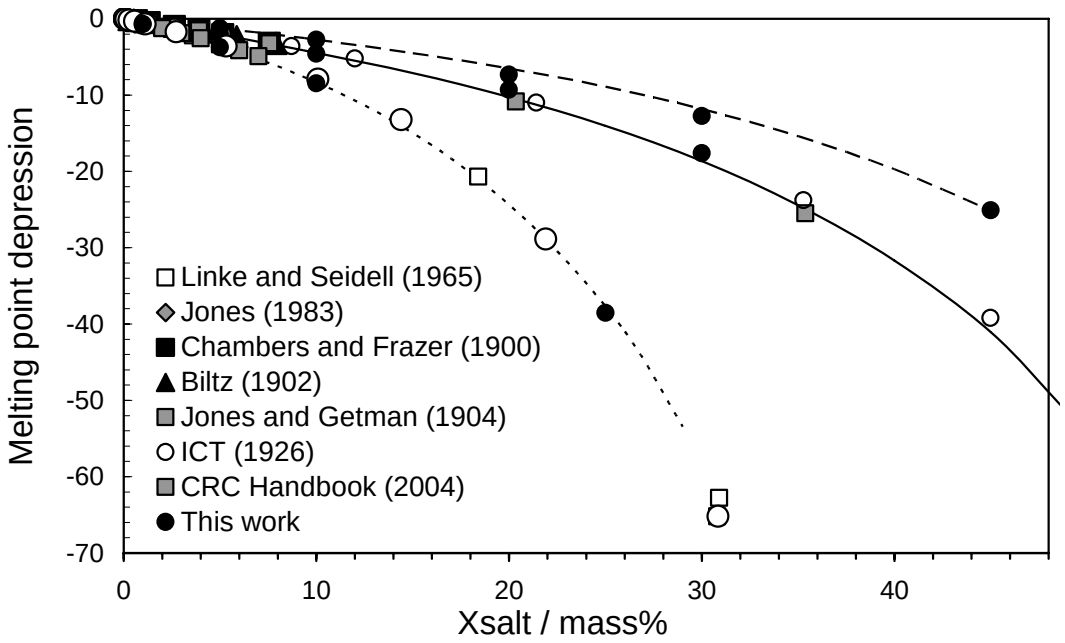

Figure 4.22 Freezing point depression in the presence of different concentrations of $ZnCl_2$, $ZnBr_2$ and KOH.
Black Line: the CPA model predictions for the $ZnCl_2$-water system. Experimental data from CRC Handbook (■), Jones, 1893 (◆), Chambers and Frazer, 1900 (■), Biltz, 1902 (▲), Jones and Getman, 1904 (■), ICT (○) and this work (●). Dotted Black line:the CPA model predictions for the $ZnBr_2$-water system, experimental data from this work (●). Dashed line: the CPA model predictions for the KOH-water system, experimental data from Linke and Seidell, 1965 (□), CRC Handbook, 2004 (■), ICT, 1926 (○) and this work (●).

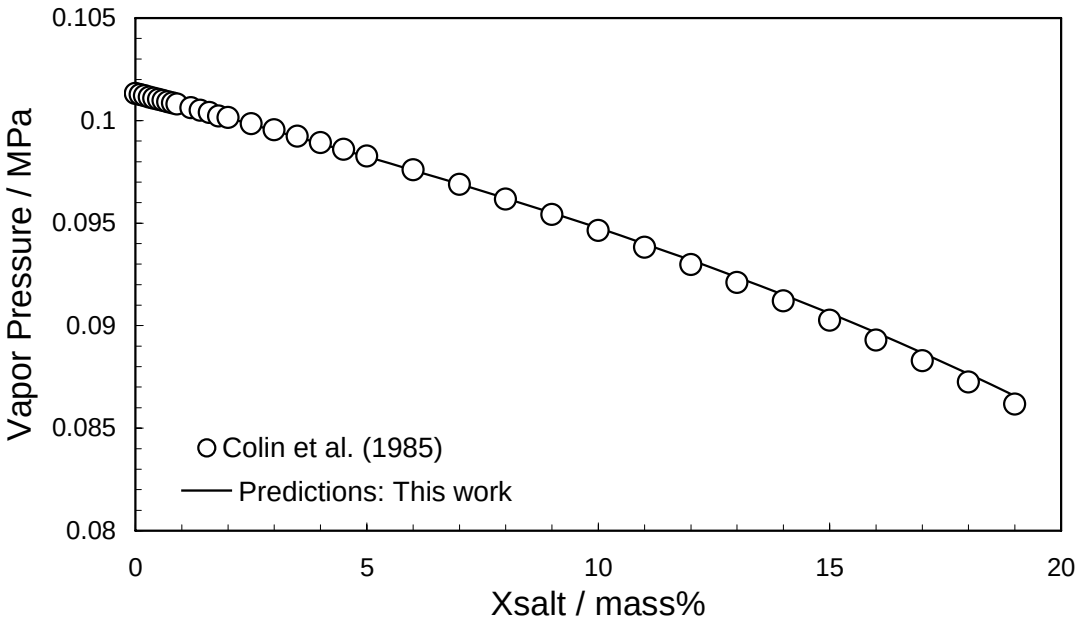

Figure 4.23 Experimental and predicted (using the CPA model developed in this work) vapour pressure of water in the presence of different concentration of NaCl at 373.15K. Experimental data from Colin et al., 1985 (○).

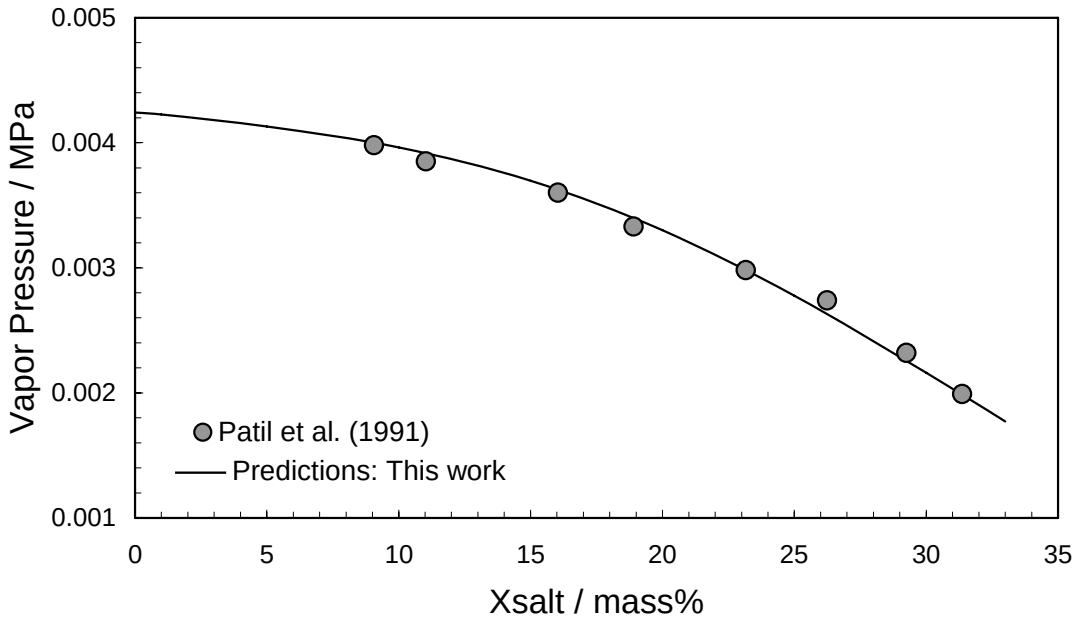

Figure 4.24 Experimental and predicted (the CPA model developed in this work) vapour pressure of water in the presence of different concentrations of $MgCl_2$ at 303.15K.
Experimental data from Patil et al., 1991(●).

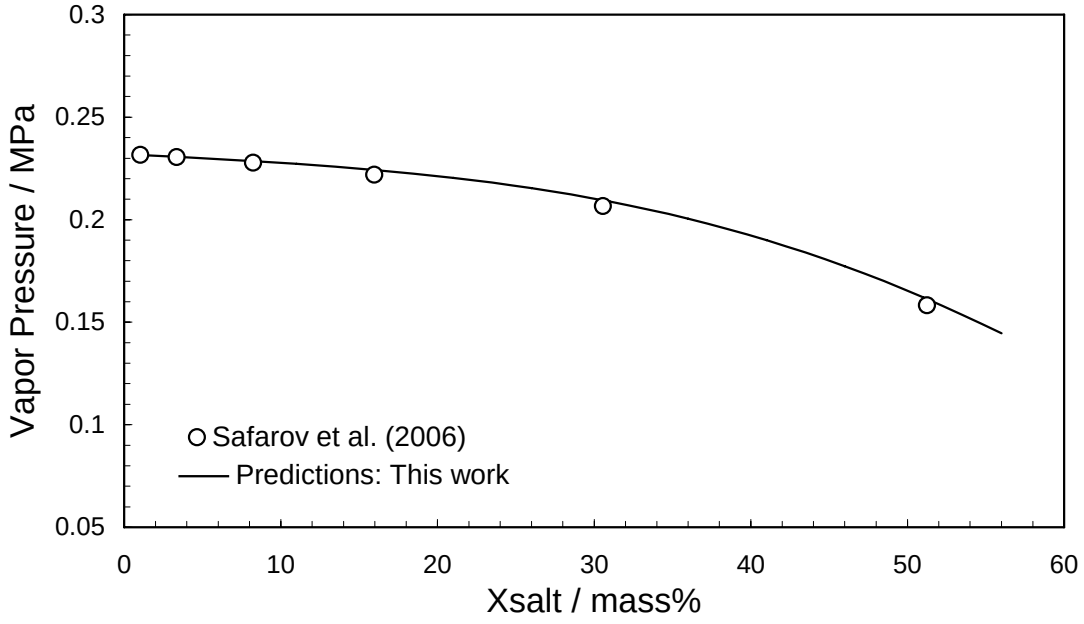

Figure 4.25 Experimental and predicted (using the CPA model developed in this work) vapour pressure of water in the presence of different concentrations of $ZnCl_2$ at 398.15K.
Experimental data from Safarov et al., 2006 (○).

Experimental freeing point depression for four mixed electrolyte solutions (H_2O-NaC1-KCl, H_2O-NaC1-$CaCl_2$, H_2O-KC1-$CaCl_2$, and H_2O-NaC1-$MgCl_2$) measured by a reliable differential thermal analysis technique are presented in Chapter 2 (Table 2.3).

As shown in Figures 4.26 to 4.29, the CPA model developed in this work can accurately predict the freezing point depression. It should be noted that none of the experimental data were used in the tuning of the model.

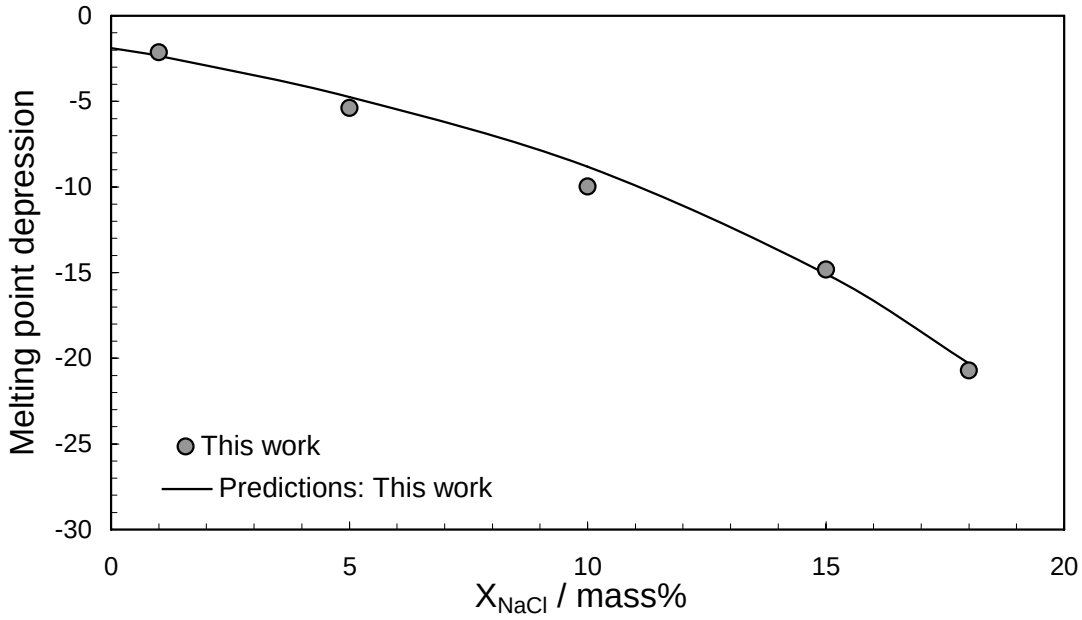

Figure 4.26 Experimental and predicted (using the CPA model developed in this work) freezing point depression of aqueous solutions of NaCl and 3 mass% $CaCl_2$. Experimental data from this work (●).

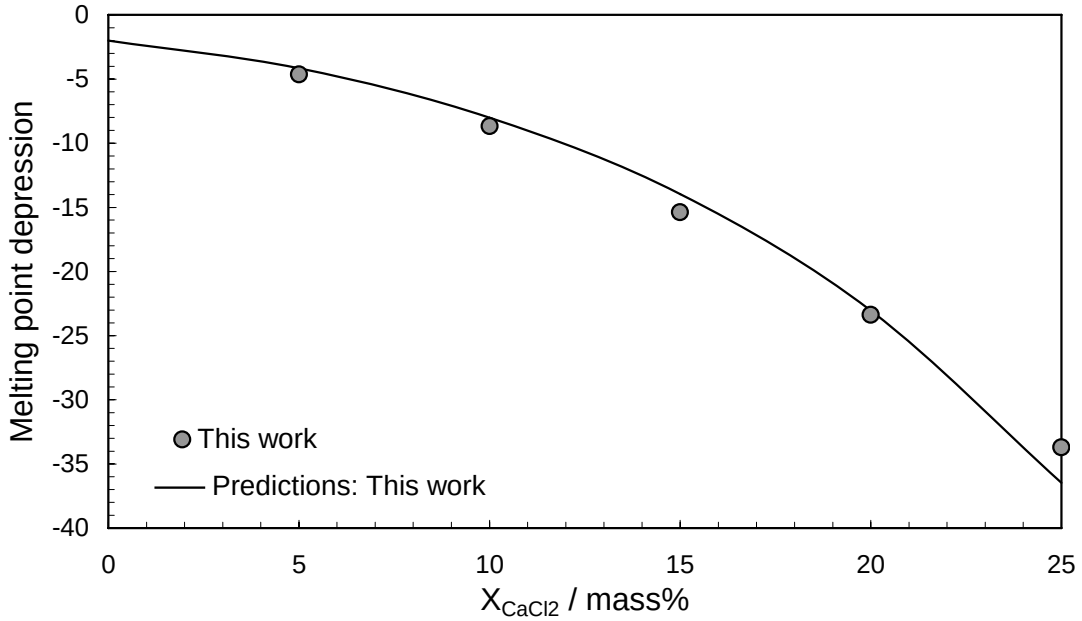

Figure 4.27 Experimental and predicted (using the CPA model developed in this work) freezing point depression of aqueous solutions of $CaCl_2$ and 3 mass% KCl. Experimental data from this work (●).

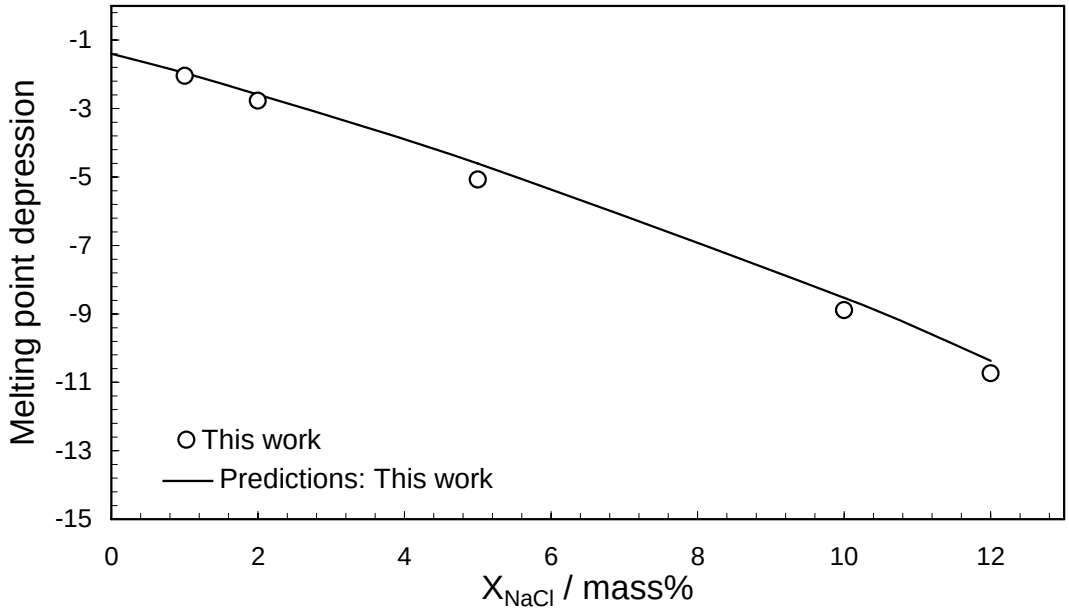

Figure 4.28 Experimental and predicted (using the CPA model developed in this work) freezing point depression of aqueous solutions of NaCl and 3 mass% KCl. Experimental data from this work (○).

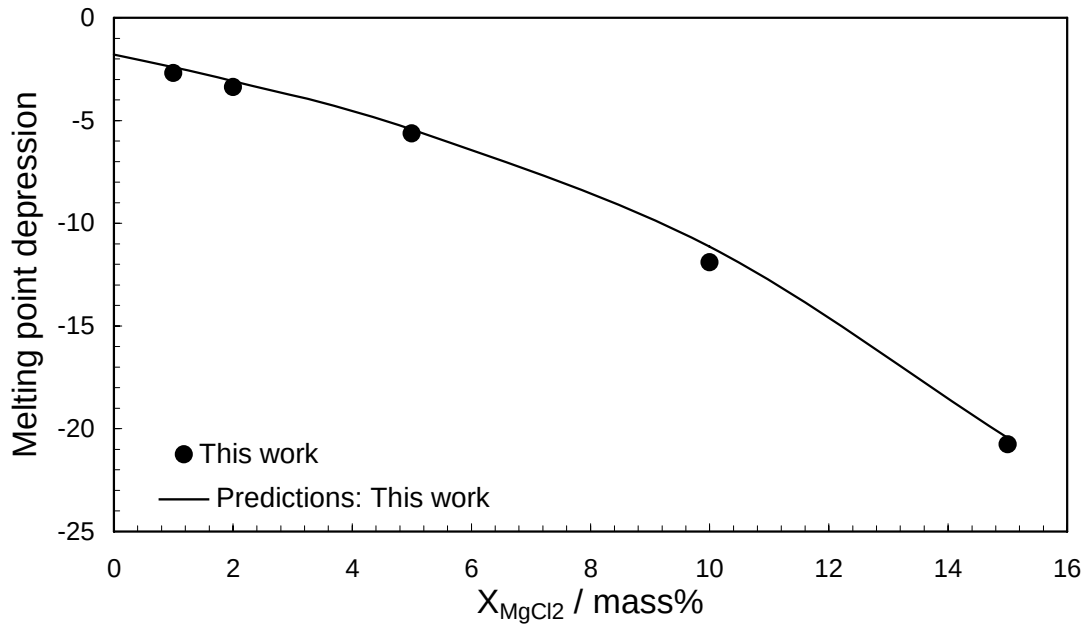

Figure 4.29 Experimental and predicted (using the CPA model developed in this work) freezing point depression of aqueous solution of $MgCl_2$ and 3 mass% NaCl. Experimental data from this work (●).

4.5 Conclusion and Perspectives

The primary target for this part of this thesis was to review and develop a reliable thermodynamic model capable of describing accurately phase equilibria for multi-component multiphase mixtures containing light and heavy hydrocarbons, water,

hydrate inhibitors and salts. In this work, the Cubic-Plus-Association (CPA) equation of state has been applied to multiphase equilibria in mixtures with complex compositions, containing water, methanol, ethanol, *n*-propanol and MEG. The CPA model reflects a new thermodynamic concept, which explicitly takes into account the association contribution. Binary interaction parameters, tuned using experimental data on binary systems, are required for the equation of state to predict the correct phase behaviour of these complex systems. Additionally the CPA model has been extended for taking into the account the effect of salt when electrolytes are present. The predictions of the model with the optimised binary interaction parameters were compared with the experimental data in the literature. A good agreement between predictions and experimental data is observed, supporting the reliability of the developed model. The CPA EoS is shown to be a strong tool and a very successful model for multiphase multi-component mixtures containing hydrocarbons, alcohols, glycols and water. This validation study is the initial stage for further investigation in the capability of the developed model for hydrate inhibition effect of electrolyte solutions and/or organic inhibitors as described in the next chapter.

References

Althaus K., 1999, *Relationship between water content and water dew point keeping in consideration the gas composition in the field of natural gas*, Fortschritt - Berichte VDI. Reihe, **3**, 350-352

Amirijafari R., Campbell J., 1972, *Solubility of Gaseous Hydrocarbon Mixtures in Water*, Soc. Pet. Eng. J., 21-27

Anderson R., Chapoy A., Tanchawanich J., Haghighi H., Lachwa-Langa J., Tohidi B., 2008, *Binary ethanol−methane clathrate hydrate formation in the system $CH_4−C_2H_5OH−H_2O$: experimental data and thermodynamic modelling*, the 6th International Conference on Gas Hydrates (ICGH)

Assarsson G., 1949, On the winning of salt from the brines of southern sweden, Sveriges Geologiska Undersökning, Stockholm, **42**, 501

Bakhuis Roozeboom M.H.W., 1889, *Étude expérimentale et théorique sur les conditions de l'équilibre entre les combinaisons solides et liquides de l'eau avec des sels, particulièrement avec le chlorure de calcium*, Rec. Trav. Chim. Pays-B, **8**, 1

Bergman A.G., Vlasov N.A., 1949, Homeomorphism of potassium halide salts and the polytherms of the systems KCl-KBr-H_2O, NaCl-NaBr-H_2O, and NaCl-KCl, *Izv. Sektora Fiz.-Khim Analiza Akad. Nauk USSR*, **17**, 312

Biltz W., 1902, *Zur kenntnis der lösungen anorganischer salze in wasser*, Z. Phys. Chem., **40**, 185-221

Brunner E., 1990, *Hueltenschmidt W., Fluid mixture at high pressures VIII. Isothermal phase equilibria in the binary mixtures: (ethanol+hydrogen or methan or ethane)*, J. Chem. Thermodyn., **22**, 73-84

Brunner E., Hueltenschmidt W., Schlichthaerle G., 1987, *Fluid mixtures at high pressures IV. Isothermal phase equilibria in binary mixtures consisting of (methanol + hydrogen or nitrogen or methane or carbon monoxide or carbon dioxide)*, J. Chem. Thermodyn., **19**, 273-291

Chiavone-Filho O., Proust P., Rasmussen P., 1993, *Vapor-liquid equilibria for glycol ether + water systems*, J. Chem. Eng. Data, 38, 128-131

Chambers V.J., Frazer J.C.W., 1900, *On a Minimum in the Molecular Lowering of the Freezing Point of Water, Produced by Certain Acids and salts*, Am. Chem. J., **23**, 512

Chapoy A., Cocquelet C., Richon D., 2003, *Solubility measurement and modeling of water in the gas phase of the methane/water binary system at temperatures from 283.15 to 318.15 k and pressures up to 35 MPa*, Fluid Phase Equilibr., **214**, 101-107

Chapoy A., Mohammadi A.H., Richon D., Tohidi B., 2004, *Gas solubility measurement and modeling for methane–water and methane–ethane–n-butane–water systems at low temperature conditions,* Fluid Phase Equilibr., **220**(1), 111-119

Chiavone-Filho O., Proust P., Rasmussen P., 1993, *Vapor-liquid equilibria for glycol-. ether + water systems*, J. Chem. Eng. Data, **38**, 128-131

Colin E., Clarke W., Glew D.N., 1985, *Evaluation of the thermodynamic functions for aqueous sodium chloride from equilibrium and calorimetric measurements below 154C*, J. Phys. Chem. Ref. Data., **14**, 489-610

Conrad F.H., Hill E.F., Ballman E.A., 1940, *Freezing points of the system ethylene glycol–methanol–water*, Ind. Eng. Chem., **32**, 542-543

Cordray D.R., Kaplan L.R., Woyciesjes P.M., Kozak T.F., 1996, *Solid - liquid phase diagram for ethylene glycol + water*, Fluid Phase Equilibr., **117**, 146-152

Culberson O.L., J.J. Mc Ketta J., 1951, *Phase equilibria in hydrocarbon-water systems III, The solubility of methane in water at 10000 psia*, AIME, **192**, 223-226

Dalager P., 1969, *Vapor-liquid equilibriums of binary systems of water with methanol and ethanol at extreme dilution of the alcohols*, J. Chem. Eng. Data, **14**, 298-301

Duffy J.R., Smith N.O., Nagy B., 1961, *Solubility of natural gases in aqueous salt solutions. 1. Liquidus surfaces in the system CH_4–H_2O–NaCl–$CaCl_2$ at room temperatures and at pressures below 1000 psia*, Geochim. Cosmochim. Acta, **2** (1–2), 23–31

Esteban A., Hernandez V., Lunsford K., 2000, *Exploit the benefits of methanol*, Proceedings of 79th GPA Annual Convention. Atlanta, GA: Gas Processors Association

Feldman H.B., Dahlstrom W.G., 1936, *Freezing points of the ternary system glycerol-methanol-water*, Ind. Eng. Chem., **28**, 1316-1317

Folas G.K., Berg O.J., Solbraa E., Fredheim A.O., Kontogeorgis G.M., Michelsen M. L., Stenby E.H., 2007, *High-pressure vapor–liquid equilibria of systems containing ethylene glycol, water and methane Experimental measurements and modeling*, Fluid Phase Equilibr., **251**, 52–58

Conard F.H., Hill E., Ballmak E.A., 1940, *Freezing Points of the System Ethylene Glycol-Methanol-Water*, Ind. Eng. Chem., **32**, 542-543

Gibbard H.F., Fong S.L., 1975, *Freezing points and related properties of electrolyte solutions iii. the systems NaCl-$CaCl_2$-H_2O and NaCl-$BaCl_2$-H_2O*, J. Solution Chem., **4**, 863-872

Grass E.H., 1976, *Alcohols comes on strong as fracturing fluids*, Drilling-DCW, **34**, 64-67

Haghighi H., Chapoy A., Burgess R., Mazloum S. , Tohidi B., 2009, *Phase equilibria for petroleum reservoir fluids containing water and aqueous methanol solutions: Experimental measurements and modelling using the CPA equation of state*, Fluid Phase Equilibr., **278**, 109-116

Hall D.L, Sterner S.M., Bodnar R.J., 1988, *Freezing point depression of NaCl-KCl-H_2O solutions*, Econ. Geol., **83**, 197-202

Hemmaplardh B., King A.D., 1972, *Solubility of methanol in compressed nitrogen, argon, methane, ethylene, ethane, carbon dioxide and nitrous oxide. Evidence for association of carbon dioxide with methanol in the gas phase*, J. Phys. Chem., **76**, 2170-2175

Hong J.H., Kobayashi R., 1988, *Vapor-liquid equilibrium studies for the carbon dioxide-methanol system*, Fluid Phase Equilib., **41**(3), 269-276

Hong J.H., Malone P.V., Jett M.D., Kobayashi R., 1987, *The measurement and interpretation of the fluid-phase equilibria of a normal fluid in a hydrogen bonding solvent: the methane-methanol system*, Fluid Phase Equilibr., **38**, 83-96

Jones H.C., 1893, *Über die bestimmung des gefrierpunktes sehr verdünnter satzlösungen*, Z. Phys. Chem. (Leipzig), **11**, 529-551

Jones H.C., Bassett H.P., 1905, *The approximate composition of the hydrates formed by certain electrolytes in aqueous solutions at different concentration*, Am. Chem. J., **33**, 534-539

Jones H.C., Pearce J.N., 1907, *Dissociation as measured by freezing point lowering and by conductivity - bearing on the hydrate theory*, Am. Chem. J., **38**, 683-743

Jones H.C., Getman F.H., 1904, *Über das vorhandensein von hydraten in konzentrierten wsserigen l sungen*, Z. Phys. Chem., **49**, 385-455

Jou F.Y., Deshmukh R.D., Otto F.D., Mather A.E., 1990, *Vapor-liquid equilibria of H2S and CO2 and ethylene glycol at elevated pressures*, Chem. Eng. Commun., **87**, 223-231

Jou F.Y., Otto F.D., Mather A.E., 1994, *Solubility of methane in glycols at elevated pressures*, Can. J. Chem. Eng., **72**, 130-133

Kato M., Konishi H., Hirata M., 1970, *New apparatus for isobaric dew and bubble point method. Methanol-water, ethyl acetate-ethanol, water-1-butanol, and ethyl acetate-water systems*, J. Chem. Eng. Data, **15**(3), 435–439

Keeney B.R, Frost J.G., 1975, *Guidelines regarding the use of alcohols in acidic stimulations fluids*, J. Prt. Technol., **27**, 552-554.

Kim Y.S., Ryu S.K., Yang S.O., Lee C.S., 2003, *Liquid water-hydrate equilibrium measurements and unified predictions of hydrate-containing phase equilibria for methane, ethane, propane, and their mixtures*, Ind. Eng. Chem. Res., **42**, 2409-2414

Kosyakov N.E., Ivchenko B.I., Krishtopa P.P., 1982, *Vopr.* Khim. Tekhnol., **68**, 33-36

Krichevsky I., Koroleva M., 1941, *The solubility of methanol in compressed gases*, Acta Physicochim. URSS, **15**, 327-342

Kurihara K., Minoura T., Takeda K., Kojima K., 1995, *Isothermal Vapor-Liquid Equilibria for Methanol + Ethanol + Water, Methanol + Water, and Ethanol + Water*, J. Chem. Eng. Data, **40**, 679-684

Laursen T., Andersen S.I., 2002, *High-pressure vapor−liquid equilibrium for nitrogen + methanol*, J. Chem. Eng. Data, **47**, 1173-1174

Lee H.S., Yoon J.H., Lee H., 1992, *VLE for the systems water-ethylene glycol, methanol-ethylene glycol and pentanol-ethylene glycol*, HWAHAK KONGHAK, **30,** 553-558

Leu A.D., Chung S.Y.K., Robinson D.B., 1991, *The equilibrium phase properties of (carbon dioxide + methanol)*, J. Chem. Thermodyn., **23**, 979-985

Lide D.R., 2004, *Hand book of chemistry and physics*, 85th edition; CRC Press, Boca Raton, FL, 8-59

Linke W.F., Seidell A., 1965, *Solubilities of inorganic and metal-organic compounds*, Van Nostrand: New York

Loomis, E. H., 1896, *On the freezing-points of dilute aqueous solutions*, Phys. Rev., **3**, 257-287

Maripuri V.O., Ratcliff G.A., 1972, *Measurement of isothermal vapor-liquid equilibriums for acetone-n-heptane mixtures using modified Gillespie still*, J. Chem. Eng. Data, **17**, 366-369

McDaniel A.S., 1911, *The absorption of hydrocarbon gases by non-aqueous liquids, J. Phys. Chem.,* **15**, 587-610

Mellan I., 1977, *Industrial Solvents Handbook*, Noyes Publishing: New Jersey, USA

Menzel H., Neue E., 1927, *Thermometerform zur kryoskopie wässriger lösungen*, Angw. Phys. Chem., **33**, 63-72

Nallet A., Paris R.A., 1956, *Equilibrium solubilities of chlorides and chlorates of sodium and of potassium in water*, I. B. Soc. Chim. Fr., **3**, 488

Oakes C.S., Bodnar R.J., Simonson J.M., 1990, *The system NaCl-$CaCl_2$-H_2O: the ice liquidus at 1 atm total pressure*, Geochim. Cosmochim. Ac., **54**, 603-610

Qlsen J.C., Brunjes A.S., Qlsen J.W., 1930, *Freezing and flow points for glycerol, prestone, denatured alcohol, and methanol*, Ind. Eng. Chem., **22**, 1315-1317

Ott J.B., Goates J.R., Waite B.A., 1979, *(Solid + liquid) phase equilibria and solid-hydrate formation in water + methyl, + ethyl, + isopropyl, and + tertiary butyl alcohols*, J. Chem. Thermodyn., **11**, 739-746

Patil K.R., Tripathi A.D., Pathak G., Katti S.S., 1991, *Thermodynamic properties of aqueous electrolyte solutions. 2. vapor pressure of aqueous solutions of NaBr, NaI, KCI, KBr, KI, RbCl, CsCl, CsBr, CsI, $MgCl_2$, $CaCl_2$, $CaBr_2$, CaI_2, $SrCl_2$, $SrBr_2$, SrI_2, $BaCl_2$ and $BaBr_2$*, J. Chem. Eng. Data, **36**, 225-230

Potter R.W., Clynne M.A., 1978, *Solubility of highly soluble salts in aqueous media. part 1. sodium chloride, potassium chloride, calcium chloride*, J. Res. U.S. Geol. Surv., **6**, 701-705

Pushin N.A., Glagoleva A.A., 1922, *The equilibrium in systems composed of water and alcohols: methyl alcohol, pinacone, glycerol, and erythritol*, J. Chem. Soc. Trans., **121**, 2813-2834

Reichl H., 1996, Ph.D. Thesis, Tech. Univ. Berlin

Rieder R.M., Thompson A.R., 1949, *Vapor–liquid equilibria measured. by a gillespie still. ethyl alcohol–water system*, Ind. Eng. Chem., **41**, 2905-2908

Rigby M., Prausnitz J.M., 1968, *Solubility of water in compressed nitrogen, argon and methane*, J. Phys. Chem., **72**, 330-334

Rivett A.D.C., 1912, *Neutralsalzwirkung auf die gefrierpunkte von mischungen in wässeriger lösung*, Z. Phys. Chem. (Leipzig), **80**, 537-542

Rodebush W.H., 1918, *The freezing points of concentrated solutions and the free energy of solutions of salts*, J. Am. Chem. Soc., **40**, 1204-1213

Ross H.K., 1954,*Cryoscopic Studies - Concentrated Solutions of Hydroxy Compounds*, Ind. Eng. Chem., **46**(3), 601-610

Safarov J.T., Jannataliyev R.M., Shahverdiyev A.N., Egon Hassel P., 2006, *Thermal properties and apparent molar volumes V of $ZnCl_2$ (aq) in high temperatures and pressures*, J. Mol. Liq., **128**, 127-133

Schlichting H., 1991, PhD Thesis, Technische Universitat Miinchen, Germany

Schlichting H., Langhorst R., Knapp H., 1993, *Saturation of high pressure gases with low volatile solvents: experiments and correlation*, Fluid Phase Equilibr., 84, 143-163

Schroeder W.C., Gabriel A., Partridge E.P., 1935, *Solubility equilibria of sodium sulfate at temperatures of 150 to 350°. I. effect of sodium hydroxide and sodium*, J. Am. Chem. Soc., **57**, 1539-1546

Schneider R., PhD Thesis, TUB, Berlin, 1978

Sloan E.D., 1998, *Clathrate hydrates of natural gases*, 2nd edition, Marcel Dekker Inc., New York

Spangler J., Davies E., 1943, *Freezing points, densities, and refractive indexes of system glycerol-ethylene glycol-water*, Ind. Eng. Chem. Anal., Ed. 15, 96-99

Suzuki K., Sue H., Itou M., Smith R.L., Inomata H., 1990, *Isothermal vapor-liquid equilibrium data for binary systems at high pressures: carbon dioxide-methanol, carbon dioxide-ethanol, carbon dioxide-1-propanol, methane-ethanol, methane-1-propanol, ethane-ethanol, and ethane-1-propanol systems*, J. Chem. Eng. Data, **35**, 63-66

Tohidi B., Burgass R.W., Danesh A., Todd A.C., 2000, Østergaard K.K., *Improving the accuracy of gas hydrate dissociation point measurements*", *Ann. N.Y. Acad. Sci.*, **912**, 924-931

Trimble H.M., Potts W., *Glycol-water mixtures vapor pressure-boiling point-composition relations*, Ind. Eng. Chem., **27**, 1935, 66-68

Ukai T., Kodama D., Miyazaki J., Kato M., 2002, *Solubility of methane in alcohols and saturated density at 280.15 K*, J. Chem. Eng. Data, **47**, 1320-1323

Van't Hoff J.H., Meyerhoffer W., 1898, *Ueber anwendungen der gleichgewichtslehre auf die bildung oceanischer salzablagerungen, mit besonderer bercksich*, Z. Phys. Chem., **27**, 75

Wang L.K., Chen G.J., Han G.H., Guo X.Q., Guo T.M., 2003, *Experimental study on the solubility of natural gas components in water with or without hydrate inhibitor*, Fluid Phase Equilibr., **207**(1-2), 143-154

Wang Y., Han B., Yan H., Liu R., 1995, *Solubility of CH_4 in the mixed solvent t-butyl alcohol and water*, Thermochim. Acta., **253**, 327-334

Washburn E.W., 1926–1930, *International Critical Tables (ICT) of Numerical Data, Physics*, Chemistry and Technology. National Research Council

Weber W., Zeck S., Knapp H., 1984,*Gas solubilities in liquid solvents at high pressures: apparatus and results for binary and ternary systems of N_2, CO_2 and CH_3OH*, Fluid Phase Equilibr., **18**, 253-278

Yanateva O.K., 1946, *Solubility polytherms in the systems $CaCl_2$-$MgCl_2$-H_2O and $CaCl_2$-NaCl-H_2O*, *Zh. Prikl. Khim.*, **19**, 709

Yang S.O., Cho S.H., Lee H., Lee C.S., 2001, *Measurement and prediction of phase equilibria for methane + water in hydrate forming conditions*, Fluid Phase Equilibr., **185**, 53-63

Yarym-Agaev N.L., Sinyavskaya R.P., Koliushko I.I., Levinton L.Y., 1985, *Zh. Prikl. Khim.* **58**, 165-168

Yokoyama C., Wakana, S., Kaminishi G. I., Takahashi S., 1988, *Vapor-liquid equilibria in the methane-diethylene glycol-water system at 298.15 and 323.15 K*, J. Chem. Eng. Data., **33**, 274-276

Yorizane M., Sadamoto S., Masuoka H., Eto Y., 1969, *Gas solubilities in methanol at high pressures*, Kogyo Kagaku Zasshi, **72**, 2174-2177

Zheng D.Q., Ma W.D.; Wei R., Guo T.M., 1999,*Solubility study of methane, carbon dioxide and nitrogen in ethylene glycol at elevated temperatures and pressures*, Fluid Phase Equilibr., **155**, 277-286

CHAPTER 5 – VALIDATION OF THERMODYNAMIC MODEL (In the presence of hydrates)

5.1 Introduction

The main objective of this work was to develop a reliable thermodynamic model, in an attempt to improve prediction of the phase behaviour of complex systems containing highly polar components (hydrate inhibitors) when hydrate is present. In order to accomplish this goal, the thermodynamic formulations in Chapter 3 were used in order to find a relationship for calculating the fugacity of different phases, including the hydrate phase, and the algorithm described was used to model fluid phases for different systems. In Chapter 4, the binary interaction parameters (BIP) between different molecules were tuned for the CPA equation of state and used to validate the capability of the model for predicting the phase behaviour of various systems. In this chapter, the performance of the model in predicting the hydrate stability zone in the absence and presence of electrolyte solutions has been evaluated. The new experimental data for different concentrations of salt(s) and organic inhibitor(s) measured in this work (Chapter 2), in addition to the data from the literature, have been used for evaluating the model. A detailed description of the model for hydrate-forming conditions has been detailed previously in Chapter 3. The performance of the model has been tested by comparing the predictions with the most reliable experimental data for hydrate stability zone. An excellent agreement between the experimental data and predictions is observed, supporting the reliability of the developed model. It should be noted that these data could be regarded as independent data as they were not used in the development and optimisation of the thermodynamic model.

In addition to conventional hydrate calculations, the reliability of the developed model has been evaluated under several challenging conditions, including:

- Gas hydrate in low water content gases
- Prediction of hydrate inhibitor distribution in multiphase systems
- Hydrate stability zone of oil/condensate in the presence of produced water and inhibitors.

The results for the above systems are also presented in this chapter.

5.2 Inhibition Effect of Electrolyte Solutions

Following the tuning of BIPs between hydrocarbons-water and water-salt interaction coefficients for different salts, assessing the ability of the model to predict the salt effect on the solubility of each component in aqueous phase was critical. Figure 5.1a presents the results of prediction of methane iso-solubility lines in distilled water and Figure 5.1b presents the results of prediction of methane iso-solubility lines in the presence of 5 mass% of NaCl in the temperature and pressure range of interest. As shown higher pressure is required to get the same amount of solubility of methane in saline water at the same temperature or in other words the solubility of methane has been reduced by adding salt to the system.

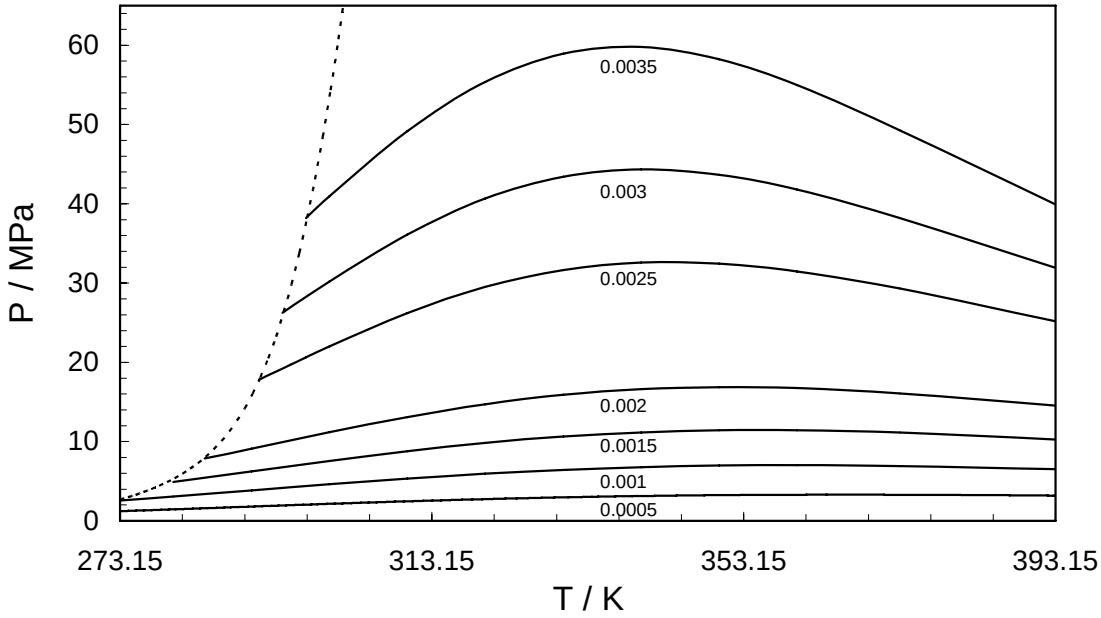

Figure 5.1a Predicted methane iso-solubility lines (in mole fraction) in distilled water in the temperature and pressure ranges of interest.
Black lines are model predictions and the dotted black line shows the methane hydrate phase boundary

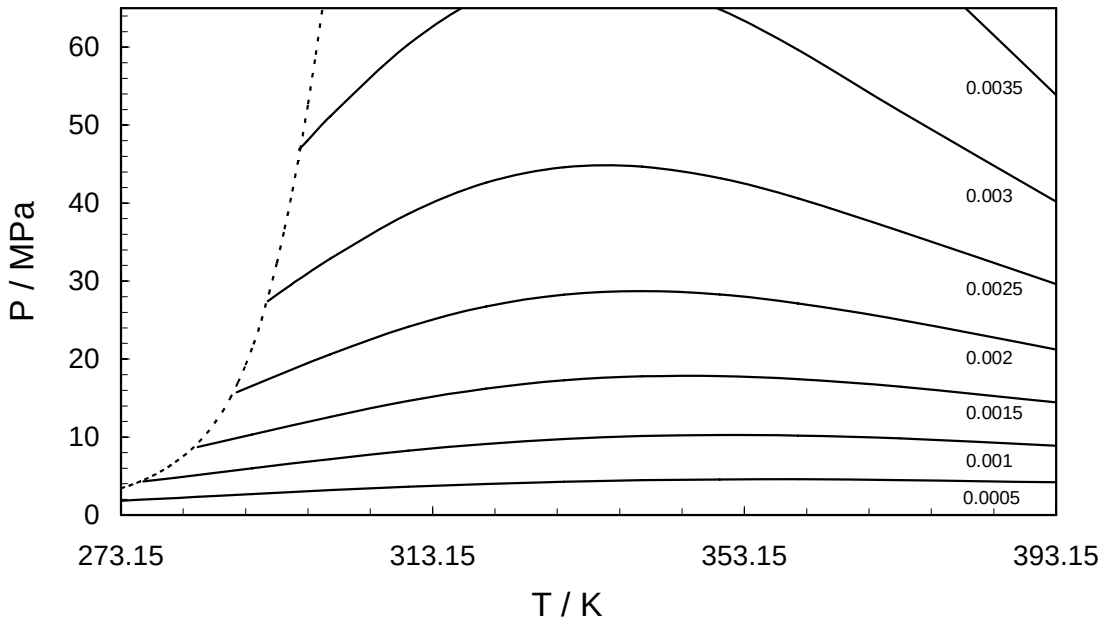

Figure 5.1b Predicted methane iso-solubility lines (in mole fraction) in the presence of 5 mass% of NaCl aqueous solution.
Black lines are model predictions and the dotted black line shows the methane hydrate phase boundary in presence of salt

The next step was to evaluate the performance of the developed model in predicting the hydrate stability zone in the presence of electrolyte solutions. The available experimental data from the literature have been used for evaluating the model. Most of the experimental work has focused on hydrate dissociation pressures or temperatures with distilled water. Experimental studies on hydrate dissociation for systems containing salts have not been investigated to the same extent; only a few authors have presented experimental results for hydrate inhibition (Haghighi et al., 2009). The presence of a salt moves the conditions required for gas hydrate formation to lower temperatures and/or higher pressures. As shown in Figures 5.2 to 5.5, the model can accurately predict the inhibition effect of salts on the hydrate stability conditions; good agreement with most of the published experimental data and the data generated in this work are observed for both single and mixed electrolyte solutions. However, the published experimental data by Kang et al. (1998) for 15 mass % of $MgCl_2$ are consistently displaced to lower pressures as compared to the data from Atik et al. (2006) and our own experimental data (see Figure 5.3).

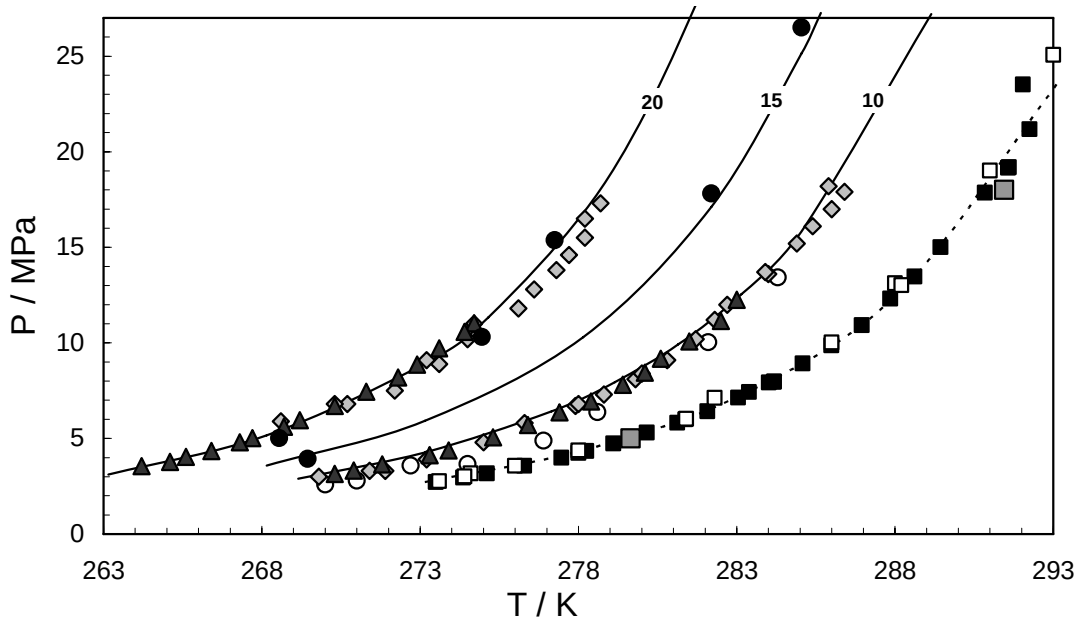

Figure 5.2 Experimental and predicted methane hydrate dissociation conditions in the presence of NaCl.
Experimental data in presence of 10 mass% of NaCl from: Kobayashi et al., 1951 (○), Maekawa et al., 1995 (◆) and Maekawa and Imai, 1999 (▲). Experimental data in presence of 15 mass% of NaCl from: this work (●). Experimental data in presence of 20 mass% of NaCl from: Maekawa et al., 1995 (◆), Maekawa and Imai, 1999 (▲) and this work. Experimental data for methane hydrate (distilled water) from: Blanc and Tournier-Lasserve, 1990 (■), Ross and Tocyzylkin, 1992 and (□), Nixdorf and Oellrich, 1997 (■). Black lines are the predicted methane hydrate phase boundary in presence of NaCl. Dotted black line is the predicted methane hydrate phase boundary (distilled water).

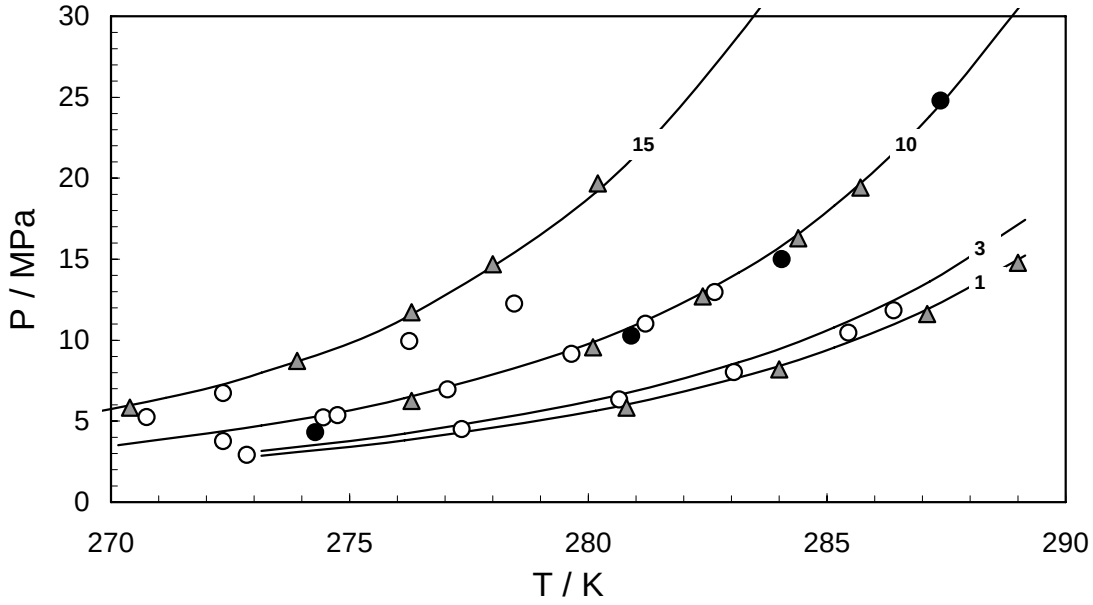

Figure 5.3 Experimental and predicted methane hydrate dissociation conditions in the presence of $MgCl_2$.
Experimental data in presence of 1 mass% of $MgCl_2$ from: Atik et al., 2006 (▲). Experimental data in presence of 3 mass% of $MgCl_2$ from: Kang et al., 1998 (○). Experimental data in presence of 10 mass% of $MgCl_2$ from: Kang et al., 1998 (○), Atik et al., 2006 (▲) and this work (●). Experimental data in presence of 10 mass% of $MgCl_2$ from: Kang et al., 1998 (○) and Atik et al., 2006 (▲). Black lines are the predicted methane hydrate phase boundary in presence of $MgCl_2$.

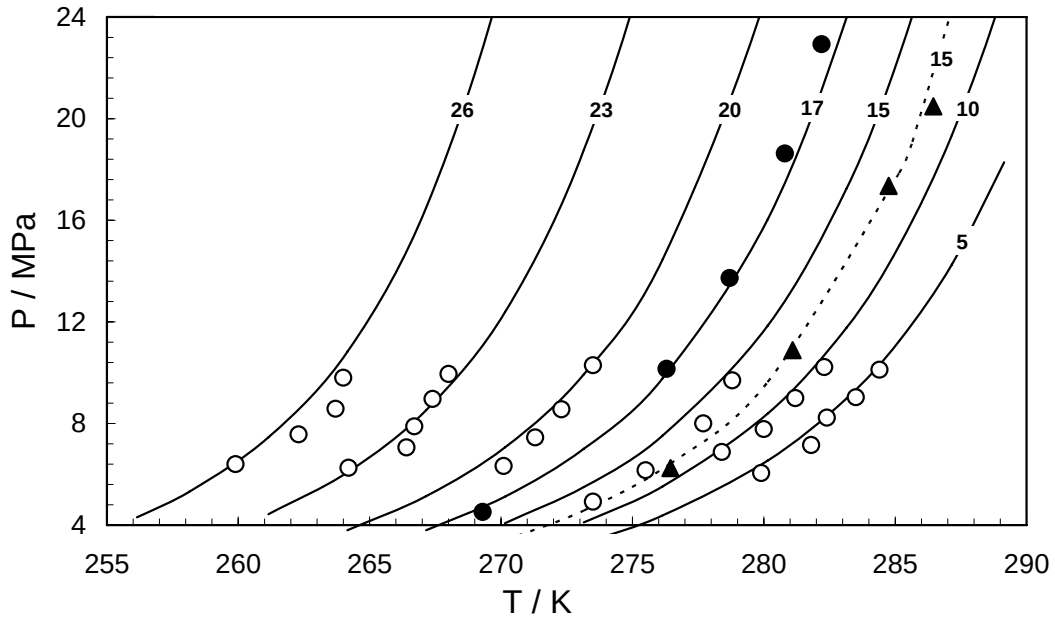

Figure 5.4 Experimental and predicted methane hydrate dissociation conditions in the presence of $CaCl_2$ or KCl.
Experimental data in presence of 5, 10, 15, 20, 23 and 26 mass% of $CaCl_2$ from: Kharrat and Dalmazzone, 2003 (○). Experimental data in presence of 17 mass% of $CaCl_2$ from: Atik et al., 2006 (●). Experimental data in presence of KCl from: this work (▲). Black lines are the predicted methane hydrate phase boundary in presence of $CaCl_2$. Dotted black line is the predicted methane hydrate phase boundary in presence of KCl.

Table 5.1 Methane hydrate dissociation data in the presence of mixed NaCl and KCl electrolyte solutions (Dholabhai et al., 1991)

Solutions	NaCl (mass%)	KCl (mass%)	T / *K*	P/ *MPa*
Na3K3	3	3	271.35 – 279.65	2.70– 5.86
Na3K5	3	5	270.32 – 281.46	2.83 – 9.38
Na5K10	5	10	267.49 - 279	2.57 – 9.05
Na5K15	5	15	266.29 – 276.19	2.91 – 8.69
Na10K12	10	12	264.58 – 274.23	2.99 – 8.82
Na15K8	15	8	265.41	3.61 – 8.84

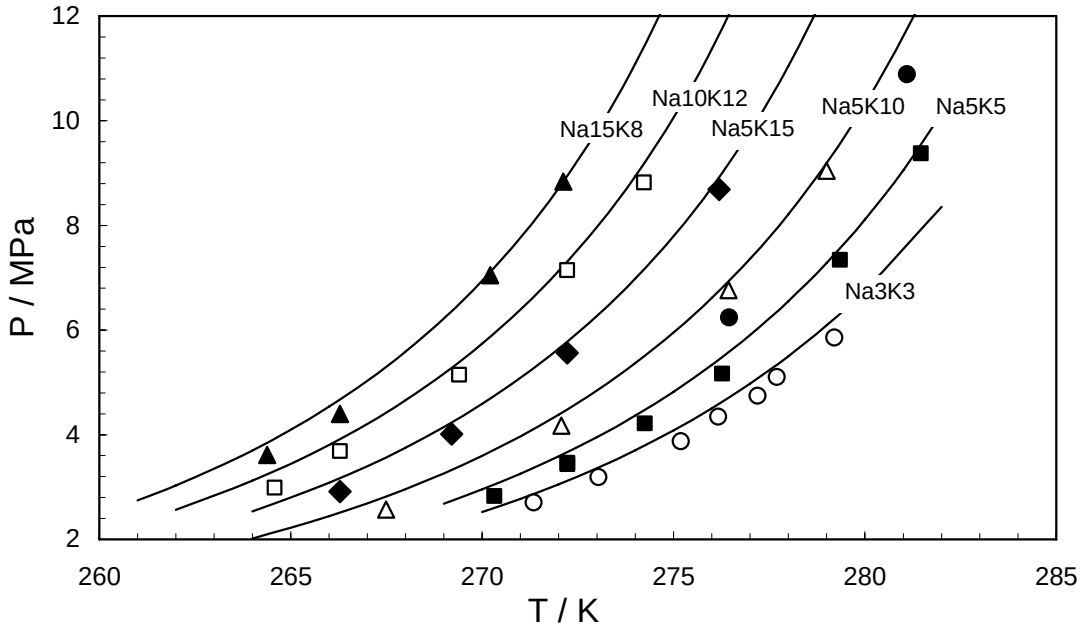

Figure 5.5 Experimental and predicted methane hydrate dissociation conditions in the presence of mixture of NaCl and KCl.
Experimental data from: Dholabhai et al., 1991. Black lines are the predicted methane hydrate phase boundary in presence of the salt mixture

Figures 5.6 and 5.7 presents the experimental and predicted hydrate stability zone of a natural gas in the presence of single electrolyte solutions as well as the new experimental data measured in this work as a reference for evaluation. The calculated hydrate dissociation conditions are seen to agree well with the experimental data.

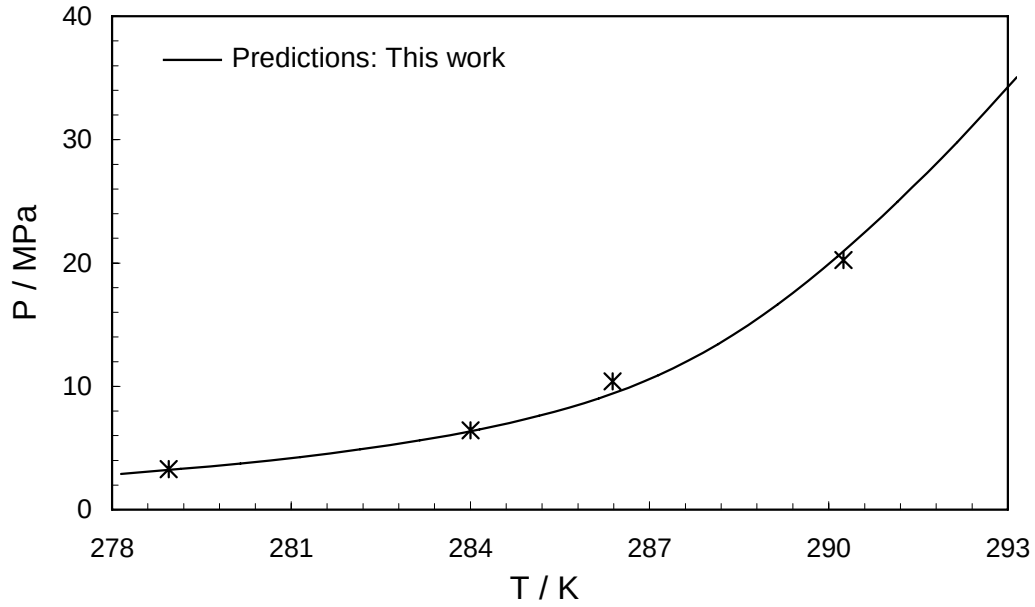

Figure 5.6 Experimental (this work) and predicted natural hydrate (NG1) dissociation conditions in the presence of 10 mass% of NaCl.

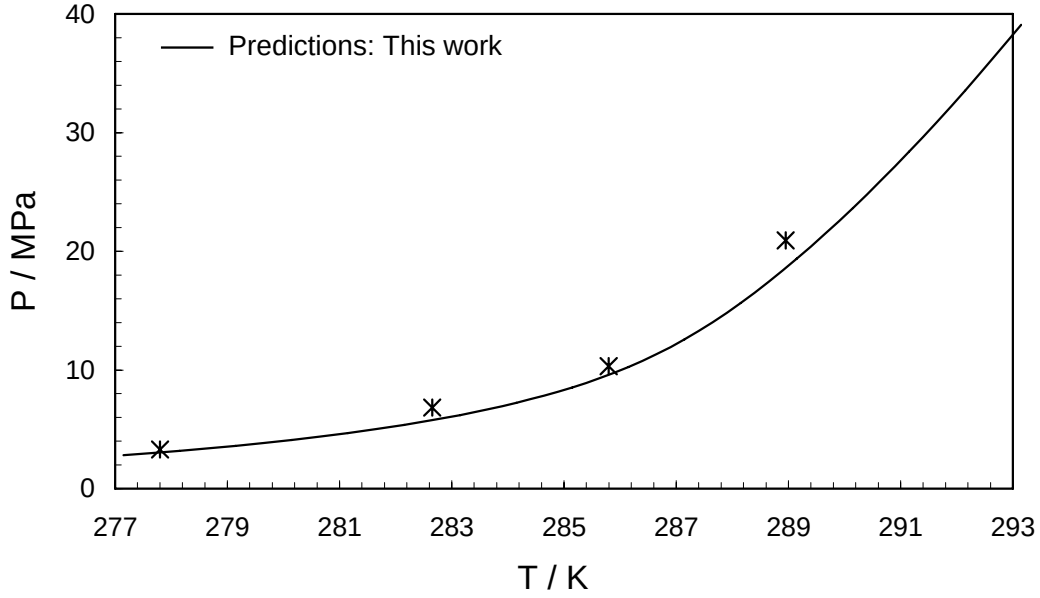

Figure 5.7 Experimental (this work) and predicted natural gas (NG1) hydrate formation conditions in the presence of 10 mass% of $MgCl_2$.

5.3 Effect of Thermodynamic Inhibitors on Gas Hydrate Stability Zone

The CPA EoS was further tested for hydrate formation predictions of methane/natural gas in the presence of methanol, and MEG in this chapter. The experimental data and the calculated hydrate dissociation conditions for methane and natural gas in the presence of different concentration of methanol and MEG up to 70 MPa are presented in Figures 5.8 through 5.11. As shown in the figures, the model predictions are seen to

agree well with the experimental data. The validation of the model for systems containing ethanol has been presented in Chapter 6.

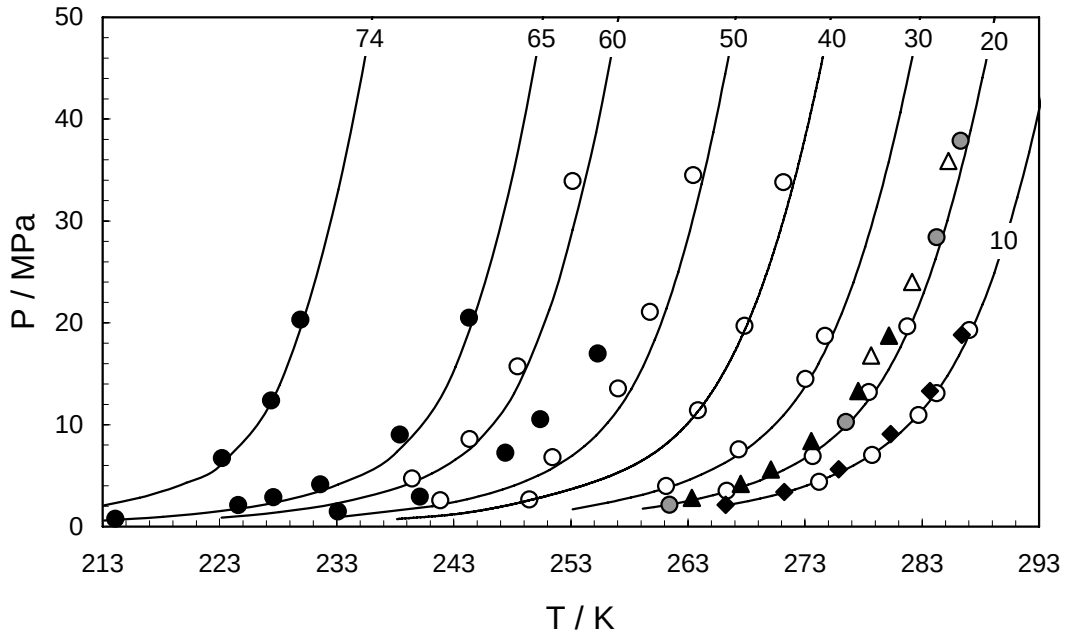

Figure 5.8 Experimental and predicted (black lines) methane hydrate dissociation (structure I) conditions in the presence methanol aqueous solutions (in mass%).
Experimental data from Ng and Robinson, 1985 (◆), Ng, et al., 1987 (●), Blank and Tournier-Lasserve, 1990 (△), Svartas and Fadnes, 1992 (●), and this work (○) (model predictions are independent from experimental data).

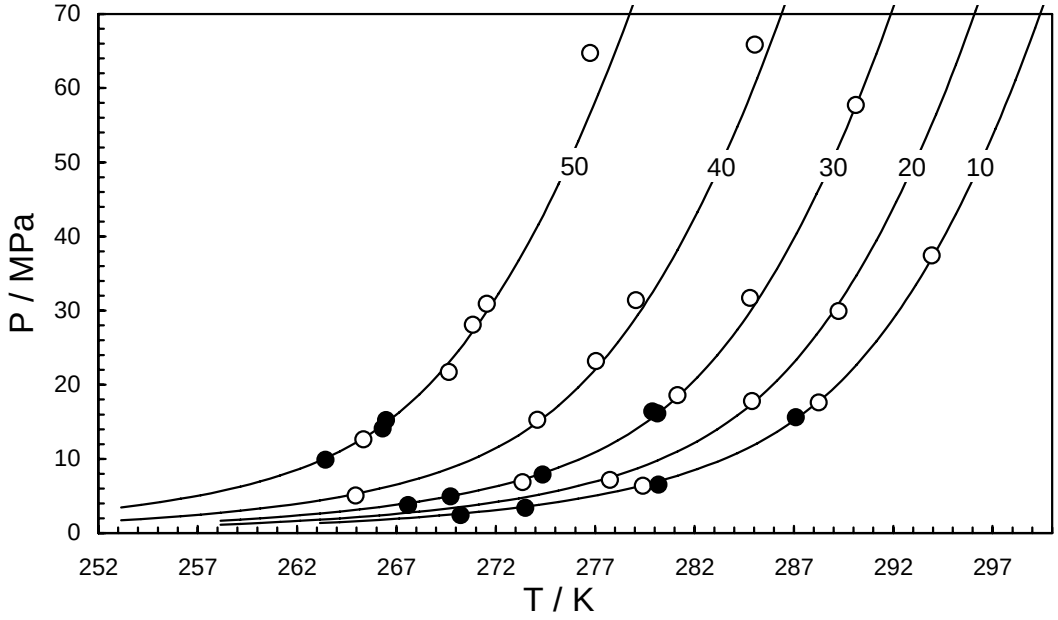

Figure 5.9 Experimental and predicted (black lines) methane hydrate dissociation (structure I) conditions in the presence monoethylene glycol aqueous solutions (in mass%).
Experimental data from Robinson and Ng, 1986 (●), and this work (○) (model predictions are independent from experimental data).

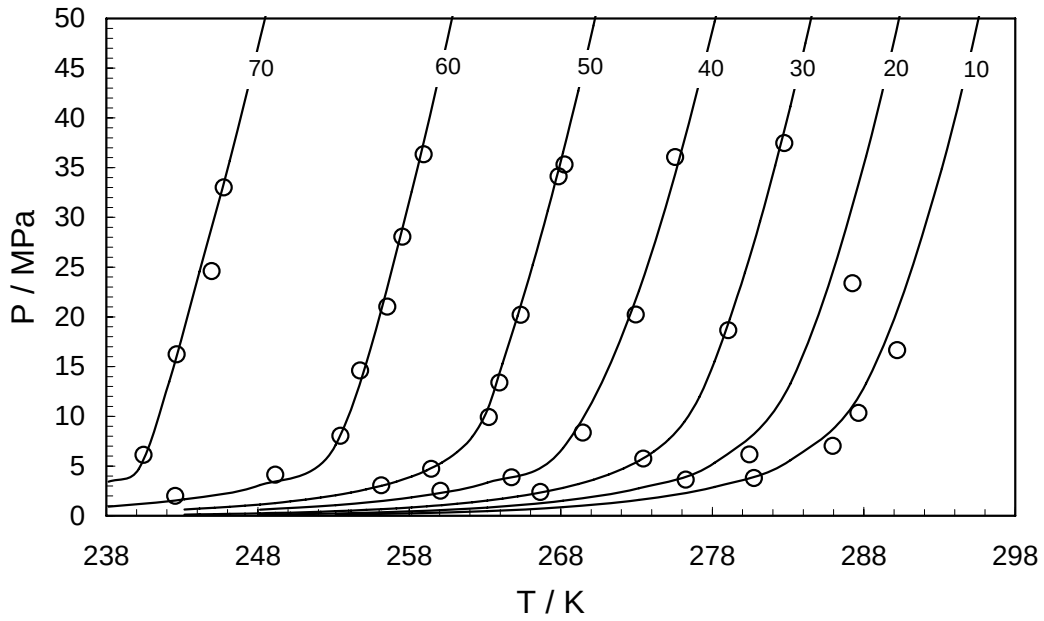

Figure 5.10 Experimental (this work) and predicted (black lines) hydrate dissociation conditions (structure II) for the natural gases (compositions reported in Chapter 2, Table 2.1) in with the presence of methanol aqueous solutions (in mass%).

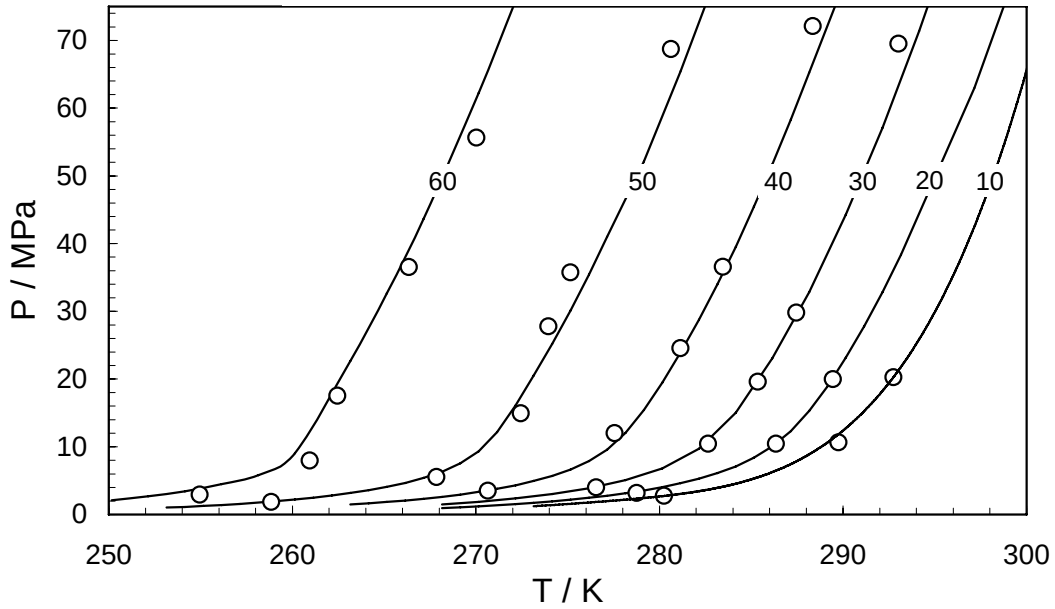

Figure 5.11 Experimental (this work) and predicted (black lines) hydrate dissociation conditions (structure II) for the natural gases (compositions reported in Chapter 2, Table 2.1) in the presence of monoethylene glycol aqueous solutions (in mass%).

Based on the fact that the data published by Song and Kobayashi (1989) are the only data set published for structure II hydrate equilibria at high MEG concentrations, these data have been used and compared with the predictions of the model developed in this work. The experimental data from Song and Kobayashi (1989) together with the predicted hydrate dissociation conditions are plotted in Figure 5.12. However, the data

reported by are consistently at much higher equilibrium temperature as compared to the predictions of the model (even for distilled water). Song and Kobayashi have used a continuous-heating technique for measuring the hydrate dissociation conditions, and it has been proven that this method particularly for multi-component systems is not accurate. Song and Kobayashi used 0.2-0.5^{o}C/h heating rate whereas in this work/laboratory a step-heating method is/recommended used. Tohidi et al. (2000) have demonstrated the superior accuracy and repeatability of hydrate equilibrium dissociation point data determined by the step-heating method, when compared to continuous heating. The principal problem with continuous heating is that equilibrium is practically unachievable in a system where temperature is constantly changing, even if the rate of change is slow. Two common characteristics of non-equilibrium resulting from continuous heating are dissociation at temperatures higher (or pressures lower) than the true equilibrium conditions and poor repeatability (Tohidi et al., 2000) and that might explain why the data published by Song and Kobayashi (1989) look very scattered.

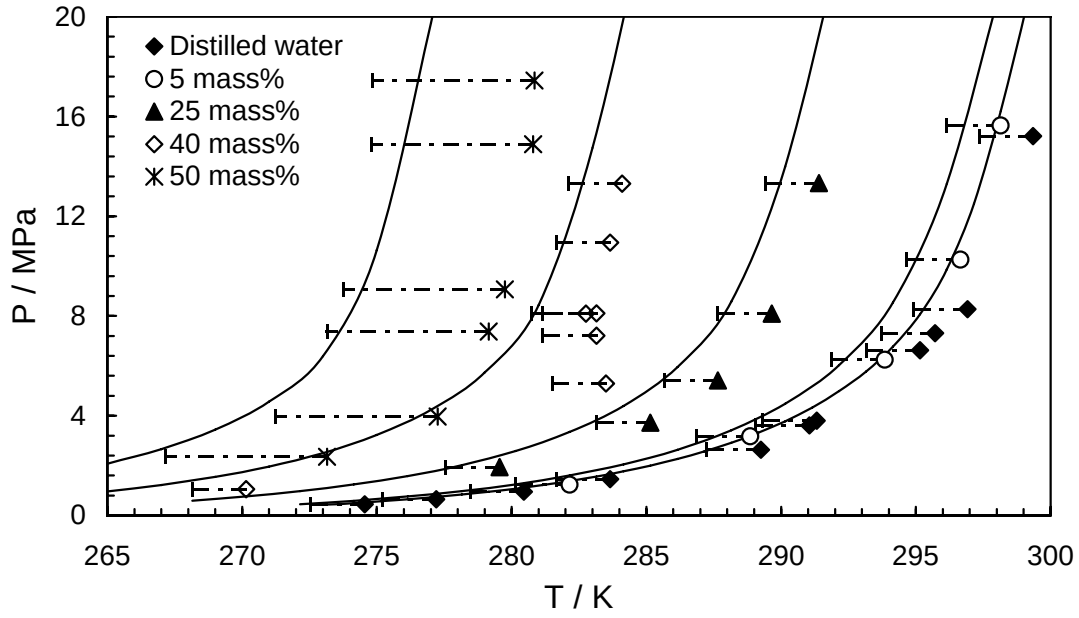

Figure 5.12 Experimental and predicted (black lines) hydrate dissociation conditions (structure II) for a synthetic gas mixture containing 88.13 mol.% methane and 11.87 mol.% propane in with the presence of MEG aqueous solutions (Experimental data from Song and Kobayashi, 1989).
(Error bars: - 2^{o}C for 5 to 40 mass % and -6^{o}C for 50 mass %)

To evaluate the capability of the CPA model developed in this work for more complicated systems containing hydrate inhibitors and salts simultaneously, two tests have been performed for natural gas system in the presence of MEG and salt. The experimental data has been presented in Chapter 2. The experimental data and the

calculated hydrate dissociation conditions up to high range of pressure are presented in Figure 5.13, wherein the model predictions are seen to agree well with the experimental data.

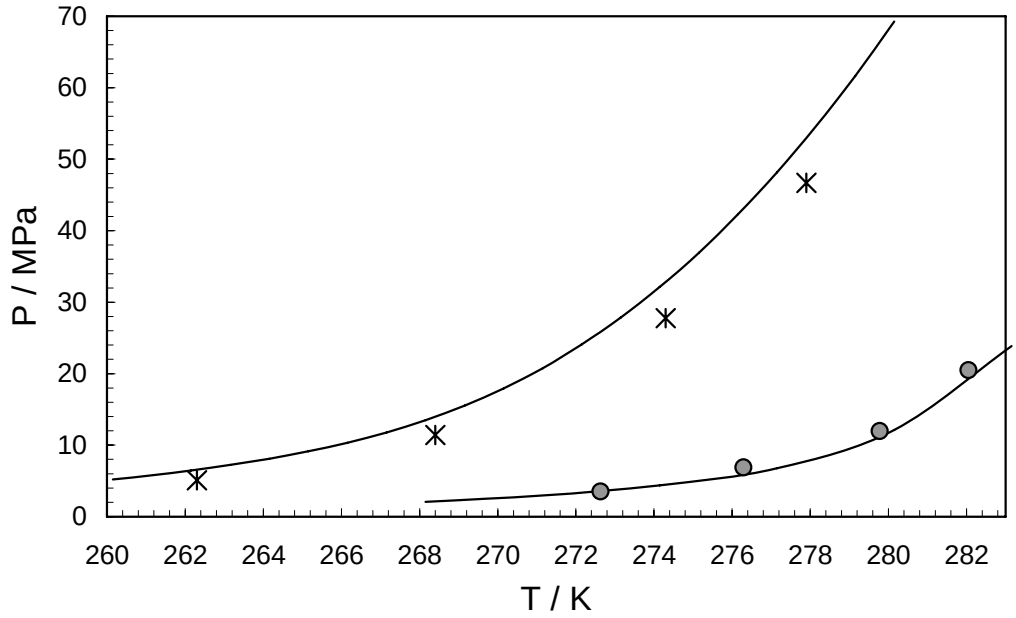

Figure 5.13 Experimental and predicted (black lines) natural gas (NG3) hydrate dissociation conditions in the presence of 30 mass% MEG and 5 mass% NaCl (●), from this work and methane hydrate formation conditions in the presence of 21.3 mass% MEG and 15 mass% NaCl (✱), from Masoudi et al., 2004.

It is worth mentioning that the MEG molecules have more functional groups for association than methanol. Thus, its associating behaviour is expected to be stronger than that of methanol. It can be seen from the work by other researchers calculations that the stronger the associating behaviour of the fluid, the stronger the predictive capability of the models considering association interaction (Li et al. 2006). Further investigations are necessary to extend the capability of the CPA model by selecting the best scheme for associating compounds to get the best performance.

5.4 Gas Hydrate in Low Water Content Gases

Natural gases are normally saturated with water at reservoir conditions. During production, transportation and processing, the dissolved water in the gas phase may form liquid water phase, ice and/or gas hydrates. Forming a liquid water phase may lead to gas hydrates and/or ice formation and cause blockage. Reducing the water content of gas streams is commonly used as a means of preventing gas hydrate problems associated with hydrate formation from condensed water. However, severe hydrate blockages have occurred in pipelines transporting so-called dry gases (Hatton and Kruka, 2002 and Austvik et al., 1995). This could be partly due to the build up of

gas hydrates on the hydrophilic pipeline wall. In most cases, it is believed that the introduction of off-spec gas has provided the required water for hydrate formation and the consequent blockage. The capability to accurately predict the water content of gas in equilibrium with water, ice or hydrates is therefore essential to asses and plan for the above flow assurance problems. This information is essential for determining the dehydration requirements for a given gas system at given operating conditions. The dehydration requirements have direct impact on CAPEX and OPEX of the dehydration units, which in-turn have a significant impact on the field development economics.

Accurate and reliable experimental water content data for single and multi-component gases composed of hydrocarbon and non-hydrocarbon gases (e.g. nitrogen and carbon dioxide) is required for the development and validation of a mathematical model. There is a scarcity of experimental data on water content for gases, particularly at high pressure and low temperature conditions, i.e., near and inside the hydrate stability region. The available data from measurements conducted at Heriot-Watt University, Institute of Petroleum Engineering, and those from literature have been used for evaluation of the model. The experimental water content data for methane-water system in the presence of hydrate and prediction by the model are reported in Tables 5.2 and 5.3 and plotted in Figures 5.14 and 5.15. As shown in the following tables and figures, the predictions of the developed model are in good agreement with the isothermal P, y_w data sets for the methane–water systems.

Table 5.2 Water content of methane in equilibrium with hydrate or liquid water at 3.44 MPa

T/ K	P/ MPa	y_w/ ppm		AD%
		Exp.	Pred.	
250.95	3.44	32.3	25.9	24.5
255.35	3.44	47.7	39.9	19.4
260.05	3.44	71.4	62.4	14.4
264.75	3.44	105.0	96.4	8.8
266.75	3.44	123.0	114.9	7.0
271.05	3.44	171.2	167.4	2.3
271.95	3.44	183.3	182.1	0.7
273.45	3.44	204.8	205.4	0.3
275.75	3.44	243.4	250.9	3.0
278.75*	3.44	302.0	308.4	2.1
282.55*	3.44	392.6	397.9	1.3
283.55*	3.44	420.6	424.9	1.0
287.05*	3.44	531.9	532.7	0.2
288.15*	3.44	573.6	571.3	0.4
			AAD%=	6.1

**in equilibrium with liquid water*

Table 5.3 Water content of methane in equilibrium with hydrate or liquid water at 6.89 MPa

T/ K	P/MPa	y_w / ppm		AD%
		Exp.	Pred.	
250.55	6.89	14.8	14.7	0.6
253.25	6.89	19.0	18.9	0.5
255.55	6.89	23.2	23.4	0.8
259.15	6.89	33.6	32.4	3.5
260.65	6.89	38.3	37.1	3.2
264.15	6.89	51.7	50.0	3.4
269.15	6.89	74.9	77.3	3.2
274.15	6.89	116.8	117.0	0.2
275.15	6.89	126.1	126.8	0.6
279.15	6.89	170.6	174.6	2.3
283.65*	6.89	237.8	248.6	4.3
288.15*	6.89	328.0	329.9	0.6
			AAD%=	1.9

**in equilibrium with liquid water*

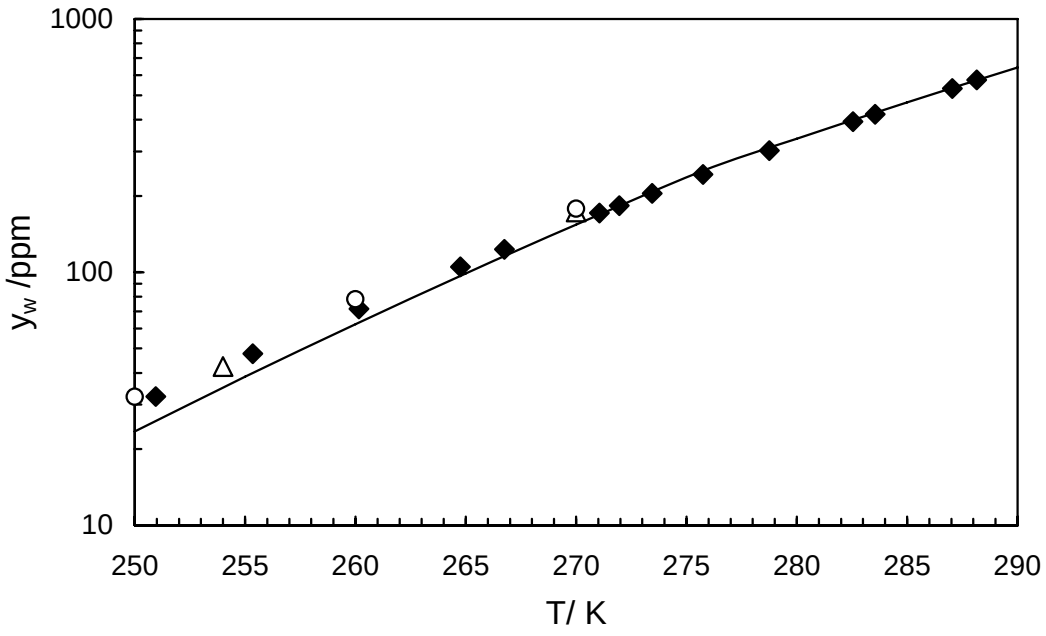

Figure 5.14 Experimental and predicted water content (ppm mole) of methane in equilibrium with liquid water or hydrate at 3.44 MPa.
◆*: Chapoy et al., 2009;* ○*: data from Aoyagi et al., 1979 and 1980;* △*: data from Song et al., 1997. Solid lines: Model predictions.*

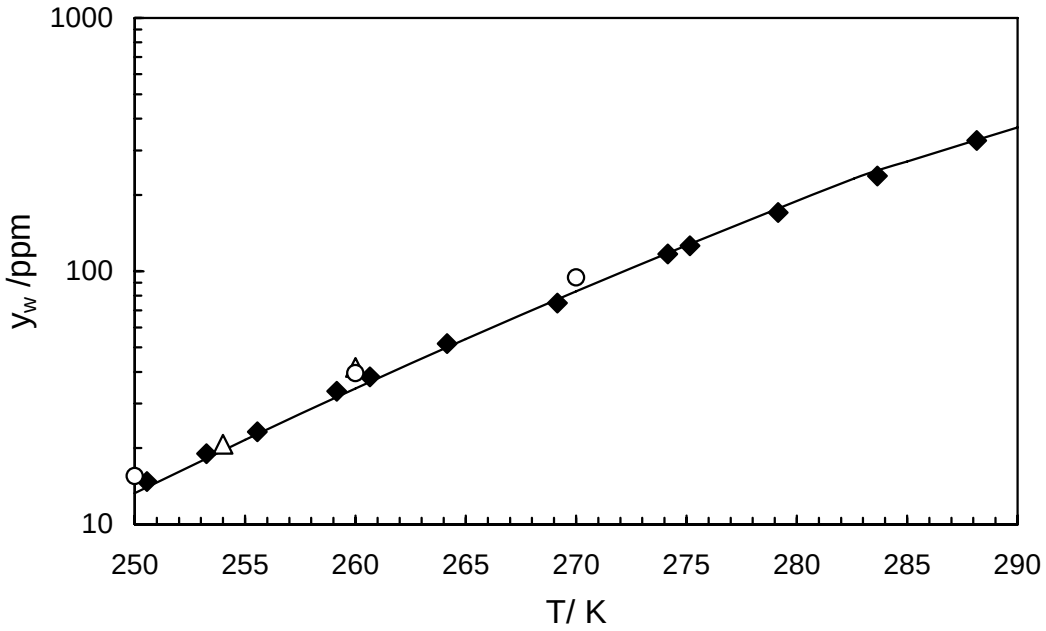

Figure 5.15 Experimental and predicted water content (ppm mole) of methane in equilibrium with liquid water or hydrate at 6.89 MPa.
◆*: Chapoy et al., 2009;* ○*: data from Aoyagi et al., 1979 and 1980;* △*: data from Song et al., 1997. Solid lines: Model predictions.*

In addition to the methane-water system, experimental gas phase water content data from Chapoy et al. (2009) for 2 synthetic gas mixtures (composition can be found in Table 5.4) in equilibrium with hydrate at pressures of 5 to 40 MPa and temperatures ranging from 253.15 to 283.15 K used for validation of the model. The experimental water content measurements (inside the hydrate stability zone) made with Mix. 1 and Mix. 2 are given in Tables 5.5 and 5.6, respectively and shown along with predictions of the CPA model in Figures 5.16 and 5.17. As can be seen the agreement between the experimental data and the model predictions is good.

Table 5.4 Gas compositions (in mol.%)

Component	Mix 1 / Mol.%	Mix 2 / Mol.%
C_1	86	94
C_2	5	2
C_3	6	1.5
nC_4	3	0
N_2	0	2
CO_2	0	0.5
Total	100	100

Table 5.5 Water content of Mix 1 in equilibrium with hydrate (Experimental data from Chapoy et al., 2009)

T/K	P / MPa	y_w / ppm		AD %
		Exp.	Pred.	
283.15	5	266.0	274.0	3.0
273.35	5	121.0	119.7	1.1
263.15	5	50.0	49.1	1.8
253.15	5	19.0	18.8	1.1
283.15	10	159.0	161.7	1.7
273.25	10	71.0	73.1	2.9
263.15	10	30.0	31.3	4.5
253.15	10	13.0	12.8	1.9
283.15	15	132.0	131.0	0.8
273.15	15	63.0	61.0	3.1
263.15	15	25.0	27.1	8.4
253.15	15	11.0	11.4	3.9
283.15	25	104.0	106.6	2.5
273.25	25	50.0	51.0	2.0
263.15	25	23.0	23.2	0.9
251.65	25	9.0	8.8	2.6
283.15	30	98.0	99.4	1.4
273.35	30	46.0	47.8	4.0
263.15	30	21.0	21.9	4.3
251.65	30	8.0	8.3	4.0
283.15	35	94.0	93.6	0.4
273.35	35	45.0	45.2	0.6
263.15	35	20.0	20.8	4.0
251.65	35	8.0	7.9	0.8
283.15	40	90.0	88.7	1.4
273.35	40	44.0	43.0	2.2
263.15	40	19.0	19.9	4.5
251.65	40	8.0	7.6	5.0
			AAD%=	2.7

Table 5.6 Water content of Mix 2 in equilibrium with hydrate (Experimental data from Chapoy et al., 2009)

T/K	P / MPa	y_w / ppm		AD %
		Exp.	Pred.	
283.15	5	279.7	294.4	5.2
273.35	5	125.7	128.8	2.5
263.15	5	47.4	53.0	11.8
253.15	5	17.4	20.3	16.6
283.15	10	159	172.2	8.3
273.25	10	73.1	77.7	6.2
263.15	10	28.9	33.0	14.2
253.15	10	13.3	13.3	0.0
283.15	15	126.6	137.5	8.6
273.15	15	59.6	63.8	7.1
263.15	15	26.3	28.2	7.2
253.15	15	11.7	11.8	0.9
283.15	25	104.4	111.3	6.6
273.25	25	52	53.2	2.3
263.15	25	23.7	24.2	2.2
253.15	25	10.7	10.4	2.8
283.15	30	100.3	103.9	3.6
273.35	30	51.5	50.0	2.9
263.15	30	23.5	23.0	2.3
253.15	30	10.2	10.0	2.3
283.15	35	95.3	98.0	2.8
273.35	35	49.4	47.5	3.9
263.15	35	22.4	21.9	2.2
253.15	35	9.5	9.6	0.5
283.15	40	92.2	93.1	1.0
273.35	40	49.6	45.0	9.3
263.15	40	22.1	20.9	5.4
253.15	40	9.6	9.2	4.4
			AAD%=	5.1

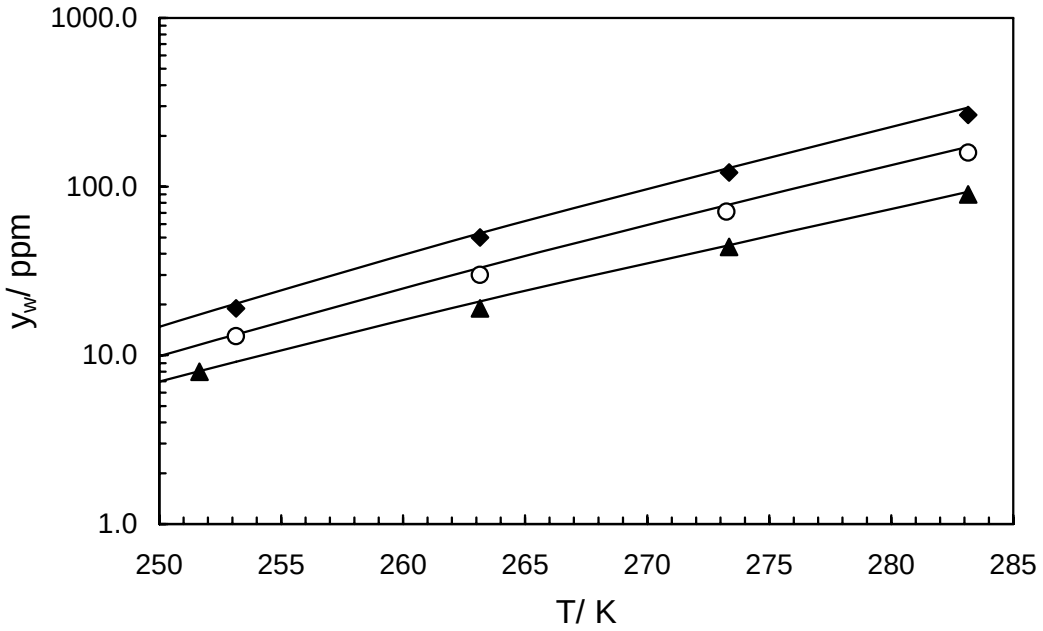

Figure 5.16 Experimental and predicted water content (ppm mole) of Mix 1 in equilibrium with hydrate.
◆: 5 MPa; ○: 10 MPa; ▲: 40 MPa. Experimental data from Chapoy et al., 2009. Solid lines: Model predictions.

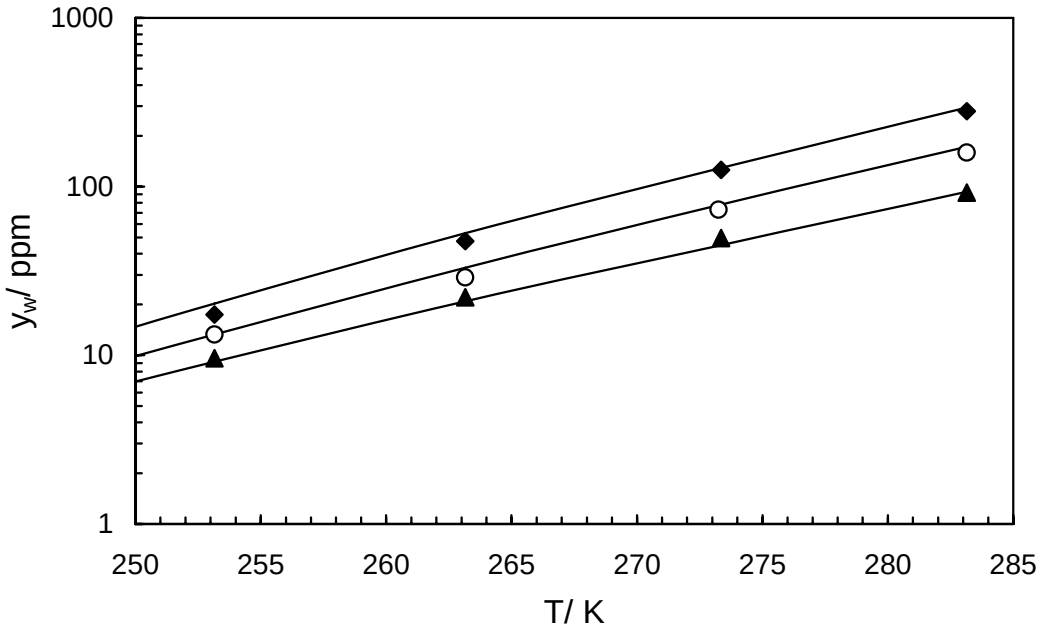

Figure 5.17 Experimental and predicted water content (ppm mole) of Mix 2 in equilibrium with hydrate.
◆: 5 MPa; ○: 10 MPa; ▲: 40 MPa. Experimental data from Chapoy et al., 2009. Solid lines: Model predictions.

5.5 Prediction of Hydrate Inhibitor Distribution in Multiphase Systems

As mentioned previously, in recent years there has been a renewed interest in gathering data on the pressures and temperatures where gas hydrates will form, in determining the degree to which the gas must be dried to prevent hydrate formation, or in calculating the amount of inhibitors required to prevent hydrate formation at operating conditions. As new resources of natural gas and gas-condensates are found offshore in deep cold water or onshore in colder climates, the risk of hydrate formation will increase. Injection of gas hydrate inhibitors at the upstream of oil/gas pipelines is normally based on the calculated/measured hydrate stability zone, operating P&T conditions, amount and composition of the aqueous phase, and the inhibitor loss to the non-aqueous phases. The partition of inhibitors to hydrocarbon phases is important as it not only determines the impurity level in the hydrocarbon phase, but also inhibitor loss, as only inhibitor concentration in the aqueous phase determines its hydrate inhibition characteristics.

Figures 5.18 and 5.19 present the predicted methanol loss in gas and liquid hydrocarbon phases for a synthetic gas-condensate mixture, along with the experimental data form Chen et al. (1988) and Bruinsma et al. (2004), respectively. The composition of the synthetic gas-condensate used by the above authors, is given in Table 5.7.

Table 5.7 Composition of the synthetic gas-condensate used by Chen et al. (1988) and Bruinsma et al. (2004)

Component	35 mass % of MeOH	70 mass % of MeOH
Methane	30.06	34.81
Heptane	20.04	23.21
Methanol	11.61	23.83
Water	38.28	18.15
Total	100.00	100.00

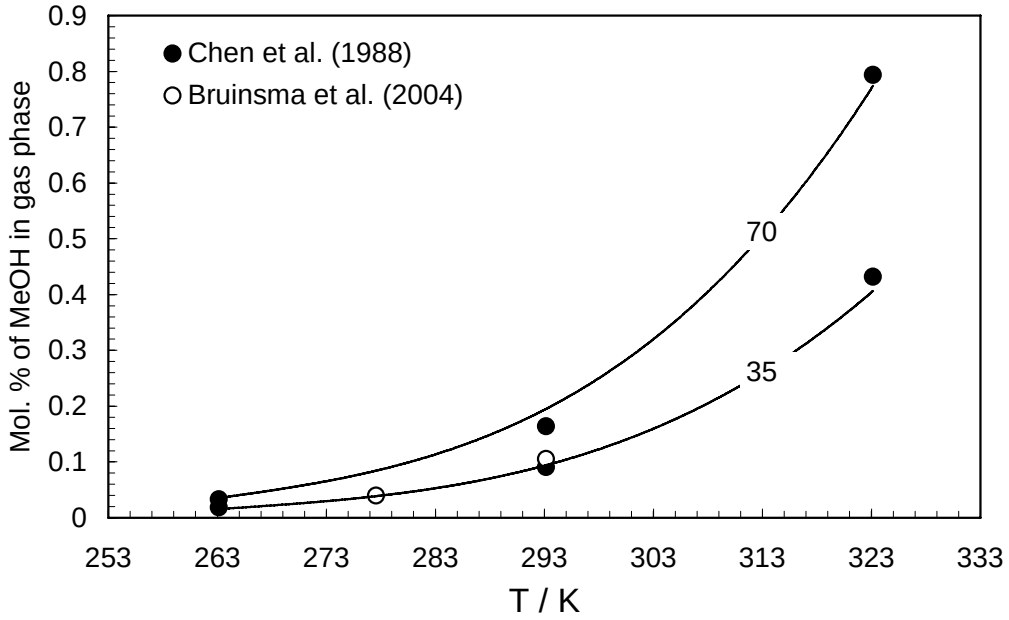

Figure 5.18 Experimental and predicted (black lines) methanol loss in gas phase of a synthetic gas-condensate at 6.9 MPa in the presence of 35 and 70 mass% methanol aqueous solutions

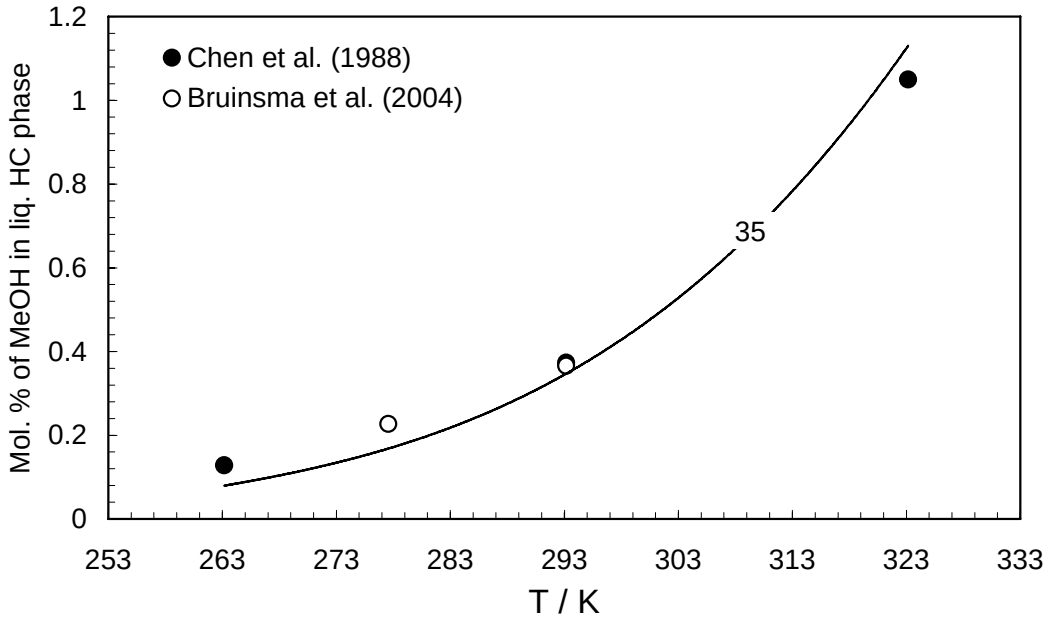

Figure 5.19 Experimental and predicted (black line) methanol loss in liquid hydrocarbon phase of a synthetic gas-condensate at 6.9 MPa in the presence of 35 mass% methanol aqueous solutions

As shown in Figures 5.18 and 5.19, the CPA model predictions are in excellent agreement with the experimental data. It should be noted that these data could be regarded as independent as they were not used in the development and optimisation of the thermodynamic model.

5.6 Hydrate Stability Zone of Oil/Condensate in the Presence of Produced Water and Inhibitors

For further investigation on the capability of the developed model, hydrate formation condition of a gas-condensate has been modelled and compared with the experimental data from Ng et al. (1985) for a gas condensate well-stream in the presence of methanol/ MEG aqueous solutions. The composition of the gas condensate used by Ng et al. (1985), can be found in Table 5.8.

Table 5.8 Composition of the gas condensate used in the tests reported Ng et al. (1985)

Component	Mol.%	Component	Mol.%
C_1	74.1333	C_{17}	0.0080
C_2	7.2086	C_{18}	0.0065
C_3	4.4999	C_{19}	0.0021
iC_4	0.8999	C_{20}	0.0014
nC_4	1.8088	C_{21}	0.0008
iC_5	0.8702	C_{22}	0.0007
nC_5	0.8889	C_{23}	0.0005
C_6	1.4582	C_{24}	0.0004
C_7	1.5170	C_{25}	0.0004
C_8	1.4400	C_{26}	0.0003
C_9	0.8364	C_{27}	0.0003
C_{10}	0.6047	Met.Cyc.C_5	0.3635
C_{11}	0.3296	Benzene	0.0424
C_{12}	0.1529	Cyclo-C_6	0.7284
C_{13}	0.1012	Met.Cyc.C_6	1.1961
C_{14}	0.0538	Toluene	0.3874
C_{15}	0.0208	m-Xylene	0.3577
C_{16}	0.0117	o-Xylene	0.0654
		100.00	100

Figures 5.20 and 5.21 present the experimental data Ng et al. (1985) and the CPA model predictions for the above gas-condensate in the presence of methanol and MEG aqueous solutions, respectively. As shown in the figures, the CPA model predictions are in a

very good agreement with the experimental hydrate dissociation data, demonstrating the reliability of the model.

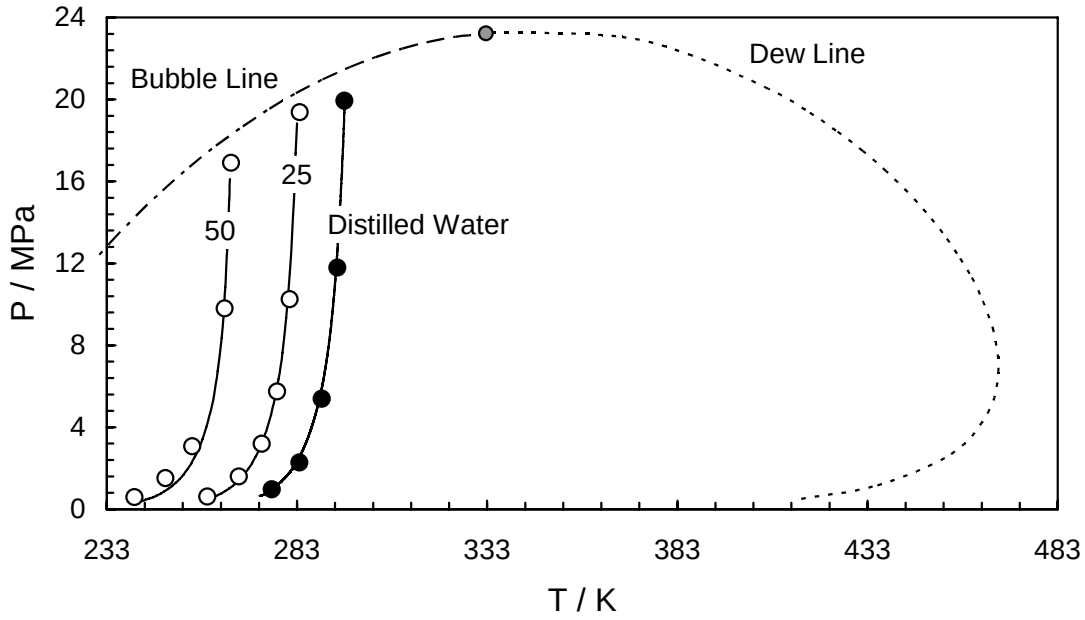

Figure 5.20 Experimental and predicted hydrate dissociation conditions and predicted phase envelope for the gas condensate well-stream in the presence of methanol aqueous solutions (Experimental data from Ng et al., 1985).
Black lines are the predicted hydrate phase boundary in the presence of various concentrations of aqueous methanol solutions. The CPA model developed in this work has been used in all predictions.

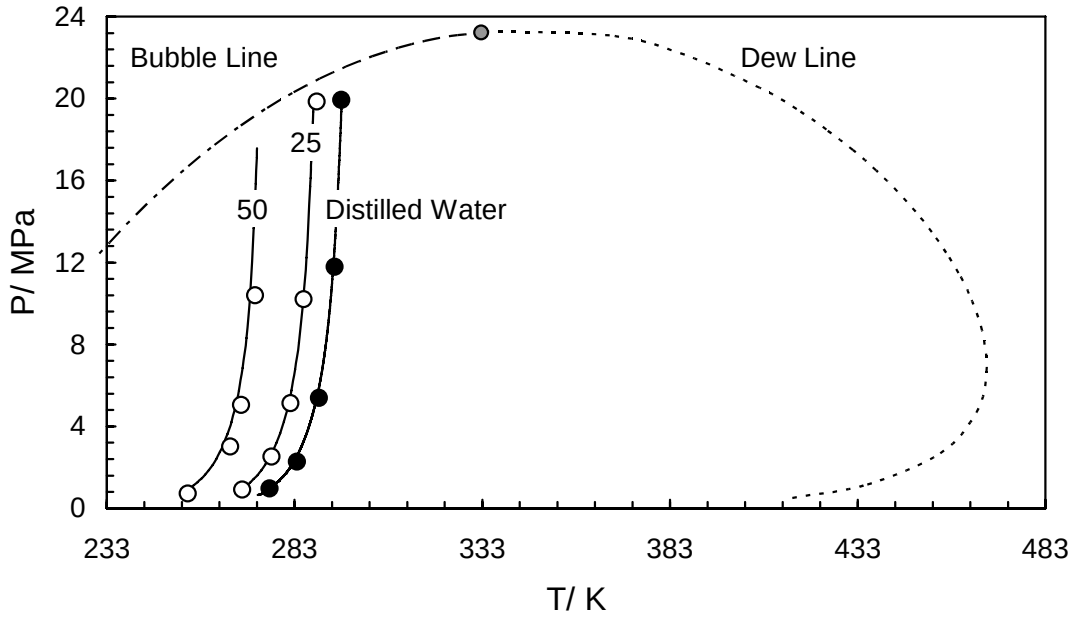

Figure 5.21 Experimental and predicted hydrate dissociation conditions and predicted phase envelope for the gas condensate well-stream in presence of MEG aqueous solutions (Experimental data from Ng et al., 1985).
Black lines are the predicted hydrate phase boundary in the presence of various concentrations of aqueous MEG solutions. The CPA model developed in this work has been used in all predictions.

5.7 Conclusion and Perspectives

The primary target for this part of the thesis was to review and develop a reliable thermodynamic model capable of describing accurately phase equilibria for multi-component multiphase mixtures containing light and heavy hydrocarbons, water, organic hydrate inhibitors and salts. In this chapter, the Cubic-Plus-Association (CPA) equation of state has been applied to multiphase equilibria in mixtures containing water, methanol, and MEG in the presence or absence or salts. The predictions of the developed CPA model are validated against independent experimental data and the data generated in this work over a wide range of temperature and pressure conditions, salt and/or inhibitor concentrations.

Additionally, this work focuses on the capability of this model for conventional as well as challenging hydrates calculations, including; (1) gas hydrate in low water content gases, (2) hydrate stability zone of oil/condensate in the presence of produced water and inhibitors, and (3) prediction of hydrate inhibitor distribution in multiphase systems. For all of the above cases, good agreements between the CPA model predictions and experimental data is observed, supporting the reliability of the developed model. The CPA EoS is shown to be a strong tool and very successful EoS for multiphase multi-component mixtures containing hydrocarbons, alcohols, glycols and water.

References

Aoyagi K., Song K.Y., Kobayashi R., Sloan E.D., Dharmawardhana P.B., 1980, (I) *The water content and correlation of the water content of methane in equilibrium with hydrates*. (II) *The water content of a high carbon dioxide simulated prudhoe bay gas in equilibrium with hydrates*, GPA Research Report **45**, Tulsa, OK, December

Aoyagi K., Song K.Y., Sloan E.D., Dharmawardhana P.B., Kobayashi R., 1979, *Improved measurements and correlation of the water content of methane gas in equilibrium with hydrate*, 58th Annual GPA Convention, Denver, CO.

Atik Z., Windmeier C., Oellrich L.R., 2006, *Experimental gas hydrate dissociation pressures for pure methane in aqueous solutions of $MgCl_2$ and $CaCl_2$ and for a (Methane + Ethane) gas mixture in an aqueous solution of ($NaCl + MgCl_2$)*, J. Chem. Eng. Data, **51**, 1862-1867

Austvik T., Hustvedt E., Meland B., Berge L.I., Lysne D., 1995, in: 7th BHRA Int. Conference on Multiphase Flow, Publication 14, Cannes, FR 6/7-9/95, 539.

Blank C., Tournier-Lasserve J., 1990, *Controlling hydrates in high-pressure flow lines*, *World Oil*, **211**(5), 63-68

Boyer F.L., Bircher L.J., 1960, *The solubility of nitrogen, argon, methane, ethylene and ethane in normal primary alcohols*, J. Phys. Chem., **64**, 1330-1331

Bruinsma D.F.M., Desens J.T., Notz P.K., Sloan Jr. E.D., 2004, *A novel experimental technique for measuring methanol partitioning between aqueous and hydrocarbon phases at pressures up to 69MPa*, Fluid Phase Equilibr., **222-223**, 311–315

Chen C.J., Ng H.J., Robinson D.B., 1988, *The solubility of methanol or glycol in water-hydrocarbon system*s, GPA Research Report RR-**117**

Chapoy A., Haghighi H., Burgass R., Tohidi B., 2009, *Gas hydrates in low water content gases: experimental measurements and modelling using the CPA equation of state*, Submitted to the J. Fluid Phase Equilibr.

Dholabhai P.D., Englezos P., Kalogerakis N., Bishnoi P.R., 1991, *Equilibrium conditions for methane hydrate formation in aqueous mixed electrolyte solutions*, Can. J. Chem. Eng., **69**, 800-805

Haghighi H., Chapoy A., Tohidi B., 2009, *Methane and water phase equilibria in the presence of single and mixed electrolyte solutions using the Cubic-Plus-Association equation of state*, J. Oil Gas Sci. Technol., **64**(2), 141-154

Hatton G.J., Kruka V.R., 2002, *Hydrate blockage formation—Analysis of Werner Bolley field test data*, DeepStar CTR, 5209.

Kang S.P., Chun M.K., Lee H., 1998, *Phase equilibria of methane and carbon dioxide hydrates in the aqueous $MgCl_2$ solutions*, Fluid Phase Equilibr., **147**, 229-238

Kharrat M., Dalmazzone D., 2003, *Experimental determination of stability conditions of methane hydrate in aqueous calcium chloride solutions using high pressure differential scanning calorimetry*, J. Chem. Thermodyn., **35**, 1489-1505

Kobayashi R., Withrow H.J., Williams G.B., Katz D.L., 1951, *Gas hydrate formation with brine and ethanol solutions*. *Proceeding of the 30th Annual Convention, Natural Gasoline Association of America*, **27-31**

Li X.S., Wu H.J., Englezos P., 2006, *Prediction of gas hydrate formation conditions in the presence methanol, glycerol, ethylene glycol, and triethylen glycol with the statistical associating fluid theory equation of state*, Ind. Eng. Chem. Res., **45**, 2131-2137

Maekeawa T., Imai N., 1999, *Equilibrium conditions of methane and ethane hydrates in aqueous electrolyte solutions, The 3rd ICGH*

Maekawa T., Itoh S., Sakata S., Igari S.I., Imai N., 1995, *Pressure and temperature conditions for methane hydrate dissociation in sodium chloride solutions*, Geochem. J., **29**, 325-329

Masoudi R., Tohidi B., Anderson R., Burgass R.W., Yang J., 2004, *Experimental measurement and thermodynamic modelling of clathrate hydrate equilibria and salt solubility in aqueous ethylene glycol and electrolyte solutions*, Fluid Phase Equilibr., **219**, 157–163

Ng H.J., Robinson D.B., 1985, *Hydrate formation in system containing methane, ethane, propane, carbon dioxide or hydrogen sulphide in the presence of methanol*, Fluid Phase Equilibr., **21**, 144-155

Ng H.J., Chen C.J., Robinson D.B., 1985, *Effect of ethylene glycol or methanol on hydrate formation in systems containing ethane, propane, carbon dioxide, hydrogen sulfide or a typical gas condensate*, GPA Research Report RR-**92**

Ng H.J., Chen C.J., Saeterstad T., 1987, *Hydrate formation and inhibition in gas condensate and hydrocarbon liquid systems*, Fluid Phase Equilibr., **36**, 99-106

Nixdorf J., Oellrich L.R., 1997, *Experimental determination of hydrate equilibrium conditions for pure gases, binary and ternary mixtures and natural gases*, Fluid Phase Equilibr., **139**, 325-333

Robinson D.B., Ng H.J., 1986, *Hydrate formation and inhibition in gas or gas condensate streams*, J. Can. Pet. Technol., **25**(4), 26–30

Ross M.J., Toczylkine L.S., 1992, *Hydrate dissociation pressures for methane or ethane in the presence of aqueous solutions of triethylene glycol*, J. Chem Eng. Data, **37**(4), 488-491

Song K.Y., Fneyrou G., Martin R., Lievois J., Kobayashi R., 1997, *Solubility measurements of methane and ethane in water and near hydrate conditions*, Fluid Phase Equilibr., **128**, 249-260

Song K.Y., Kobayashi R., 1989, *Final hydrate stability conditions of a methane and propane mixture in the presence of pure water and aqueous solutions of methanol and ethylene glycol*, Fluid Phase Equilibr., **47**, 295-308

Svartas T.M., Fadnes F.H., 1992, *Methane hydrate equilibrium data for the methane-water-methanol system up to 500 bara*, The 2nd International Offshore and Polar Engineering Conference, **1**, 614-619

Tohidi B., Burgass R.W., Danesh A., Todd A.C., Østergaard K.K., 2000, *Improving the Accuracy of Gas Hydrate Dissociation Point Measurements*, Ann. N.Y. Acad. Sci., **912**, 924-931

CHAPTER 6 – APPLICATION OF THE MODEL TO NEW HYDRATE FORMERS AND HYDRATES IN POROUS MEDIA

6.1 Introduction

Alcohols such as methanol are generally known to be inhibitors for hydrate formation. Addition of alcohols to water reduces hydrate stability, causing a shift in the hydrate equilibrium conditions to lower temperature and higher pressure (Sloan, 1998). It has been recently demonstrated that some alcohols like *i*-propanol (Østergaard et al., 2002), *n*-propanol (Chapoy et al., 2008) and ethanol (Anderson et al., 2008) can form hydrates and do not have the inhibition effect expected from an alcohol. Ohmura et al. (2007) investigated clathrate hydrates formed from methane and a 16.4 mass% aqueous solution of *i*-propanol using X-ray diffraction analysis. Mores, this research showed that structure II hydrates formed as opposed to structure I hydrates normally formed with methane and pure water. Equilibrium conditions for clathrate hydrates formed from methane and different concentrations of *n*-propanol or *i*-propanol aqueous solutions were also experimentally determined by Maekawa (2008). It has been investigated that propanol has an inhibiting and/or promoting effect on hydrate formation depending on the concentration. A structural transition from a structure I to a different hydrate structure occurred at concentrations between 3 and 5 mass% for *n*-propanol and between 2 and 3 mass% for *i*-propanol (Maekawa, 2008). This investigation has been followed by Aladko et al. (2009) for *i*-propanol. The phase diagram of the binary system of *i*-propanol –water was investigated by means of differential thermal analysis and powder X-ray diffraction. Two incongruently melting polyhydrates with the compositions close to the molar ratio of *i*-propanol to water of 1 to 5 has been reported by Aladko et al. (2009).

In addition to the above, freezing point data of ethanol and *n*-propanol solutions (up to 80 mass%) has been presented by Chapoy et al. (2008) and Anderson et al. (2008), respectively. These data suggest existence of a peritectic point and formation of clathrate hydrate in *n*-propanol/ethanol-water systems. To confirm that *n*-propanol and ethanol (similar to *i*-propanol) form double hydrates with small molecules at elevated pressures, hydrate dissociation points were measured and presented for aqueous solution of different concentration of *n*-propanol/ethanol in the presence of methane and natural gas by the above authors.

In this work, the hydrate formation conditions for two natural gas systems in the presence of aqueous solution with different ethanol concentrations were measured and reported in Chapter 2 (Table 2.12). In addition, by using the CPA model, *n*-propanol and ethanol have been modelled as hydrate-forming compounds using a thermodynamic model. Comparisons between the experimental hydrate dissociation data and model predictions strongly suggest that *n*-propanol and ethanol take part in structure II hydrate formation, occupying the large cavity of the structure.

Further to the above, the capability of model for predicting the hydrate dissociation conditions in porous media has been evaluated. Methane gas hydrates have been widely touted as a potential new source of energy. Methane hydrates have been found to form in various rocks or sediments given suitable pressure and temperature conditions, and supplies of water and methane. The hydrate dissociation conditions in mesoporous silica have been modelled by using the method presented in Chapter 3. In this chapter, the predictions of the model for different pore sizes have been validated against independent experimental data generated in mesoporous silica media.

6.2 Optimization of Kihara Parameters for Alcohols

Alcohols are generally considered hydrate inhibitors. While all available evidence suggests methanol, the most common alcohol used for hydrate inhibition, does not form clathrates, despite a favourable ratio of molecular size to simple hydrate cavity radii (see Table 6.1), the fact that *i*-propanol, in addition to tert-butanol (Murthy, 1999), can form hydrates, demands further investigation. In the past we have investigated hydrate characteristics of *i*-propanol and the experimental and modelling results suggested that *i*-propanol entered and stabilized the large $5^{12}6^4$ cavity of structure II (sII) hydrates (Østergaard et al., 2002). Subsequent independent Raman Spectroscopy studies by Ohmura et al. (2004) confirmed these findings.

Recently Chapoy et al. (2008), and Anderson et al. (2008) investigated the equilibrium conditions of clathrate hydrates formed from methane and *n*-propanol/ethanol aqueous solutions, and found that similar to *i*-propanol, *n*-propanol and ethanol do not have the inhibition effect expected from an alcohol. The only explanation for the observed behaviour is that *n*-propanol and ethanol enter and stabilize hydrate structure; thus, it can be considered as a hydrate former. In light of this, it was decided to investigate this

phenomenon further by thermodynamic modelling. The available experimental data from the literature could give us enough material to be able to model these compounds and investigate their hydrate formation characteristics. The modelling could also help us to find out the best hydrate structure that can describe the observed phase behaviour.

Table 6.1 Ratios of cavity radius and n-propanol and ethanol radius

		Molecular Radius / Cavity radius						
		Structure I		Structure II		Structure H		
Guest	R /Å	5^{12} 2.55[a] /Å	$5^{12}6^{12}$ 2.90[a] /Å	5^{12} 2.51[a] /Å	$5^{12}6^{4}$ 3.33[a] /Å	5^{12} 2.51[a] /Å	$4^{3}5^{6}6^{3}$ 2.66[a] /Å	$5^{12}6^{8}$ 4.31[a] /Å
MeOH	2.3	0.90	0.79	0.92	0.69	0.92	0.86	0.53
EtOH	2.8	1.10	**0.97**	1.12	**0.84**	1.12	1.05	0.65
n-POH	3.3	1.29	1.14	1.31	**0.99**	1.31	1.24	**0.77**
i-POH	3.33[b]	1.31	1.15	1.33	**1.00**	1.33	1.25	**0.77**

[a] *Cavity radius minus the van der Waals radius of the water molecule (1.4Å)*[b]*; from Østergaard et al., 2002.*

Considering molecular size of ethanol and cavity sizes of different hydrate structures, it can be concluded that ethanol molecules are far too small to stabilize the large cavity of structure H (sH) hydrates (smallest guest known to stabilize the large cavity of sH is adamantine with a radius of 3.7 Å) but they could be accommodated in the large cavities of sI and sII (see Table 6.1), hence stabilising these two structures. With the same logic by considering *n*-propanol molecular size and cavity sizes, one can conclude that *n*-propanol could be accommodated in large cavities of sII and sH. As detailed below, the experimental data generated from the literature were used in optimising the Kihara parameters for ethanol and *n*-propanol.

A general phase equilibrium model based on the uniformity of component fugacities in all phases has been extended to model *n*-propanol/ethanol clathrate hydrate equilibria by using the CPA model in Chapter 3. The hydrate phase is modelled using the solid solution theory of van der Waals and Platteeuw (1959), as developed by Parrish and Prausnitz (1972). The Kihara model for spherical molecules is applied to calculate the potential function for compounds forming hydrate phases (Kihara, 1953).

Methane − *n*-propanol/ethanol and water − *n*-propanol/ethanol binary interaction parameters have been optimised using gas solubility data in *n*-propanol/ethanol, and a combination of VLE and ice melting point data respectively. Optimized binary interaction parameters have been reported in Chapter 4.

The thermodynamic model has been extended to include *n*-propanol and ethanol as hydrate formers by optimizing the Kihara potential parameters. The hard-core radius, α, of the Kihara potential parameter for *n*-propanol and ethanol was calculated from correlations given by Tee et al. (1966). This value was considered acceptable for hydrate modelling, given that predictions are not significantly affected by minor changes in the hard-core radius.

The two remaining Kihara potential parameters for *n*-propanol or ethanol, i.e., the collision diameter "σ" and the depth of the energy well "ε", were optimized using the experimental methane hydrate dissociation data for *n*-propanol and ethanol presented by Chapoy et al. (2008), Maekawa (2008) and Anderson et al. (2008) (assuming sII and sH for *n*-propanol and sI and sII for ethanol) by using the method of Tohidi-Kalorazi. (1995). The resulting Kihara parameters for *n*-propanol and ethanol are presented in Tables 6.2 and 6.3, respectively. The Kihara potential parameters for methane are taken from Tohidi-Kalorazi. (1995). The resulting model has been used to predict the H-L-V experimental data generated on the above systems.

6.2.1 *n-Propanol−Water−Methane and n-Propanol−Water−Natural Gas Systems*

Figure 6.1 shows experimental data and predicted hydrate dissociation conditions for the system methane-distilled water, alongside measured data for hydrate formed from aqueous *n*-propanol solutions in the presence of methane. In the above predictions *n*-propanol is assumed a non-hydrate former and a hydrate inhibitor. It is clear from Figure 6.1 that there are significant deviations between experimental data and predicted hydrate phase boundaries for *n*-propanol solutions if *n*-propanol is considered as an inhibitor. When compared to experimental data for methane-distilled water system, it is clear that *n*-propanol has a considerably lower inhibition effect than what would be expected from an alcohol acting as a hydrate inhibitor.

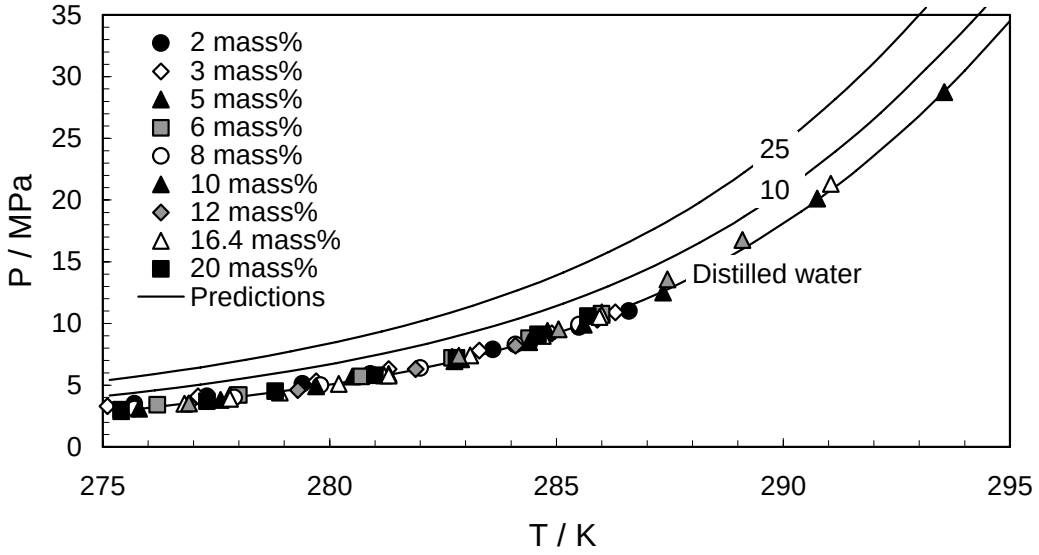

Figure 6.1 Experimental hydrate dissociation conditions for methane- distilled water and methane-n-propanol aqueous solutions, compared to model predictions (black lines) of 10 and 25 mass% n-propanol assuming n-propanol as a hydrate inhibitor (Experimental data form Chapoy et al., 2008 and Maekawa, 2008).

This is a similar pattern to what seen for *i*-propanol, and supports formation of double methane−*n*-propanol clathrates (Østergaard et al., 2002). The only feasible explanation for the observed increase in the hydrate stability is that *n*-propanol enters and stabilizes hydrate structure; thus, it can be considered as a hydrate former.

To further investigate the potential structure(s) in *n*-propanol hydrates, experimental and predicted hydrate dissociation conditions for *n*-propanol-methane and *n*-propanol-natural gas systems are presented in Figures 6.2a-b and Figures 6.2c-d, respectively. In calculating the hydrate phase boundaries for the above systems three conditions were considered, 1) assuming *n*-propanol as an inhibitor, 2) a hydrate sII former, and 3) as a hydrate sH former. The three possible prediction scenarios are also shown in Figure 6.2.

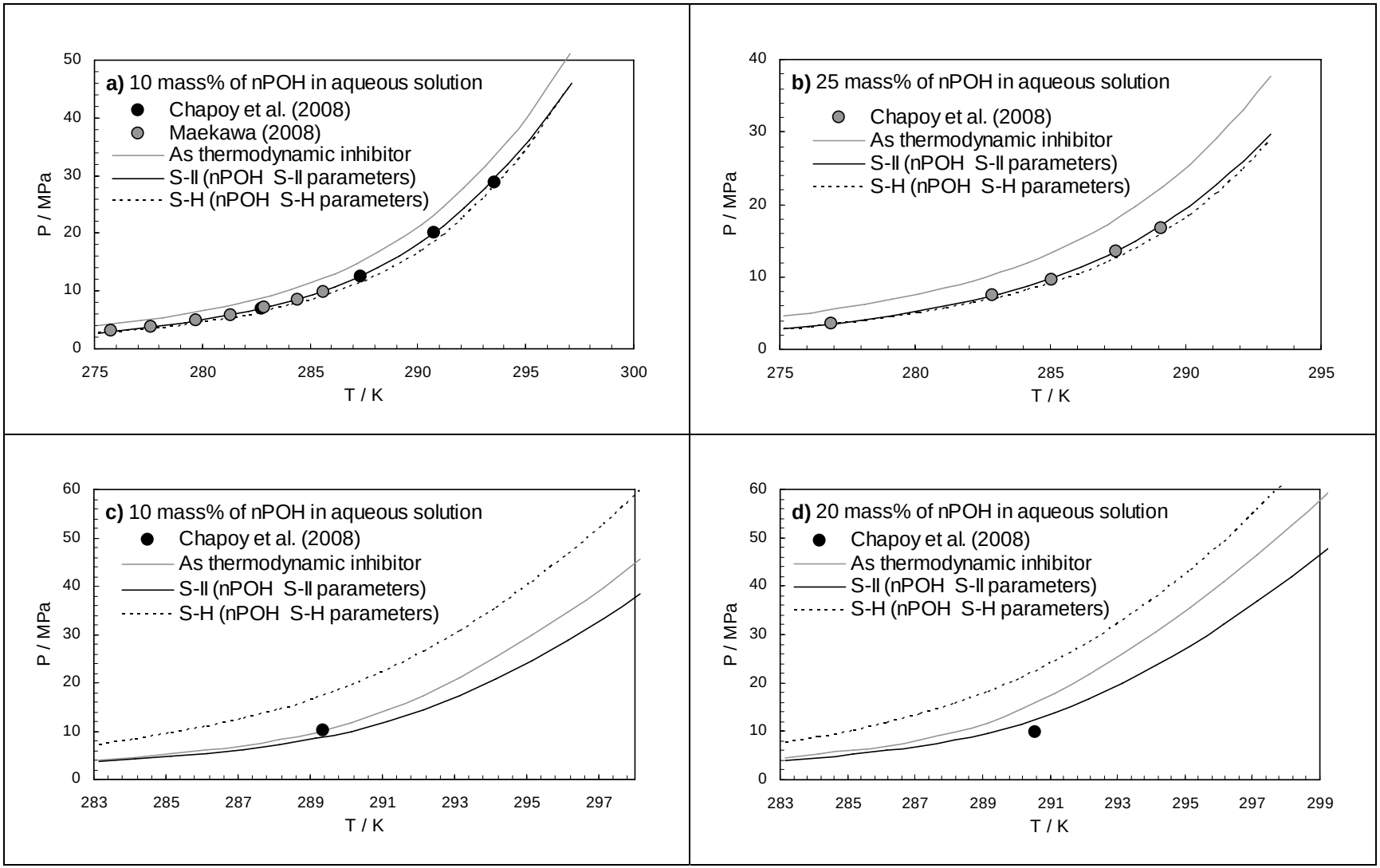

Figure 6.2 Calculated methane (a & b) and natural gas (NG 1) (c & d) hydrate dissociation condition in the presence of aqueous n-propanol solutions

Where *n*-propanol is assumed to be either an inhibitor or a sH hydrate former, the predictions are in significant disagreement with the measured experimental hydrate dissociation data (Figure 6.2). By contrast, the closest agreement between predicted values and experimental data is where *n*-propanol is assumed to be a sII hydrate former. To better understand how *n*-propanol acts to stabilize hydrates, it is important to establish the particular cavity and structure it can enter. With respect to the molecular diameter, *n*-propanol is too large to fit into any of the cavities of sI hydrates, but it could be accommodated by the large cavities of sII hydrates, as illustrated in Table 6.1. In terms of sH, *n*-propanol is probably too small to stabilize the large cavity. It is important to note that size alone does not determine whether a component is a hydrate former because other parameters such as the chemical nature of the potential guest molecule are also important. Both experimental and modelling results suggest that *n*-propanol forms sII hydrates, occupying the large cavity of this structure. However, confirmation of sII hydrate formation with *n*-propanol by direct measurement of the hydrate phase is required for a final validation.

Table 6.2 Optimized Kihara Parameters for n-propanol (α = Collision Diameter, ε = Depth of Energy Well, k = Boltzmann's Constant)

Structure	α /Å	σ^{*a} /Å	(ε / k)/K
sII	1.2664	2.873	248.61
sH	1.2664	3.116	336.86

[a] $\sigma^{*} = \sigma - 2\alpha$

6.2.2 *Ethanol−Water−Methane and Ethanol−Water−Natural Gas Systems*

As presented for *n*-propanol system, Figure 6.3 shows experimental and predicted hydrate dissociation conditions for methane-distilled water system, alongside measured data for hydrates formed in the presence of aqueous ethanol solutions. Also shown are model predictions assuming ethanol is a hydrate inhibitor. From Figure 6.3, it can be observed that there are deviations between the experimental data and predictions if ethanol is considered as an inhibitor especially at higher concentrations of ethanol. It can be concluded that ethanol has a considerably lower inhibition effect than what would be expected if it was purely an inhibitor.

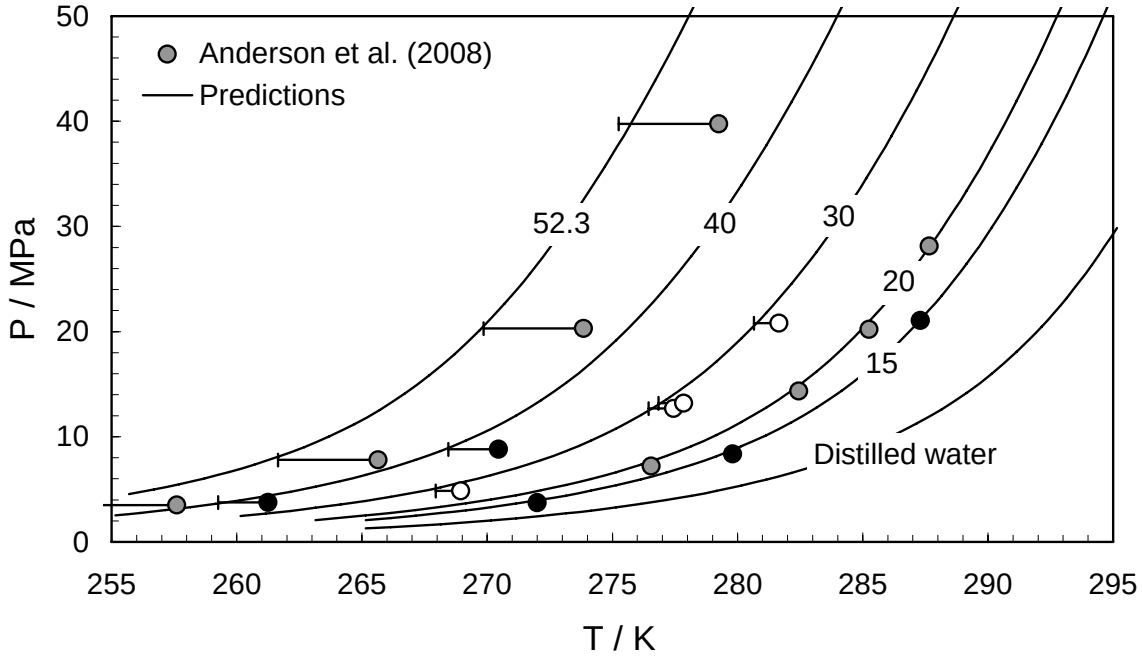

Figure 6.3 Experimental hydrate dissociation conditions for methane-distilled water and methane-ethanol aqueous solutions, compared to model predictions (black lines) for different concentration of ethanol in the aqueous phase (in mass%) assuming ethanol as an inhibitor

As it has been suggested by Anderson et al. (2008), this might be explained by formation of mixed (double) methane−ethanol clathrates. From Table 6.1 ethanol can take part in hydrate structures I or II filling large cavities in these structures. To further investigate the stable hydrate structure in methane-ethanol systems, the experimental hydrate dissociation points are plotted in Figure 6.4 along with two possible prediction scenarios, i.e, 1) assuming ethanol as a sI hydrate former, and 2) as a sII hydrate former. Experimental hydrate dissociation data for methane-ethanol-water systems are also included in Figure 6.4 for comparison. As can be seen from predictions for ethanol as an s-I or s-II former are both quite similar and comparatively close to experimental data. As such, predictions do not provide evidence in favour of either structure. Kihara parameters are presented in Table 6.3.

Table 6.3 Optimized Kihara Parameters for ethanol (α = Collision Diameter, ε = Depth of Energy Well, k = Boltzmann's Constant)

Structure	α /Å	σ^{*a} /Å	(ε / k)/K
sI	1.2664	2.349	290.91
sII	1.2664	2.491	365.95

[a] $\sigma^{*} = \sigma - 2\alpha$

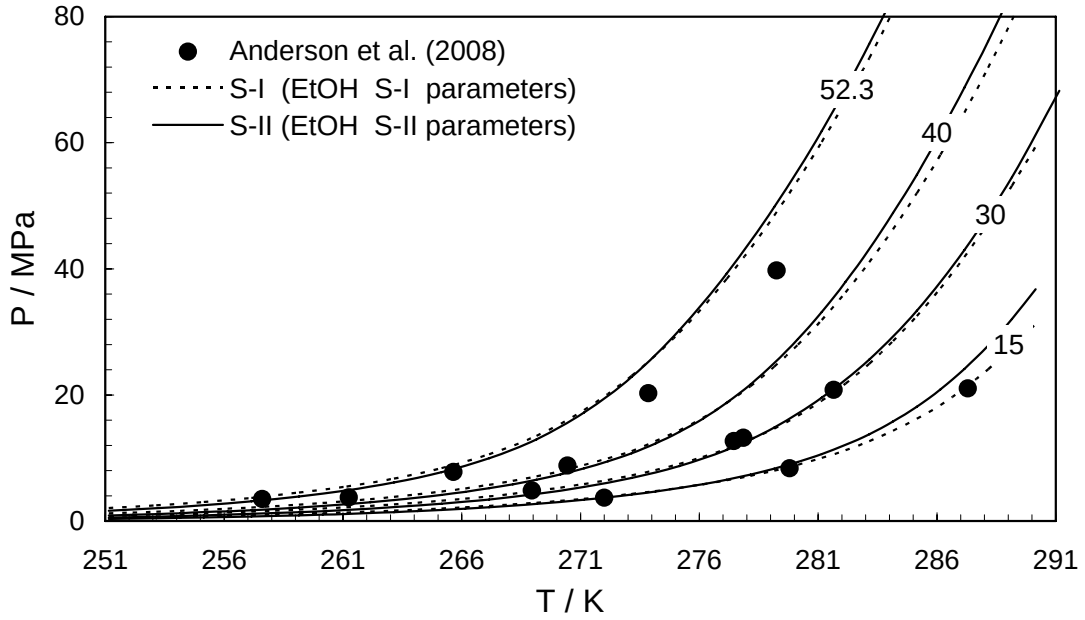

Figure 6.4 Comparison of experimental and predicted hydrate dissociation conditions for methane-ethanol aqueous solutions (15, 30, 40 and 52.3 mass% ethanol in the aqueous solutions) in three phase L-H-V region.
Two scenarios have been considered for predictions, e.g., 1) ethanol takes part in sI hydrates, 2) ethanol takes part in sII hydrates.

In light of the above, new experimental data were generated for aqueous ethanol in the presence of a North Sea natural gas (NG5), which typically forms structure-II (composition and experimental data given in Chapter 2, Table 2.12). Experimental data are compared with three model prediction options in Figure 6.5: (1) sII hydrate formation with ethanol considered as a sII former, (2) s-II hydrate with ethanol considered as an s-I former, and (3) as a thermodynamic inhibitor. As can be seen, the best agreement between predictions and experimental data is for when ethanol is considered as a sII former, occupying the large $5^{12}6^4$ cavity, however there is a deviation of up to 2 K in some cases. This may be attributed to the hydrate formed not being a true sII, but a modified structure, although this ultimately requires further confirmation, ideally through structural studies (e.g. X-ray or neutron diffraction).

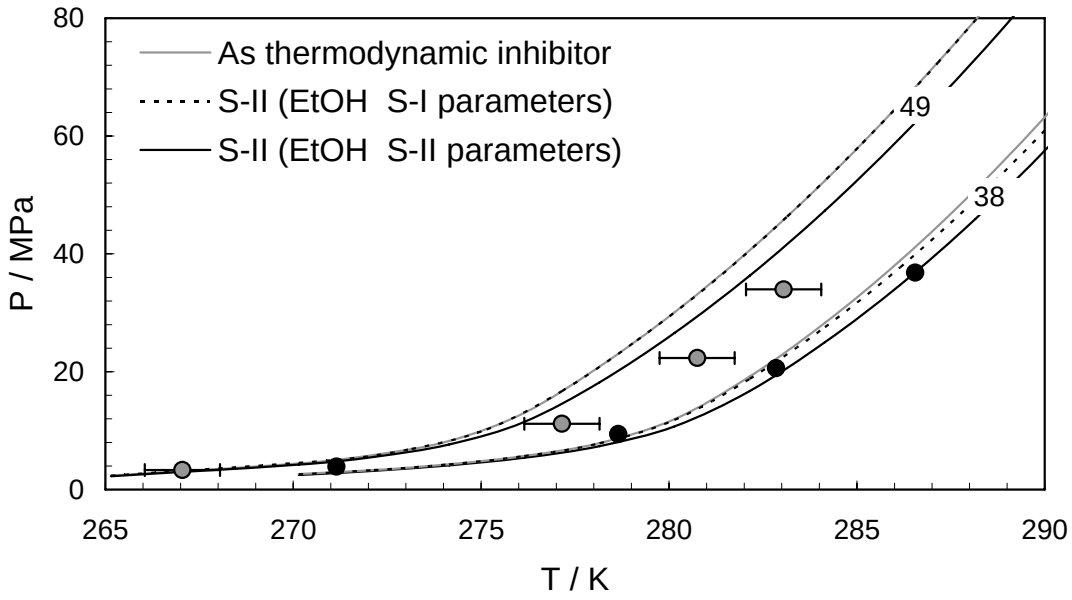

Figure 6.5 Comparison of experimental and predicted hydrate phase boundary for a natural gas in the presence of ethanol aqueous solutions.
Three scenarios have been considered in calculating the hydrate stability zone, i.e., 1) ethanol as a hydrate inhibitor which does not take part in hydrate structure, 2) assuming sI Kihara parameters for ethanol, 3) assuming sII Kihara parameters for ethanol. (Experimental data for 38 and 49 mass% of ethanol aqueous solution; from this work).

6.3 The Capillary Effect on the Hydrate Stability Condition in Porous Media

As a potential energy source, naturally occurring gas hydrates are attracting significant attention. Current estimates put the hydrate resources on the earth twice as great as the combined fossil fuel reserve (Sloan, 1998). In spite of such importance, most measurements and models are for bulk gas hydrates (i.e., not taking into account the effect of porous media). In nature, hydrates occur in porous media, e.g., clay, silt, and sand. Therefore the hydrate stability zone is expected to be a function of capillary pressure, wettability, sediment mineralogy as well as over burden pressure. Furthermore the pore water in sediments is generally saline, containing a mixture of salts. In this work the effect of capillary pressure and salts on the hydrate stability zone has been addressed.

Since Handa and Stupin (1992) first measured the equilibrium dissociation conditions of methane hydrate and propane hydrate in porous media, researchers have carried out many investigations into the hydrate equilibrium dissociation conditions for different porous media, and obtained a range of experimental data. However, some recent literature reviews suggest that the results of many existing studies are questionable. It

was first Clarke et al. (1999) and Wilder et al. (2001) who offered the explanation that the porous media used in the experiment by different researches were not a single pore size but had a distribution of the pore sizes. In a more recent work by Anderson et al. (2003a), it was revealed that the opinions differ significantly among researchers, with respect to appropriate experimental techniques and interpretation of the results. This can explain significant disagreement among the reported results.

Similar to the experimental techniques, there are some disagreements among the researchers for modelling hydrate formation in porous media. Applying Gibbs–Thomson equation to account for the capillary effect arising from the small pore size, Clennell et al. (1999) and Henry et al. (1999) developed a thermodynamic model to predict the three phase equilibrium of CH_4 hydrate in marine sediments. Later, Klauda and Sandler (2001, 2003) proposed an improved model and predicted the distribution of methane hydrate in ocean sediment. However, these models used incorrect interface parameters (Llamedo et al., 2004). The shape factor (curvature) of hydrate – liquid interface assumed by them corresponds not to hydrate equilibrium dissociation, but to hydrate growth. Therefore, these models overestimate the inhibition effect of the capillary force on equilibrium condition.

The purpose of this part of the research is to develop an accurate model to predict the *P-T* condition for gas hydrate formation in marine environments by taking into account the effect of temperature, pressure, salinity and capillary forces together. As presented in Chapter 3, the CPA model has been extended to take into account the effect of capillary pressure of hydrate formation in porous media by the approach introduced by Llamedo et al. (2004). The Debye Hückel electrostatic term has been used for taking into account the effect of salt on the fugacity of water when electrolytes are present (Aasberg-Petersen et al., 1991).

6.3.1 *Equilibrium Condition in Porous Media in Presence of Pure Water*

As mentioned previously, one of the main sources of deviation between the predictions by the thermodynamic model and the experimental results could be due to the questionable experimental methods used by different researchers and methods for interpretation of the results. It should be considered that the pore sizes of the porous media used have a distribution in radii, not a single size in radii. Regarding data interpretation of experimental results, dissociation conditions have been interpreted by

some researchers in terms of the mean pore diameter, directly contradicting proposals by others that this is not possible. As Anderson et al., (2003a) concluded, for samples with a simple, unimodal distribution; it is possible to determine dissociation conditions for the mean pore size. By assuming the volume of hydrate formed within pores is proportionate to the sample pore volume distribution, then, because the slope of the heating curve reflects the volume of hydrate dissociated with each temperature step, the point of slope inflection (from increasing to decreasing slope) should approximate the dissociation in pores with diameters close to the mean of the distribution (if the mean pore diameter matches the diameter of maximum porosity). If the distribution is more complex, e.g., unevenly spread, with many peaks, then considering the dissociation point taken is attributed to mean pore diameter is likely to cause inaccuracy in results, generally underestimating inhibition (Anderson et al., 2003a).

In this section, the model predictions of CH_4 and CO_2 hydrate dissociation conditions for different pore sizes have been validated against independent experimental data generated in mesoporous silica media. The experimental data and the calculated methane and carbon dioxide hydrate dissociation conditions are presented in Figures 6.6 and 6.7, wherein the model predictions are seen to agree well with the experimental data. It is worthy to note, the experimental data from Anderson et al. (2003b) have been measured by using a step-heating method as recommended by Tohidi et al. (2000) and are for mean pore diameter. It should be also mentioned that these data could be regarded as independent as hydrate dissociation data have not been used in extending the thermodynamic model to porous media.

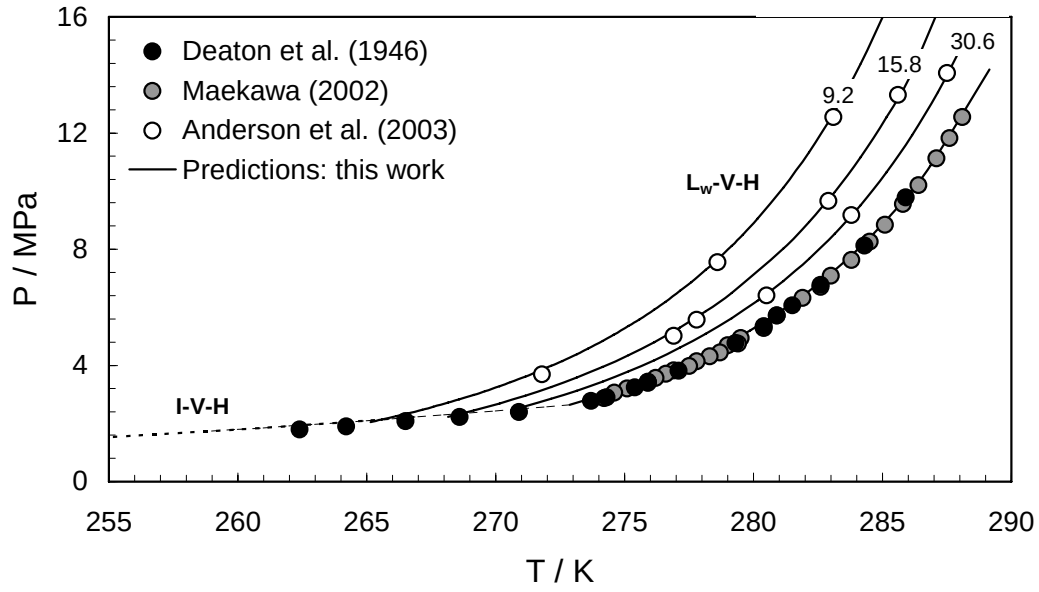

Figure 6.6 Methane hydrate dissociation conditions in mesoporous silica for different pore sizes (i.e, 9.2, 15.8, and 30.6 nm).
Black lines are the predicted methane hydrate phase boundary in porous media in the L_w-V-H region. Dotted black lines are the predicted methane hydrate phase boundary in porous media in the I-V-H region. The CPA model developed in this work has been used in all predictions.

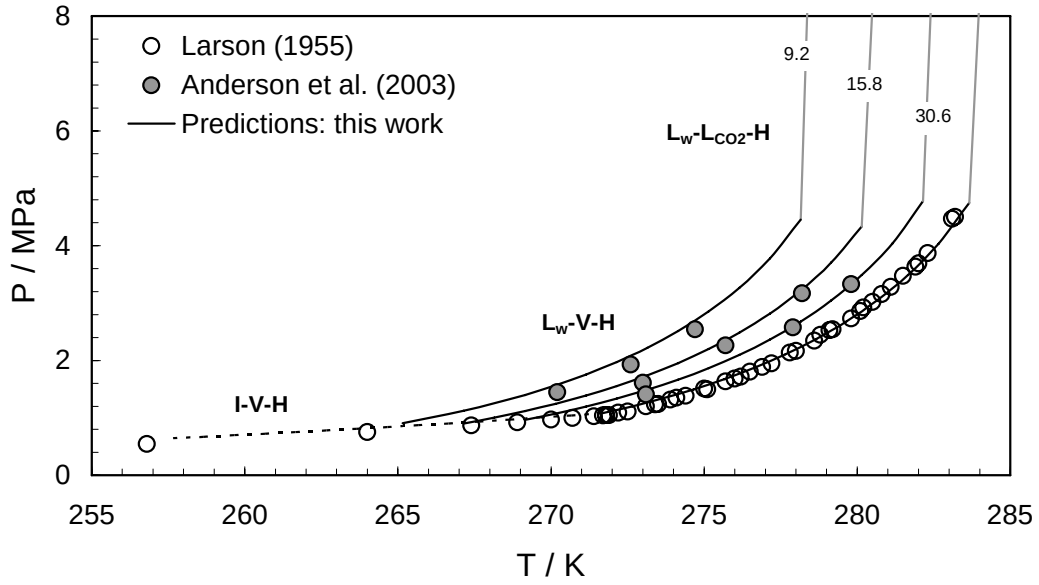

Figure 6.7 Carbon dioxide hydrates dissociation conditions in mesoporous silica for different pore sizes (i.e, 9.2, 15.8, and 30.6 nm).
Black lines are the predicted Carbon dioxide hydrate phase boundary in porous media in the L_w-V-H region. Dotted black lines are the predicted Carbon dioxide hydrate phase boundary in porous media in the I-V-H region. Gray solid lines are the predicted Carbon dioxide hydrate phase boundary in porous media in the L_W-L_{CO2}-H region. The CPA model developed in this work has been used in all predictions.

Seo and Lee (2003) have also reported some experimental data for dissociation conditions of CH_4/CO_2 hydrate in the porous media, using a continuous heating (non-equilibrium) method. The rate of temperature change was 0.05~0.1 K/h. The dissociation equilibrium point in silica gel pores was chosen by Seo and Lee (2003) as the cross point between the maximum inclination line and complete dissociation line. They considered this point corresponds to the dissociation of hydrate in the pores of the mean diameter of used silica gels. The experimental data have been used for validation of the model. Figure 6.8 presents the modelling results along with the predictions of the thermodynamic model.

It should be noted that whatever the nature of the pore size distribution, the final dissociation point should always correspond to dissociation in pores of maximum diameter (of detectable porosity). This means that the last hydrate dissociation point which corresponds to the dissociation condition in the largest pore size has been reported as the dissociation pint for the mean diameter of the used silica gel by Seo and Lee (2003). This incorrect determination of dissociation conditions with respect to mean pore diameter interpretative methods can be considered as source of deviation between prediction and experimental results in Figure 6.8.

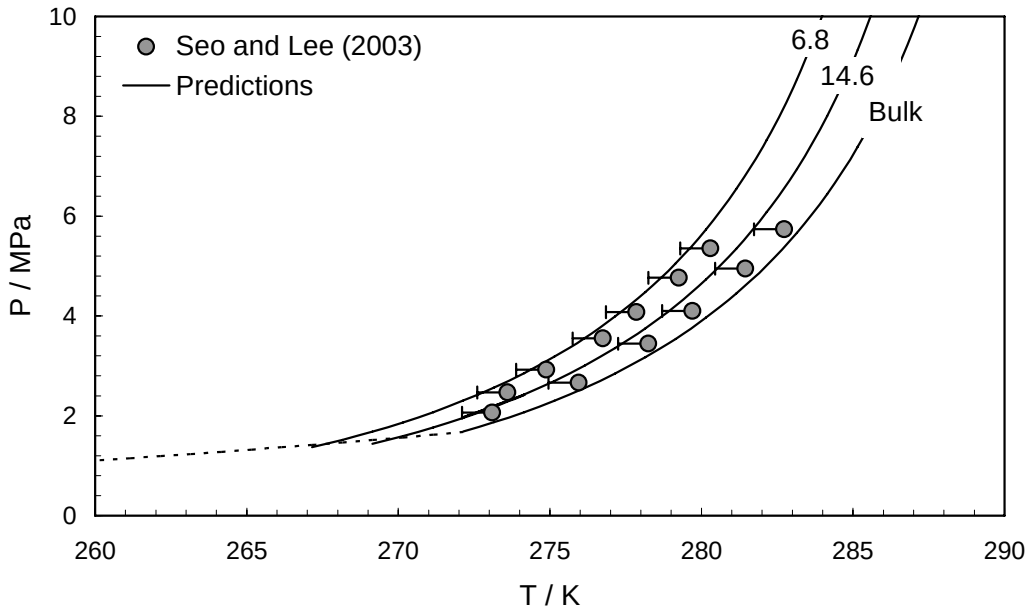

Figure 6.8 CH_4(60 mol.%)/CO_2 hydrate dissociation pressure in mesoporous (6.8 and 14.6 nm).
Black lines are the predicted hydrate phase boundary in porous media in the L_w-V-H region. Solid black lines are the predicted hydrate phase boundary in the L_W-L_{CH4}-$_{CO2}$-H region (Error bars: ± 0.5 K). Dotted black lines are the predicted hydrate phase boundary in porous media in the I-V-H region. The CPA model developed in this work has been used in all predictions.

6.3.2 *Equilibrium Condition in Porous Media in Presence of Electrolyte Solutions*

As one step towards a better understanding of the occurrence of gas hydrate in nature, the effects electrolyte solutions on phase equilibria in porous media must be known. The model has been successfully tested for prediction of hydrate formation conditions in the presence of salts and organic inhibitors in bulk (Chapter 5). In this section, this model has been further evaluated to model methane and carbon dioxide hydrate dissociation condition in presence of NaCl (Figures 6.9 and 6.10). As mentioned in the previous section, the interpretative method used by Seo et al. (2002) and Seo and Lee (2003) could be considered as a source of the deviation between modelling prediction and experimental results.

There is another issue regarding the available hydrate dissociation experimental data in presence of salts is about how the pore samples have been washed up after each test. Porous media sample should be clean up before running each series of tests but it could be considered as impossible to remove salts completely by usual methods. This is an important issue that does have effect on the experimental results. However due to limitation of experimental data for these systems, there is no other source of data available which can be used for evaluation of the experimental data used in this section. As it can be seen from Figures 6.9 and 6.10, the deviations between predictions and experimental data increase by increasing the concentration of salt. It could be explained by the fact that the porous media samples used for the tests were not washed or replaced with fresh sample and the accumulation of salt in each step causes this shift in the equilibrium condition.

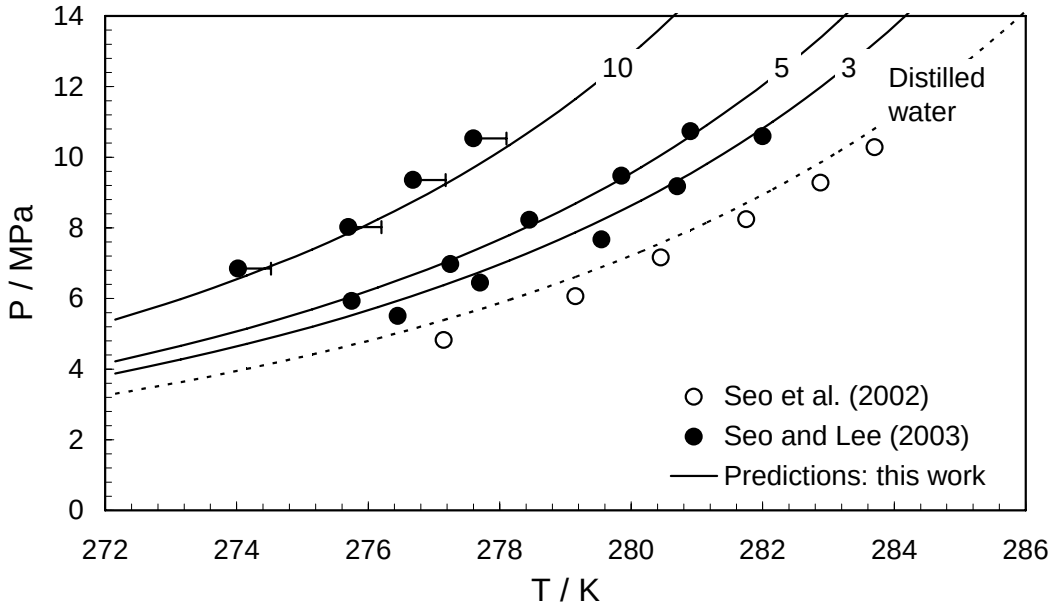

Figure 6.9 Methane hydrate dissociation conditions in mesoporous (15 nm) in the presence of different concentrations of NaCl (i.e., 3, 5 and 10 mass%).
Black lines are the predicted methane hydrate phase boundary in porous media in the presence of NaCl aqueous solution. Dotted black lines are the predicted methane hydrate phase boundary with no salt presents (distilled water) (Error bars: ± 1 K). The CPA model developed in this work has been used in all predictions.

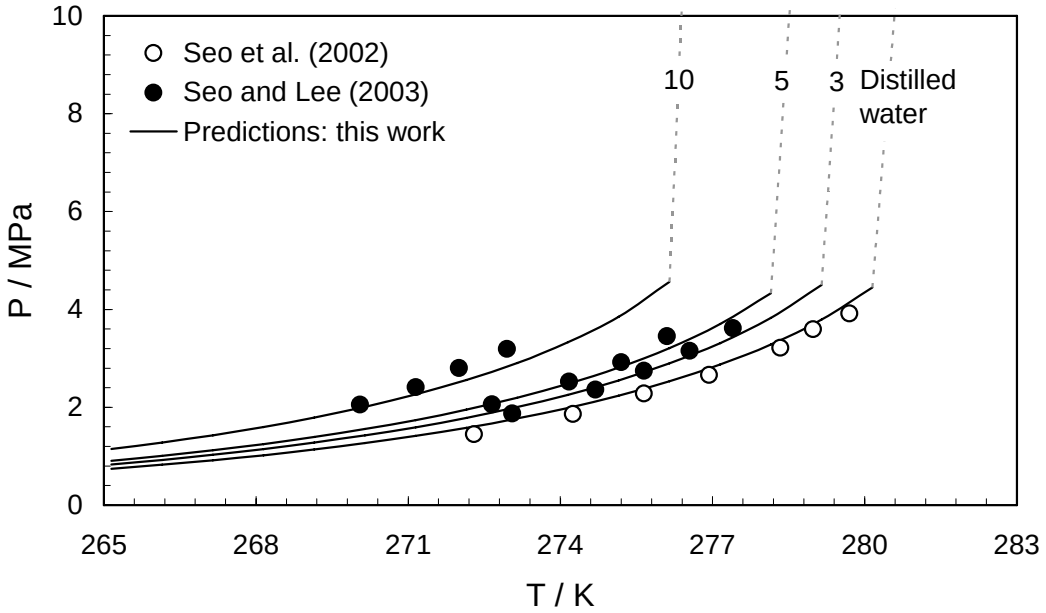

Figure 6.10 Carbon dioxide hydrate dissociation conditions in mesoporous (15 nm) in the presence of different concentrations of NaCl (i.e., 3, 5 and 10 mass%).
Black lines are the predicted carbon dioxide hydrate phase boundary in porous media in the L_w-V-H region. Dotted grey lines are the predicted carbon dioxide hydrate phase boundary in the L_W-L_{CO2}-H region. The CPA model developed in this work has been used in all predictions.

6.3.3 *Equilibrium Condition in Porous Media in Presence of Methanol*

To use methane hydrate as an energy resource, production methods need to be established to extract methane-rich hydrocarbons from methane hydrate. Consequently, finding an efficient, safe method of triggering the dissociation of methane hydrate is an important factor in production. Conventional methods for gas hydrate production include depressurization, thermal stimulation, and inhibitor injection, or a combination of the above. In the inhibitor injection, inhibitors such as methanol or electrolytes are injected from surface down to methane hydrate-bearing layers (Rose and Pfannkuch, 1982 and Tohidi et al., 1993). This method results in methane hydrate dissociation by shifting the local hydrate stability zone to the left. Thus, there has been a strong interest in developing either predictive thermodynamic models or correlations capable of predicting hydrate phase boundaries in porous media for systems containing electrolytes or alcohols. In this section the effect of methanol on hydrate formation condition in porous media has been addressed.

The experimental data from Llamedo et al. (2004), which have been used in this section, have been measured by using a step-heating method. Note that experimental dissociation data for methanol aqueous solutions are for silica sample maximum pore diameters, determined through NMR studies (Anderson et al., 2003b). Maximum pore diameters were used because of the effects of inhibitor mass transfer in systems. As aqueous inhibitor concentrations increase proportionally with the volume of hydrate present, dissociation conditions for sample, mean pore diameters (where a considerable volume of hydrate will still be present) will be representative of an inhibitor concentration higher than that of initial solution.

The effect of methanol on hydrate formation condition in porous media has been tested and presented in Figure 6.11, wherein the model predictions are seen to agree well with the experimental data.

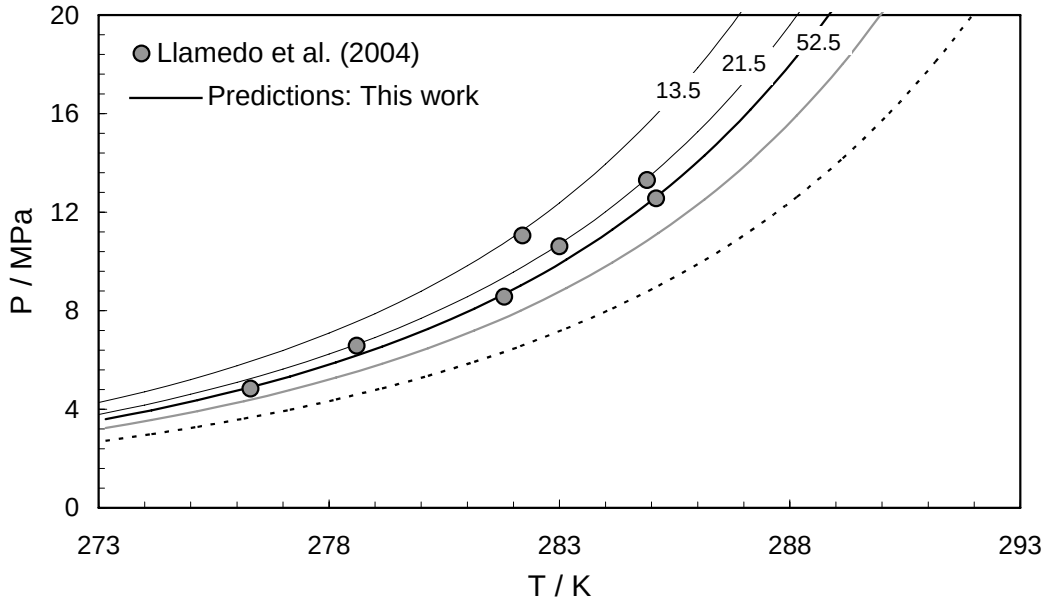

Figure 6.11 Methane hydrate dissociation conditions in mesoporous silica for different pore sizes in the presence of MeOH (3.5, 3.6 and 3.9 mass% of MeOH aqueous solutions were used for 13.5, 21.5 and 52.5 nm pore diameter, respectively).
Black lines are the predicted methane hydrate phase boundary in porous media. Gray line is the the predicted methane hydrate phase boundary in bulk in the presence of 3.5 mass% of MeOH. Dotted black lines are the predicted methane hydrate phase boundary in porous media (distilled water). The CPA model developed in this work has been used in all predictions.

6.4 Conclusions

In this work, the experimental data for *n*-propanol and ethanol clathrates have been used in the optimization of Kihara potential parameters, facilitating the extension of the CPA thermodynamic model to predicting the hydrate phase boundary for systems containing *n*-propanol and ethanol, taking into account their hydrate formation and inhibition characteristics.

Model predictions show the best agreement with the experimental data when *n*-propanol is considered as a hydrate former. Both experimental (Maekawa, 2008) and modelling results from this work suggest that *n*-propanol forms sII hydrates, occupying the large cavity of this structure.

Novel experimental incipient three-phase H-L_W-V equilibrium data for ethanol clathrate hydrates have been reported in this thesis. The results strongly suggest that ethanol is a hydrate-forming compound. Experimental phase behaviour and compositional data, combined with preliminary thermodynamic modelling studies,

suggest ethanol clathrates are most likely of sII type, although this ultimately requires further confirmation, ideally through structural studies (e.g. X-ray or neutron diffraction).

Further to the above, the model has been extended to take into account the effect of capillary pressure of hydrate formation in porous media. The hydrate equilibrium dissociation conditions for single and mixed gases in the presence of salt and alcohol are predicted successfully using the CPA model and the good agreement with experimental was achieved.

References

Aladko L.S., Manakov A.Y., Ogienko A.G., A. Ancharov I., 2009, *New data on phase diagram and clathrate formation in the system water–isopropyl alcohol*, J. Incl. Phenom. Macrocycl. Chem., **63**, 151–157

Anderson R. , Chapoy A., Tanchawanich J., Haghighi H., Lachwa-Langa J., Tohidi B., 2008, *Binary ethanol−methane clathrate hydrate formation in the system CH_4-C_2H_5OH-H_2O: experimental data and thermodynamic modelling*, 6th International Conference on Gas Hydrates (ICGH)

Anderson R., Llamedo M., Tohidi B., Burgass R., 2003a, *Characteristics of clathrate hydrate equilibria in mesopores and interpretation of experimental data*, J. Phys. Chem. B, **107**, 3500-3506

Anderson R., Llamedo M., Tohidi B., Burgass R., 2003b, *Experimental measurement of methane and carbon dioxide clathrate hydrate equilibria in mesoporous silica*, J. Phys. Chem. B, **107**, 3507-3514

Chapoy A., Anderson R., Haghighi H., Edwards T., Tohidi B., 2008, *Can n-propanol form hydrate?*, Ind. Eng. Chem. Res., **47**, 1689-1694

Clarke M.A., Darvish M.P., Bishnoi P.R., 1999, *A method to predict equilibrium conditions of gas hydrate formation in porous media*, Ind. Eng. Chem. Res., **38**, 2485-2490

Deaton W.M., Jr. Frost E.M., 1946, *Gas hydrate composition and equilibrium data*, Oil Gas J., **45**, 170-178

Handa Y.P., Stupin D., 1992, *Thermodynamic properties and dissociation characteristics of methane and propane hydrates in 70-Å-radius silica-gel pores*, J. Phys. Chem., **96**, 8599-8603

Kihara T., 1953, *Virial coefficients and models of molecules in gases*, Reviews of Modern Physics, **25**(4), 831-843

Larson S.D., 1955, *Phase studies of the two-component carbon dioxide-water system involving the carbon dioxide hydrate*, Ph.D. Thesis, University of Michigan

Llamedo M., Anderson R., Tohidi B., 2004, Thermodynamic *prediction of clathrate hydrate dissociation conditions in mesoporous media*, Am. Mineral., **89**, 1264-1270

Maekawa T., 2002, *Equilibrium conditions for gas hydrates of hydrocarbons and noble gases mixtures*, International Conference on Gas Hydrates (ICGH)

Maekawa T., 2008, *Equilibrium conditions for clathrate hydrates formed from methane and aqueous propanol solutions*, Fluid Phase Equilibr., **267**, 1–5

Murthy S.S.N., 1999, *Detailed study of ice clathrate relaxation: evidence for the existence of clathrate structures in some water-alcohol mixtures*, J. Phys. Chem. A, **103**, 7927-7937

Ohmura R., Takeya S., Uchida T., Ebinuma T., 2004, *Clathrate hydrate formed with methane and 2-Propanol: Confirmation of structure-II hydrate formation*, Ind. Eng. Chem. Res., **43**, 4964-4966

Østergaard K.K., Tohidi B., Anderson R., Todd A.C., Danesh A., 2002, *Can 2-propanol form clathrate hydrates?*, Ind. Eng. Chem. Res., **41**, 2064-2068

Parrish W.R., Prausnitz J.M., 1972, *Dissociation pressures of gas hydrates formed by gas mixtures*, Ind. Eng. Chem. Process Des. Dev., **11**(1), 26–35

Rose W., Pfannkuch H.O., 1982, *Unconventional ideas about unconventional gas*, SPE Unconventional Gas Recovery Symposium, Pittsburgh, Pennsylvania

Seo Y., Lee H., 2003, *Hydrate phase equilibria of the ternary CH_4 + NaCl + water, CO_2 + NaCl + water and CH_4 + CO_2 + water mixtures in silica gel pores*, J. Phys. Chem. B, **107**(3), 889-894

Seo Y., Lee H., Uchida T., 2002, *Methane and carbon dioxide hydrate phase behavior in small porous silica gels: three-phase equilibrium determination and thermodynamic modelling*, Langmuir, **18**(24), 9164-9170

Sloan E.D., 1998, *Clathrate hydrates of natural gases*, Marcel Dekker Inc., New York

Tee L.S., Gotoh S., Stewart W.E., 1966,*Molecular parameters for normal fluids*, Ind. Eng. Chem. Fundam., **5**, 363-367

Tohidi B., Burgass R.W., Danesh A., Todd A.C., 1993, *Gas hydrates, problem or source of energy*, International Non-Renewable Energy Sources Congress, Tehran, Iran

Tohidi-Kalorazi B., 1995, *Gas hydrate equilibria in the presence of electrolyte solutions*, Ph.D. Thesis., Heriot-Watt University

Van der Waals J.H., Platteeuw J.C., 1959, *Clathrate solutions*, Advances in Chemical Physics, **2**, 1–57

Wilder J.W., Seshadri K., Smith D.H., 2001, Modeling hydrate formation in media with broad pore size distributions, Langmuir, **17**, 6729- 6735.

CHAPTER 7 – CONCLUSIONS AND RECOMMENDATIONS

7.1 Introduction

In this thesis the phenomenon of gas hydrate formation in relation to petroleum exploration and production was investigated. The investigations covered both experimental and theoretical aspects for a wide variety of systems including salts and/or organic inhibitors such as methanol, ethanol, *n*-propanol and MEG. The main achievements are summarised below.

(1) An extensive literature survey was conducted in order to extract experimental data for systems containing hydrocarbons, water, organic inhibitor(s) and salt(s) available in the literature (Chapter 2). The data was used for tuning and validation of the developed model,

(2) New experimental freezing point depression data for aqueous solutions of methanol, ethanol, monoethylene glycol and single or mixed salt(s) aqueous solutions, were generated (Chapter 2) in order to produce the necessary data for modelling purposes.

(3) The incipient equilibrium methane and natural gas hydrate conditions in presence of salt(s) and/or thermodynamic inhibitors (methanol, ethanol and MEG) have been experimentally measured (Chapter 2) and used as independent data for validation of the model.

(4) Thermodynamic modelling of phase equilibria, including an equation of state called CPA (Cubic-Plus-Association) and extensions of the model to take into account the effect of electrolyte solutions and the capillary effect in porous media has been presented. In addition hydrate-forming conditions have been modelled using the solid solution theory of van der Waals and Platteeuw (1959) and also the Kihara potential model (Chapter 3).

(5) In order to enable an equation of state to predict the correct phase behaviour of the fluid, the available experimental data (Chapter 2) were used for tuning the binary interaction parameters between molecules. After tuning, both the validity and reliability of the model were investigated in Chapter 4.

(6) The performance of the model in predicting the hydrate stability zone in the absence and presence of organic inhibitors and electrolyte solutions has been

evaluated. The new experimental data for different concentrations of salt(s) and organic inhibitor(s) measured in this work, in addition to the data from the literature, have been used for evaluating the model (Chapter 5).

(7) After showing the strength of the model for systems with and without hydrate (Chapters 3 to 5), further investigation have been conducted to model new applications such as recently discovered hydrate formers and hydrate in porous media (Chapter 6).

The conclusions drawn during the course of this study and the main features of the developed model will be described in this chapter. Some suggestions and recommendations of future work are also presented for further modification and validation of the thermodynamic model.

It is worth noting that, the CPA model developed in this work was also evaluated recently by Total SA for conventional and challenging hydrates calculations (Haghcheno and Duchet-Suchaux, 2009). In each case, the predictions were compared with independent experimental data, demonstrating the range of applicability of the model. The results show that the CPA model (HWHYD 2.1) consistently performs better than other thermodynamic models.

7.2 Literature Survey

The primary aim of this study was to develop a reliable thermodynamic model capable of describing accurately phase equilibria for multi-component multiphase mixtures containing light and heavy hydrocarbons, water, hydrate inhibitors and salts. For accurate prediction of phase behaviour using a thermodynamic model, the interaction between components in the system should be adjusted/tuned by minimising the error between reliable experimental data and the model predictions. For this reason, an extensive literature survey was conducted to find the relevant reliable experimental data on systems containing hydrocarbons, water, organic inhibitor(s) and salt(s) available in the literature (Chapter 2).

7.3 Experimental Work

After tuning the thermodynamic model (presented Chapter 4), the next step was to validate the model by using reliable experimental data. Although gas hydrates and flow assurance are major problems in oil and gas production and processing, the existing experimental data are relatively limited particularly for the real petroleum reservoir fluids. Furthermore, the limited data that are available in the literature are scattered and shows some discrepancies, highlighting the need for reliable measurements (this has been outlined in Chapter 5). In this work, experimental data on the incipient hydrate formation conditions on methane and natural gases in the presence of salt(s) and/or thermodynamic inhibitors have been generated, as well as freezing point depression data for aqueous solution of methanol, ethanol, monoethylene glycol and single or mixed salt(s) aqueous solutions (Chapter 2).

7.4 Thermodynamic Modelling

A statistical thermodynamic model based on the CPA-EoS and the classical mixing rules for fugacity calculations in all fluid phases was used in thermodynamic model (Chapter 3). The CPA-EoS has been extended to predict fluid phase equilibria in the presence of single or mixed electrolyte solutions by combining the equation of state with the Debye-Hückel electrostatic contribution for taking into the account the effect of salt. Hydrate-forming conditions are modelled by the solid solution theory of van der Waals and Platteeuw (1959). Langmuir constants have been calculated using the Kihara potential model (Kihara, 1953).

7.5 Validation of the Model

The predictions of the model (in the presence or absence of hydrates) were compared for a wide range of experimental data simulating various fluid systems and scenarios to validate the developed model (Chapters 4 to 6). The objective was to address three aspects of flow assurance and production technology: avoiding hydrate problems using thermodynamic inhibitors (e.g., electrolyte and/or organic inhibitors), investigation on recently discovered hydrate formers, and hydrate in porous media. In light of this, the accuracy of the model in prediction of the hydrate phase boundary in the presence of salts and/or organic inhibitors (both in bulk and porous media), as well as the potential for hydrate formation from new hydrate formers (*n*-propanol and ethanol) were examined and the model predictions were compared with the relevant experimental

data. This validation demonstrated the capabilities of the model as a design tool for oil and gas transmission lines and process facilities. The work of validating the model gave rise to the following conclusions:

(1) The CPA EoS has been shown to be a strong tool and very successful model for multiphase multi-component mixtures containing hydrocarbons, alcohols, glycols and water. Due to the scarcity and limitation of the reliable experimental data related to water/methanol/ethanol/*n*-propanol/MEG content in gases, the gas solubility in these components was employed for tuning the binary interaction parameters (BIPs). After tuning, the model could successfully predict the gas solubility in water/methanol/ethanol/*n*-propanol/MEG and water content and inhibitor distribution in vapour phase (Chapter 4). For cross associating systems, the results of this study indicate that the use of vapour-liquid equilibrium data (VLE) and ice melting point data (SLE) in the presence of aqueous inhibitor solutions for tuning the model can lead to successful predictions of hydrate phase boundaries.

(2) The model developed in this work is able to predict vapour pressure and freezing point depression of aqueous single and mixed electrolyte solutions over a wide range of temperature, and salt concentrations (Chapter 4).

(3) The hydrate inhibition effect of single and mixed electrolyte solutions with and without organic inhibitors has been modelled successfully, as demonstrated by good agreement between experimental data and the model predictions. These include predicting hydrate phase boundary for multi-component fluids in the presence of single and mixed electrolyte solutions, organic inhibitors, and mixtures of salts and organic inhibitors(Chapter 4 and 5).

(4) The capability of the model was further tested for conventional as well as challenging hydrates calculations: gas hydrate in low water content gases, prediction of hydrate inhibitor distribution in multiphase systems, and hydrate stability zone of oil/condensate in the presence of produced water and inhibitors. For all the above cases, a good agreement between predictions and experimental data was observed, supporting the reliability of the developed model (Chapter 5). Regarding gas hydrate in low water content gases, the only experimental data available for tuning the binary interaction parameters (BIPs)

between natural gas components and water were the gas solubility data in the temperature range of 273.15 K to 425.15 K (Chapter 4). The temperature-dependant interaction has been extrapolated to cover the lower temperature conditions. As the prediction results show, the model can predict the experimental water content data satisfactory and no further corrections are needed.

After showing the strength of the model for systems with and without hydrate (Chapters 4 and 5), further investigations were conducted to model new applications such as recently discovered hydrate formers and hydrate in porous media.

(5) The experimental data for *n*-propanol and ethanol clathrates have been used in the optimization of Kihara potential parameters for *n*-propanol and ethanol hydrates. Model predictions show the best agreement with the experimental data when *n*-propanol and ethanol are considered as hydrate formers. The model presented in this work demonstrates that *n*-propanol forms sII hydrates, occupying the large cavity of this structure. The experimental study (Maekawa, 2008) also confirms this conclusion. In addition experimental phase behaviour, combined with thermodynamic modelling studies from this work, suggest ethanol clathrates are most likely of sII type.

(6) The model has been extended to take into account the effect of capillary pressure on hydrate formation in porous media. The hydrate equilibrium dissociation conditions of the single and mixed gases in the presence of salt and alcohol are predicted using the CPA model and compared with experimental data available in the literature. The agreement between experimental data and predictions are acceptable (considering the potential error in experimental data).

7.6 Recommendations for Future Work

Four organic inhibitors; methanol, ethanol, *n*-propanol, and MEG and eight electrolytes; NaCl, KCl, KOH, $CaCl_2$, $MgCl_2$, $CaBr_2$, $ZnCl_2$ and $ZnBr_2$ were modelled successfully in this work, using the CPA EoS coupled with solid solution theory of van der Waals and Platteeuw (1959) for describing the phase behaviour in the presence or absence of hydrates (Chapter 4). In relation to electrolyte solutions, new salts (e.g., KBr, NaF, $BaCl_2$, $NaSO_4$) could be modelled using the developed approach in order to cover the main constituents of formation waters. This will require a comprehensive

experimental and theoretical investigation. The required experimental data for extending the model can be either, collected from open literature if available, or generated.

A few chemical inhibitors and combinations of salts and organic inhibitors, used in different drilling and production scenarios, were modelled in this work. It is recommended to extend the model to other combinations of salts and organic inhibitors (e.g., Glycerol, DEG, TEG, etc). Only very limited experimental data are likely to be available for optimisation of the relevant parameters in the thermodynamic model. In order to achieve reliable predictions for the phase behaviour, and the hydrate stability zone in these systems, reliable experimental data on freezing point depression, and boiling point elevation/lowering should be generated and used for modelling purposes. It is also recommended to further investigate high concentrations of mixed electrolyte/organic inhibitor systems for other combinations of salts and organic inhibitors and potential salting-out, both experimentally and from a modelling point of view. Furthermore no attempt was made to tune the binary interaction parameter between salt and alcohols or between two different alcohols. This was partly due to the lack of suitable experimental data.

In addition to the possibility of hydrate formation which has been addressed in this thesis, salt precipitation is also a serious concern. During production, pressure/ temperature/composition changes may result in salt precipitation (Joseph et al., 2002). Accurate thermodynamic description and prediction of this system, prone to gas hydrate and salt formation, is crucial to economical and safe design and operation of oil and gas production and transportation facilities; in particular in offshore and deepwater regions. It is recommended to further evaluate the model presented here to predict salt precipitation conditions of brine solutions in the presence or absence of hydrate organic inhibitors. For this reason the model might need to get extended by including salts as pseudo-components in the equation of state (Masoudi et al. 2004).

One area of interest to the oil industry is the potential loss of methanol, ethanol and MEG to the liquid hydrocarbon phase. There is a significant amount of binary data for the solubility of the above compounds in different hydrocarbons, but not for multi-component fluids such as condensates and oils. These data could be used to further

improve and validate the model. In this work, the prediction of the methanol loss in gas and liquid hydrocarbon phases, for a synthetic gas-condensate mixture, has been evaluated with the two available series of experimental data. In light of this, there is a need for reliable experimental data to use for validation purposes. These data are important as these compounds are only effective as a hydrate inhibitor in the aqueous phase, hence the mole fraction of inhibitor that partitions into the hydrocarbon phases must be considered lost.

As mentioned in Chapter 3, in the CPA model the total volume in each phase and therefore the fraction of non-bonded associating molecules, as well as their first- and second-order partial derivatives with respect to temperature, density, and mole fractions are calculated by iterative methods. In general, equation of state models with a chemical contribution that accounts for association effects, are computationally intensive as they have to solve an internal chemical equilibrium calculation. Tan et al. (2004) and Michelsen et al. (2001) have introduced simplified methods in order to calculate physical property calculation for association models. It is recommended the use of these methods to simplify the evaluation of physical properties from such models, in order to speed up the calculation time.

References

Joseph W.K., James B.D., 2002, *A protocol to inhibit the formation of natrium chloride salt blocks*, International Symposium on Oilfield Scale, Aberdeen, United Kingdom

Kihara T., 1953, *Virial coefficient and models of molecules in gases*, Rev. Modern Phys., **25**(4), 831– 843

Masoudi R., Tohidi B., Danesh A., Todd A.C., 2004, *A new approach in modelling phase equilibria and gas solubility in electrolyte solutions and its applications to gas hydrates,* Fluid Phase Equilibr., **215**(2), 163-174

Michelsen M.L., Hendriks E.M., 2001, *Physical properties from association models*, Fluid Phase Equilibr., **180**, 165–174

Tan S.P., Adidharma H., Radosz M., 2004, *Generalized procedure for estimating the fractions of nonbonded associating molecules and their derivatives in thermodynamic perturbation theory*, Ind. Eng. Chem. Res., **43**, 6263-6264

Van der Waals J.H., Platteeuw J.C., 1959, *Clathrate solutions*, Adv. Chem. Phys., **2**, 1–57

Haghcheno J.M., Duchet-Suchaux P., 2009, *5 comparison of some commercial programs for challenging hydrate predictions,* 20th International Oil Field Chemistry Symposium, Geilo, Norway